Determining the Relationship Between the [OIII] 5007$\AA$ Emission Line Profile and the Stellar Velocity Dispersion in Active Galaxies

Nathaniel Milgram

A Thesis presented for the degree of
Doctor of Physics

CAL POLY
SAN LUIS OBISPO

Department of Physics
California Polytechnic State University
San Luis Obispo

June 2015

Dedicated to

Human Endeavor

Abstract

The empirical relation between the stellar velocity dispersion (SVD) of the bulge and the mass of the central supermassive black hole (BH) suggests a link between host galaxy and BH evolution. For active galactic nuclei (AGNs), the BH mass (M_{BH}) can be estimated in a straightforward way from the Doppler broadening of the broad emission lines using the so-called virial method. However, the powerful AGN continuum emission often outshines the underlying stellar absorption lines, making it difficult to measure SVD of the host galaxy. Thus, the M_{BH} - SVD relation is difficult to establish for galaxies containing AGNs. As a remedy, the line-width of the [OIII] 5007$\mathring{A}$ emission line has been used as a surrogate for SVD. To probe the validity of this substitution, our team used a sample of $\sim$100 local AGNs with precise measurements of SVD from spatially-resolved high S/N Keck spectra and fitted the central [OIII] 5007$\mathring{A}$ emission lines with single Gaussian, double Gaussian, and Gauss-Hermite profiles, in both latter cases to allow for a blue or red-shifted wing due to e.g., outflows or jet interaction. For the central spectra, the study revealed no clear correlation between SVD and the [OIII] line widths. We here extend this analysis to spectra at greater distances from the nucleus thought to be less affected by outflows or jet interactions and instead dominated by the bulge potential. The results of this analysis show a loose correlation between SVD and the [OIII] line width at larger distances, albeit a large amount of scatter, suggesting that making a substitution between these two quantities should be done only for high S/N data and when there is significant confidence in the accuracy of the measurements and in the absence of interfering factors such as outflows or jet interactions, which have been shown to perturb the relation even when accounting for their effects as we have done. It was also determined that the preferred fitting method to measure the line width of the [OIII] emission is a double Gaussian, but only when there is a clear asymmetry in the profile, otherwise, a single Gaussian fit should be used. Even under ideal conditions, however, it was determined that the [OIII] line width tends to overestimate the SVD by roughly 30 $\pm$ 10%.

Declaration

The work in this thesis is based on research carried out at California Polytechnic State University. No part of this thesis has been submitted elsewhere for any other degree or qualification and it is all my own work unless referenced to the contrary in the text.

Acknowledgements

Dr. Vardha N. Bennert
Kelsi Flatland
Dr. Stefanie Komossa
Dr. Matthew W. Auger
Dr. Tommaso Treu
Charlie Showley
Jonathan Frederich
Dr. Brian Granger

Assistance from a National Science Foundation (NSF) Research at Undergraduate Institutions (RUI) grant AST-1312296 is gratefully acknowledged. Note that findings and conclusions do not necessarily represent views of the NSF.

This research has made use of the Dirac computer cluster at Cal Poly, maintained by Dr. Brian Granger and Dr. Ashley Ringer McDonald.

Data presented in this thesis were obtained at the W. M. Keck Observatory, which is operated as a scientific partnership among Caltech, the University of California, and NASA. The Observatory was made possible by the generous financial support of the W. M. Keck Foundation. The authors recognize and acknowledge the very significant cultural role and reverence that the summit of Mauna Kea has always had within the indigenous Hawaiian community. We are most fortunate to have the opportunity to conduct observations from this mountain.

This research has made use of the public archive of the Sloan Digital Sky Survey (SDSS) and the NASA/IPAC Extragalactic Database (NED) which is operated by the Jet Propulsion Laboratory, California Institute of Technology, under contract with the National Aeronautics and Space Administration.

Funding for travel to Lick observatory was provided through the College Based Fee (CBF) and the Physics department at Cal Poly.

Contents

List of Figures

List of Tables

Chapter 1

Introduction

Active galactic nuclei (AGN) are among the most exotic objects in the Universe. First observed by Edward A. Fath in 1908, these objects were originally considered quasi-stellar objects: star-like bodies within the Milky Way galaxy with uniquely non-stellar spectra. What makes these objects stand out from an observation standpoint is their strong emission line spectrum which is never exhibited by stars. It was not until 1943 that Carl Keenan Seyfert discovered that these quasi-stellar objects were not, in fact, within the Milky Way but instead contained within other far away galaxies. The extreme luminosity of these objects were the reason they had been mistaken as local objects, but not only are these objects highly luminous, they are also relatively small in size: hardly larger than our solar system as suggested by the inability to resolve these objects spatially as well as their short term variability in spectral features. The fact that the luminosity of these objects can be as high as that of an entire galaxy yet they are so small in size rules out the possibility of a star cluster as the source, since one with such characteristics would not be gravitationally stable. The unique emission spectra observed from these objects further serves to rule out stars as an explanation for these objects entirely. The only feasible explanation for these phenomena that we have is that of a super-massive black hole fed by accretion of matter. The extremely luminous power law continuum emissions from AGNs are due to the large gravitational potential of the accreting matter being converted to radiation through friction in the accretion disk (formed due to the conservation of angular momentum). It is from this power law continuum causing

ionization and recombination of the interstellar material that we observe the characteristic emission spectra. As we collect more data and further our understanding of these objects, we can begin to classify them, for there are many different types of AGNs that have been discovered. Lately, however, astronomers have embraced a more unified model of AGNs and attribute the differences to observational circumstances or evolutionary stages (note that this introduction refers to Peterson (1997)).

1.1 The Unified Model

The anatomy of a standard AGN is illustrated in Fig. 1.1. In the center of the host galaxy is the super-massive black hole. Surrounding the black hole is an accretion disk, which feeds into the black hole at typically a slow rate of roughly 1-2 $M_{\odot}$ per year. Because of the viscosity of the material being accreted, the large gravitational potential due to the vicinity to the black hole is converted into heat via friction, resulting in intense thermal radiation. Unlike stellar emissions, however, which are single black-body in nature, the resulting emission is a power law. This is due to the non-uniformity of the accretion disk; matter that is closer to the black hole is subject to greater gravitational forces and will thus have a higher temperature. This relation between distance and temperature results in a culmination of many black body curves, taking the shape of a power law continuum in the optical-UV wavelength range.

In addition to this power law continuum, emission lines are also observed emanating from active galaxies from regions which have been separately classified as the broad line region (BLR) and the narrow line region (NLR), depending on the width of the emission lines that they exhibit (see below). The BLR resides very close to the black hole, while the NLR is further out. There is also a torus of dust encircling the BLR which acts as an obscuring medium if present within the line of sight. Seyfert galaxies have been classified into type-1 and type-2, along with several sub-classes, with the major difference being the noteworthy absence of broad lines in type-2 Seyfert galaxy spectra (Fig. 1.2). The reason for this is the obscuration of

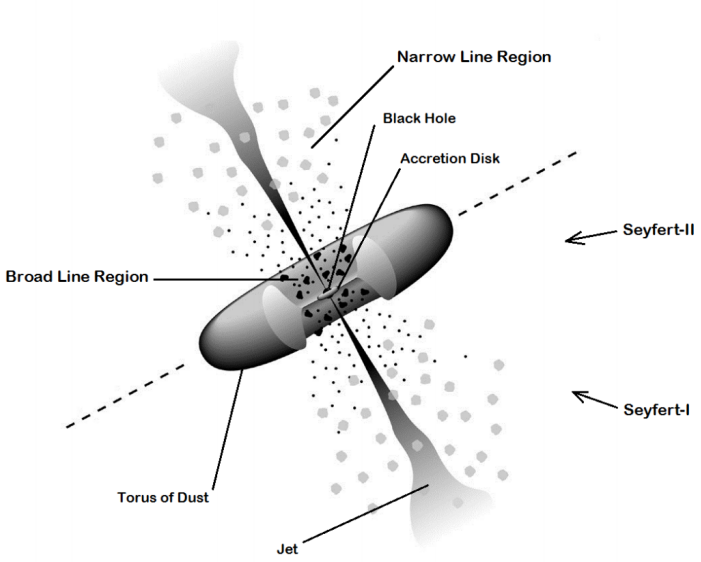

Figure 1.1: The geometry of an AGN. Each component is labeled, as well as the difference in viewing angles for Seyfert galaxies. Image adapted from Urry and Padovani (1995).

the BLR due to the dusty torus in the case of type-2 Seyfert galaxies, whereas for type-1 Seyfert galaxies, the dusty torus is not present along our line of sight. This suggests a fundamental similarity between type-1 and 2 Seyfert galaxies, with the apparent difference being due only to our observation angle.

1.1.1 The Broad-Line Region

The BLR consists of very hot and dense gas clouds surrounding the accretion disk. The central power law continuum will cause the material such as hydrogen and helium within these clouds to become photo-ionized and subsequently undergo recombination, resulting in the emission lines that we observe. Typically, however, only certain emission lines are observed emanating from this region, most notably the Balmer series characterized by electrons transitioning down to the n=2 orbital. The motion of these clouds are dictated by the gravitational potential of the black hole. Because of the strong gravitational potential present, these clouds reach velocities between 10^3 and 10^4 km/s. The result of this is extreme Doppler broadening within the emission lines that are eminent from this region. It is because of this broadening that it is called the broad line region.

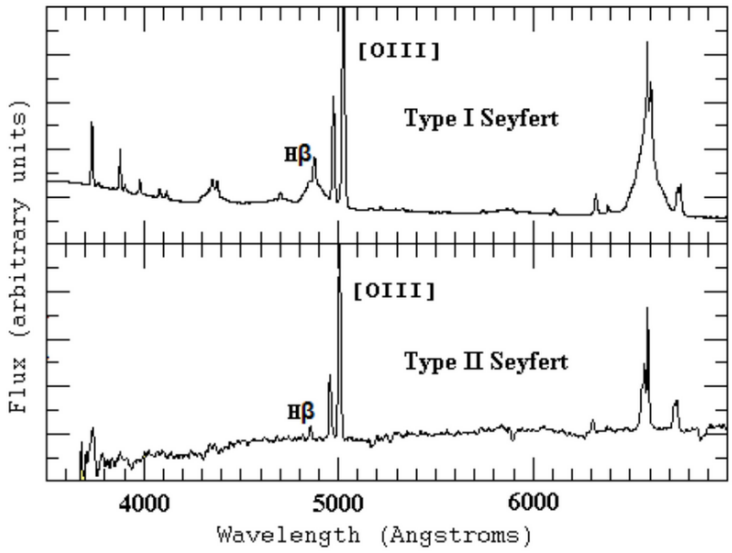

Figure 1.2: Sample spectra from type-1 and type-2 Seyfert galaxies. Note that Hβ and Hα have broad components in type-1, but not in type-2 Seyferts, whereas [OIII] is narrow in both cases. Image adapted from http://www.astr.ua.edu/keel/agn/spectra.html.

1.1.2 The Narrow-Line Region

Further from the central object than the BLR, yet in many ways similar, the NLR is characterized by its low density in comparison with the BLR as well as its greater distance from the central object, resulting in a smaller range in velocities (10^2 - 10^3 km/sec) and thus narrower emission lines. Like the BLR, the NLR is comprised of gas clouds which undergo photo-ionization and subsequent recombination, resulting in an emission spectrum, however this process occurs only for hydrogen and helium. Heavier elements will also create narrow emission lines due to electron transitions to lower energy levels, a process which does not occur in the BLR due to the high likelihood of collisional de-excitation in this dense region. Many more spectral lines are observed emanating from the NLR than from the BLR because of this. The NLR extends beyond the dusty torus as is seen in Fig. 1.1, meaning that it is seldom obscured to the observer. Indeed the NLR is typically large enough to be spatially resolved and is often observed in the form of large ionization cones for type-2 objects (Fig. 1.3), which gives further credence to the unified model.

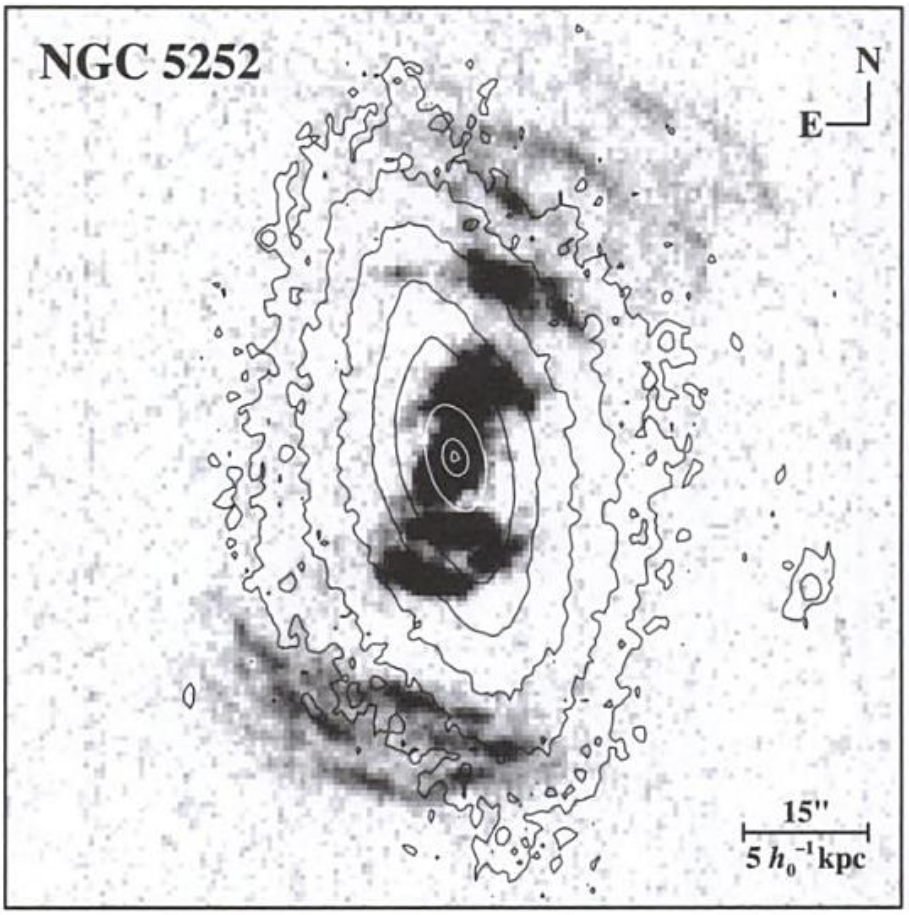

Figure 1.3: A map of the [OIII] 5007$\AA$ line emissions from NGC 5252, which shows the ionized regions taking the shape of cones. Figure taken from *An Introduction to Active Galactic Nuclei* by Bradley M. Peterson and composed by R.W. Pogge.

1.2 Measuring Black Hole Mass

In order to measure the mass of a black hole at the center of a galaxy, there are multiple methods that may be employed depending on the information available. If the galaxy is close enough, the gravitational sphere of influence of the black hole can be spatially resolved using distance information along with velocity data from stars or gas orbiting the black hole. If the gravitational sphere of influence cannot be spatially resolved, however, it is only possible to measure the black hole mass if the galaxy contains an AGN via the so called virial method. The technique of reverberation mapping involves measuring the time delay between variations in the power law continuum from the accretion disk and variations in the BLR (Fig.

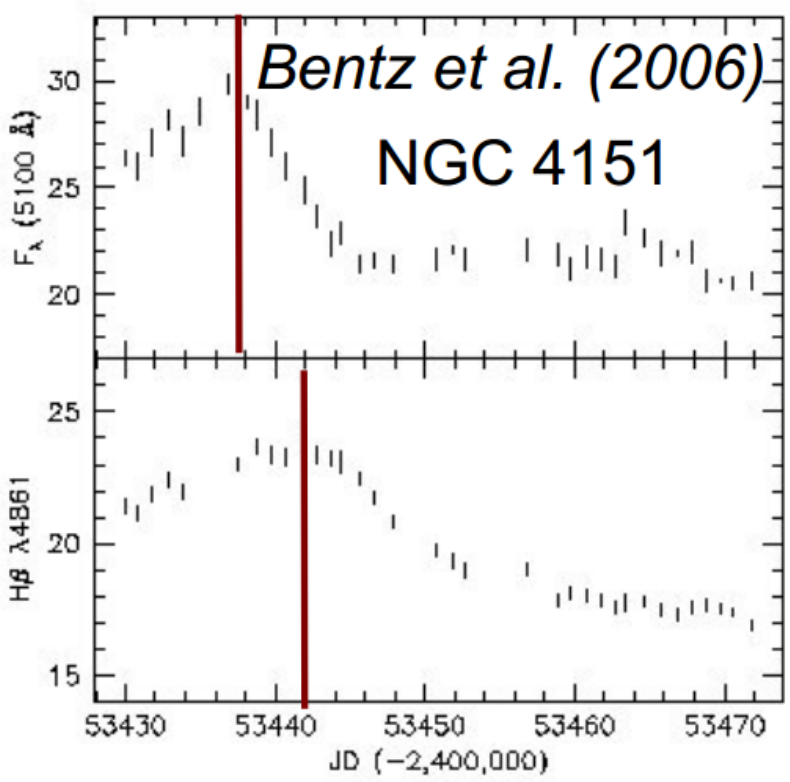

Figure 1.4: An example of measuring the time difference between central emissions and broad line region signals in order to perform reverberation mapping (Bentz et al. 2006).

1.4). By combining this time lag along with the speed of light, it is possible to calculate the distance between the BLR and the black hole (because on such scales, the distance from the accretion disk is essentially the same as the distance from the black hole). Using this information along with the observed Doppler broadening of the broad emission lines allows us to estimate the black hole mass without having to spatially resolve its gravitational sphere of influence. The mass of the black hole can be calculated using the formula:

$$M_{BH} = f\frac{v_{BLR}^2 R_{BLR}}{G} \tag{1.2.1}$$

where M_{BH} is the black hole mass, v_{BLR} is the orbital velocity of the broad line region, R_{BLR} is the distance of the BLR from the black hole, G is the gravitational constant, and f is the "virial coefficient" which depends on the geometry and kinematics of the BLR and is responsible for most of the uncertainty when measuring black hole mass using this method. f is usually found by matching the relation

between black hole mass and stellar velocity dispersion (see section 1.3) for inactive galaxies with that for active galaxies. This calculation can be used only if R_{BLR} is known from reverberation mapping. If it is not known, the so called single epoch method can be used, which involves the empirical relation found between the size of the BLR and the luminosity of the AGN. This relation obeys the following formula (Fig. 1.5, Bentz et al. 2007):

$$R_{BLR} \propto \sqrt{L_{5100\mathring{A}}} \tag{1.2.2}$$

where R_{BLR} is in light days and $L_{5100\mathring{A}}$ is the luminosity of the $5100\mathring{A}$ emission from the AGN power law continuum. This allows us to use the luminosity of the AGN measured in a single spectrum (hence the term "single epoch") as a proxy for the size of the BLR. Making this substitution into equation 1.2.1, M_{BH} can be calculated using the formula:

$$M_{BH} = f\frac{v_{BLR}^2\sqrt{L_{5100\mathring{A}}}}{G}. \tag{1.2.3}$$

Because it is only possible to measure the mass of the central black hole for distant unresolved galaxies if it contains an AGN, the measurement of black hole masses at the center of AGNs is potentially very illuminating when observing galaxies at high redshifts and may further our understanding of the galaxy-black hole mass scaling relation (Bennert et al. 2015).

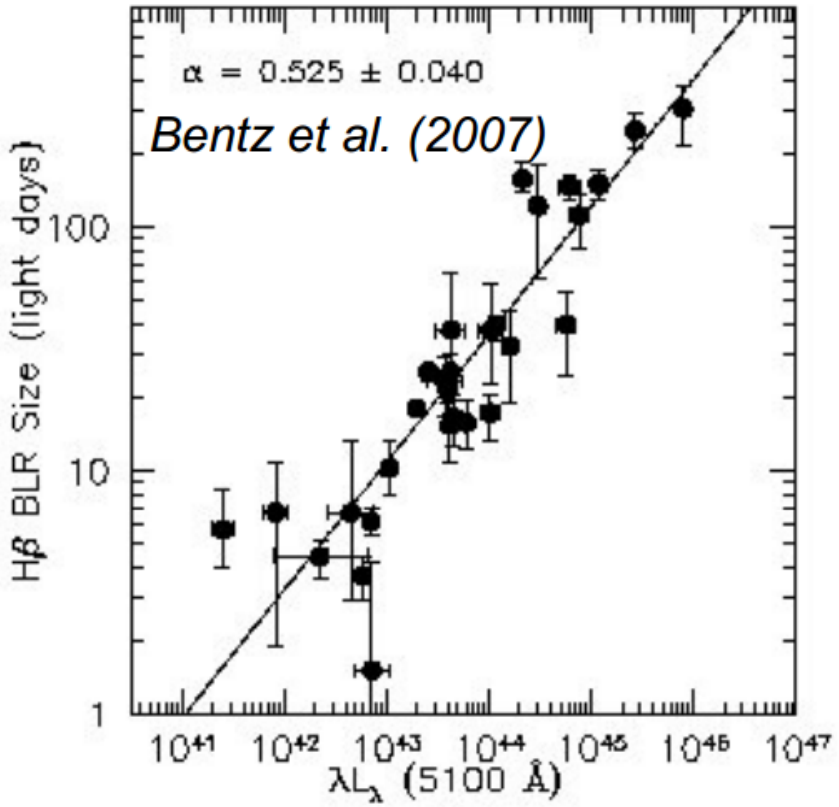

Figure 1.5: The empirical relation found between the AGN luminosity and the BLR size (Bentz et al. 2007).

1.3 Stellar Velocity Dispersion

When observing elliptical galaxies or galactic bulges, astronomers will often measure the stellar velocity dispersion (SVD). This quantity is derived from the broadening that is observed in the stellar absorption lines and is indicative of the overall orbital velocity of the stars (Fig. 1.6) and thus can be used to estimate the mass of the bulge. When comparing this quantity to the mass of the black hole at the center, an empirical relation has been found between the two (Fig.1.7, e.g., Gultekin et al. 2009). Because the mass of the black hole does not contribute significantly to the gravitational potential of the bulge or galaxy itself (the mass ratio between the bulge and the black hole is typically a factor of ∼1000), it is not clear why M_{BH} and σ should be correlated. It suggests a co-evolution between the central black hole and the galaxy. This co-evolution is not fully understood. In order to

further our understanding, it is desirable to study this evolution by carrying out observations of galaxies at very high redshift, which is possible only with AGNs so that we may measure M_{BH}. The problem with this, however, is the fact that the stellar emissions from galaxies containing AGNs are almost entirely outshone by the nuclear emissions, making the measurement of the SVD in AGNs very difficult.

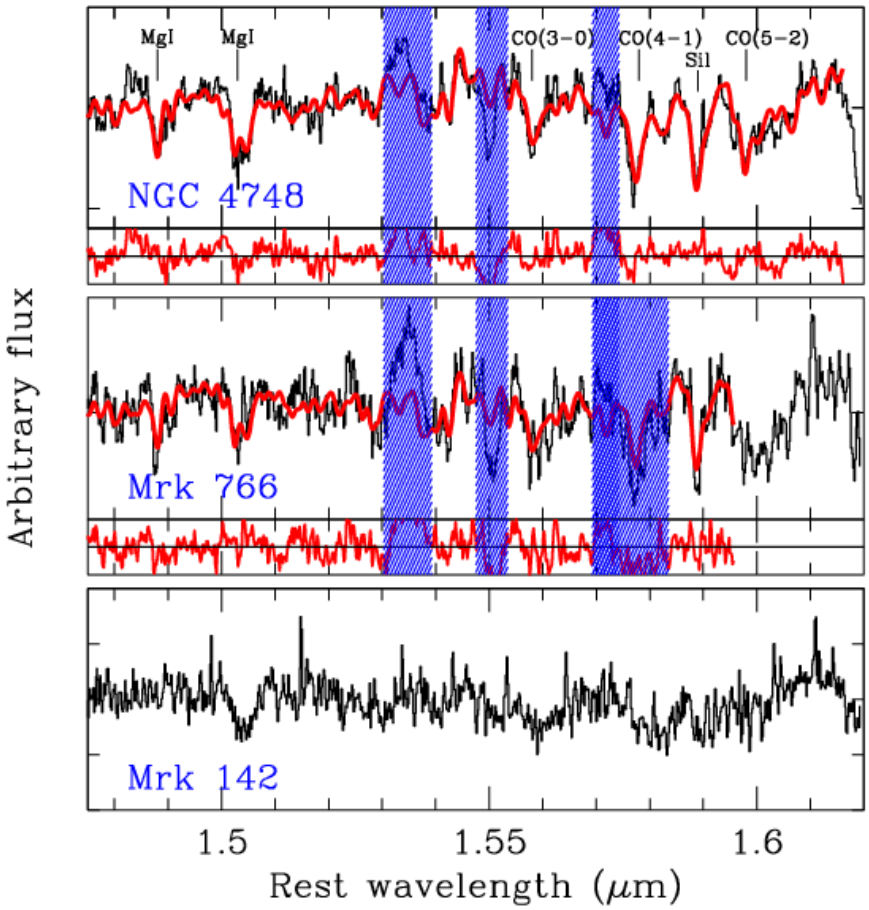

Figure 1.6: An example of measuring stellar velocity dispersion using stellar absorption lines.

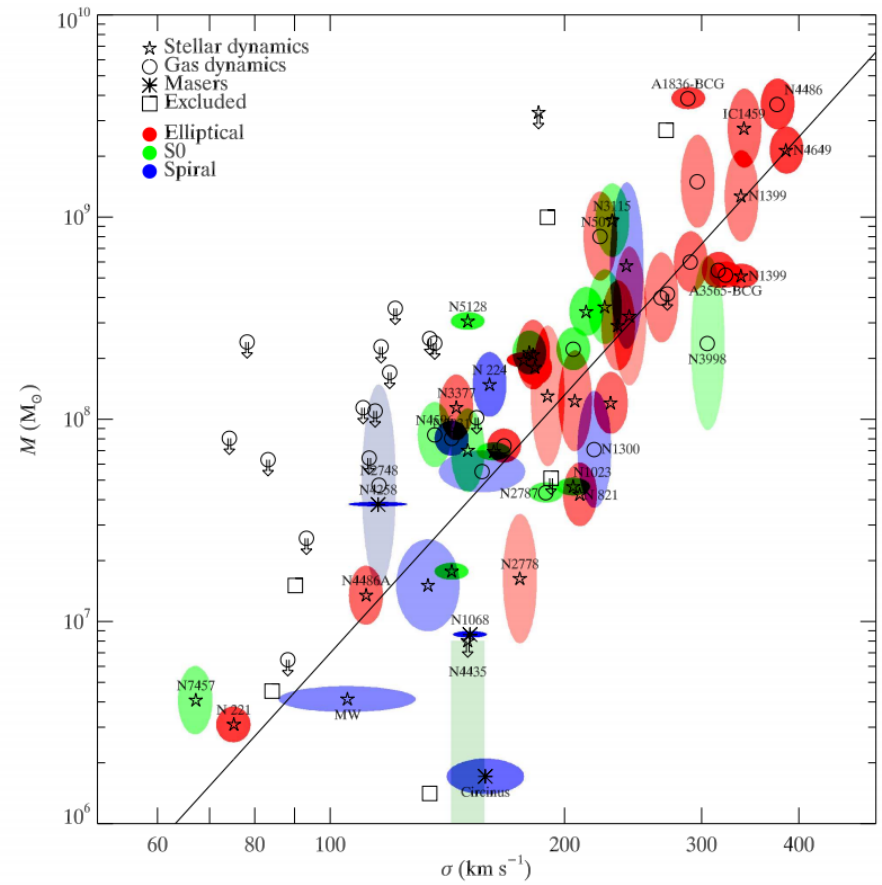

Figure 1.7: The relation between M_{BH} and σ. Figure from Gultekin et al. (2009).

1.4 Literature Discussion

It has been suggested to use the line widths observed from the NLR as a surrogate for the SVD for AGNs, particularly the strong [OIII] 5007$\AA$ emission line, which is easy to observe. This line originates in the NLR, which is extended, and the kinematics of the gas clouds are most likely dominated by the bulge potential. However, the tightness of the relation between the SVD and the line widths of the NLR has been questioned, since interferences such as jet interactions, outflows and inflows may alter the emission line profiles of the NLR gas. Nelson & Whittle (1996) was among the first to study the relation between the [OIII] line width and the SVD and found a moderately strong correlation between the two, yet they acknowledged the possibility of strong jet interactions perturbing this relation. Boroson (2003) tested this relation and came to the conclusion that "the correlation is real, but

the scatter is large" and that the [OIII] width could only be used to predict M_{BH} to a factor of 5. Boroson (2005) continued this line of research and finds [OIII] line blueshift in a large fraction of active galaxies, which correlates with a larger line width measurement. Komossa and Xu (2007) and Shields et al. (2003) both assumed this relation when studying the $M_{BH} - \sigma$ relation of AGNs and found the [OIII] line width to be a suitable surrogate for the SVD. Dasyra et al. (2011), in the endeavor to gather kinematic data from the NLR of 81 AGNs, came to the conclusion that the velocity dispersion of the NLR gas is systematically greater than that of the stars by 50 - 100 km/sec. All in all, it seems that the assumed correlation exists at least to a certain degree, but whether it is suitable for substitution is a question that is as of yet unanswered.

1.5 Goal of Thesis

In this thesis, we attempt to determine if the aforementioned relation exists. According to the findings of Kelsi Flatland (Flatland senior thesis 2012), no such relationship exists for these objects when considering only the spectrum collected by integrating the emissions from a relatively small region about the center. Here, this analysis has been extended to consider other spectra collected at various distance intervals from the center in order to determine if the relationship is present at these greater distances where previously mentioned interferences might be less or absent.

Chapter 2

Sample Selection, Observations, and Data Reduction

For this experiment, a sample of ∼100 Seyfert-1 galaxies in the local universe (0.02 <z <0.1) were selected from the Sloan Digital Sky Survey (SDSS) having black hole masses of no less than $10^7 M_\odot$. These objects were chosen because not only are they relatively close, making it possible to spatially resolve the host galaxy, they are also relatively dim for AGNs. This allows us to measure their SVD. The spectra for each object were collected from January 2009 to March 2010. The mass of the black hole in each AGN was measured using the broad Hβ lines (Bennert et al. 2015) and the SVD for 82 of these objects was measured using stellar absorption lines (Harris et al. 2012).

For each of the objects in our sample, long slit spectroscopy was utilized to gather multiple spectra from each object. This was performed using the Keck-10m telescope's Low Resolution Imaging Spectrometer (LRIS) and involved placing a 1" wide slit along the major axis of an object and collecting a set of 11 spectra at certain angular increments along the slit. The D560 dichroic was used for spectra taken in 2009, while the D680 dichroic was used for spectra taken in 2010. A 600/4000 grism was also used in order to collect blue spectra at a resolution of 90km/s and a wavelength range of 3200 - 5600$\AA$. The typical exposure time used was 600-1200 sec (Bennert et al. 2011). Each set of spectra consisted of a c, m5, m12, m21, m32, m45, p5, p12, p21, p32, and p45 spectrum, where c refers to the central spectrum,

m refers to "minus" and p refers to "plus" (arbitrary directions along the slit), and the following number refers to the number of pixels from the center of the object the spectrum was collected at (the pixel size used was 0.135").

The data was then reduced in order to remove the stellar absorption lines and the underlying power law continuum to ensure that only the AGN emission spectra was considered. Additionally, it was necessary to have spectra that were de-redshifted from the observed wavelengths to the rest frame wavelengths. This process of reduction and de-redshifting was performed using a Python script designed to follow standard procedures such as wavelength calibration and corrections. By selecting certain wavelength ranges where no emission lines were present, this code was able to perform a fit to the stellar absorption lines as well as the power law continuum and effectively remove them, and by matching known emission lines to their corresponding rest frame wavelengths using arc lamp calibration, the spectra were shifted down to their rest frames. This reduction and de-redshifting was carried out prior to my own research by Dr. Vardha N. Bennert and Chelsea Harris and is published in Harris et al. (2012).

Chapter 3

Spectral Analysis

In order to perform spectral analysis on our spectra, several Python codes were utilized. The original author of these codes is Dr. Matthew W. Auger, but the codes have been altered and re-written by Dr. Vardha N. Bennert, Kelsi Flatland, and myself in part with the help of Dr. Matthew W. Auger and Jon Frederic. The analysis is limited to the [OIII] 5007$\AA$ (hereafter [OIII]) emission line since this is the strongest AGN emission line present and thus easiest to analyze. The goal of the analysis is to determine the line width of the [OIII] emission line profile in order to compare these to the known SVD for each object. Three different fitting methods are used: single Gaussian, double Gaussian, and Gauss-Hermite Polynomials.

3.1 Single Gaussian Fit

If dominated by Doppler broadening from Keplerian motion, the emission line profile observed is expected to resemble a single Gaussian profile. There are a fair number of spectra from our sample ($\sim 80\%$) in which the emission line profile resembles this simplest form, and for these cases it is appropriate to apply a single Gaussian fit and measure the line width (standard deviation) directly from it.

3.2 Double Gaussian Fit

There are, however, other factors which can alter the shape of the profile. In many cases, the [OIII] emission line profile is observed to have either a blue wing or a red wing, which are slight asymmetries caused by inflow, outflow, or jet interactions with the NLR. The nature of these wings are complex, but typically it is appropriate to apply a Gaussian fit to these features. While this is an oversimplification, the fits are quite accurate. Moreover, we are only interested in the main component, which is defined here as the Gaussian whose peak aligns with that of the [OIII] line profile. Thus, it is appropriate to use a double Gaussian fit and to collect the linen width from the main Gaussian, with the secondary Gaussian used to exclude any asymmetries caused by non-Keplerian motion. For this fitting, an automated procedure was developed to determine if the fit produced was realistic, and if not, to attempt different sets of initial parameters. For instance, if the code generated a fit to a noise peak or in some other way produced an undesirable fit, it would recognize this and attempt a new set of initial parameters to which the code was sensitive. If no realistic double Gaussian fits could be generated, a single Gaussian fit was performed instead. This procedure was successful and required only minimal quality control (see the Appendix for further details).

3.3 Gauss-Hermite Polynomial Fit

While Gaussian fits may be applicable for most line profiles observed, especially the combination of two Gaussians, they are not ideal for profiles with more complex asymmetries or shape aberrations. Gauss-Hermite polynomials are a product of a Gaussian function and a Hermite function (of order no more that 12 in this case), that are highly versatile and are able to fit asymmetries and/or aberrations into a single fit with an associated line width. In addition to being more versatile, this type of fitting also incorporates and asymmetries into the line width value rather than exclude them. For these reasons, it is expected that the Gauss-Hermite polynomials will produce the most accurate fit to the observed profiles. However, the line width that scales with the SVD is supposedly the one of the central, main [OIII] component

unaffected by jets/outflows/inflows, and thus we expect Gauss-Hermite polynomials to overestimate the SVD.

3.4 Comparison Between Fitting Methods

In Fig. 2.1, three characteristic examples of [OIII] emission line profiles are shown, representing three different possibilities: blue wing (left panels), no wing (middle panels), and red wing (left panels). In the case without any wing, a single Gaussian gives an accurate fit of the overall profile. If outflows (blue wing) or inflows (red wing) are present, the single Gaussian leads to an overestimate of the width of the central component. A double Gaussian gives a more accurate fit, with the best overall fit being achieved by Gauss-Hermite polynomials, which also leads to an overestimate of the width if there are asymmetries.

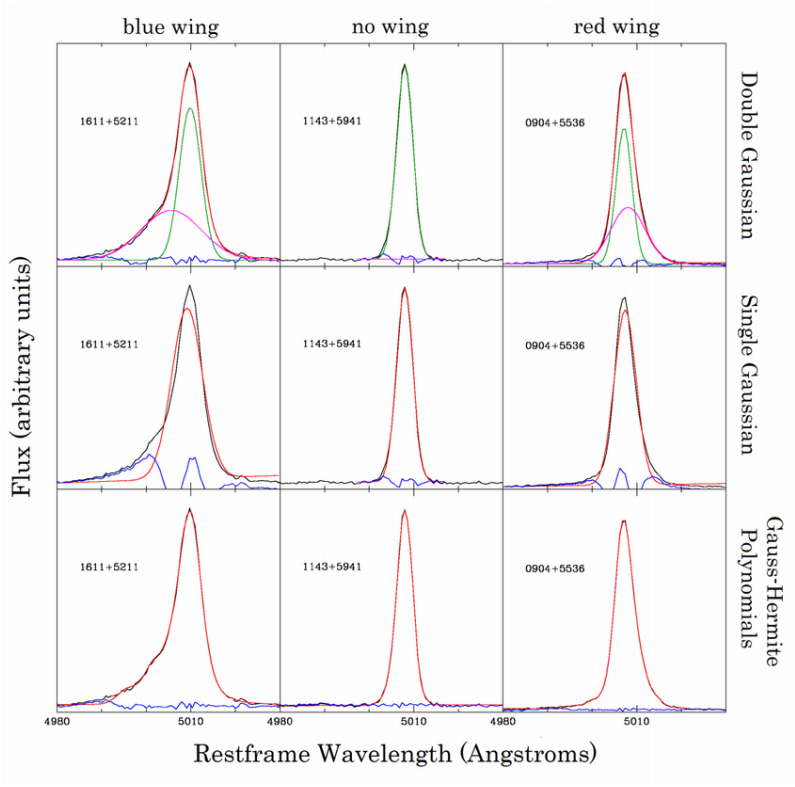

Figure 3.1: An example of the three different fitting techniques used for this study applied to three different profiles. Image from Flatland senior thesis 2012.

Chapter 4

Results and Discussion

4.1 Comparison with SVD

After collecting all [OIII] line width data and comparing it with the SVD data previously collected, a very rough relation between the two is seen. In the figure below (Fig. 3.1), the [OIII] line width divided by the SVD is plotted against the distance from the center, with each plot corresponding to a different fitting method (here we do not distinguish individual objects, all are included in the same plot). For all plots, the data points seem to congregate near the expected value of 1 (dashed line), but with a considerable amount of scatter as well as outliers. For the combined Gaussian plot, data from both single and double Gaussian fits were used, but with the goal of using double Gaussian data only in the cases of very clear blue or red wings. For the following plots, the double and single Gaussian data is plotted separately. It must be noted that the double Gaussian plot does incorporate some amount of single Gaussian data for the few cases in which no realistic double Gaussian fit could be generated. Additionally, it can be seen that the single Gaussian and Gauss-Hermite data have the largest total average values due to their inclusion of the [OIII] wing, while the double Gaussian data has the smallest total average due to its correction for it.

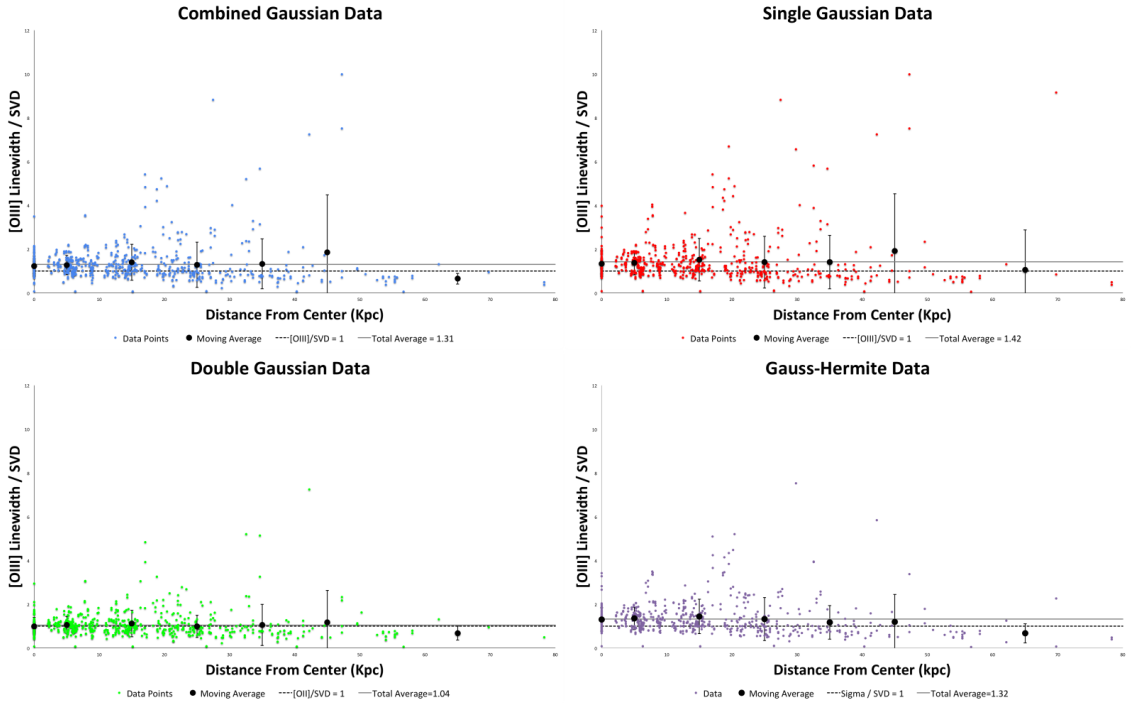

Figure 4.1: [OIII] line width / SVD vs. distance from the center (kpc) for combined Gaussian data (top left), single Gaussian data (top right), double Gaussian data (bottom left), and Gauss-Hermite data (bottom right). The moving averages have also been plotted in black. The total averages are indicated as a grey line, and [OIII]/SVD=1 is indicated as a dashed black line.

The following tables contain data for the moving average for each of the above plots (Fig. 3.1). 10 kpc bins were used in all cases except for the first and final bins for each plot, which were 0 kpc and 30 kpc respectively (the central spectra at 0 kpc from the center were to be considered separately from the rest of the bins, and the final bins were extended in order to incorporate a sufficient number of data pints). They correspond with the black data points above.

Table 4.1: Combined Gaussian Moving Average Data ($\sigma_{[OIII]}$/ SVD)

Distance interval (kpc)	Average	Standard Deviation
0 (Exactly)	1.23	0.46
0-10	1.27	0.44
10-20	1.40	0.82
20-30	1.29	1.03
30-40	1.33	1.14
40-50	1.85	2.62
50-80	0.65	0.25

Table 4.2: Single Gaussian Moving Average Data ($\sigma_{[OIII]}$/ SVD)

Distance interval (kpc)	Average	Standard Deviation
0 (Exactly)	1.34	0.58
0-10	1.38	0.55
10-20	1.52	0.98
20-30	1.41	1.18
30-40	1.41	1.22
40-50	1.91	2.62
50-80	1.05	1.83

Table 4.3: Double Gaussian Moving Average Data ($\sigma_{[OIII]}$/ SVD)

Distance interval (kpc)	Average	Standard Deviation
0 (Exactly)	0.99	0.40
0-10	1.06	0.39
10-20	1.12	0.61
20-30	0.99	0.51
30-40	1.05	0.94
40-50	1.17	1.46
50-80	0.68	0.32

Table 4.4: Gauss-Hermite Moving Average Data ($\sigma_{[OIII]}$/ SVD)

Distance interval (kpc)	Average	Standard Deviation
0 (Exactly)	1.31	0.53
0-10	1.35	0.51
10-20	1.44	0.79
20-30	1.32	0.98
30-40	1.17	0.77
40-50	1.20	1.25
50-80	0.67	0.44

4.2 Comparison with Literature

As stated earlier, our data is seen to have a large amount of scatter. This is consistent with the findings of Boroson (2003), which found a correlation coefficient of $r = 0.44$ between the [OIII] linewidth and the SVD, and it is likely due to the effects of inflow, outflow, or jet interactions on the emission line spectrum. These are effects that, although we have diligently tried to correct for them, have been known to disrupt the expected correlation between [OIII] and SVD as was seen in the findings of Kelsi Flatland (2012). These results have also indicated that the [OIII] line width is systematically greater than the SVD by 30 $\pm$ 10%, which is consistent with the findings of Dasyre et al. (2011), which found that the velocity dispersion of the NLR typically exceeds that of the stars by 50 - 100 km/sec. Considering the data obtained from the centers of the galaxies, these results are highly consistent with those found by Kelsi Flatland (2012). For double Gaussian fitting, she found an average value for $\sigma_{[OIII]}$/ SVD of 0.97 with a standard deviation of 0.32. for single Gaussian fitting, she found an average value of 1.32 with a standard deviation of 0.51. For the Gauss-Hermite polynomial fitting, he found an average value of 1.28 with a standard deviation of 0.49. Despite these results, the large amount of scatter within the data resulted in there being no clear correlation between the [OIII] line width and the SVD within Flatland's data set. While Flatland's conclusion that there is

no apparent correlation between these two quantities was reasonable given her data, the additional data that has been collected here indicates that there is indeed such a correlation, and the consistency of the shared results between Flatland's senior thesis and this project provides confidence that this research serves as a satisfactory continuation to her research.

4.3 Discussion

Overall, it can be said that the expected correlation between the [OIII] line width and the SVD is present, yet not robust. If one must make the substitution, then it is recommended that they perform fitting consistent with the combined Gaussian fitting method used here, wherein single Gaussian fits are used predominantly while double Gaussian fits are used only in cases where there are clear asymmetries to correct for. It is believed that this method is the most reliable one since it can correct for asymmetries while avoiding double Gaussian fits that are not realistic. As a recipe for studies using the [OIII] line width as a surrogate for the SVD, it is suggested to do the following:

1. Fit the [OIII] line with two Gaussians if wings/asymmetries are present, if not, fit the line with a single Gaussian instead.
2. Divide the derived quantity by 1.3 to correct for the overestimate.
3. Only perform this analysis with high S/N spectra.
4. This analysis may be performed at any location within the active galaxy, although the correlation becomes less robust the more inflows / outflows / jet interactions are present, which may be present at any location and are largely dependent on the object.
5. Due to the large scatter, it is not recommended that the [OIII] line width is used as a direct substitute for the SVD, but only as a stand in for qualitative analysis.

Chapter 5

Conclusion

In summary, this study has sought to establish the validity of using the [OIII] 5007 $\mathring{A}$ emission line width as a surrogate for the SVD in active galaxies. Such a correlation would be very useful, for one, due to the inability to measure the SVD in most active galaxies, and second, because the M_{BH} - SVD relation is crucial to our understanding of the proposed galaxy - black hole co-evolution. After performing single Gaussian, double Gaussian, and Gauss-Hermite polynomial fitting analysis on the [OIII] 5007 $\mathring{A}$ emission line on a total of 1100 spectra collected from 100 local Seyfert-1 galaxies and comparing the resulting [OIII] line widths to the SVDs published by Harris et al. (2012), it has been concluded that the expected correlation between these two quantities is present, but not robust. While it can be seen that the relation is clearly present (Fig. 3.1), there is a large amount of scatter as well as many outliers in the data collected. The most likely cause for this is either inflow, outflow, or jet interactions with the NLR occurring in many cases, which affect the emission line profiles in ways which disrupt the correlation that would otherwise be present, despite our efforts to correct for these effects. Because of this finding, it must be concluded that in order to use the [OIII] line width as a surrogate for the SVD, it is necessary to do so only under a certain set of conditions. These conditions are as follows:

1. Use a fitting method that utilizes single Gaussians when there are no asymmetries in the line, and one that utilizes double Gaussians if there are.

2. Assume that the value for the [OIII] line width is an overestimate of the SVD by roughly 30%.

3. Only perform this analysis to high S/N spectra.

4. Be mindful that the correlation becomes less robust the more inflow / outflow / jet interaction is present.

5. Because of the large scatter, do not use the [OIII] line width as a direct substitute for the SVD, but rather as a rough estimate.

In the future, there are some procedures that could potentially provide further insight into this subject: (i) A different fitting method may be used, such as Lorentzians, in order to better account for some of the underlying broad components seen in some of the profiles (see appendix). (ii) Examination of the outliers is important to determine if there is any physical phenomena within these objects that may result in such extreme relations between the [OIII] line width and the SVD. (iii) Finally, rather than compare the [OIII] line widths to the SVD of the entire object, it may be worthwhile to compare them to the SVD collected at some location closer to the location where the spectrum was collected since the SVD does have some spatial dependence. While all of this is beyond the scope of this thesis, the research will be continues along these lines.

Bibliography

Bennert, V. N., Auger, M. W., Treu, T., Woo, J.-H., & Malkan, M. A. 2011, The Astrophysical Journal, 726, 59-84: A Local Baseline of the Black Hole Mass Scaling Relations for Active Galaxies. I. Methodology and Results of Pilot Study

Bentz, M. C., Denney, K. D., Cackett, E. M., Dietrich, M., Fogel, J. K. J., Ghosh, H., Horne, K., Kuehn, C., Minezaki, T., Onken, C., A., Peterson, B., M., Pogge, R. W., Pronik, V., I., Richstone, D., O., Sergeev, S., G., Vestergaard, M., Walker, M., G., Yoshii, Y. 2006, The Astrophysical Journal, 651, 775-781: A Reverberationbased Mass for the Central Black Hole in NGC 4151

Bentz, M. C., Denney, K. D., Peterson, B., M., Pogge, R. W. 2007, ASP Conference Series, 373, 380: Refining the Radius-Luminosity Relationship for Active Galactic Nuclei

Boroson, Todd A. 2003, The Astrophysical Journal, 585, 647-652: Does the Narrow [OIII] λ5007 Line Reflect the Stellar Velocity Dispersion in Active Galactic Nuclei?

Boroson, T. A. 2005, The Astronomical Journal, 130, 381-386: Blueshifted [OIII] Emission: Indications of a Dynamic Narrow-Line Region

Dasyra, K. M., Ho, L. C., Netzer, H., Combes, F., Trakhtenbrot, B., Sturm, E., Armus, L., & Elbaz, D. 2011, The Astrophysical Journal, 740, 94: A View Of The Narrow-Line Region In The Infrared: Active Galactic Nuclei With Resolved Fine-Structure Lines In The Spitzer Archive

Gultekin, K., Richstone, D. O., Gebhardt, K., Lauer, T.A., Tremaine, S., Aller, M. C., Bender, R., Dressler, A., Faber, S. M., Filippenko, A.V., Green, R., Ho, L. C., Kormendy, J., Magorrian, J., Pinkney, J., & Siopis, C. 2009, The Astrophysical Journal, 698: The M-σ and M-L Relations in Galactic Bulges, and Determinations of Their Intrinsic Scatter.

Harris, C. E., Bennert, V. N., Auger, M. W., Treu, T., Woo, J., & Malkan, M. A. 2012, The Astrophysical Journal Supplement Series, 201, 29: A Local Baseline Of The Black Hole Mass Scaling Relations For Active Galaxies. II. Measuring Stellar Velocity Dispersion In Active Galaxies

Komossa, S. & Xu, D. 2007, The Astrophysical Journal, 667, L33-L36: Narrow-Line Seyfert 1 Galaxies and the $M_{BH} - \sigma$ Relation

Nelson, C. H. & Whittle, M. 1996, The Astrophysical Journal, 465, 96-114: Stellar and Gaseous Kinematics of Seyfert Galaxies. II. The Role of the Bulge

Peterson, B. M. *An Introduction to Active Galactic Nuclei.* Cambridge: Cambridge UP, 1997

Shields, G. A., Gebhardt, K., Salviander, S., Wills, B. J., Xie, B., Brotherton, M.S., Yuan, J., & Dietrich, M. 2003, The Astrophysical Journal, 583, 124-133: The Black HoleBulge Relationship in Quasars

Urry, M. & Padivani, P. 1995, Publications of the Astronomical Society of the Pacific, 107, 803-45: Unified Schemes for Radio-Loud Active Galactic Nuclei

Appendix A

Object List

The following is a comprehensive list of the objects used for this study. The values for SVD were taken from Table 2 - σ_{best} in Harris et al. (2012).

Table A.1: Object List

Object	**I.D.**	RA	**Dec**	**z**	**SVD (km/s)**	**Exp. Time (sec)**	**Date Taken**
0802+3104	1	08 02 43.40	+31 04 03.3	0.041	-	1200	01-21-2009
0026+0009	5	00 26 21.29	+00 09 14.9	0.06	170 ± 2	1600	09-20-2009
0353-0623	6	03 53 01.02	−06 23 26.3	0.076	196 ± 11	1200	01-22-2009
0336-0706	9	03 36 02.09	−07 06 17.1	0.097	246 ± 3	2400	09-20-2009
0813+4608	10	08 13 19.34	+46 08 49.5	0.054	120 ± 4	1200	01-14-2010
0121-0102	11	01 21 59.81	−01 02 24.4	0.054	107 ± 11	1200	1-21-2009
1116+4123	13	11 16 07.65	+41 23 53.2	0.021	131 ± 4	850	04-15-2009
1132+1017	14	11 32 49.28	+10 17 47.4	0.044	-	600	01-15-2010
1144+3653	15	11 44 29.88	+36 53 08.5	0.038	155 ± 8	600	04-16-2009
0802+3104	16	08 02 43.40	+31 04 03.3	0.0409	-	600	01-14-2014
0857+0528	19	08 57 37.77	+05 28 21.3	0.0586	127 ± 5	600	01-15-2010
0904+5536	20	09 04 36.95	+55 36 02.5	0.0371	128 ± 9	600	03-14-2010
0909+1330	21	09 09 02.35	+13 30 19.4	0.0506	91 ± 5	600	01-14-2010
0921+1017	22	09 21 15.55	+10 17 40.9	0.0392	98 ± 3	700	01-14-2010
0923+2254	23	09 23 43.00	+22 54 32.7	0.0332	129 ± 6	600	01-15-2010
0927+2301	24	09 27 18.51	+23 01 12.3	0.0262	195 ± 2	600	01-15-2010
0932+0233	26	09 32 40.55	+02 33 32.6	0.0567	124 ± 4	600	01-14-2010
0932+0405	27	09 32 59.60	+04 05 06.0	0.059	96 ± 6	600	01-14-2010
0938+0743	28	09 38 12.27	+07 43 40.0	0.0218	124 ± 4	600	01-14-2010
0948+4030	29	09 48 38.43	+40 30 43.5	0.0469	140 ± 3	900	01-15-2010
1002+2648	30	10 02 18.79	+26 48 05.7	0.0517	154 ± 8	600	01-15-2010
1029+2728	31	10 29 01.63	+27 28 51.2	0.0377	127 ± 6	600	01-15-2010
1042+0414	32	10 42 52.94	+04 14 41.1	0.0524	108 ± 10	1200	04-16-2009
1043+1105	33	10 43 26.47	+11 05 24.3	0.0475	-	600	04-46-2009
1049+2451	34	10 49 25.39	+24 51 23.7	0.055	77 ± 17	600	04-16-2009
1101+1102	35	11 01 01.78	+11 02 48.8	0.0355	144 ± 14	600	04-16-2009
1104+4334	36	11 04 56.03	+43 34 09.1	0.0493	91 ± 7	600	01-14-2010
1110+1136	37	11 10 45.97	+11 36 41.7	0.0421	-	3600	03-15-2010
1118+2827	38	11 18 53.02	+28 27 57.6	0.0599	119 ± 3	900	01-15-2010
1137+4826	39	11 37 04.17	+48 26 59.2	0.0541	166 ± 7	600	01-14-2010
1140+2307	40	11 40 54.09	+23 07 44.4	0.0348	82 ± 2	1200	01-15-2010

Continued on next page

Table A.1 – *Continued from previous page*

Object	I.D.	RA	Dec	z	SVD (km/s)	Exp. Time (sec)	Date Taken
1145+5547	41	11 45 45.18	+55 47 59.6	0.0534	118 ± 6	3600	03-14-2010
1206+4244	42	12 06 26.29	+42 44 26.1	0.052	157 ± 6	1100	03-14-2010
1210+3820	43	12 10 44.27	+38 20 10.3	0.0229	144 ± 5	600	04-16-2009
1216+5049	44	12 16 07.09	+50 49 30.0	0.0308	172 ± 7	900	03-14-2010
1223+0240	45	12 23 24.14	+02 40 44.4	0.0235	97 ± 8	600	03-15-2010
1250-0249	46	12 50 42.44	−02 49 31.5	0.047	107 ± 8	1200	04-16-2009
1306+4552	47	13 06 19.83	+45 52 24.2	0.0507	100 ± 4	3600	03-14-2010
1307+0952	48	13 07 21.93	+09 52 09.3	0.049	-	2400	03-15-2010
1323+2701	49	13 23 10.39	+27 01 40.4	0.0559	122 ± 9	700	04-16-2009
1355+3834	50	13 55 53.52	+38 34 28.5	0.0501	-	300	04-16-2009
1405-0259	51	14 05 14.86	−02 59 01.2	0.0541	123 ± 4	1600	04-16-2009
1416+0317	52	14 16 30.82	+01 37 07.9	0.0538	149 ± 4	2700	03-15-2010
1419+0754	53	14 19 08.30	+07 54 49.2	0.0558	185 ± 10	900	04-16-2009
1434+4839	54	14 34 52.45	+48 39 42.8	0.0365	114 ± 7	600	04-16-2009
1505+0342	56	15 05 56.55	+03 42 26.3	0.0358	-	1200	03-15-2010
1535+5754	57	15 35 52.40	+57 54 09.3	0.0304	116 ± 4	1200	04-15-2009
1545+1709	58	15 45 07.53	+17 09 51.1	0.0481	171 ± 5	1200	04-15-2009
1554+3238	59	15 54 17.42	+32 38 37.6	0.0483	159 ± 4	1200	04-15-2009
1557+0830	60	15 57 33.13	+08 30 42.9	0.0465	-	1200	04-15-2009
1605+3305	61	16 05 02.46	+33 05 44.8	0.0532	186 ± 8	1200	04-15-2009
1606+3324	62	16 06 55.94	+33 24 00.3	0.0585	170 ± 8	1200	04-15-2009
1611+5211	63	16 11 56.30	+52 11 16.8	0.0409	120 ± 5	1200	04-15-2009
1647+4442	64	16 47 21.47	+44 42 09.7	0.0253	-	4200	03-14-2010
2327+1524	70	23 27 21.97	+15 24 37.4	0.0458	266 ± 3	600	09-20-2009
0013-0951	71	00 13 35.3	−09 51 20.9	0.0615	134 ± 5	600	09-20-2009
0038+0034	73	00 38 47.96	+00 34 57.5	0.0805	131 ± 6	600	09-20-2009
0109+0059	74	01 09 39.01	+00 59 50.4	0.0928	165 ± 17	600	09-20-2009
0150+0057	76	01 50 16.43	+00 57 01.9	0.0847	193 ± 4	600	09-20-2009
0212+1406	77	02 12 57.59	+14 06 10.0	0.0618	188 ± 4	600	09-20-2009
0301+0110	78	03 01 24.26	+01 10 22.8	0.0715	97 ± 4	600	09-20-2009
0301+0115	79	03 01 44.19	+01 15 30.8	0.0747	90 ± 6	600	09-20-2009
0310-0049	80	03 10 27.82	−00 49 50.7	0.0801	-	600	09-20-2009
0731+4522	81	07 37 26.68	+45 22 17.4	0.0921	-	600	09-20-2009
0735+3752	82	07 35 21.19	+37 52 01.9	0.0962	156 ± 23	600	09-20-2009
0737+4244	83	07 37 03.28	+42 44 14.6	0.0882	90 ± 18	600	09-20-2009
1655+2014	88	16 55 14.21	+20 12 42.0	0.0841	199 ± 6	600	09-20-2009
1708+2153	91	17 08 59.15	+21 53 08.1	0.0722	172 ± 13	600	09-20-2009
2116+1102	96	21 16 46.33	+11 02 37.3	0.0805	-	700	09-20-2009
2140+0025	99	21 40 54.55	+00 25 38.2	0.0838	71 ± 28	600	09-20-2009
2215-0036	100	22 15 42.29	−00 36 09.6	0.0992	-	600	09-20-2009
2221-0906	102	22 21 10.83	−09 06 22.0	0.0912	115 ± 17	600	09-20-2009
2222-0819	103	22 22 46.61	−08 19 43.9	0.0821	99 ± 8	700	09-20-2009
2233+1312	106	22 33 38.42	+13 12 43.5	0.0934	198 ± 6	800	09-20-2009
2254+0046	108	22 54 52.24	+00 46 31.4	0.0907	-	600	09-20-2009
2351+1552	109	23 51 28.75	+15 52 59.1	0.0963	237 ± 9	600	09-20-2009
0811+1739	114	08 11 10.28	+17 39 43.9	0.0649	136 ± 6	2700	03-15-2010
0845+3409	126	08 45 56.67	+34 09 36.3	0.0655	121 ± 5	3600	03-14-2010
0854+1741	130	08 54 39.25	+17 41 22.5	0.0654	-	600	03-15-2010
0923+2946	138	09 23 19.73	+29 46 09.1	0.0625	143 ± 3	600	01-15-2010
0936+1014	143	09 36 41.08	+10 14 15.7	0.06	-	3600	03-15-2010
1029+1408	155	10 29 25.73	+14 08 23.2	0.0608	197 ± 5	600	01-15-2010
1029+4019	156	10 29 46.80	+40 19 13.8	0.0672	165 ± 6	600	01-14-2010
1038+4658	157	10 38 33.42	+46 58 06.0	0.0631	-	600	01-14-2010
1058+5259	162	10 58 28.76	+52 59 29.0	0.0676	121 ± 3	600	01-14-2010
1139+5911	174	11 39 08.95	+59 11 54.6	0.0612	-	600	01-14-2010
1143+5941	177	11 43 44.30	+59 51 12.4	0.0629	121 ± 6	3000	03-14-2010
1147+0902	180	11 47 55.08	+09 02 28.8	0.0688	120 ± 18	600	01-15-2010

Continued on next page

Table A.1 – *Continued from previous page*

Object	I.D.	RA	Dec	z	SVD (km/s)	Exp. Time (sec)	Date Taken
1205+4959	187	12 05 56.01	+49 59 56.4	0.063	166 ± 6	600	01-14-2010
1231+4504	196	12 31 52.04	+45 04 42.9	0.0621	228 ± 7	1200	01-15-2010
1241+3722	197	12 41 29.42	+37 22 01.9	0.0633	144 ± 4	800	01-15-2010
1246+5134	202	12 46 38.74	+51 34 55.9	0.0668	113 ± 5	600	01-15-2010
1312+2628	204	13 12 59.59	+26 28 24.0	0.0604	133 ± 9	2700	03-14-2010
1636+4202	205	16 36 31.28	+42 02 42.5	0.061	144 ± 10	1200	03-14-2010
1353+3951	207	13 53 45.93	+39 51 01.6	0.0626	168 ± 11	600	03-14-2010
0831+0521	208	08 11 10.28	+17 39 43.9	0.035	201 ± 13	600	03-15-2010
1423+2720	209	14 23 38.43	+27 20 09.7	0.0639	128 ± 7	1200	03-14-2010
1228+0951	210	12 28 11.41	+09 51 26.7	0.064	184 ± 10	600	03-15-2010
1313+3653	213	13 13 48.96	+36 53 57.9	0.0667	183 ± 24	600	03-14-2010
1543+3631	214	15 43 51.49	+36 31 36.7	0.0672	119 ± 9	1200	03-15-2010

Column 1 - Target I.D. from RA and Dec, Column 2 - Object I.D. Given for Project, Column 3 - Right Ascension, Column 4 - Declination, Column 5 - Redshift, Column 6 - Stellar Velocity Dispersion, Column 7 - Exposure Time, Column 8 - Date of Observation

Appendix B

Fits

The following sections contain the plots collected from all the fits performed for this study. Each plot is zoomed in on the wavelength range 4980 - 5030$\mathring{A}$, with the flux range being arbitrary and adjusted for each object in order to view the entire profile (each set of spectra from an individual object was plotted with the same flux range). If no fit is shown, it was determined that either there was no emission line present or that the signal to noise ratio was too small to produce a reliable fit. If the fits themselves do no encompass the full wavelength range plotted, it was because the fitting code was sensitive to the wavelength range used, and a smaller range was necessary to produce a reliable fit. Note that there are some objects here that were not included in the final data set due to the absence of SVD data. There are also objects that warrant individual discussion. The captions for the images below will be marked accordingly with certain symbols:

X - The object was not included in the final data set due to the absence of SVD data.
U - The set of spectra contains double Gaussian fits that are considered to be unrealistic. These were occurrences in which either the fit produced two Gaussians where it was unclear which should be considered as the main fit or two Gaussians where it was clear that neither should be considered as the main fit.
B - The set of spectra contain highly prominent symmetrical underlying broad components that do not resemble a blue or red wing.

H - The [OIII] lines further from the center of the object tend to increase in strength rather than decrease. This is likely due to [HII] regions within the galaxies that emit [OIII] lines due to ionization by young stars. In these cases, the line width of these profiles is still expected to be correlated to the SVD, so the data was still included. 11% of the objects showed such behavior.

* - There is a comment regarding the object in the "Individual Object Discussion" section at the end of this chapter.

B.1 Single Gaussian Fits

The following are the single Gaussian fits collected for this study, performed regardless of any asymmetries on all objects and spectral rows.

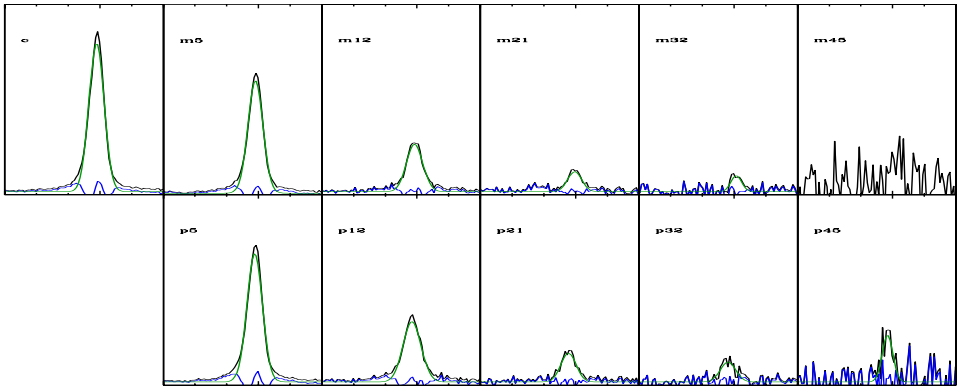

Figure B.1: SG-Object 1 [X]

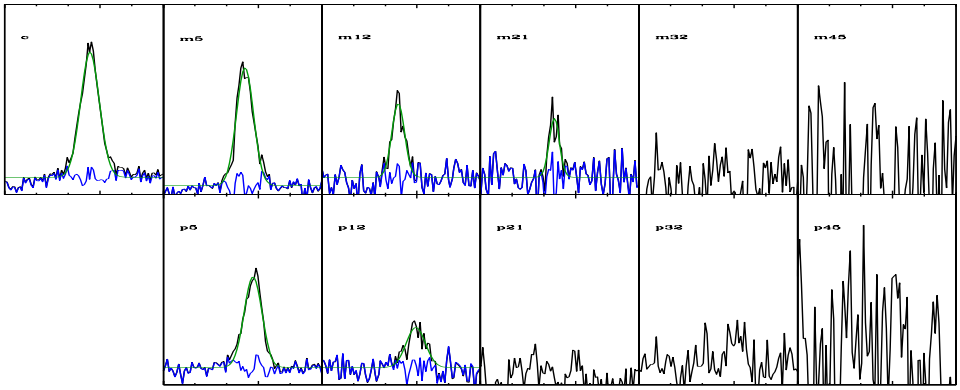

Figure B.2: SG-Object 5

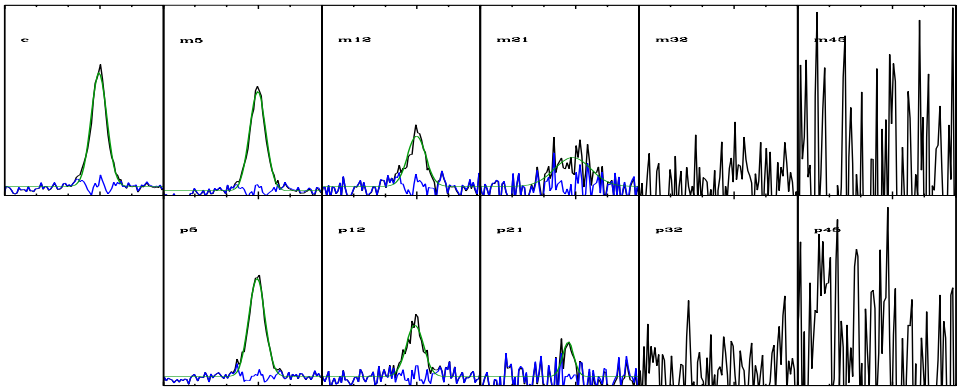

Figure B.3: SG-Object 6

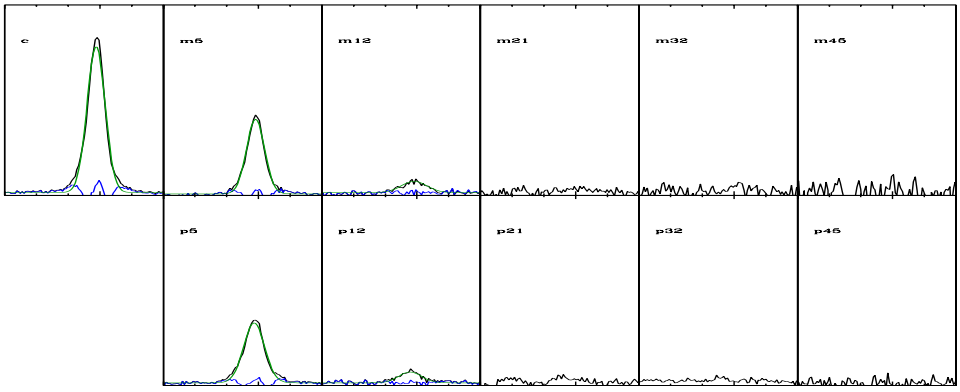

Figure B.4: SG-Object 9

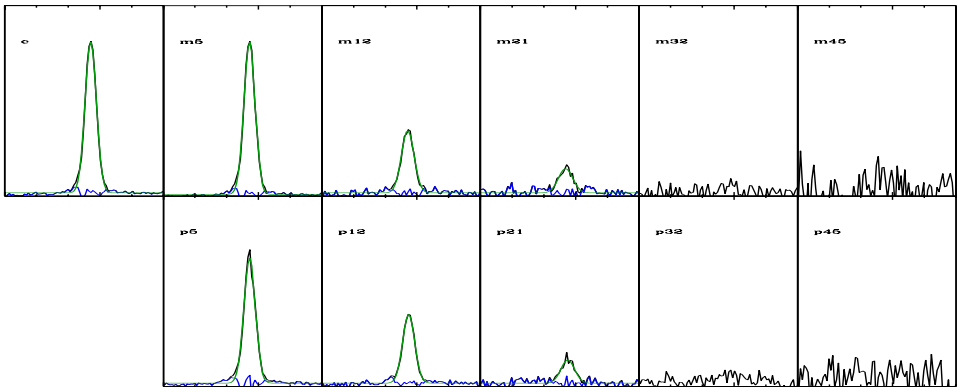

Figure B.5: SG-Object 10

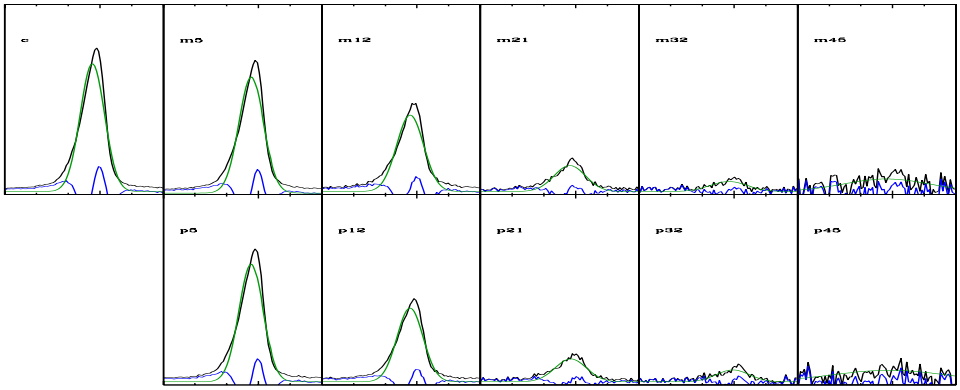

Figure B.6: SG-Object 11 [*]

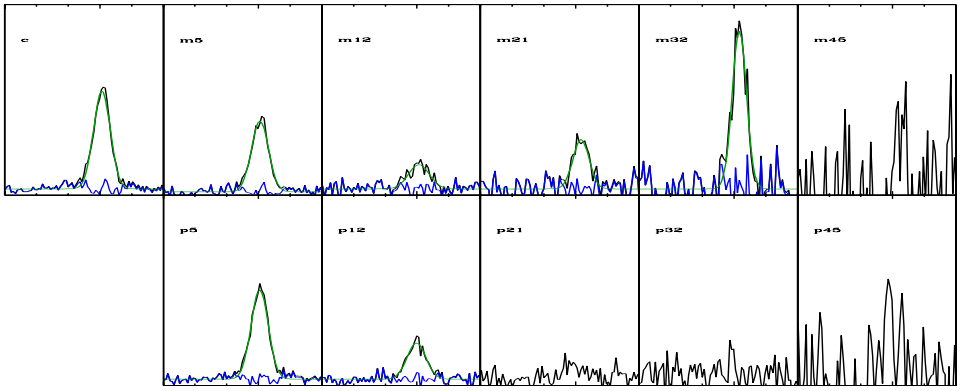

Figure B.7: SG-Object 13 [H]

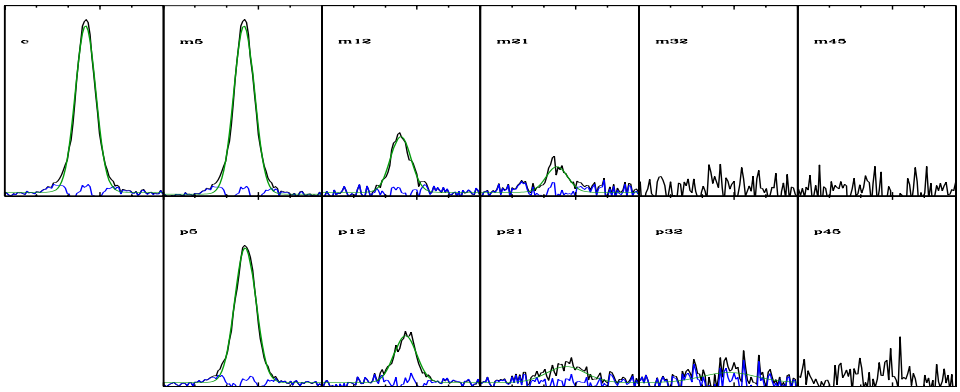

Figure B.8: SG-Object 14 [X]

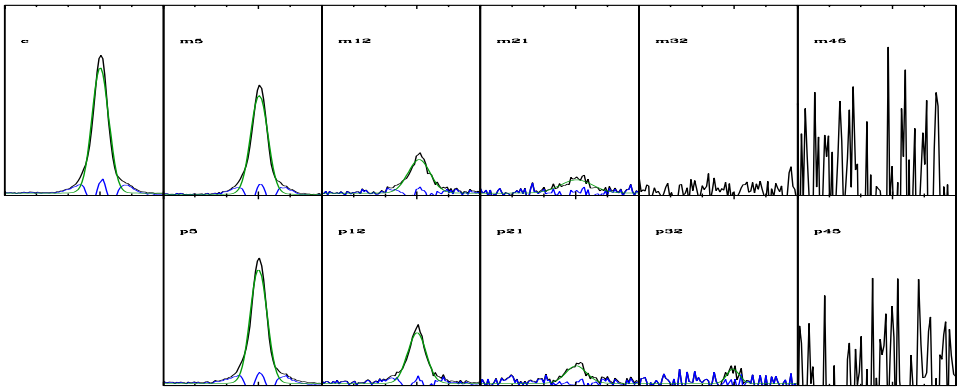

Figure B.9: SG-Object 15

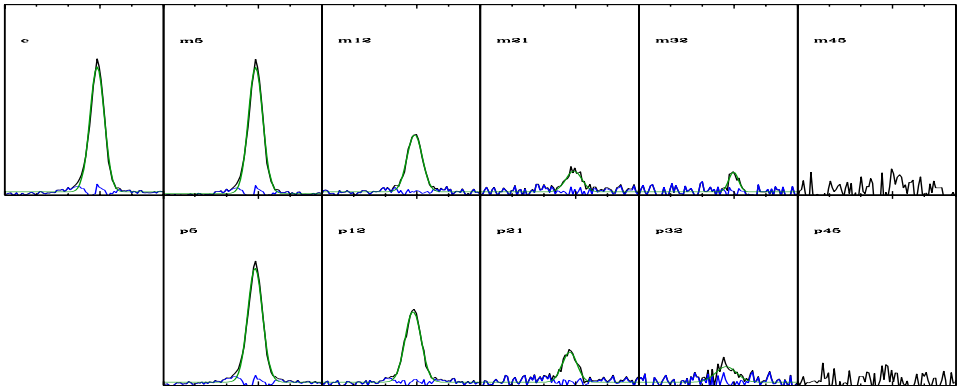

Figure B.10: SG-Object 16 [X]

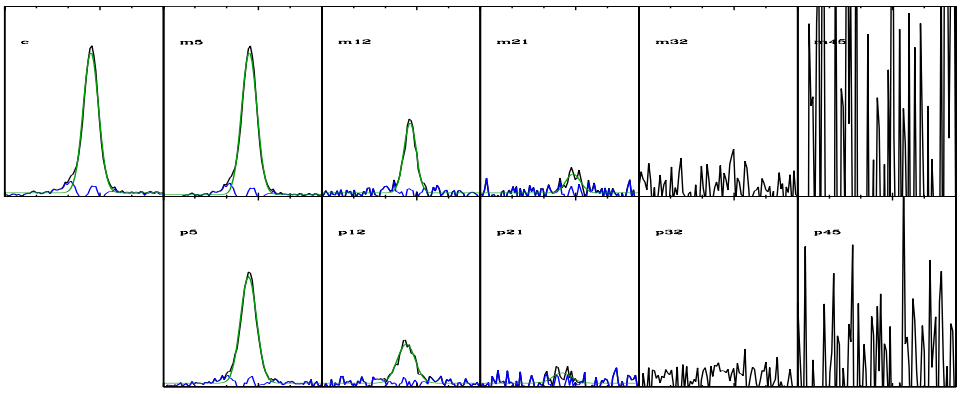

Figure B.11: SG-Object 19

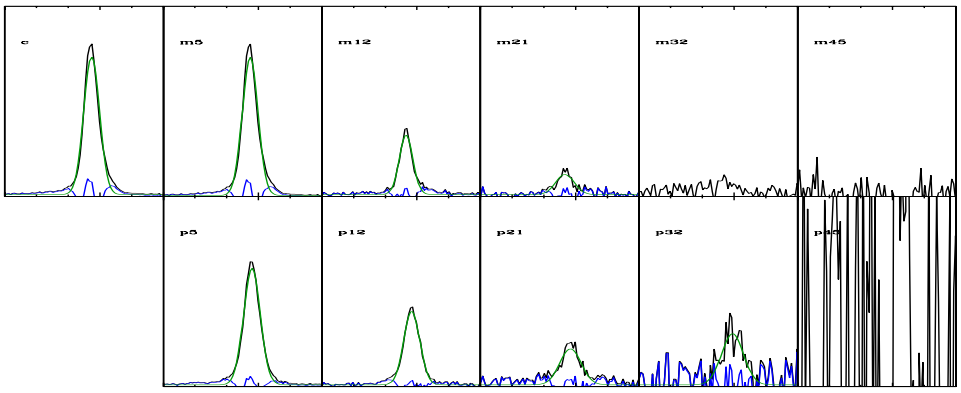

Figure B.12: SG-Object 20

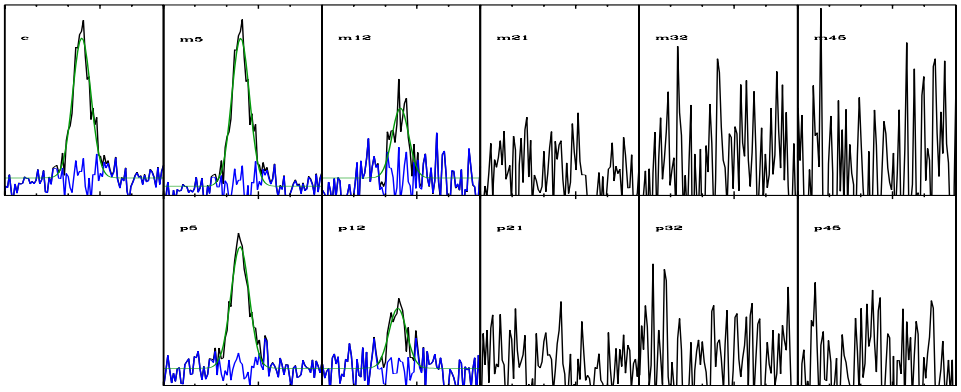

Figure B.13: SG-Object 21

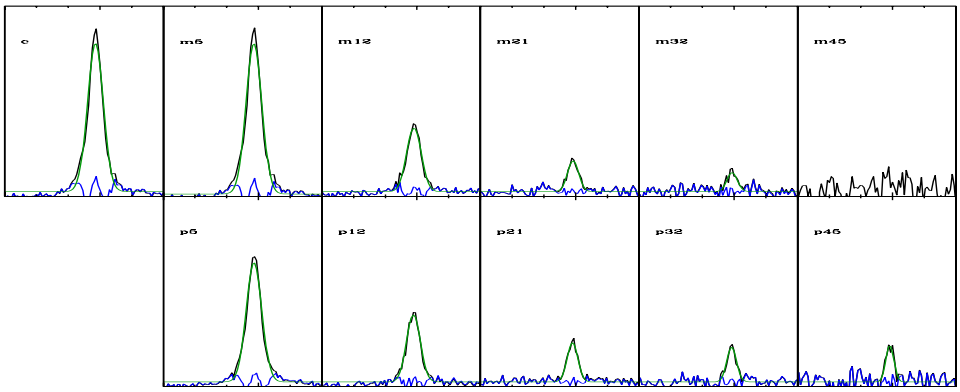

Figure B.14: SG-Object 22

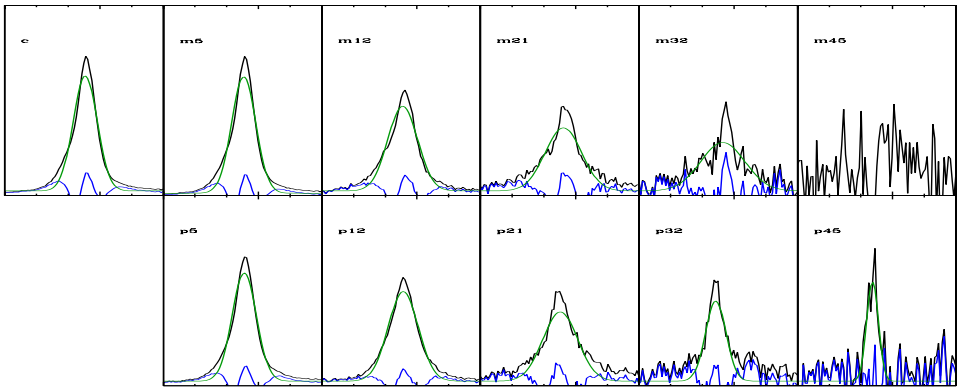

Figure B.15: SG-Object 23 [B]

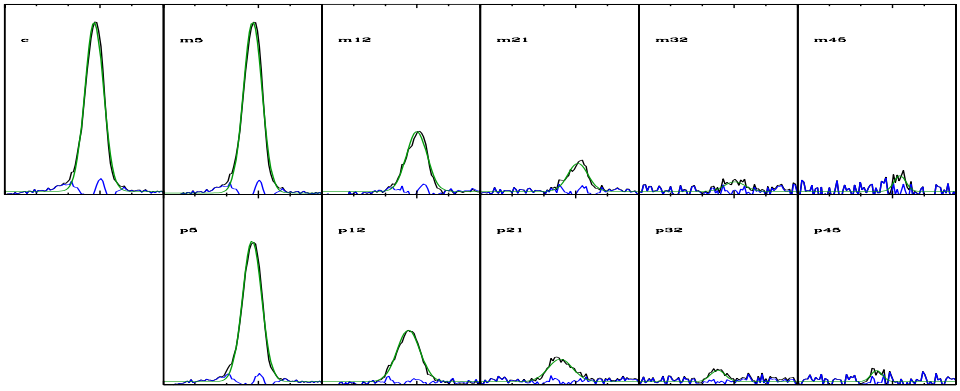

Figure B.16: SG-Object 24

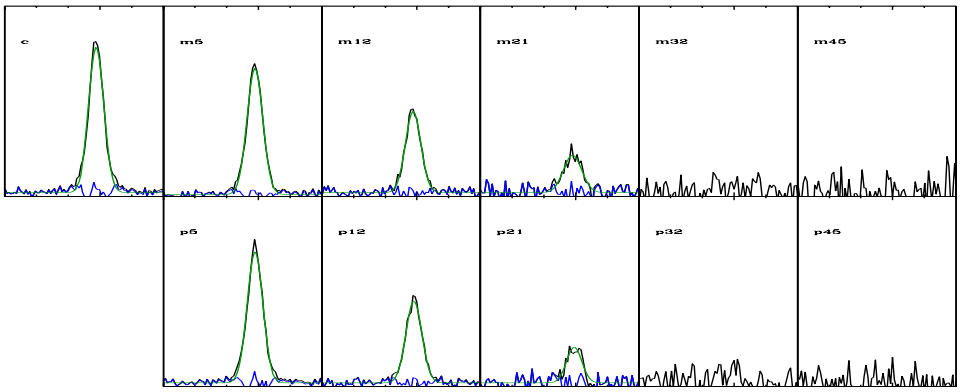

Figure B.17: SG-Object 26

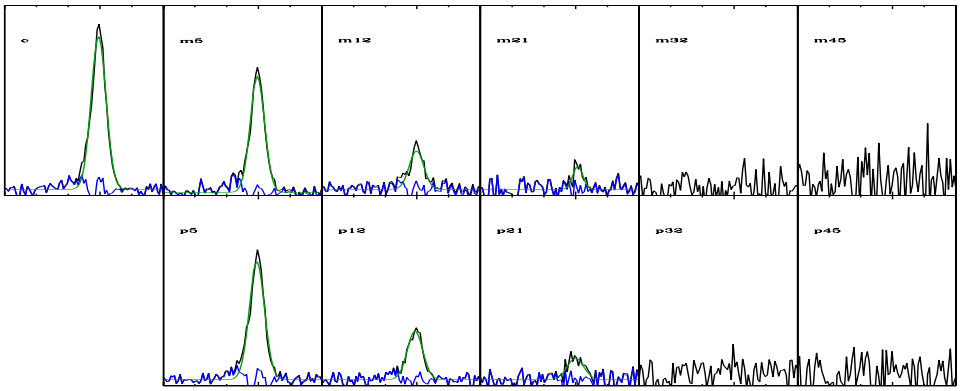

Figure B.18: SG-Object 27

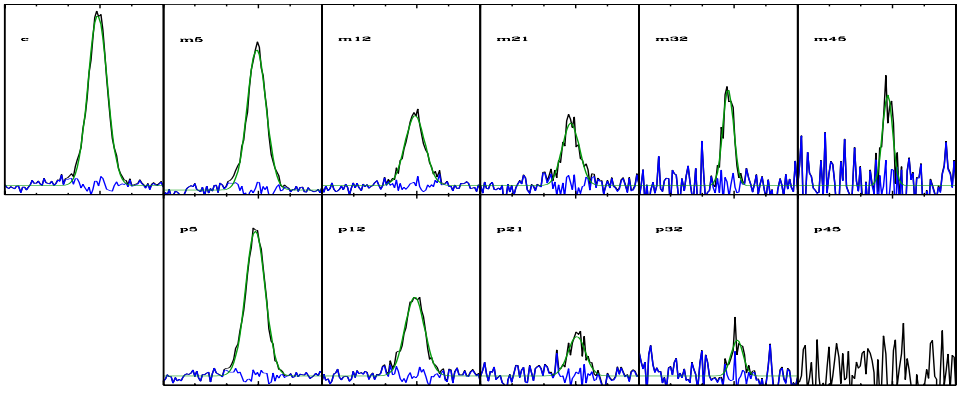

Figure B.19: SG-Object 28 [H]

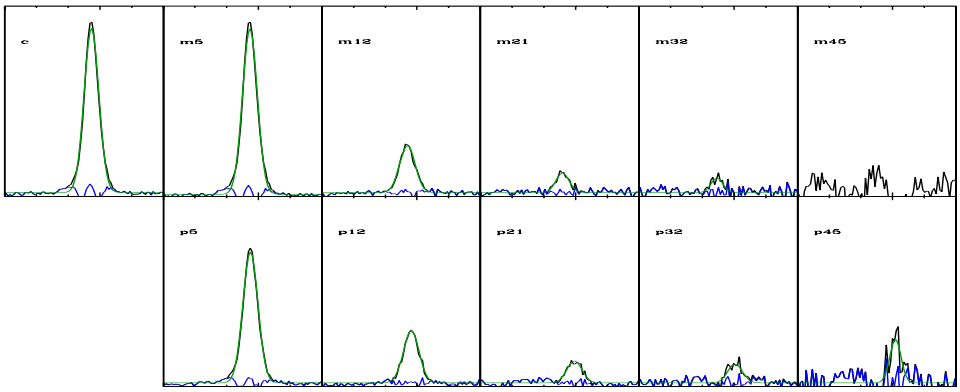

Figure B.20: SG-Object 29

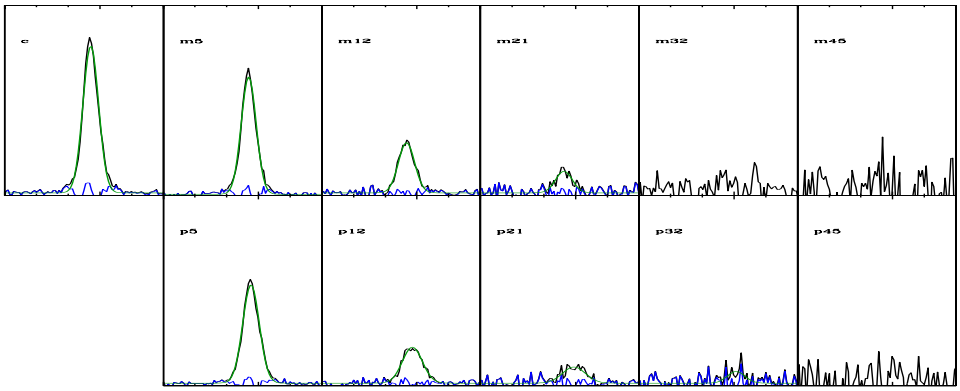

Figure B.21: SG-Object 30

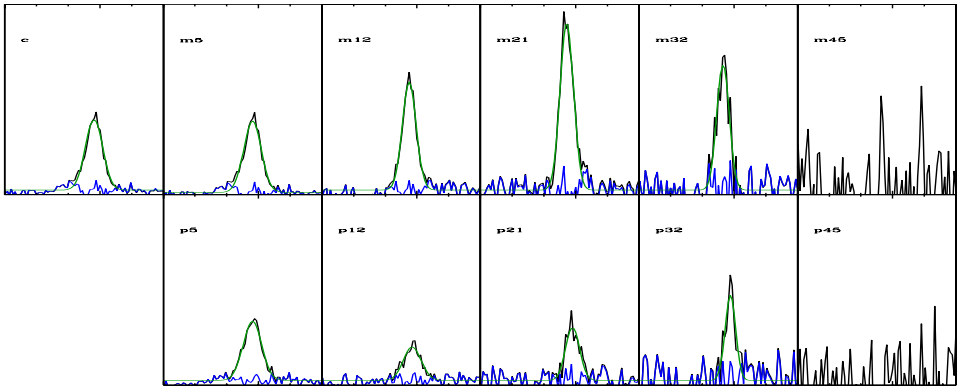

Figure B.22: SG-Object 31 [H]

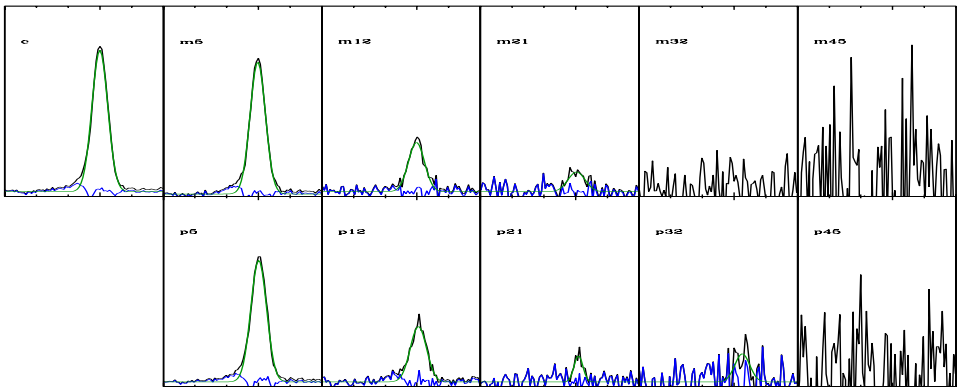

Figure B.23: SG-Object 32

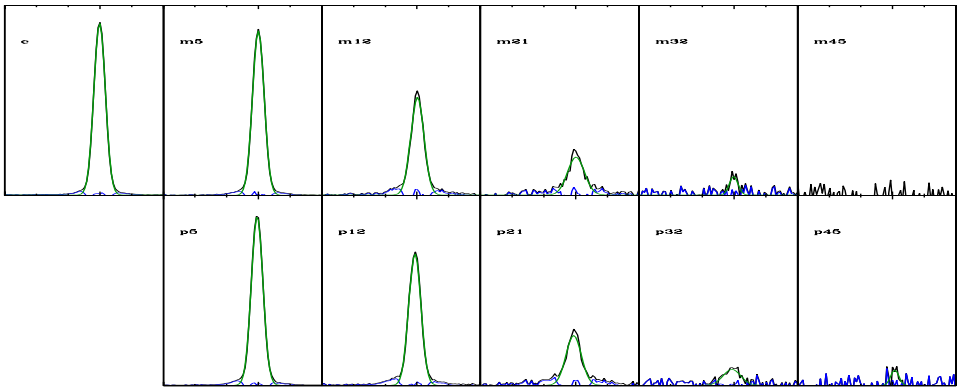

Figure B.24: SG-Object 33 [X]

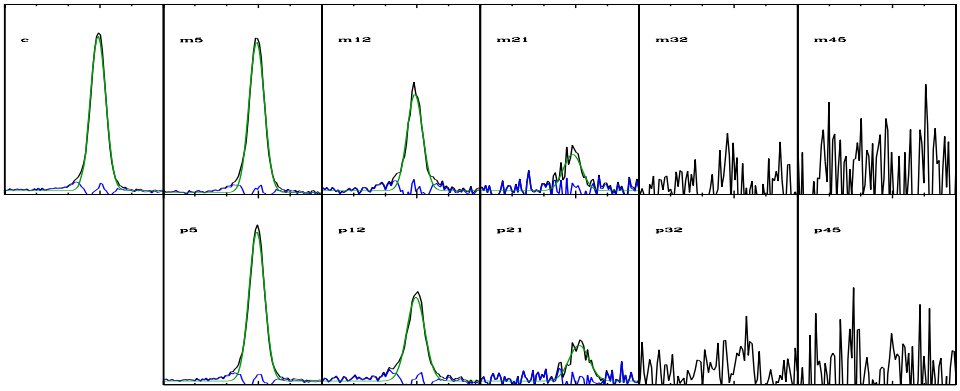

Figure B.25: SG-Object 34

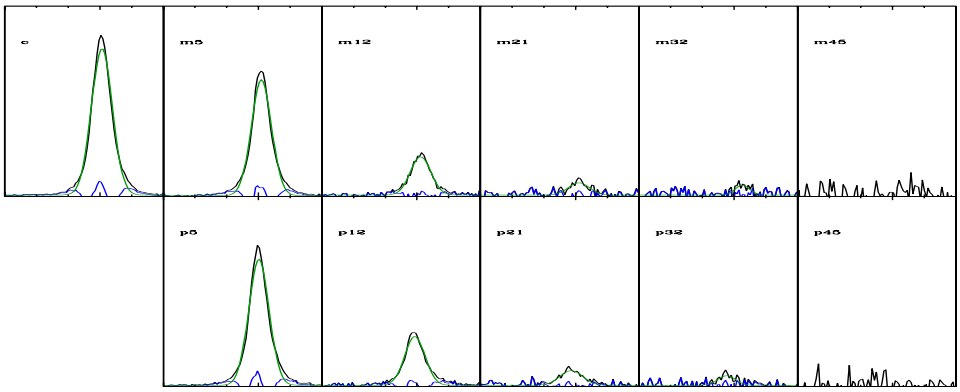

Figure B.26: SG-Object 35

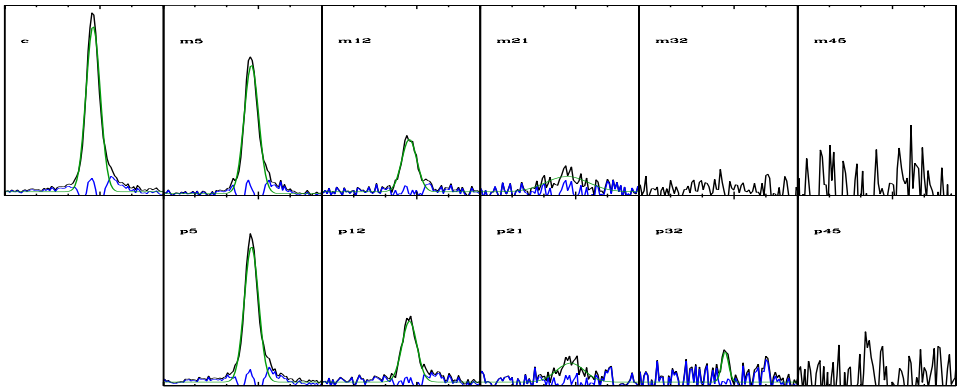

Figure B.27: SG-Object 36

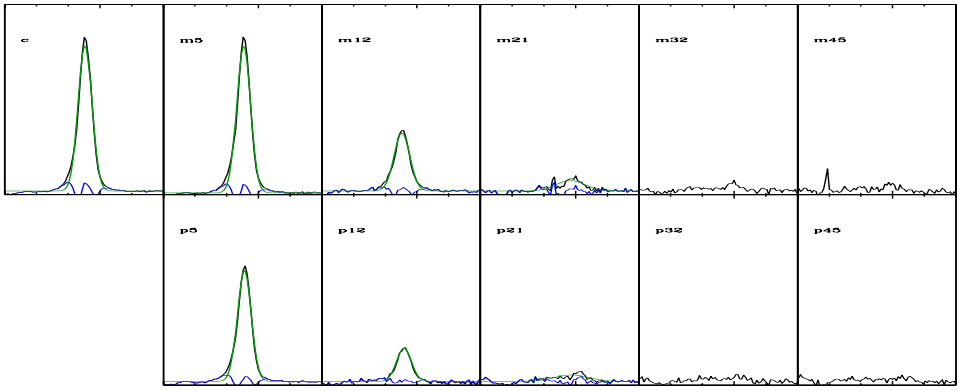

Figure B.28: SG-Object 37 [X]

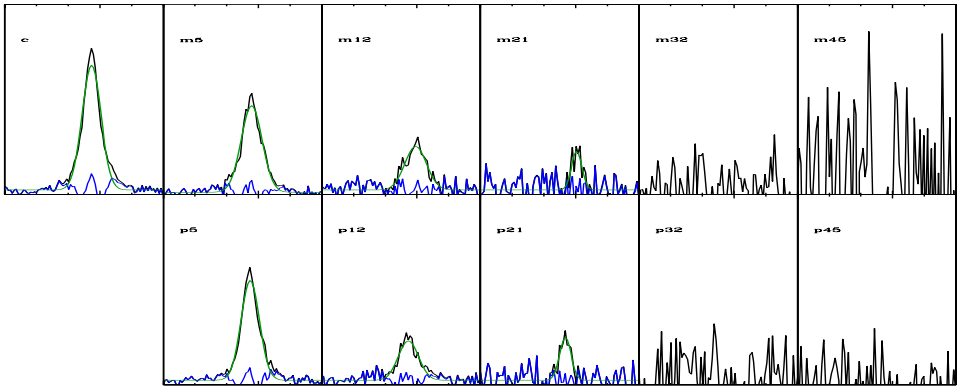

Figure B.29: SG-Object 38

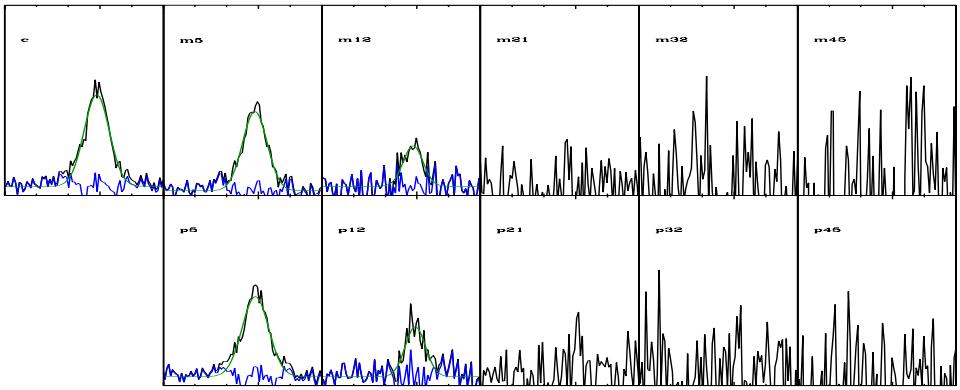

Figure B.30: SG-Object 39

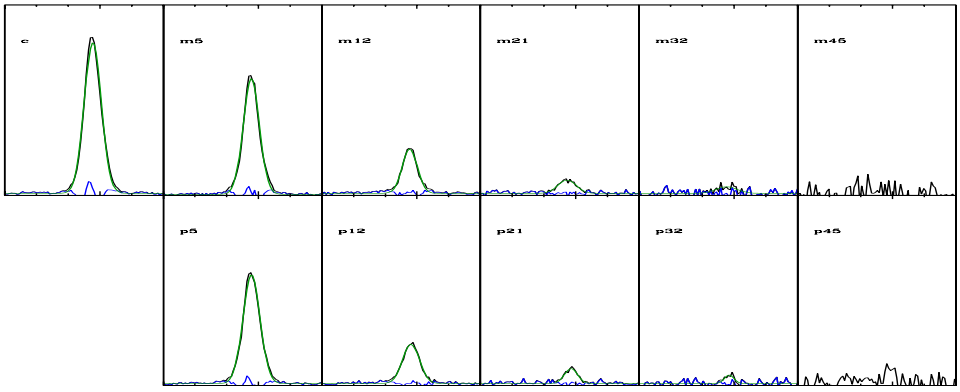

Figure B.31: SG-Object 40

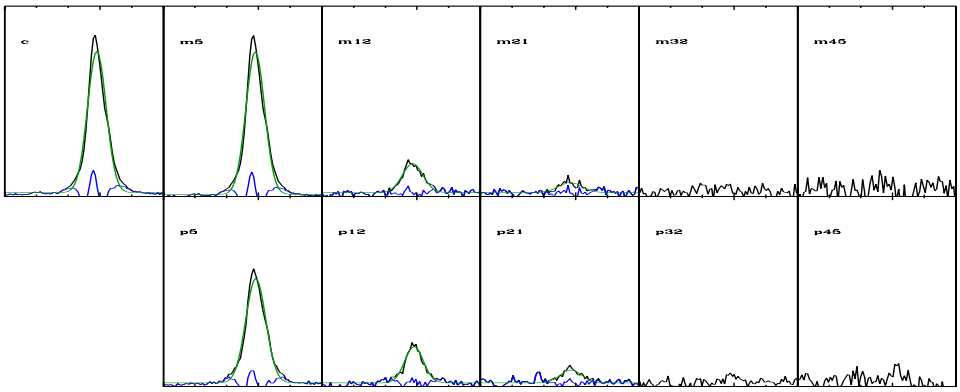

Figure B.32: SG-Object 41

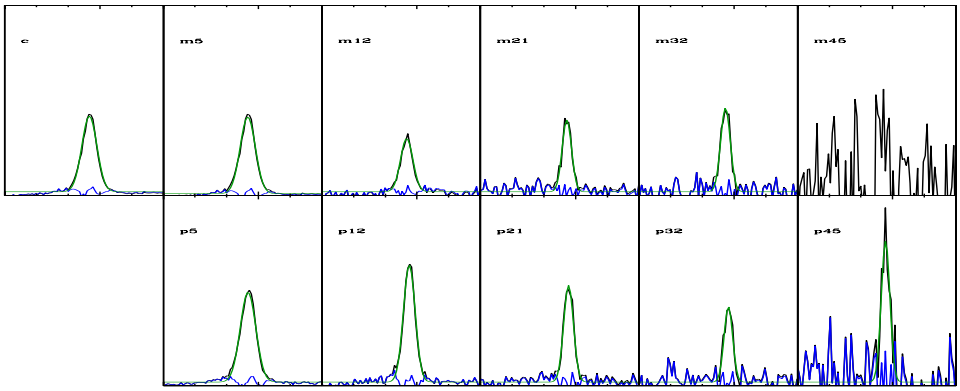

Figure B.33: SG-Object 42 [H]

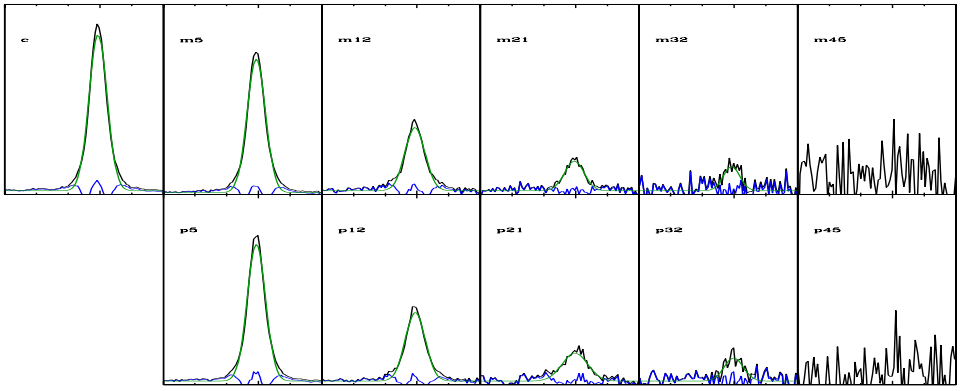

Figure B.34: SG-Object 43

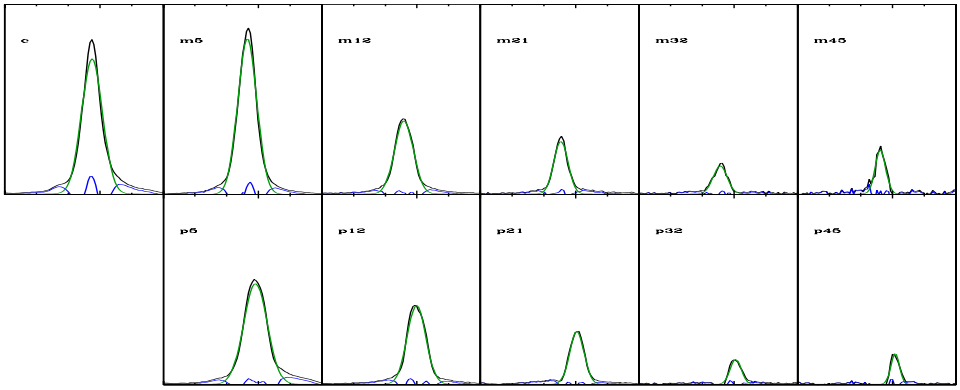

Figure B.35: SG-Object 44

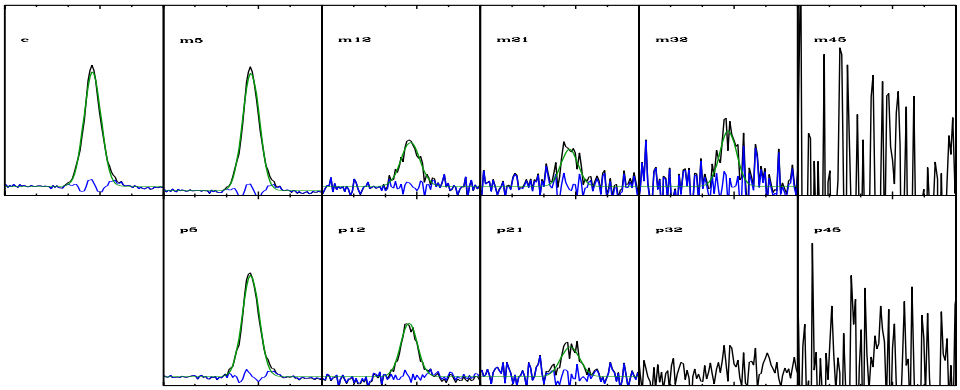

Figure B.36: SG-Object 45

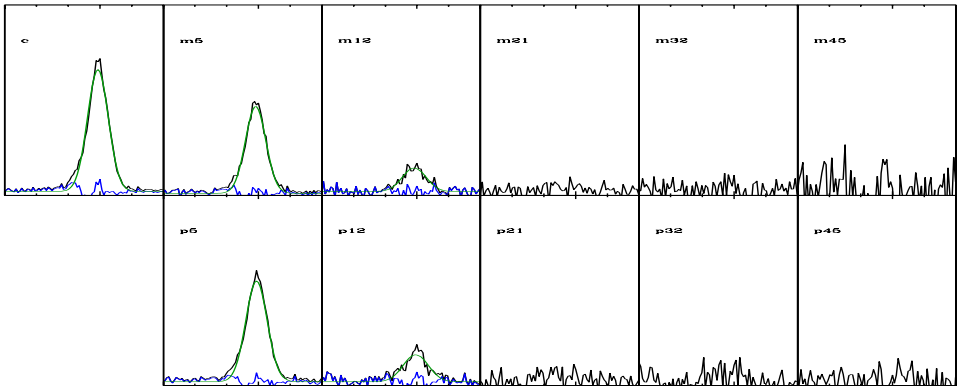

Figure B.37: SG-Object 46

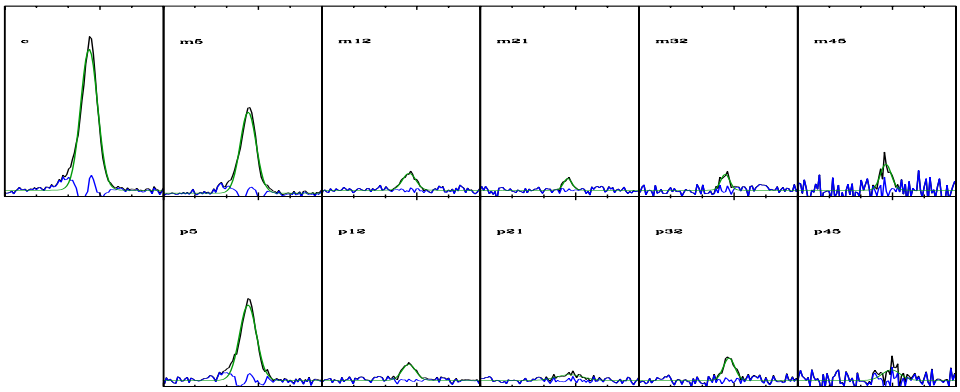

Figure B.38: SG-Object 47

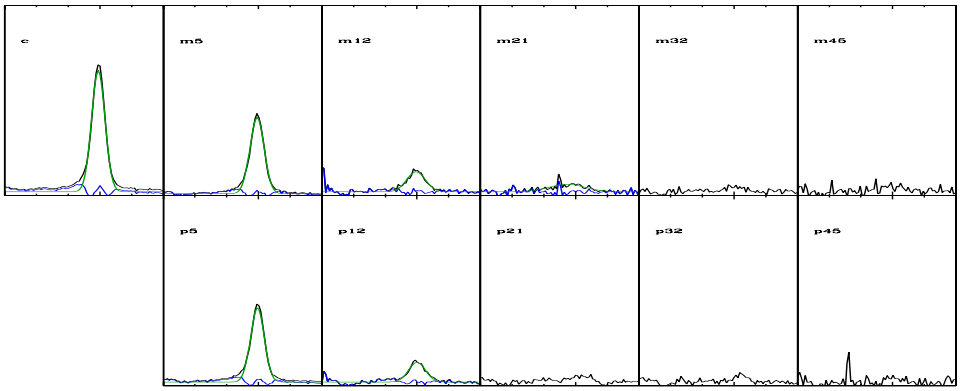

Figure B.39: SG-Object 48 [X]

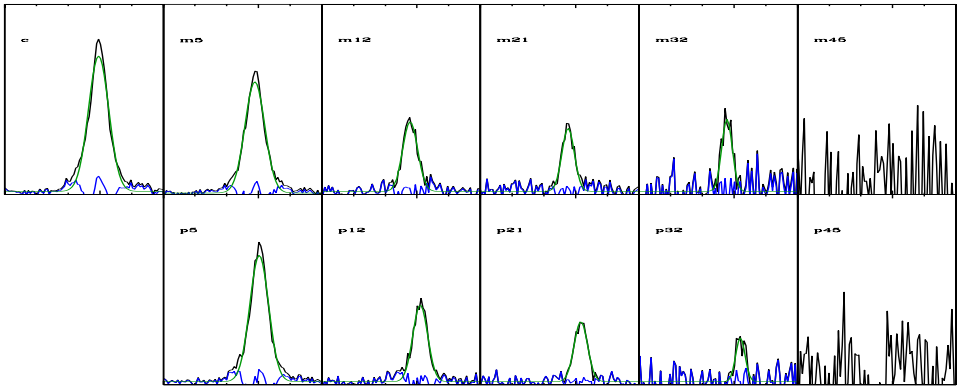

Figure B.40: SG-Object 49

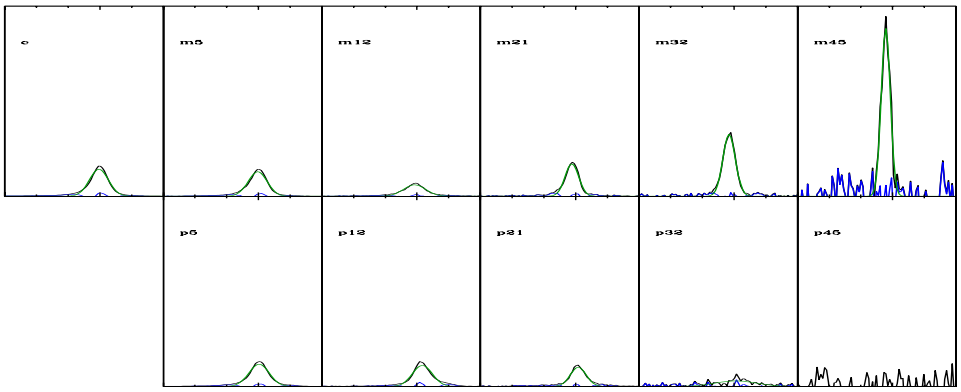

Figure B.41: SG-Object 50 [X,H]

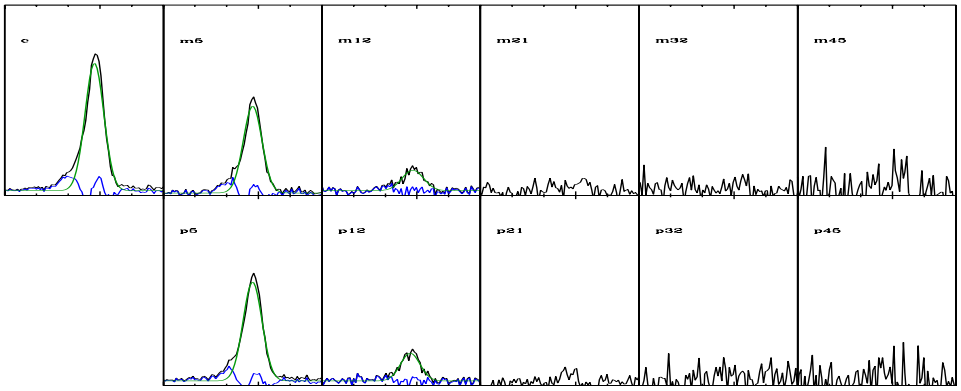

Figure B.42: SG-Object 51

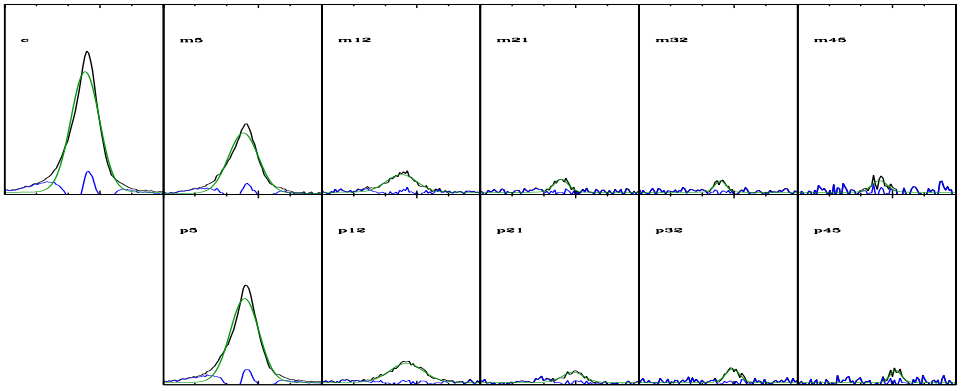

Figure B.43: SG-Object 52

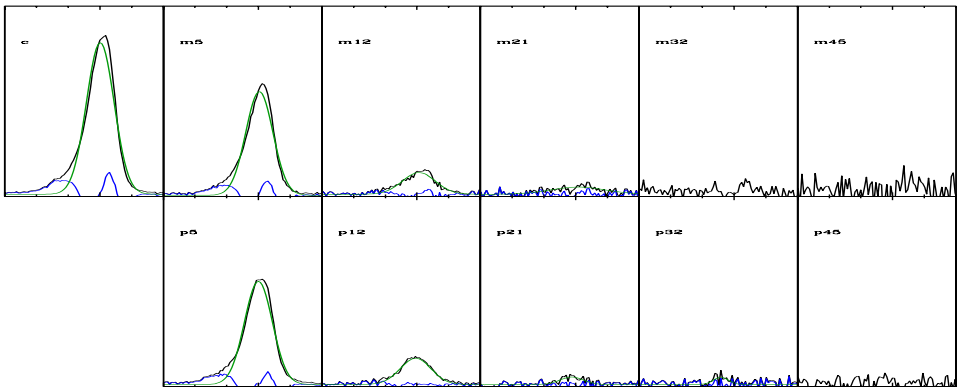

Figure B.44: SG-Object 53

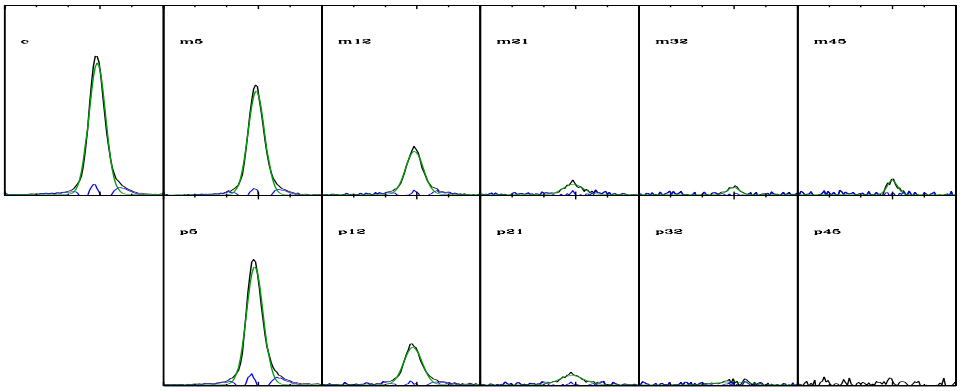

Figure B.45: SG-Object 54

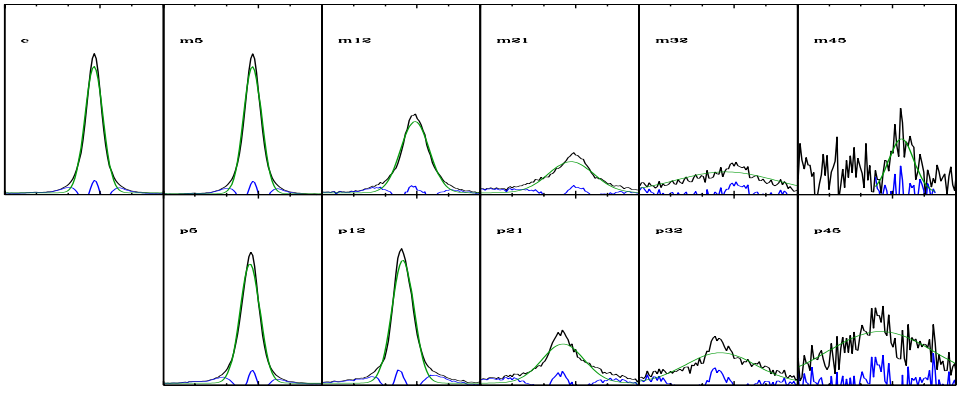

Figure B.46: SG-Object 56 X,[B]

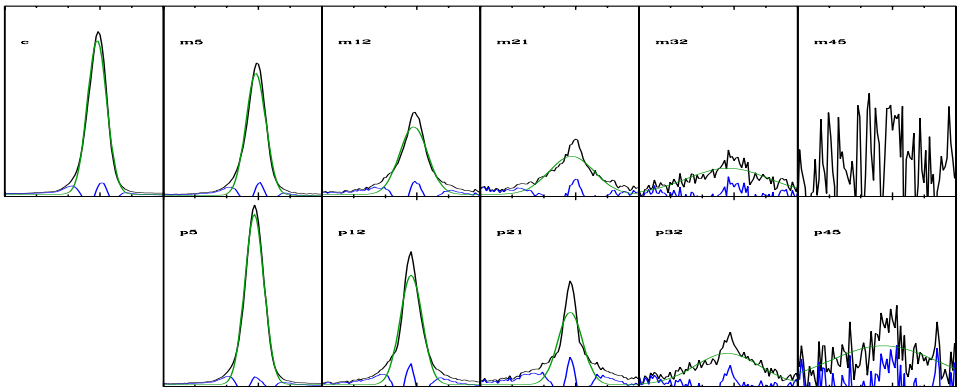

Figure B.47: SG-Object 57

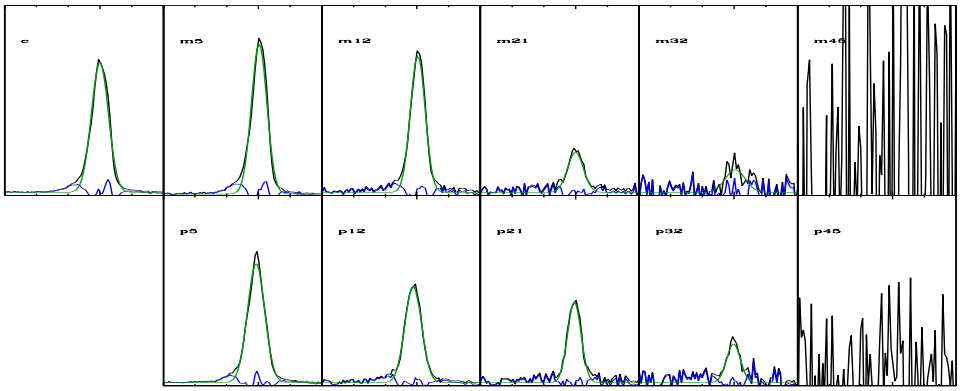

Figure B.48: SG-Object 58

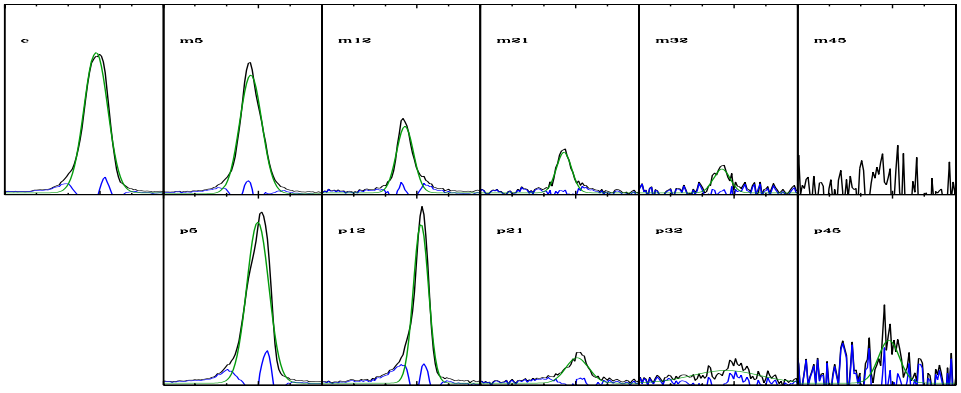

Figure B.49: SG-Object 59 [*]

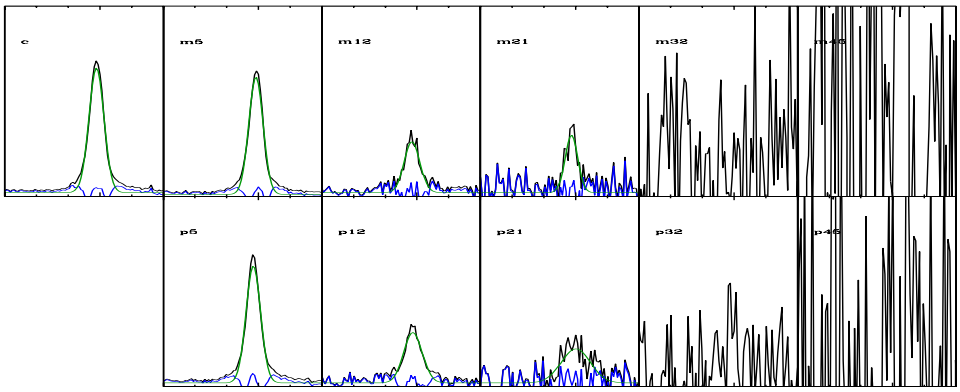

Figure B.50: SG-Object 60 [X]

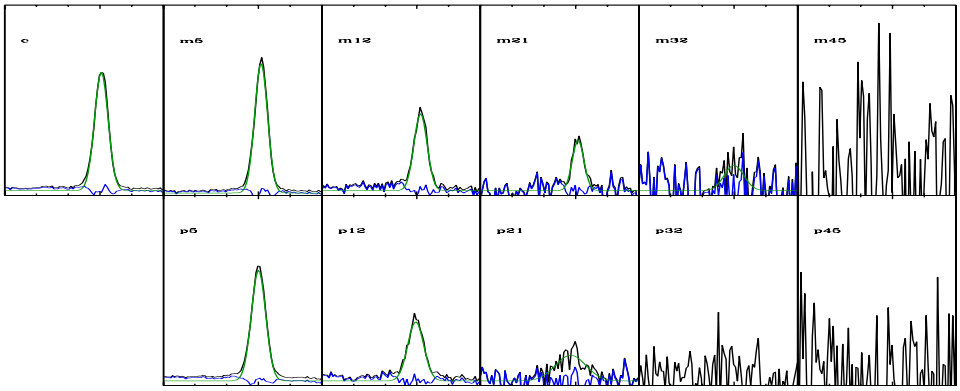

Figure B.51: SG-Object 61

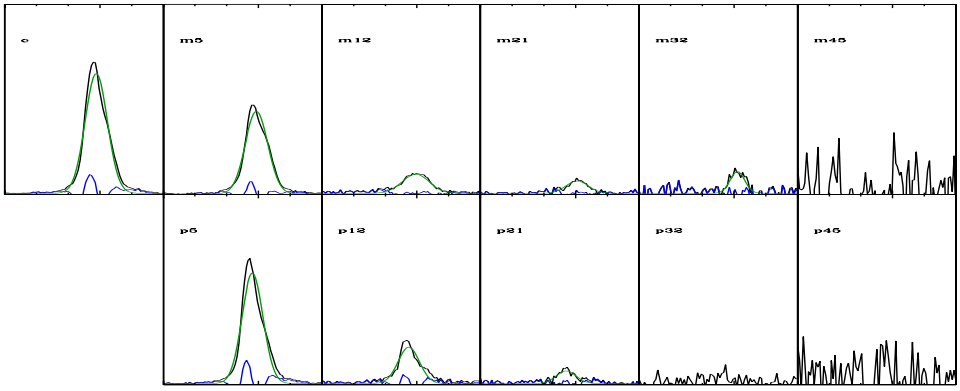

Figure B.52: SG-Object 62

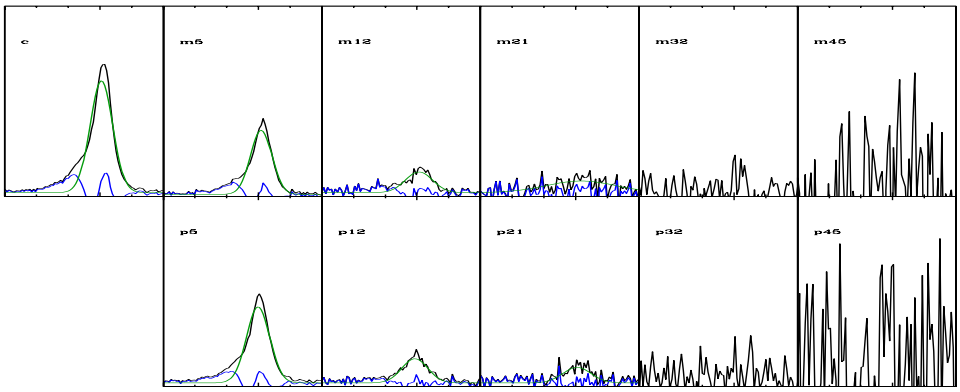

Figure B.53: SG-Object 63

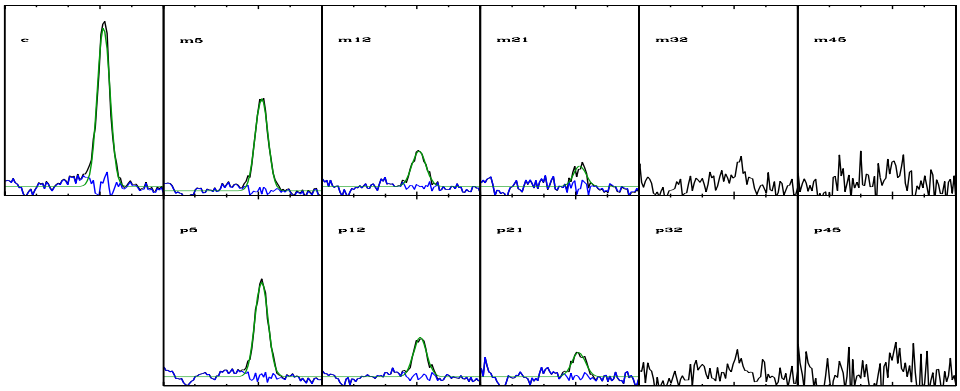

Figure B.54: SG-Object 64 [X]

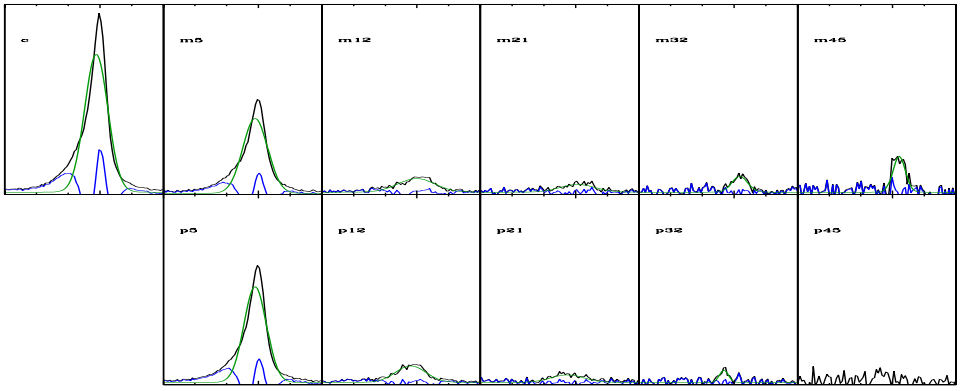

Figure B.55: SG-Object 70

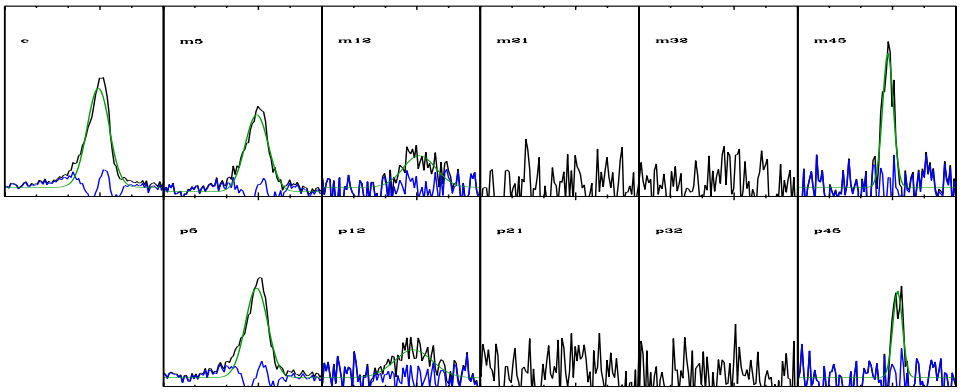

Figure B.56: SG-Object 71 [H]

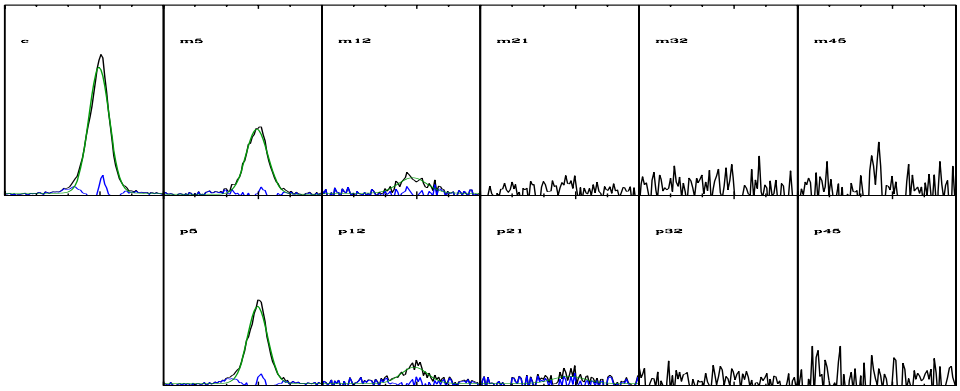

Figure B.57: SG-Object 73

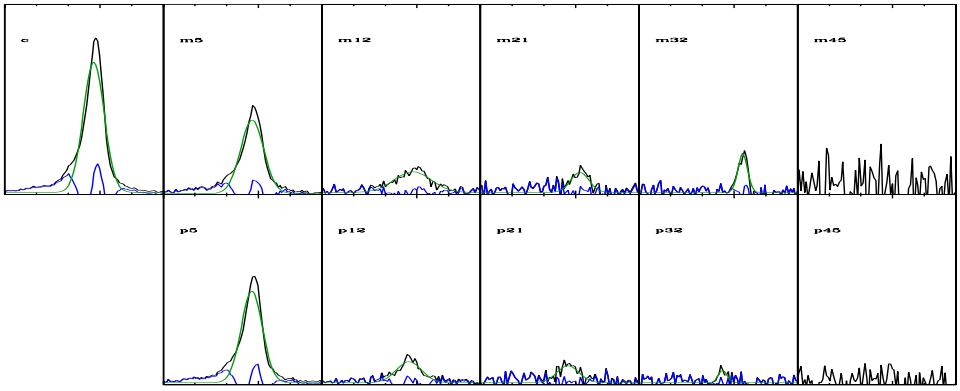

Figure B.58: SG-Object 74

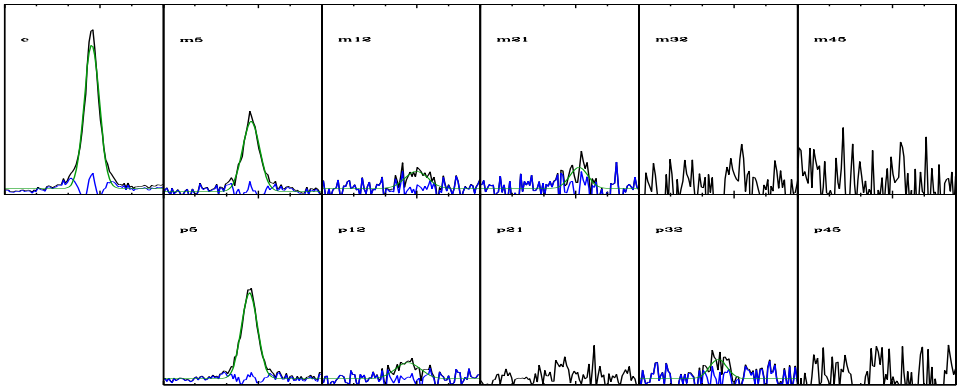

Figure B.59: SG-Object 76

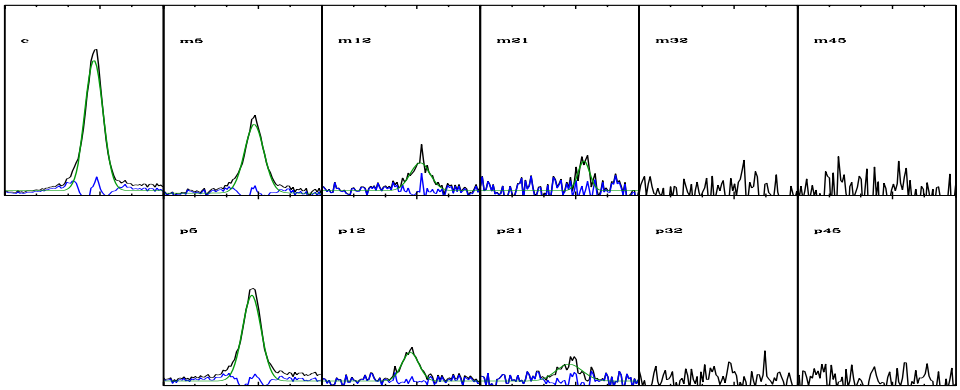

Figure B.60: SG-Object 77

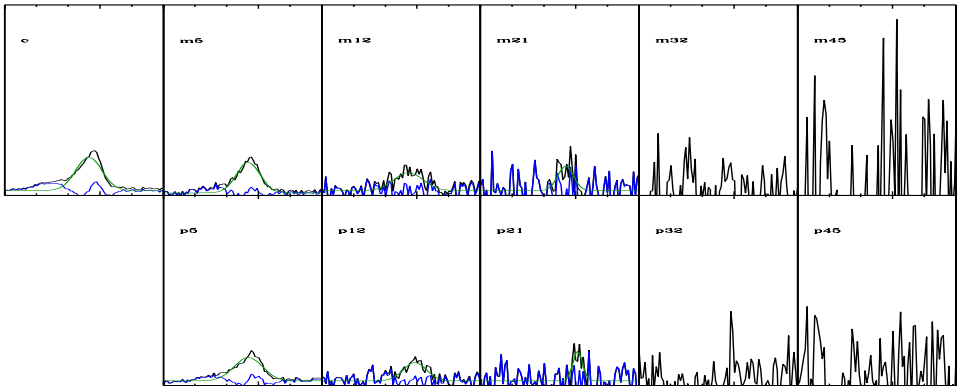

Figure B.61: SG-Object 78

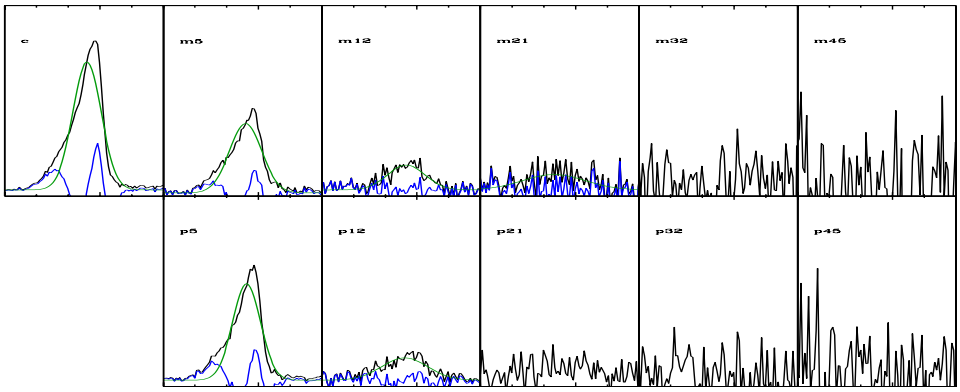

Figure B.62: SG-Object 79

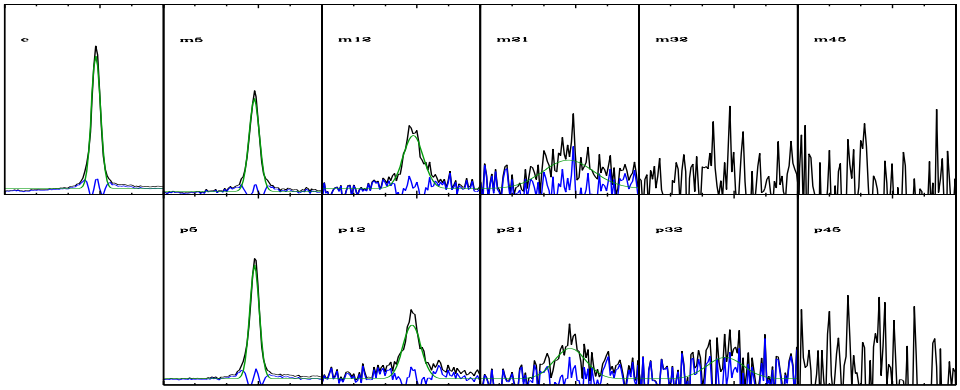

Figure B.63: SG-Object 80 [X]

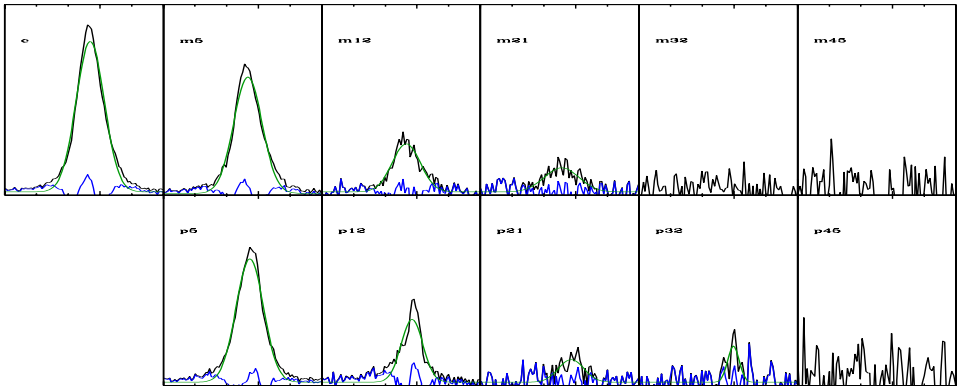

Figure B.64: SG-Object 81 [X]

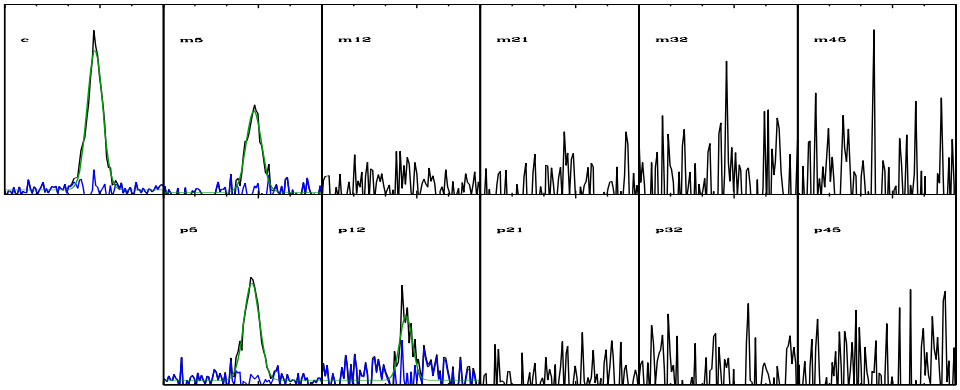

Figure B.65: SG-Object 82

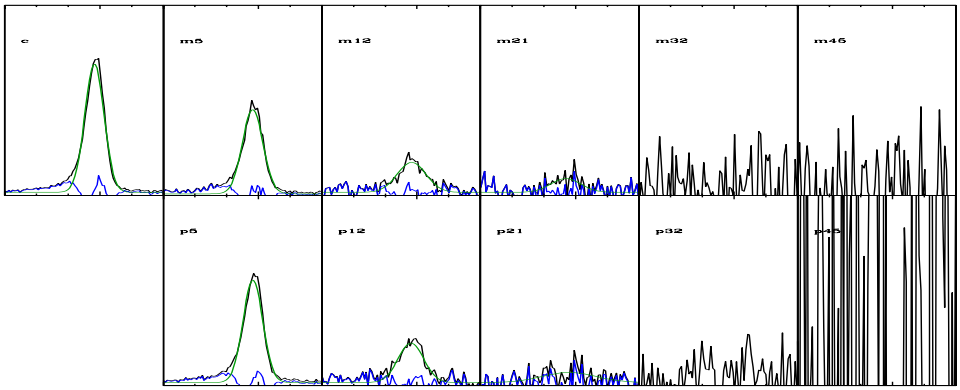

Figure B.66: SG-Object 83

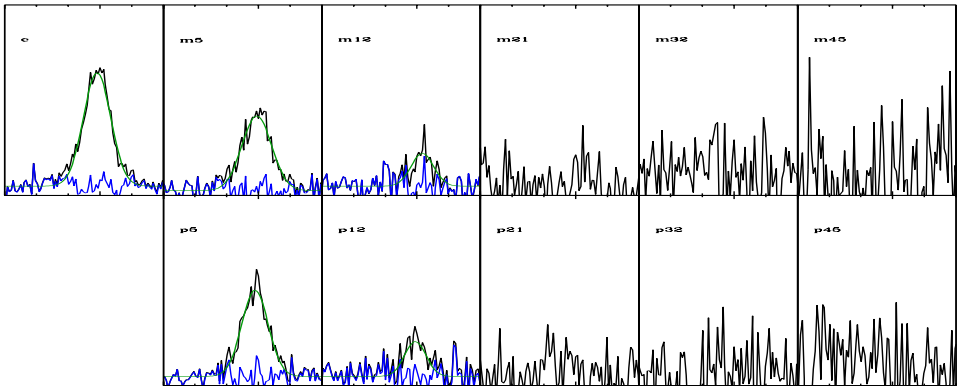

Figure B.67: SG-Object 88

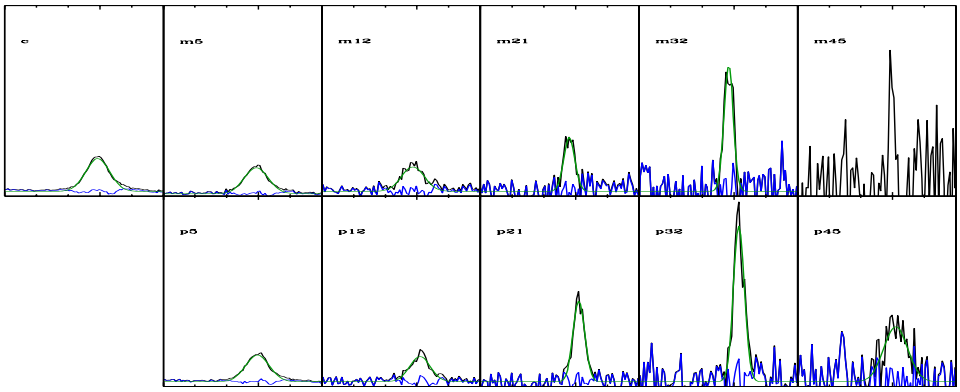

Figure B.68: SG-Object 91

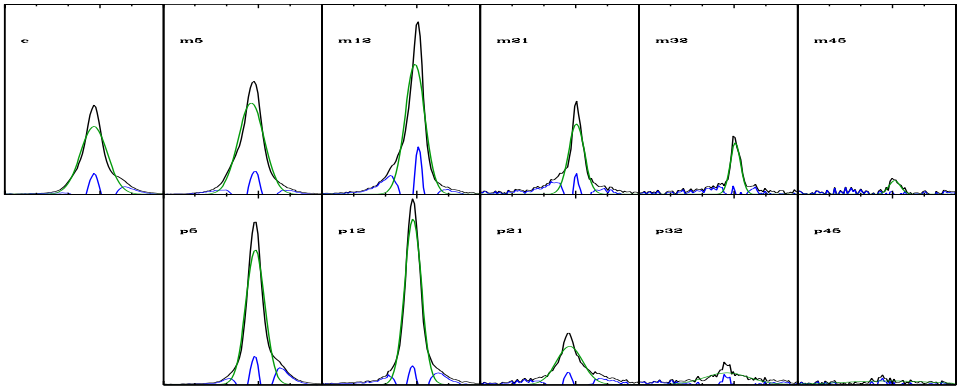

Figure B.69: SG-Object 96 [X,*]

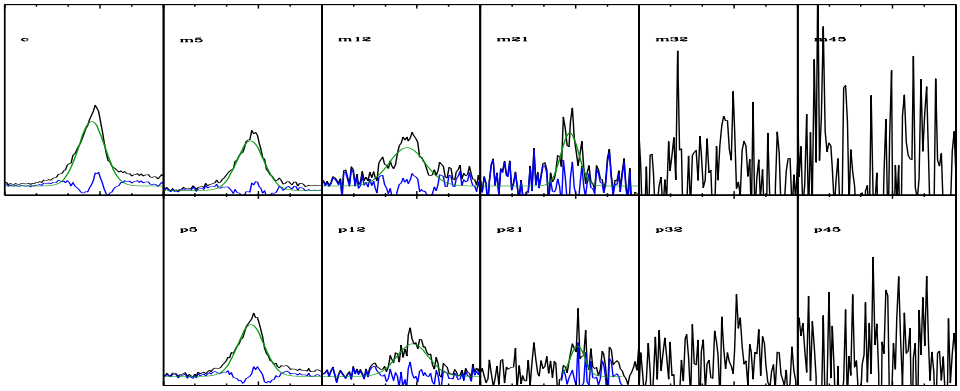

Figure B.70: SG-Object 99 [*]

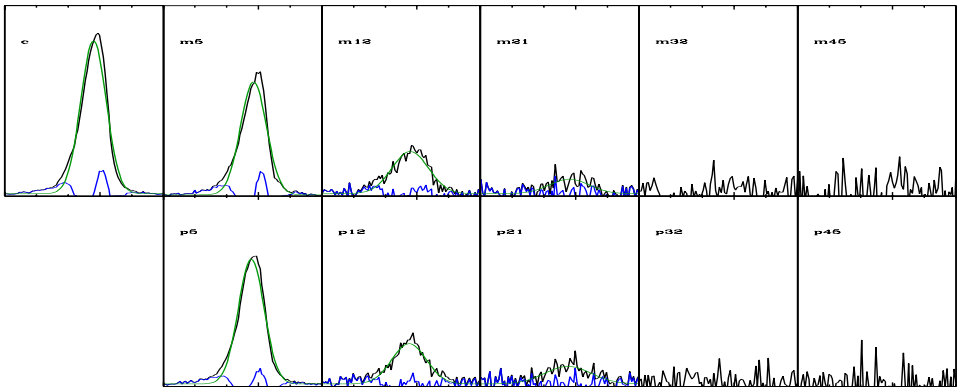

Figure B.71: SG-Object 100 [X]

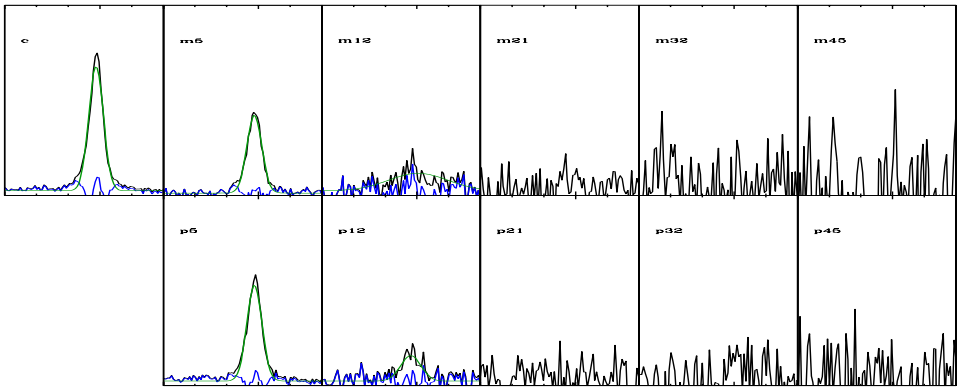

Figure B.72: SG-Object 102

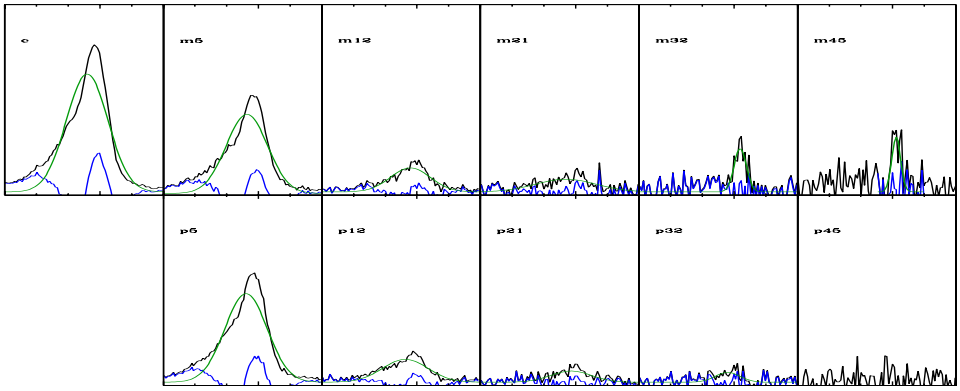

Figure B.73: SG-Object 103 [H]

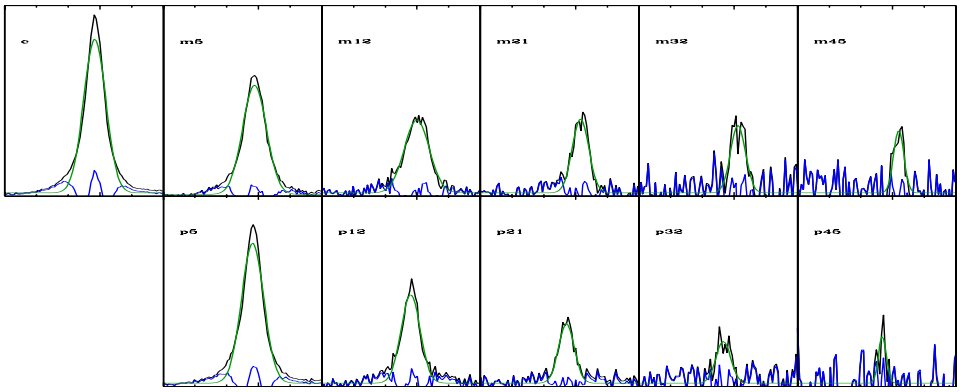

Figure B.74: SG-Object 106

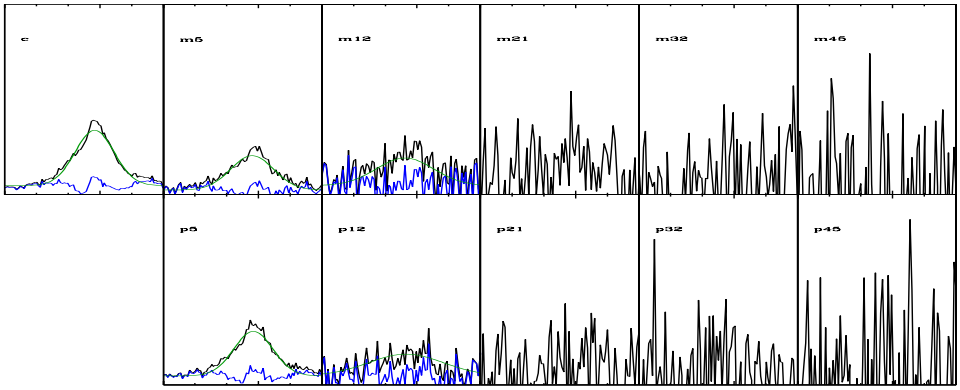

Figure B.75: SG-Object 108 [X,B]

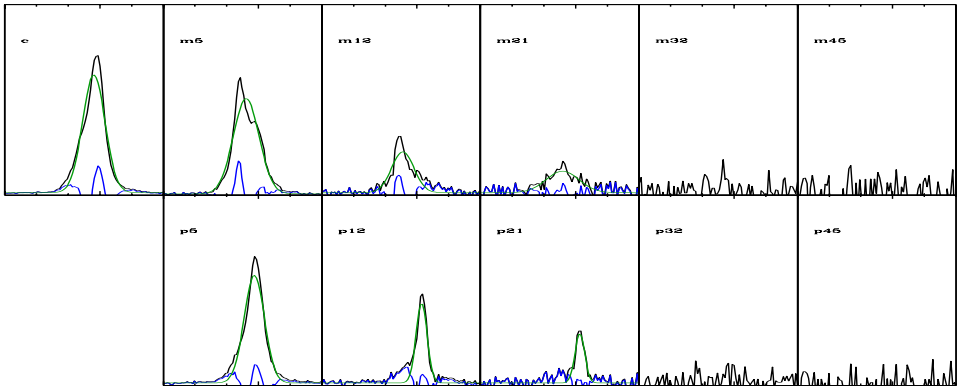

Figure B.76: SG-Object 109 [*]

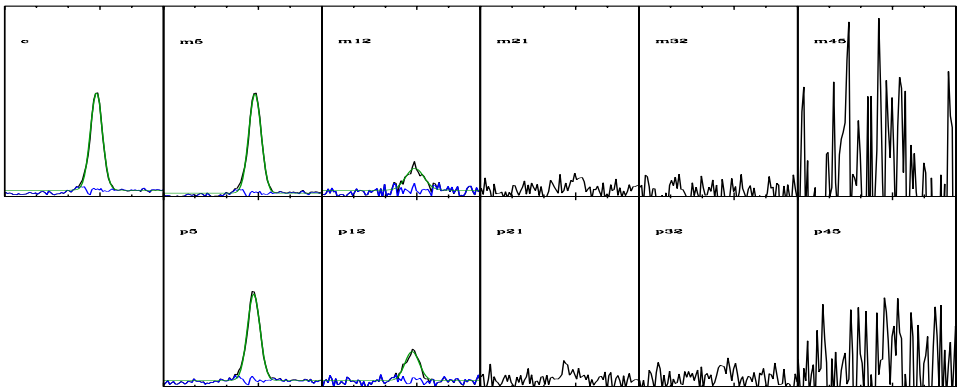

Figure B.77: SG-Object 114

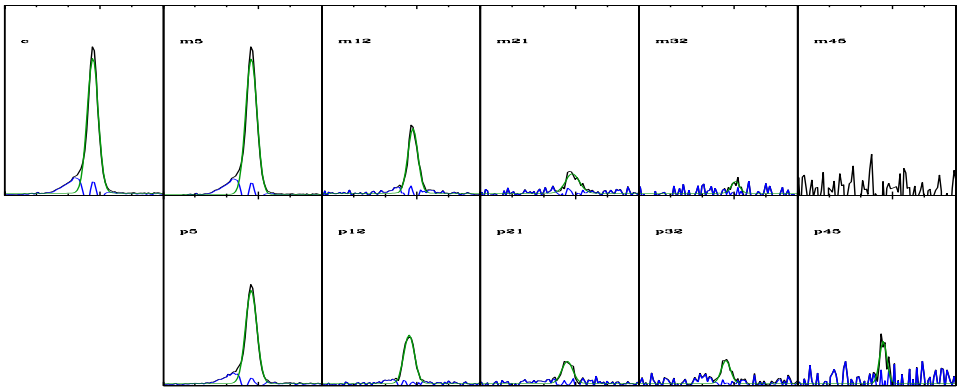

Figure B.78: SG-Object 126

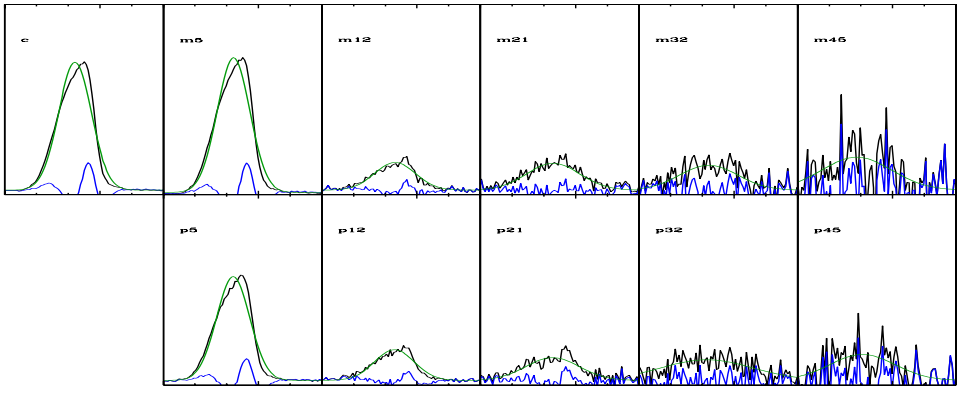

Figure B.79: SG-Object 130 [X,*]

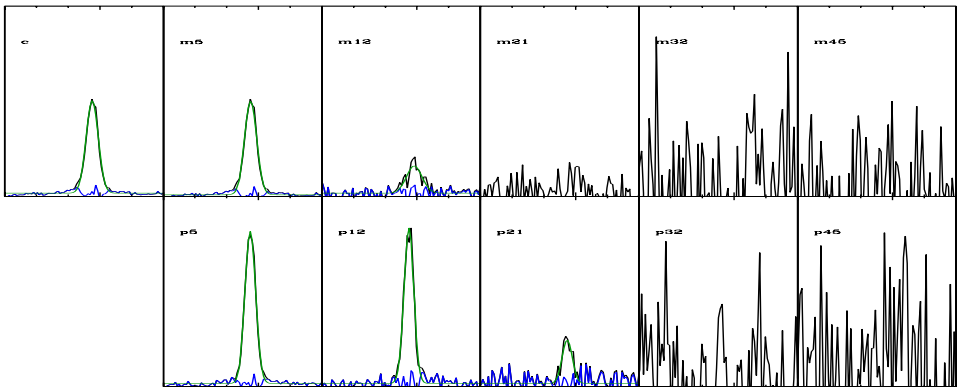

Figure B.80: SG-Object 138

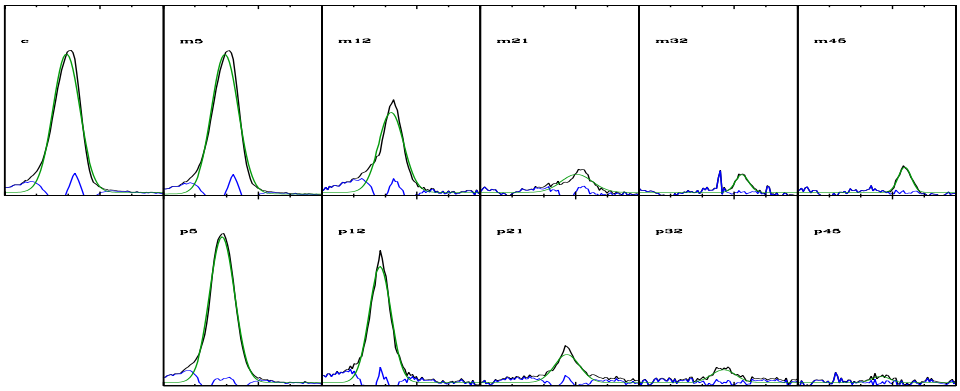

Figure B.81: SG-Object 143 [X,*]

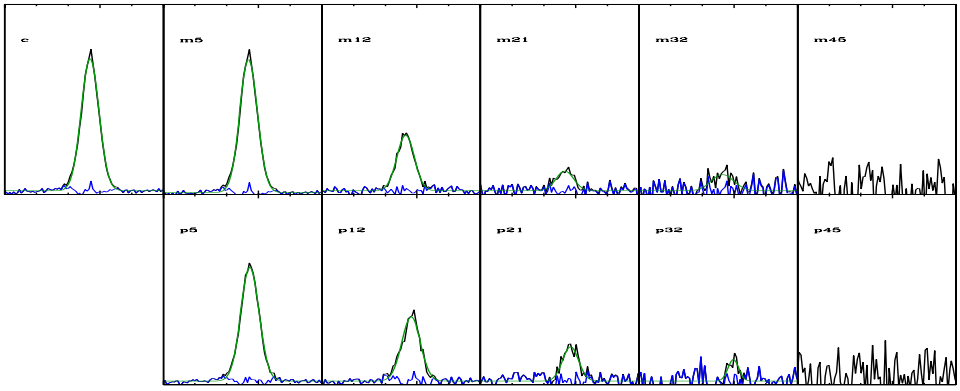

Figure B.82: SG-Object 155

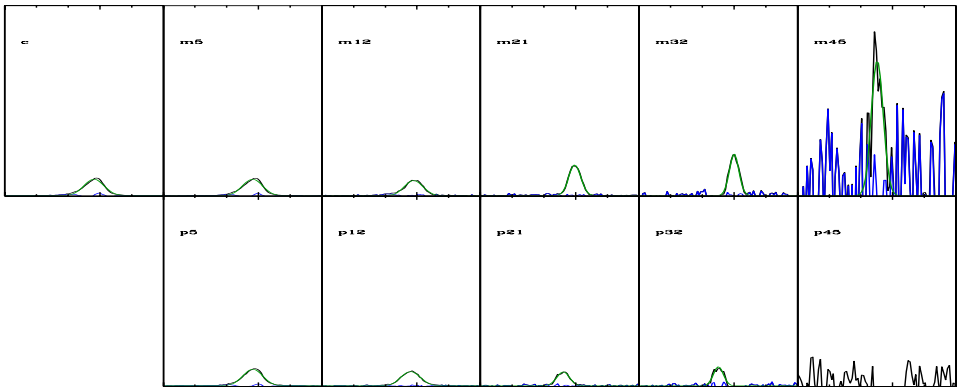

Figure B.83: SG-Object 156 [H]

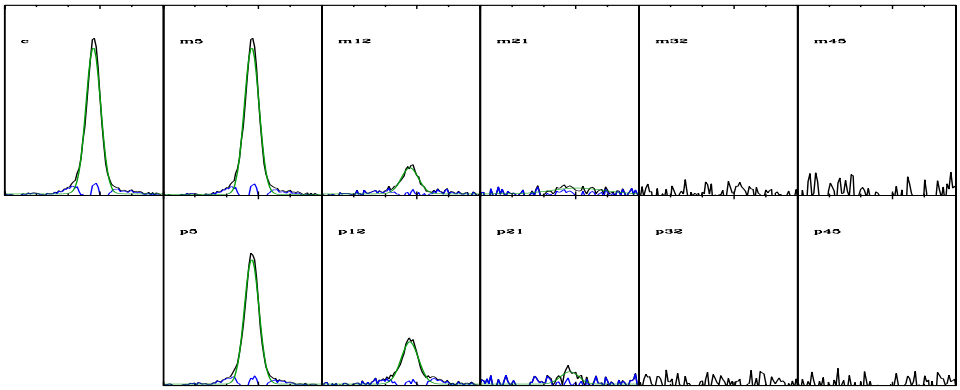

Figure B.84: SG-Object 157 [X]

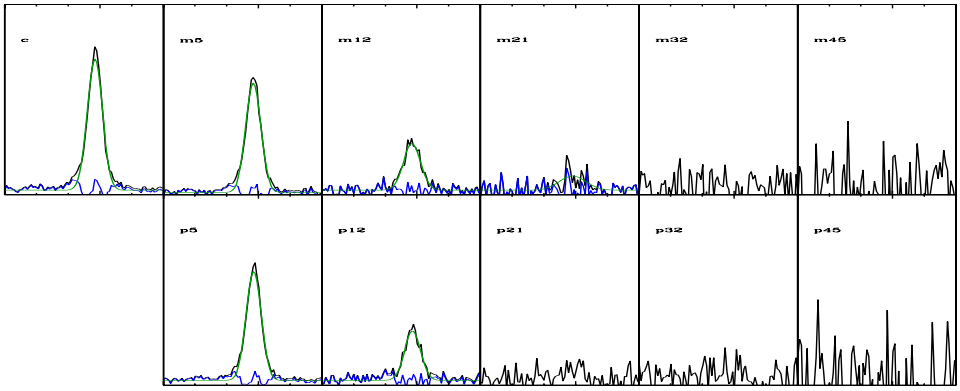

Figure B.85: SG-Object 162

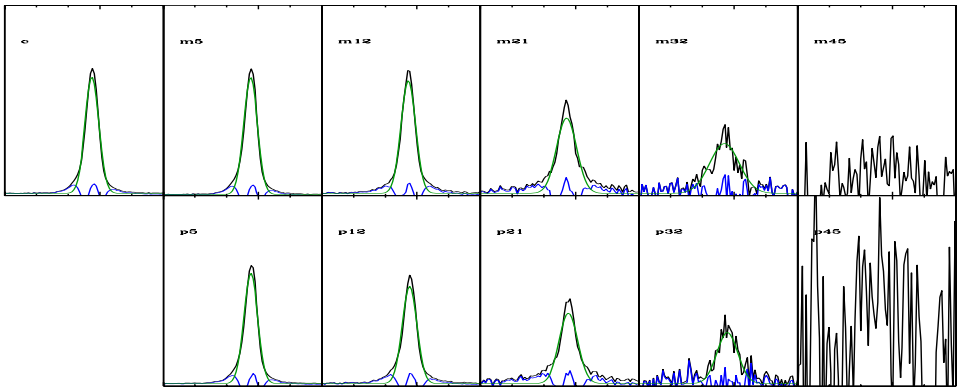

Figure B.86: SG-Object 174 [X]

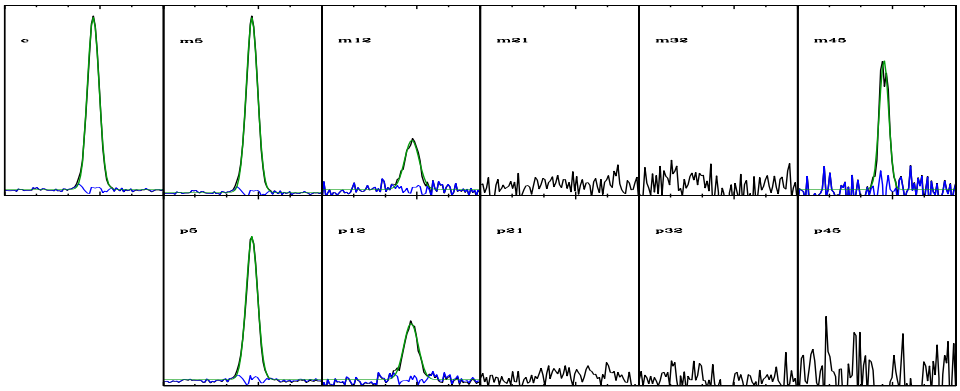

Figure B.87: SG-Object 177 [H]

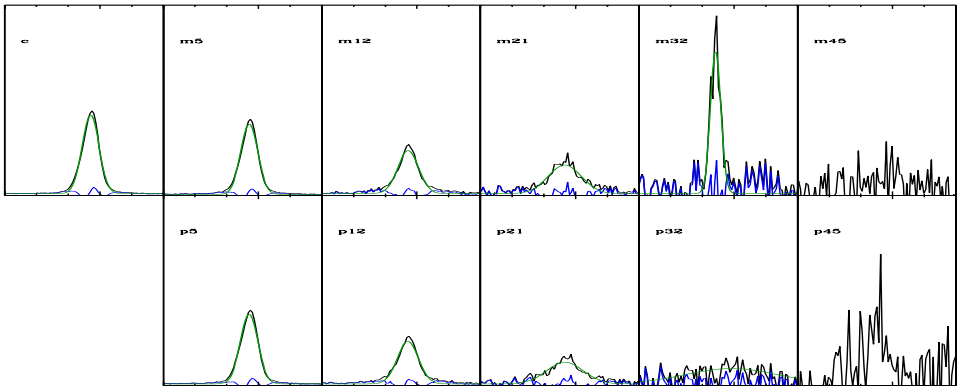

Figure B.88: SG-Object 180 [H]

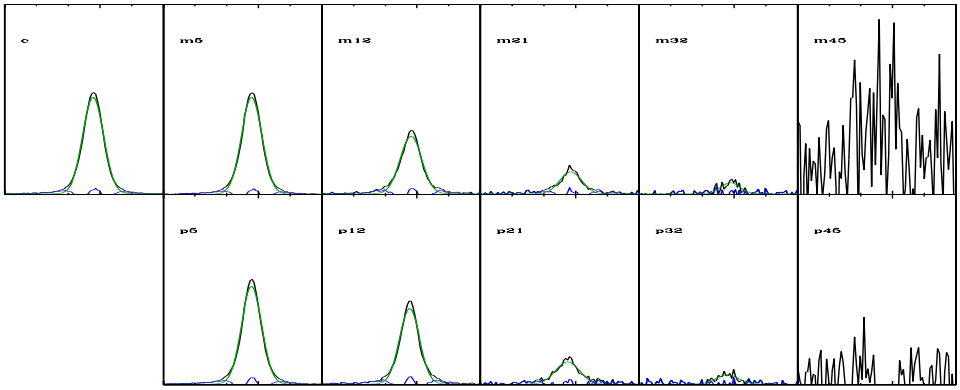

Figure B.89: SG-Object 187

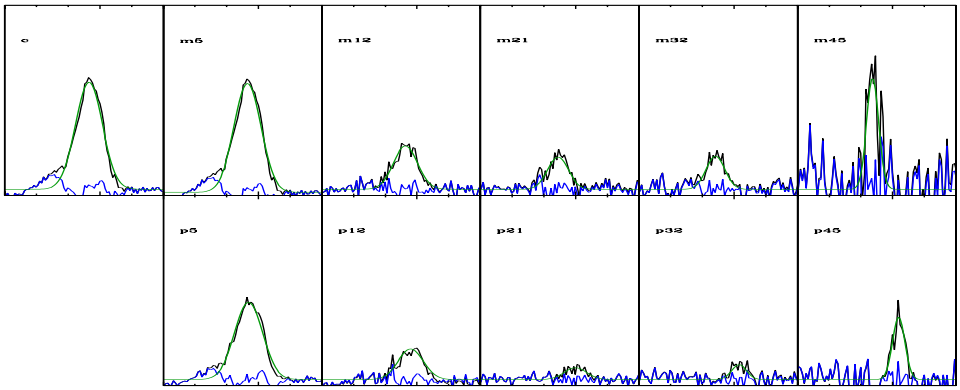

Figure B.90: SG-Object 196

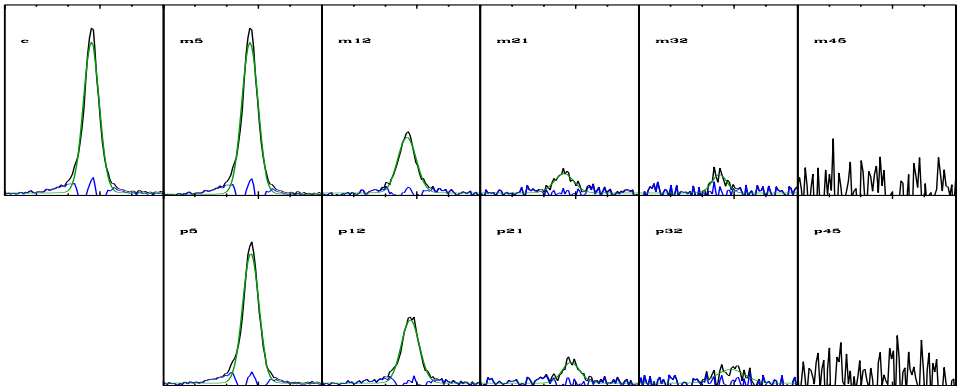

Figure B.91: SG-Object 197

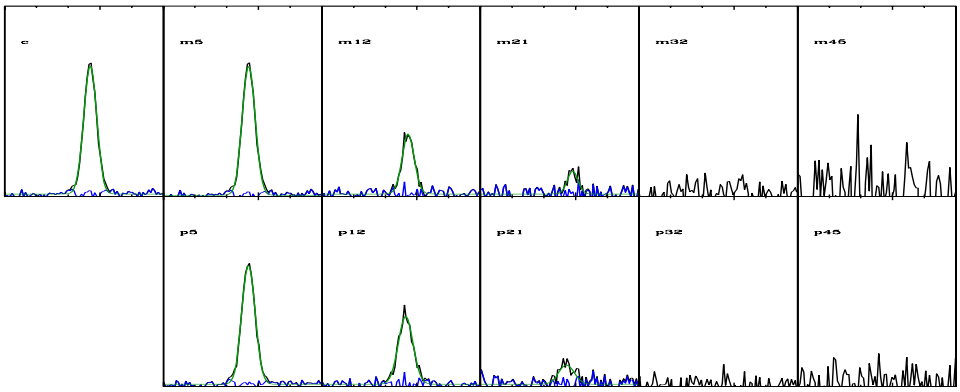

Figure B.92: SG-Object 202

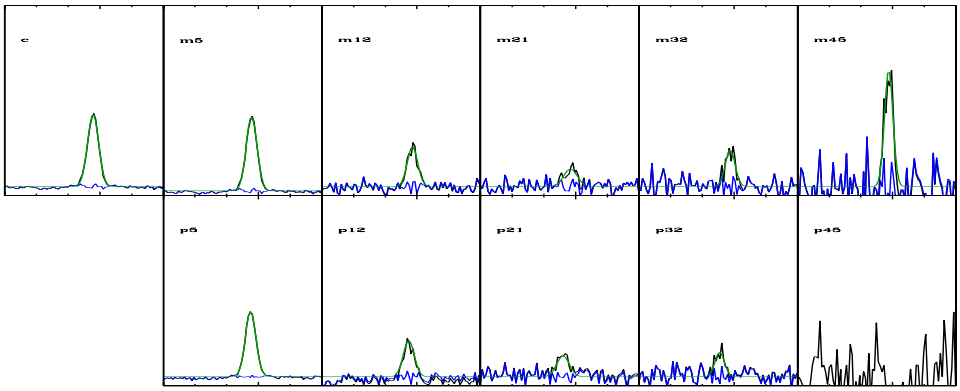

Figure B.93: SG-Object 204 [H]

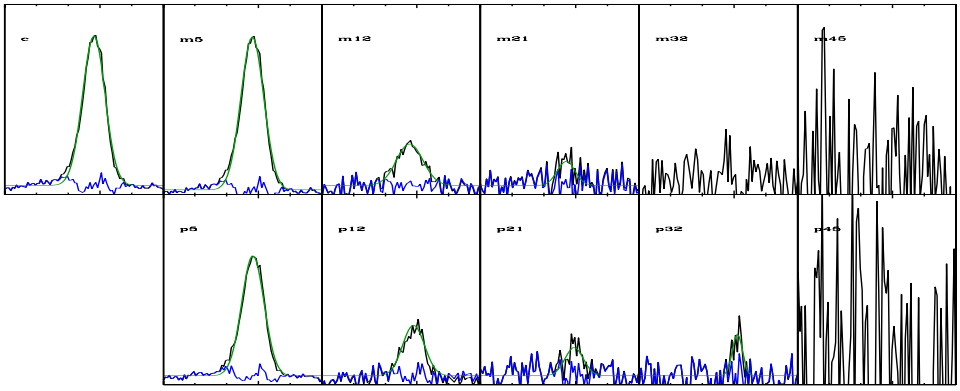

Figure B.94: SG-Object 205

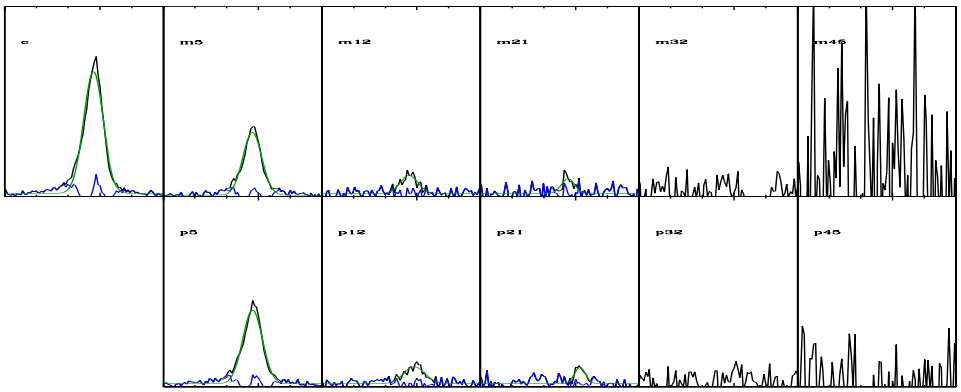

Figure B.95: SG-Object 207

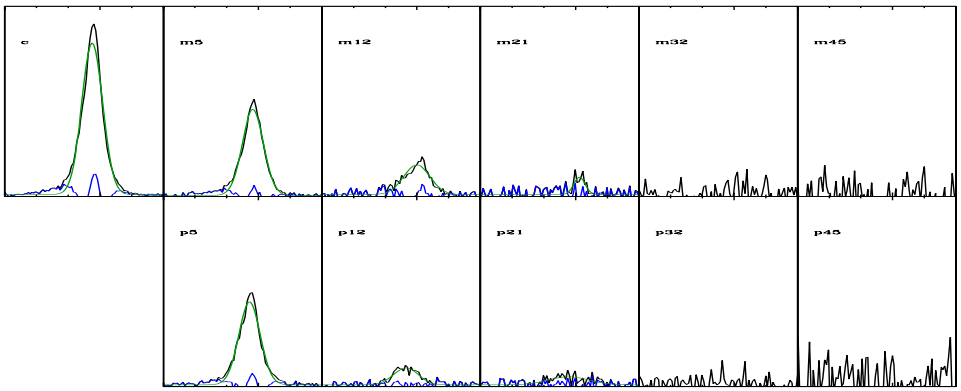

Figure B.96: SG-Object 208

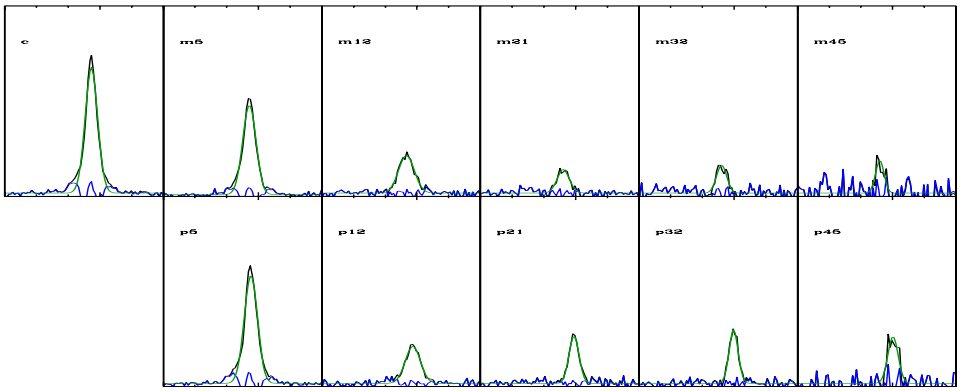

Figure B.97: SG-Object 209

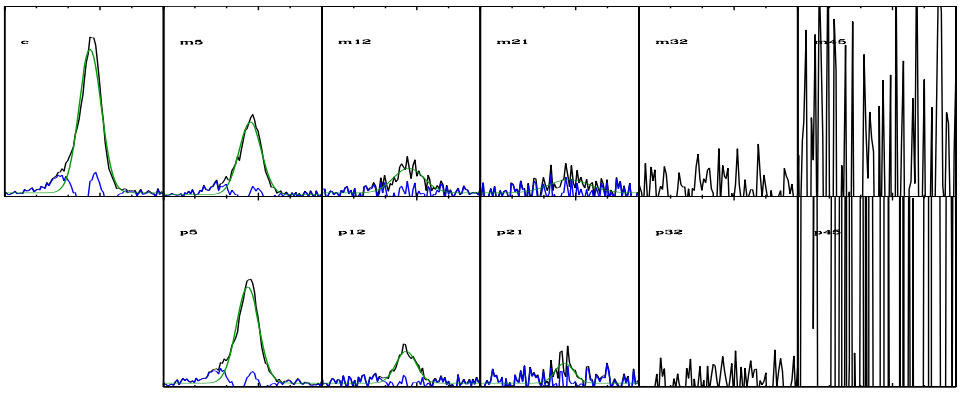

Figure B.98: SG-Object 210

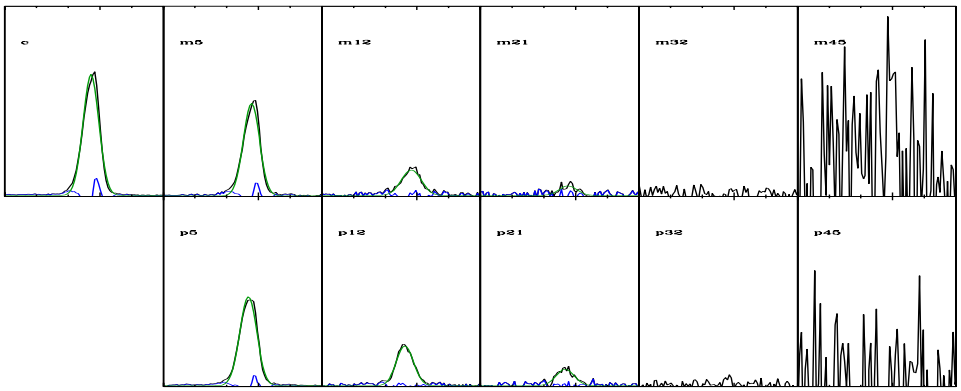

Figure B.99: SG-Object 213

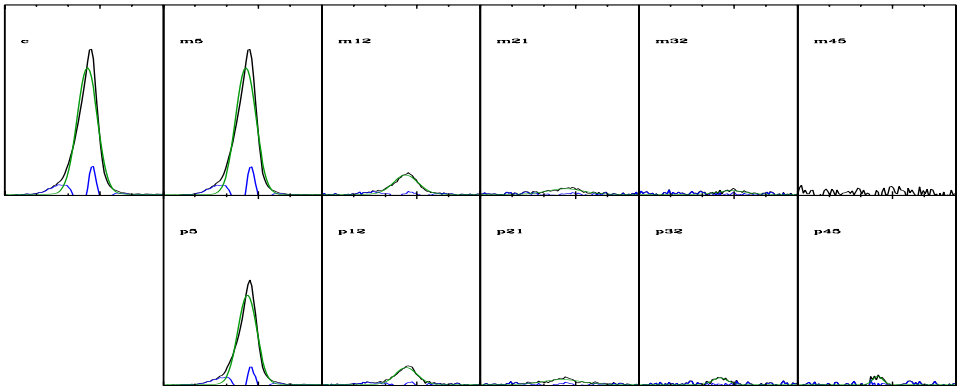

Figure B.100: SG-Object 214

B.2 Double Gaussian Fits

The following are the double Gaussian fits collected for this study. Note that the goal of these fits was to collect a double Gaussian whenever possible; some are not considered realistic. The green profiles are the main Gaussian fits, the purple profiles are the secondary Gaussian fits to the asymmetries, the red profiles are the total fits from both Gaussian fits, and the blue lines are the residuals. The main Gaussian fit was defined as that whose peak aligned with the peak of the entire [OIII] profile.

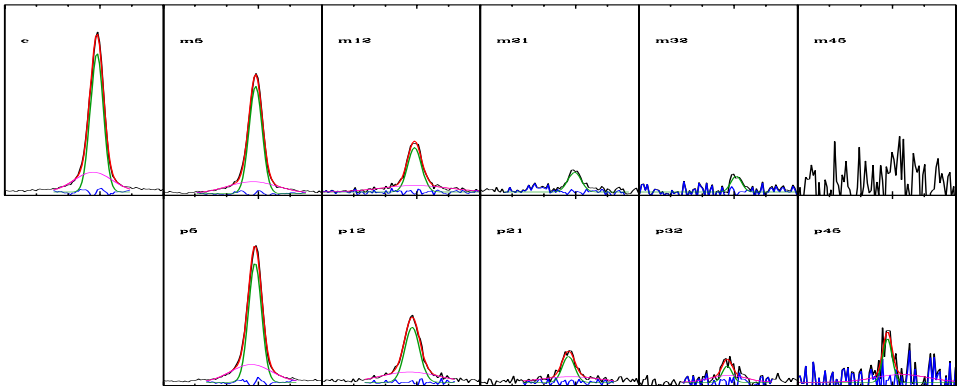

Figure B.101: DG-Object 1 [X]

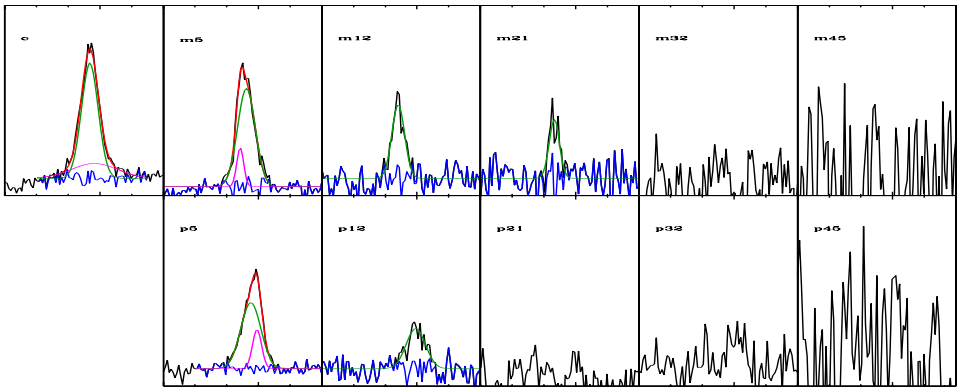

Figure B.102: DG-Object 5 [U]

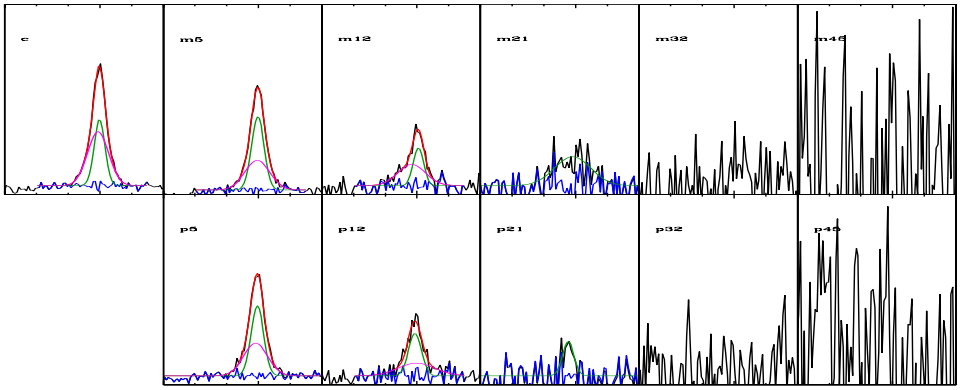

Figure B.103: DG-Object 6

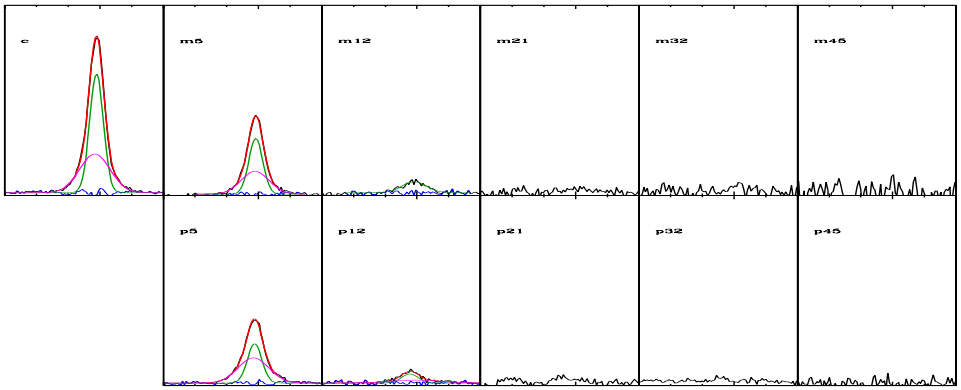

Figure B.104: DG-Object 9

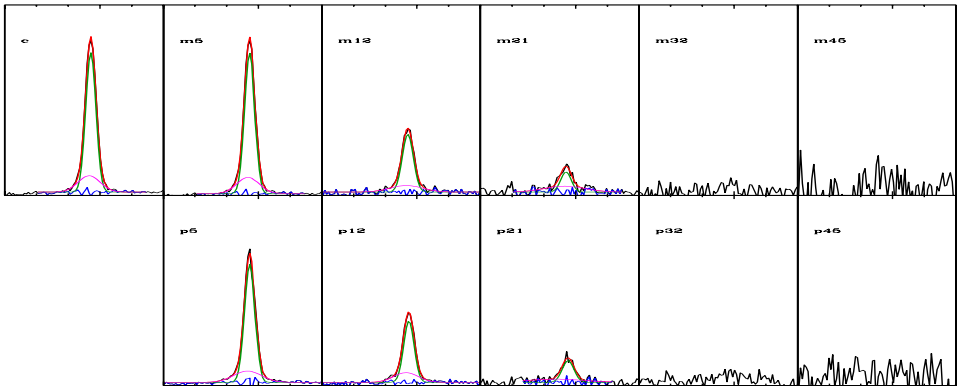

Figure B.105: DG-Object 10

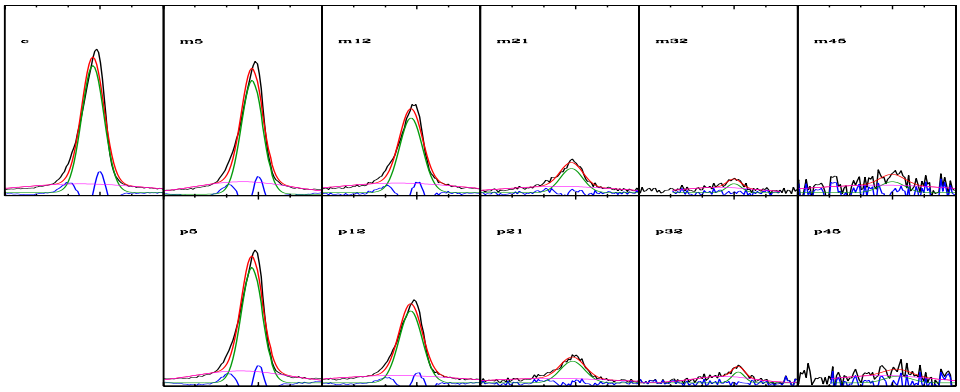

Figure B.106: DG-Object 11 [*]

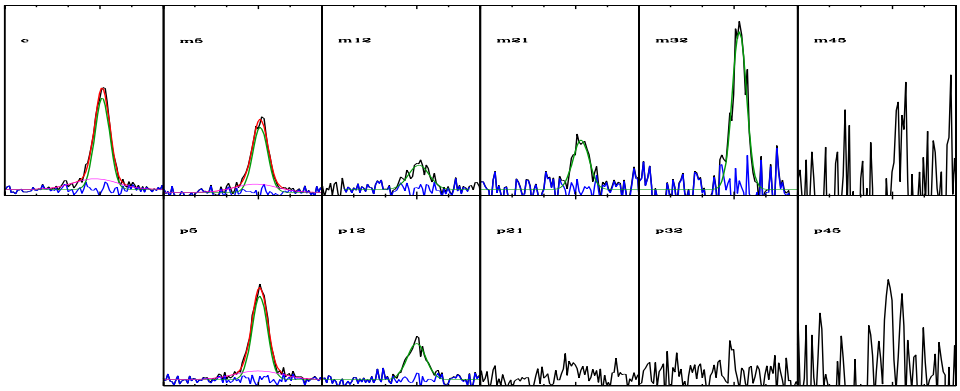

Figure B.107: DG-Object 13 [H]

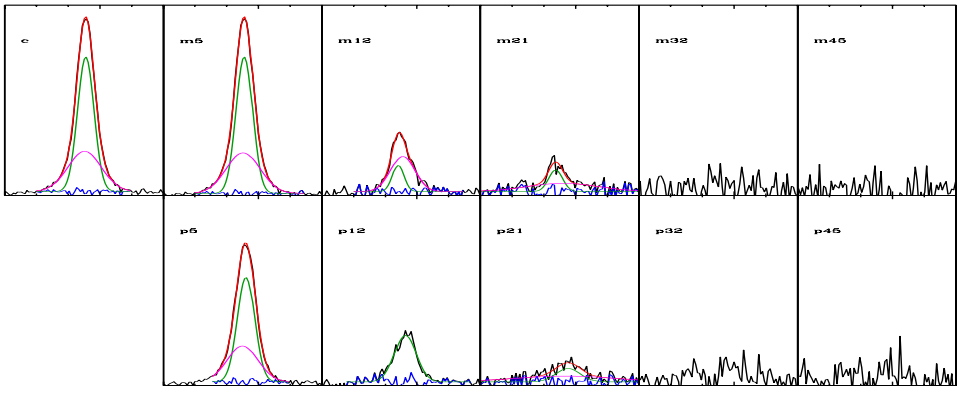

Figure B.108: DG-Object 14 [X]

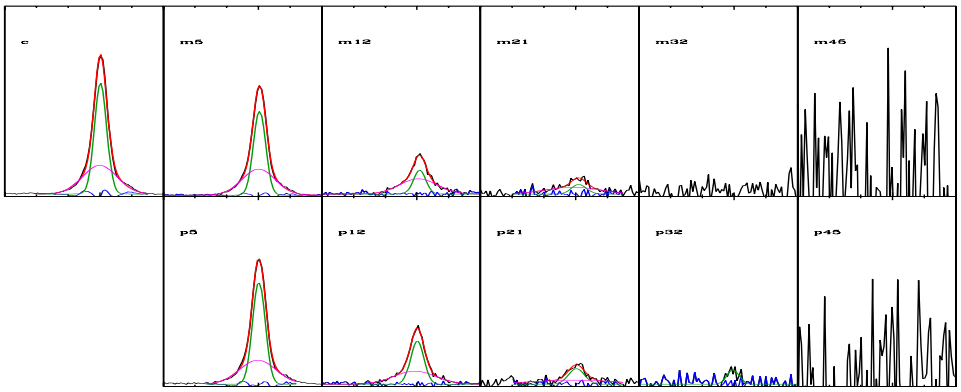

Figure B.109: DG-Object 15

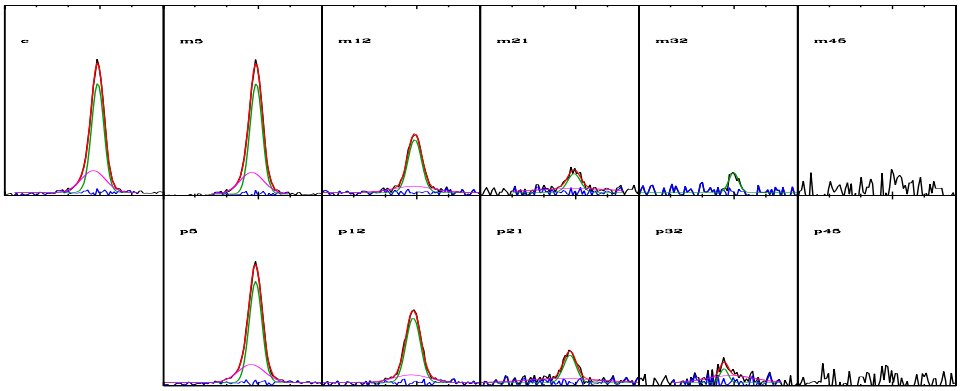

Figure B.110: DG-Object 16 [X]

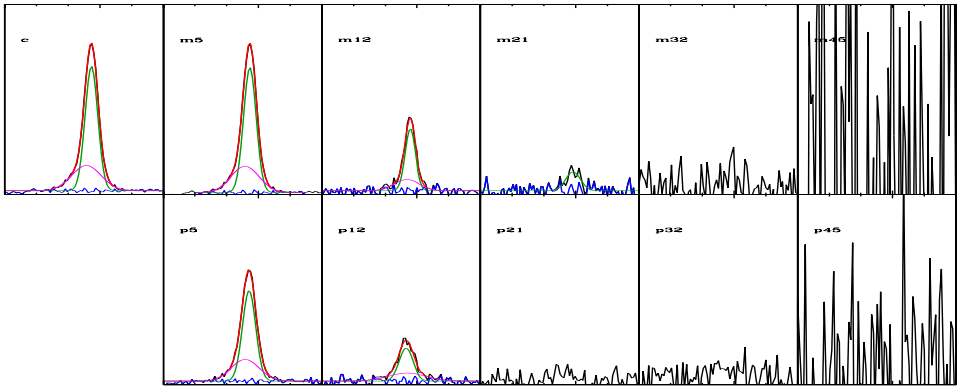

Figure B.111: DG-Object 19

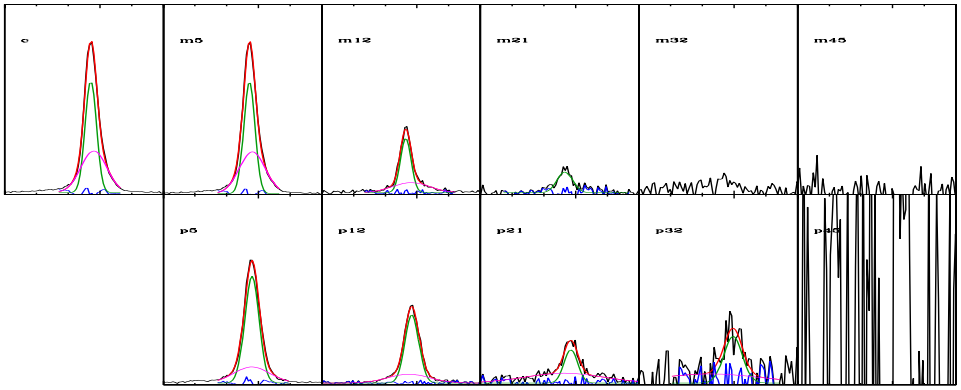

Figure B.112: DG-Object 20

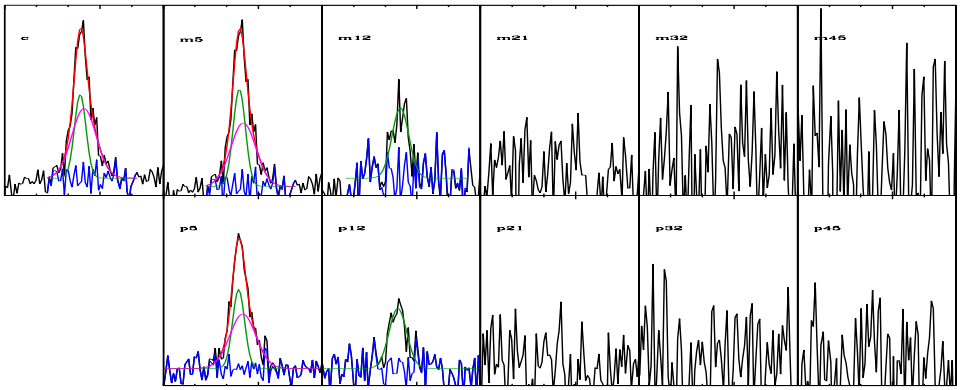

Figure B.113: DG-Object 21

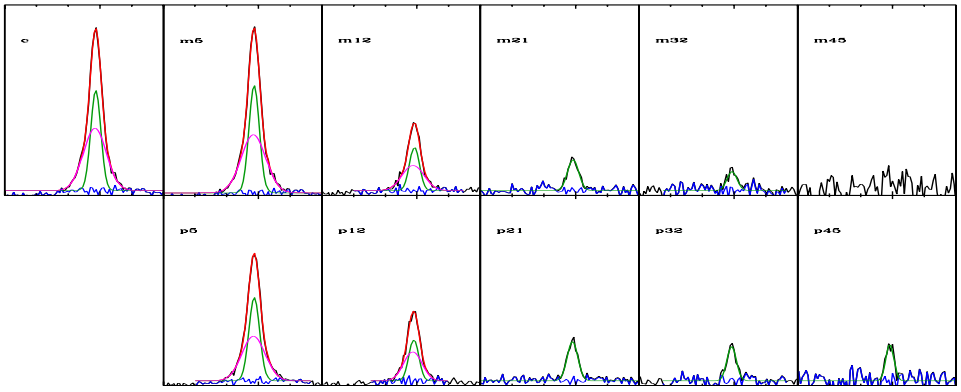

Figure B.114: DG-Object 22

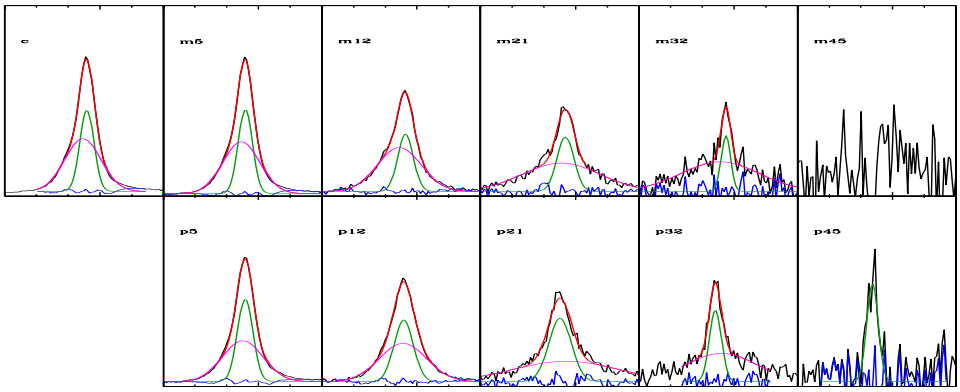

Figure B.115: DG-Object 23 [B]

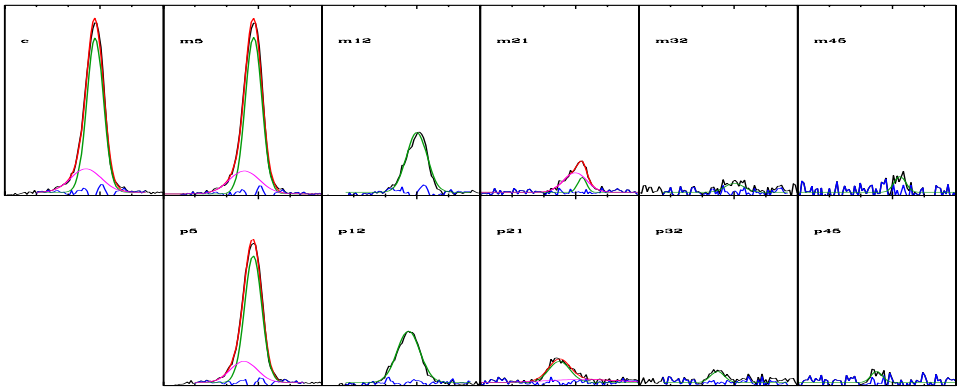

Figure B.116: DG-Object 24 [U]

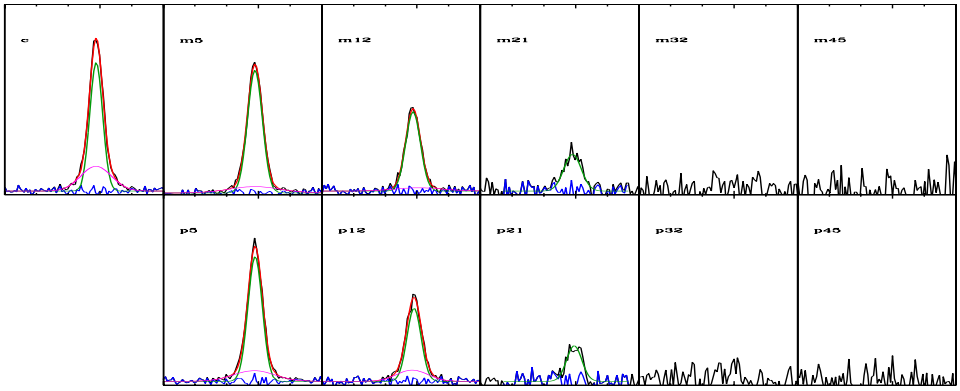

Figure B.117: DG-Object 26

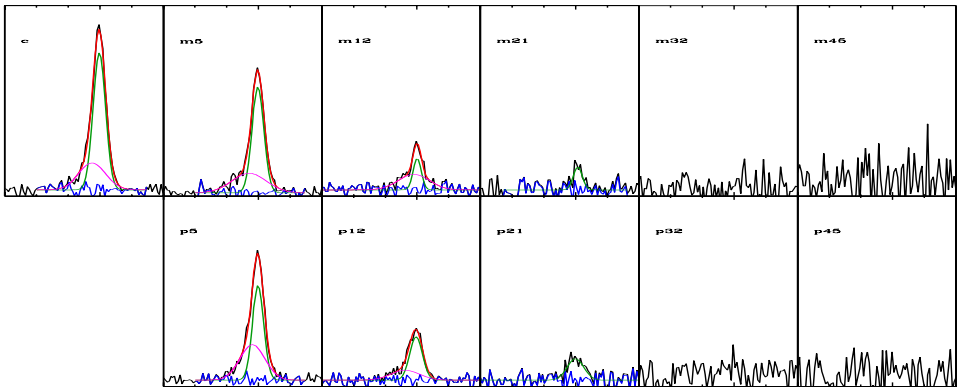

Figure B.118: DG-Object 27

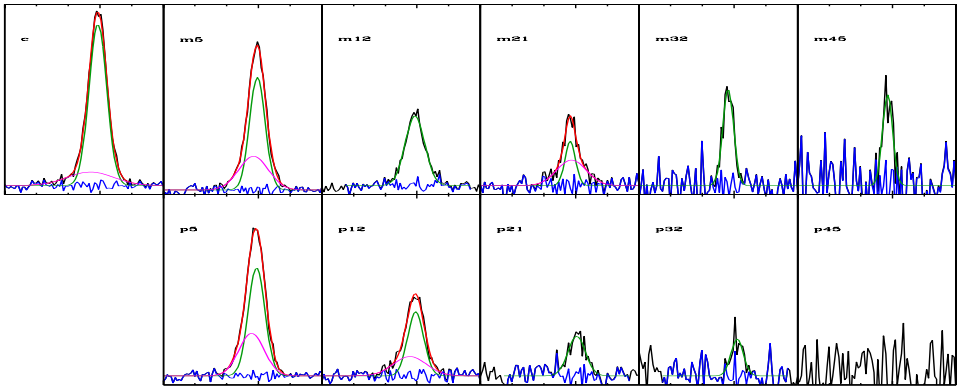

Figure B.119: DG-Object 28 [H]

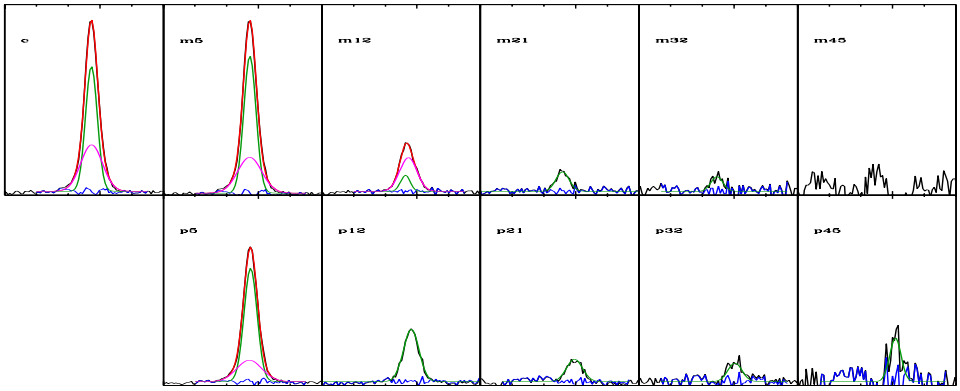

Figure B.120: DG-Object 29 [U]

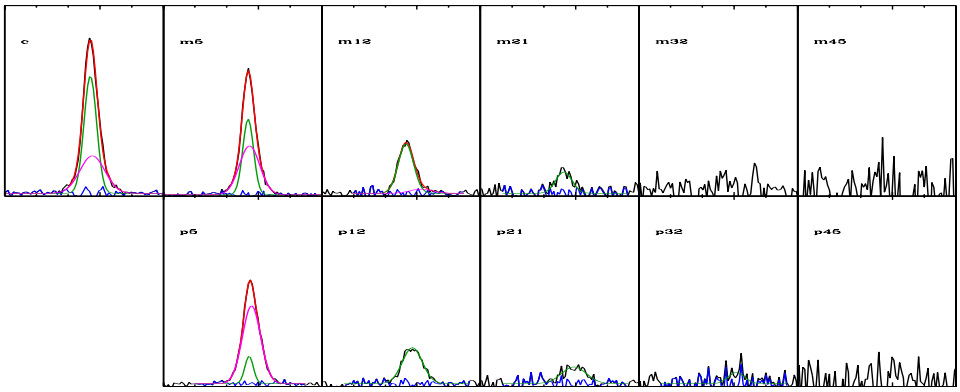

Figure B.121: DG-Object 30 [U]

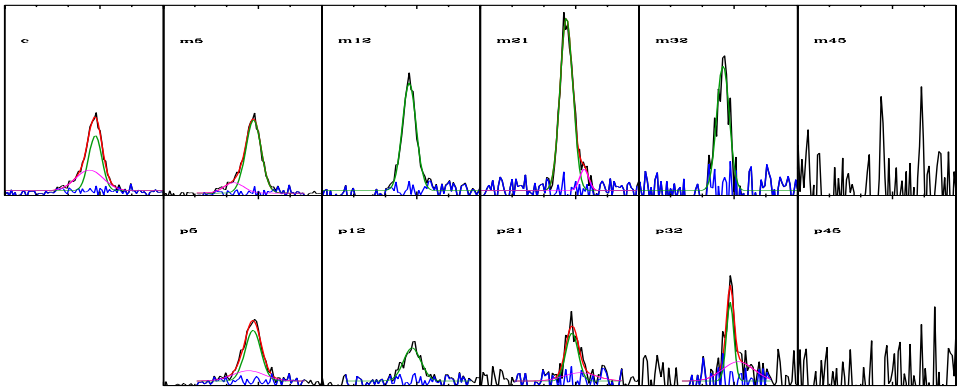

Figure B.122: DG-Object 31 [H]

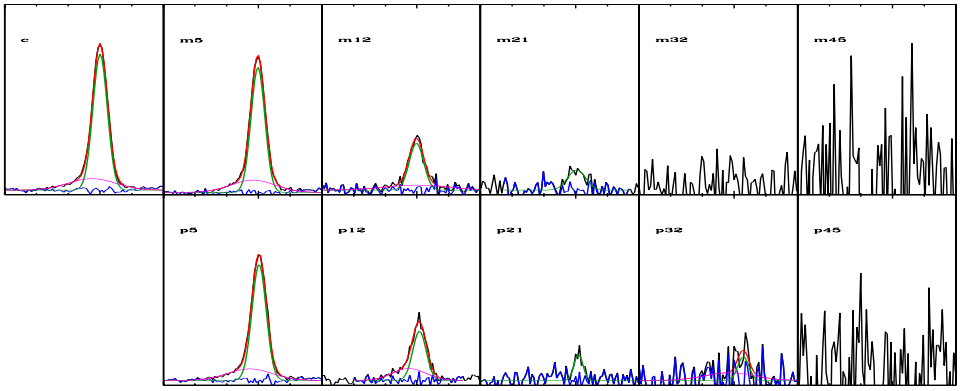

Figure B.123: DG-Object 32

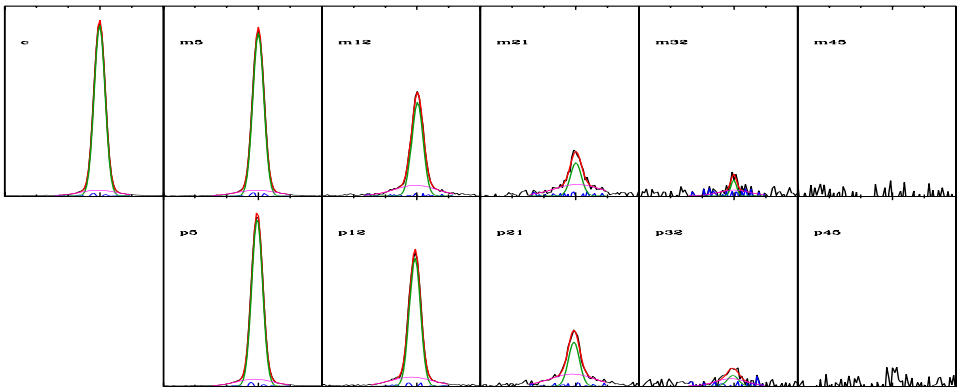

Figure B.124: DG-Object 33 [X]

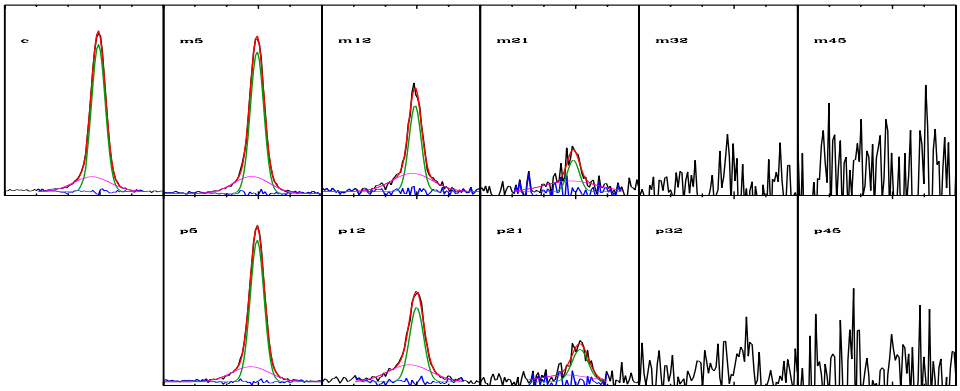

Figure B.125: DG-Object 34

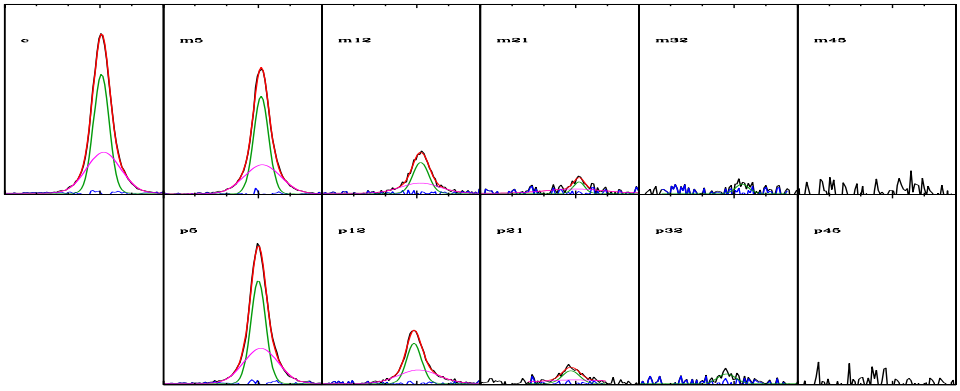

Figure B.126: DG-Object 35

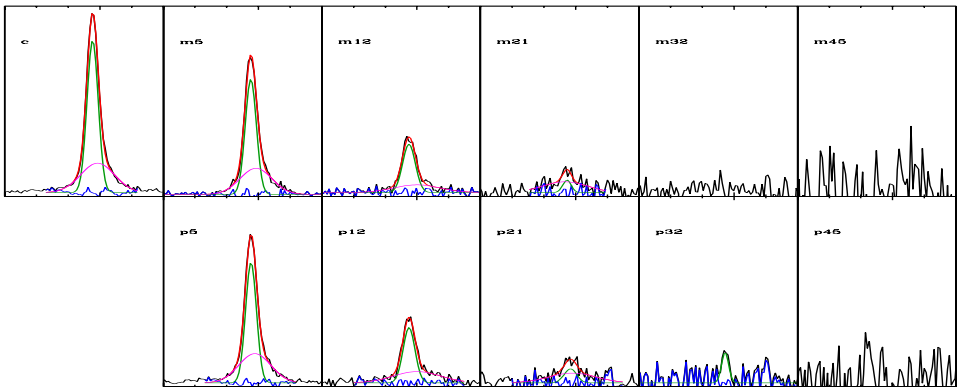

Figure B.127: DG-Object 36

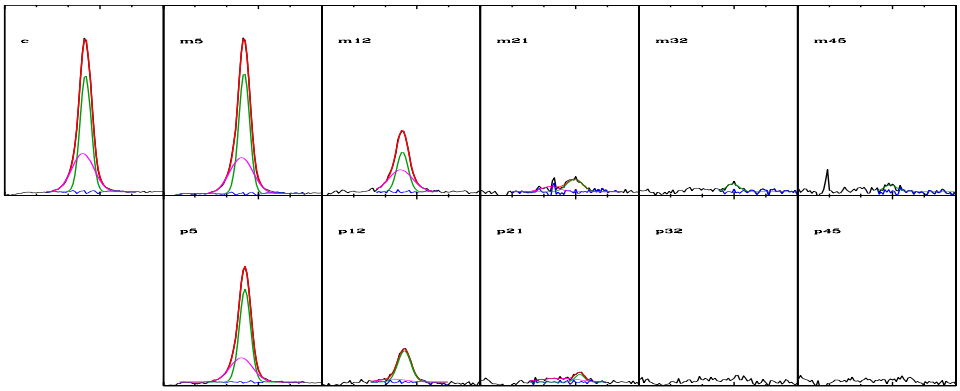

Figure B.128: DG-Object 37 [X]

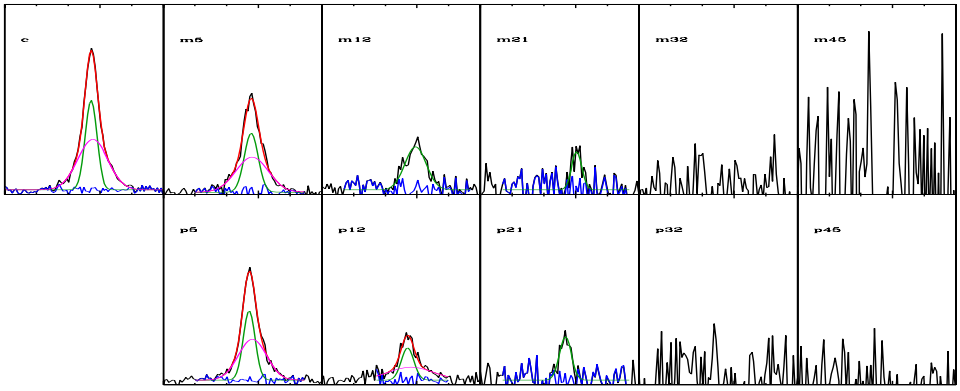

Figure B.129: DG-Object 38

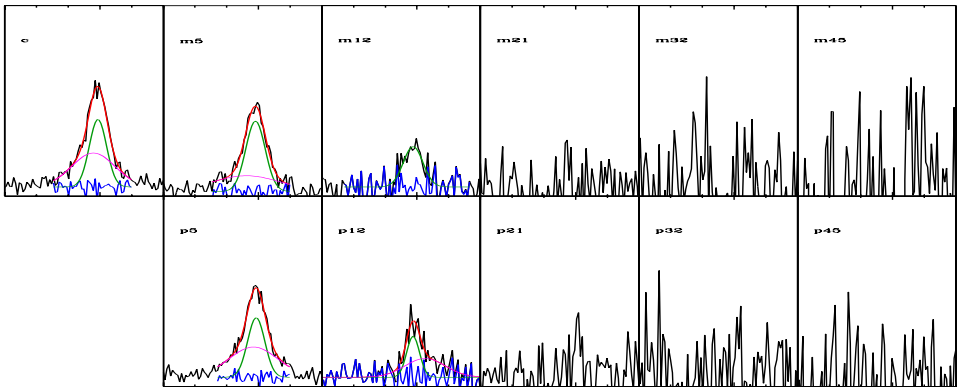

Figure B.130: DG-Object 39

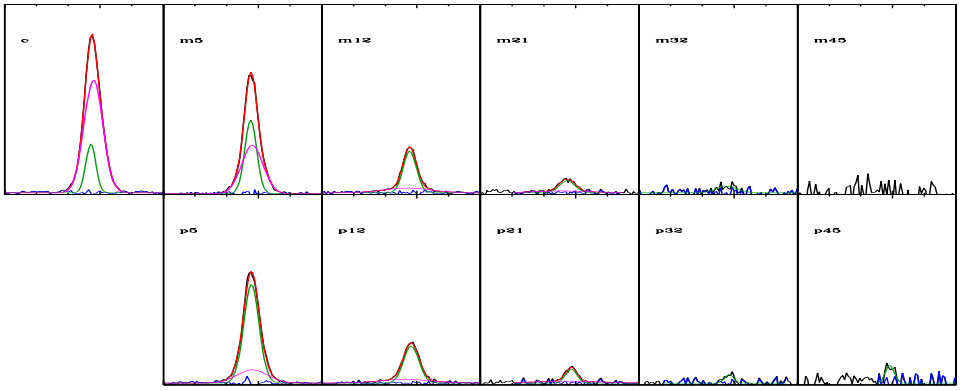

Figure B.131: DG-Object 40 [U]

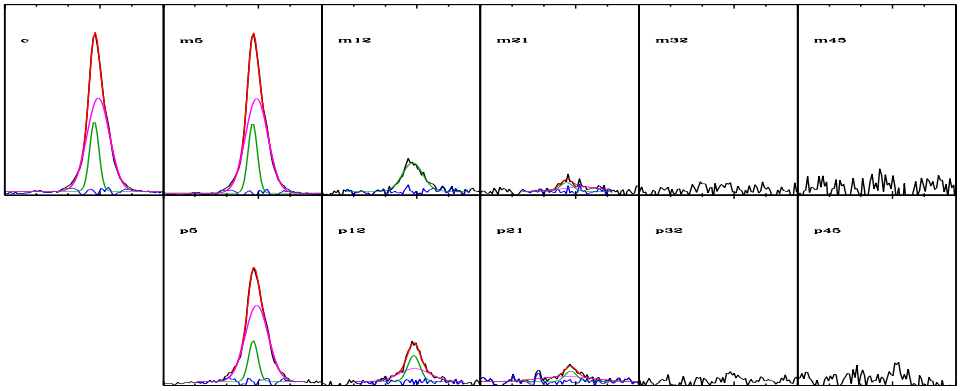

Figure B.132: DG-Object 41 [U]

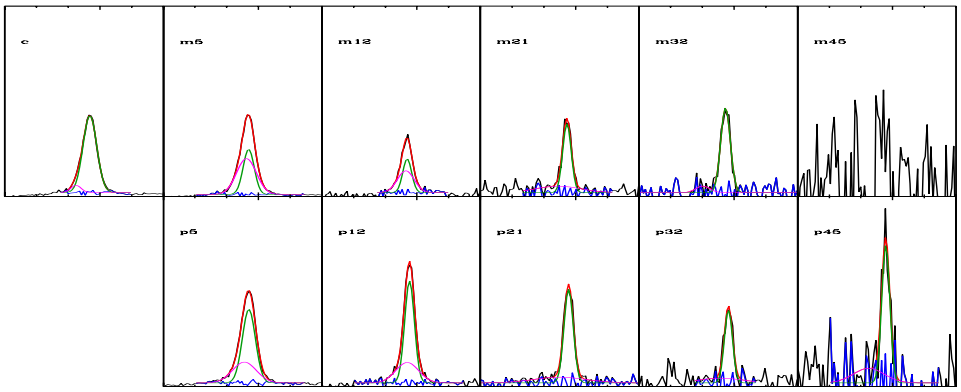

Figure B.133: DG-Object 42 [U,H]

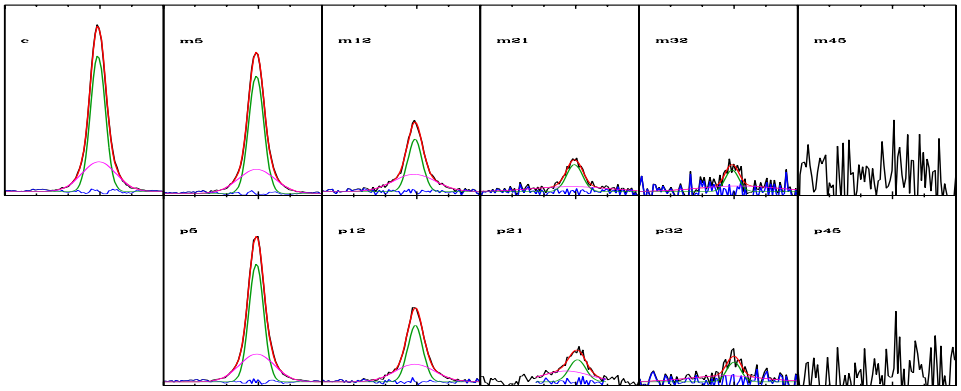

Figure B.134: DG-Object 43

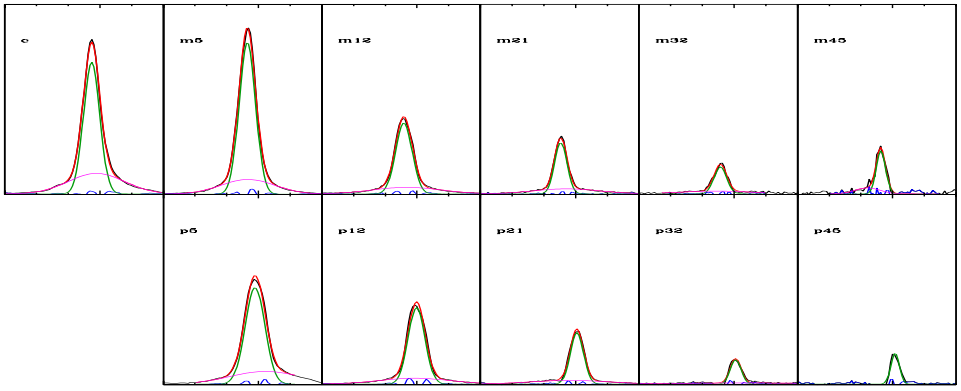

Figure B.135: DG-Object 44

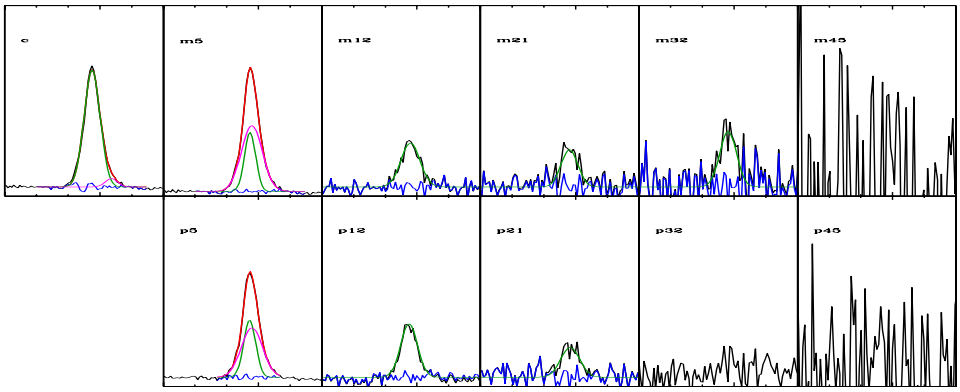

Figure B.136: DG-Object 45 [U]

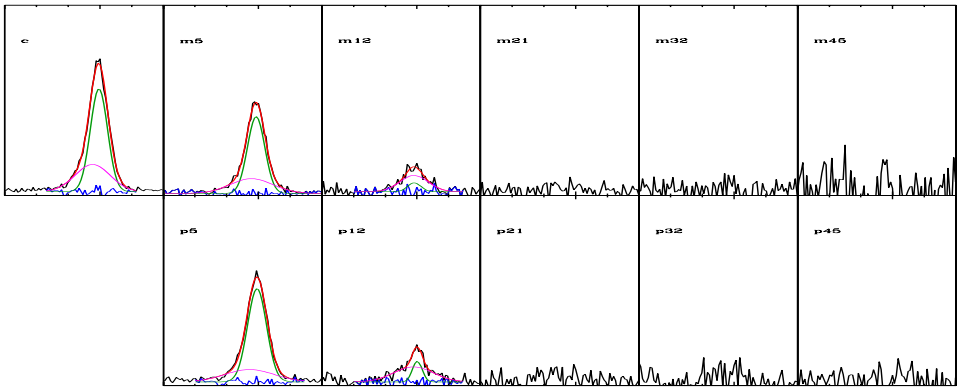

Figure B.137: DG-Object 46 [U]

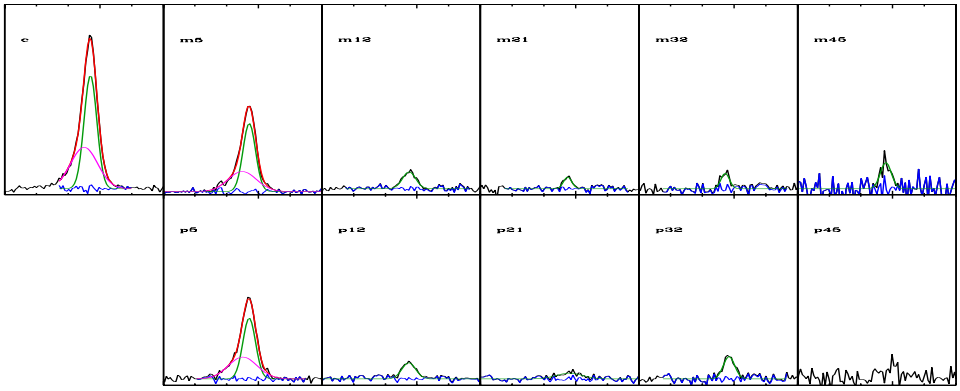

Figure B.138: DG-Object 47

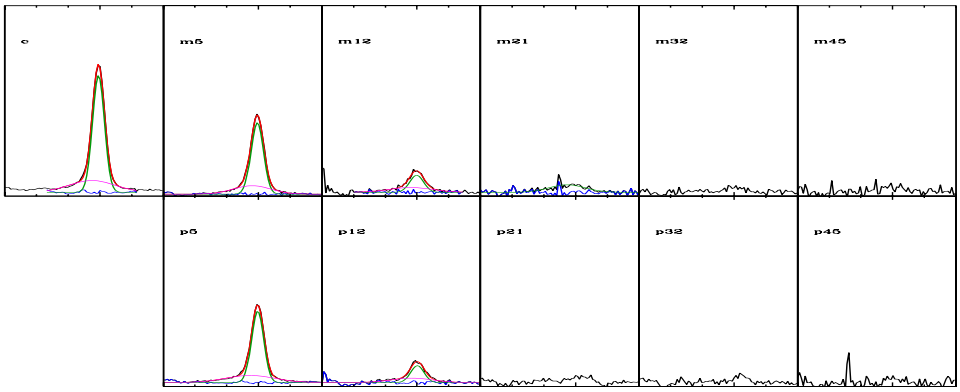

Figure B.139: DG-Object 48 [X]

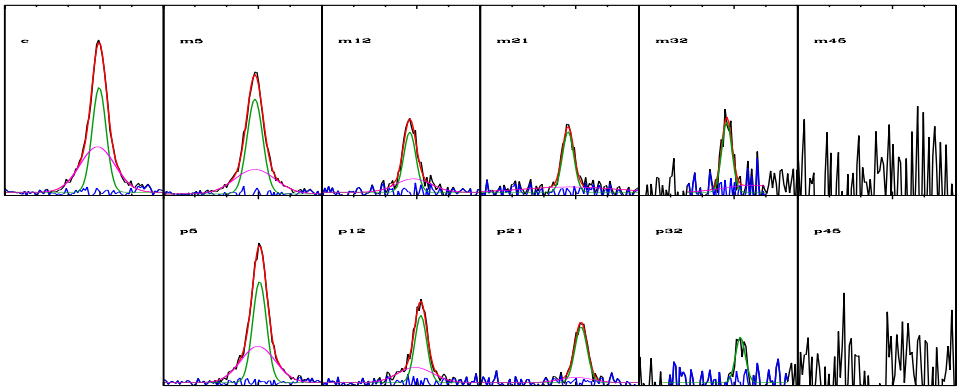

Figure B.140: DG-Object 49

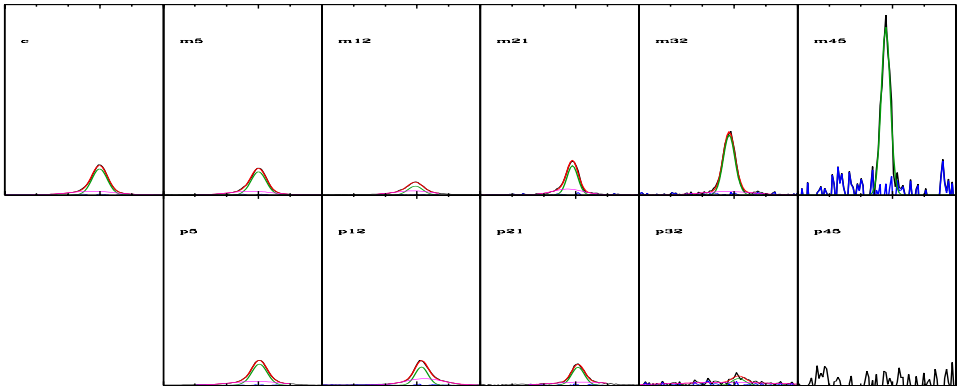

Figure B.141: DG-Object 50 [X,H]

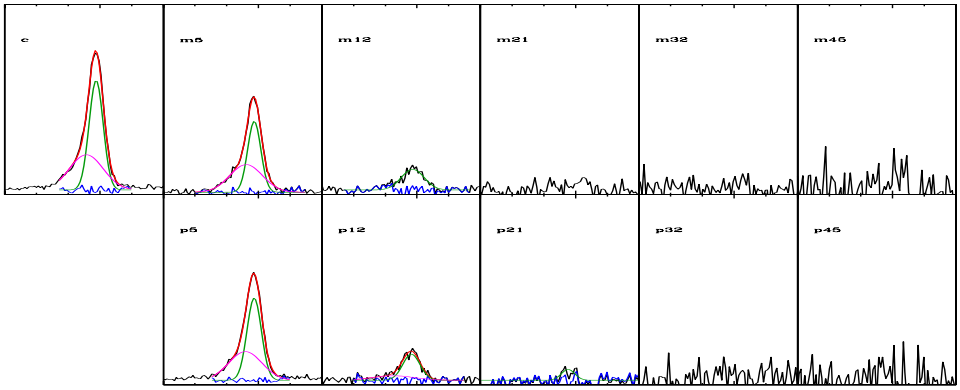

Figure B.142: DG-Object 51

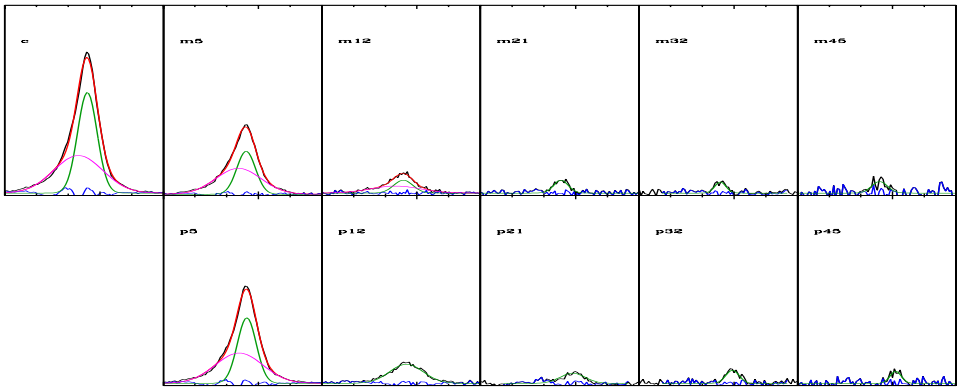

Figure B.143: DG-Object 52

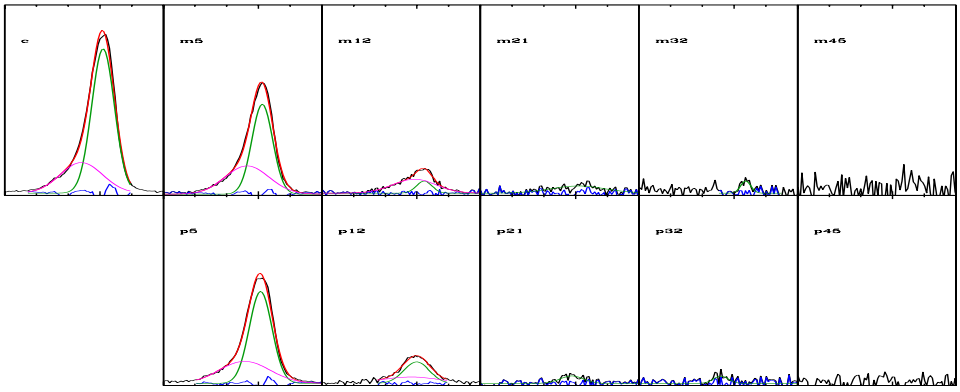

Figure B.144: DG-Object 53

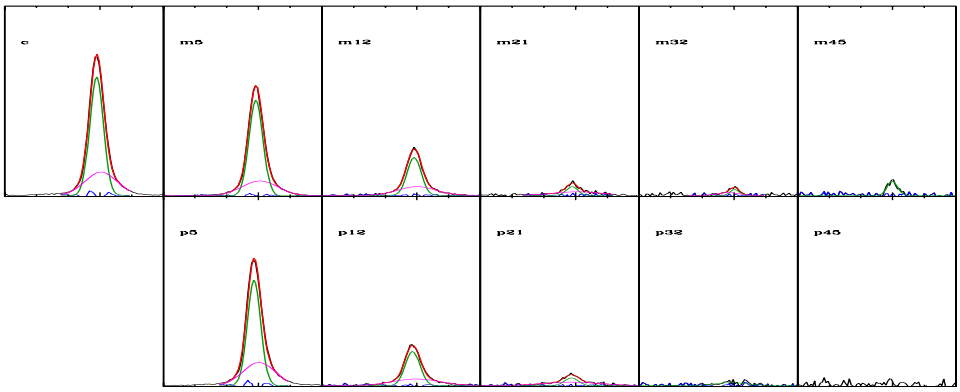

Figure B.145: DG-Object 54

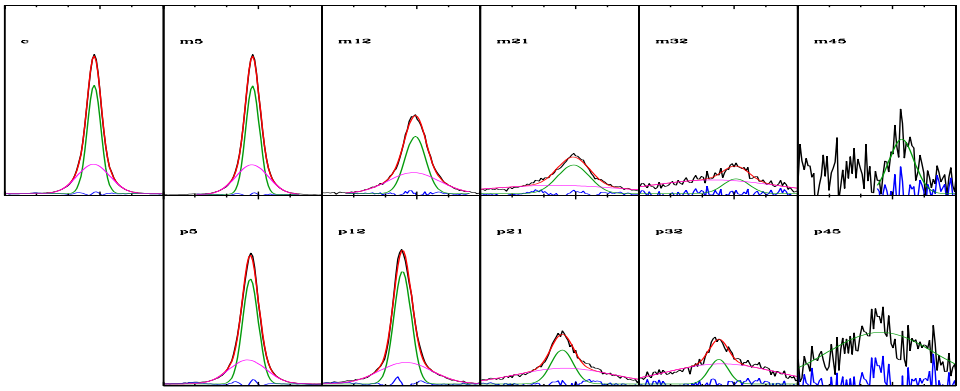

Figure B.146: DG-Object 56 [X,B]

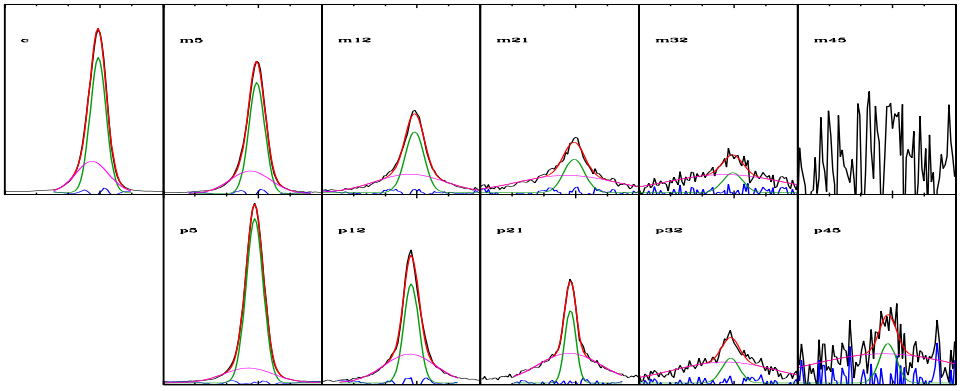

Figure B.147: DG-Object 57

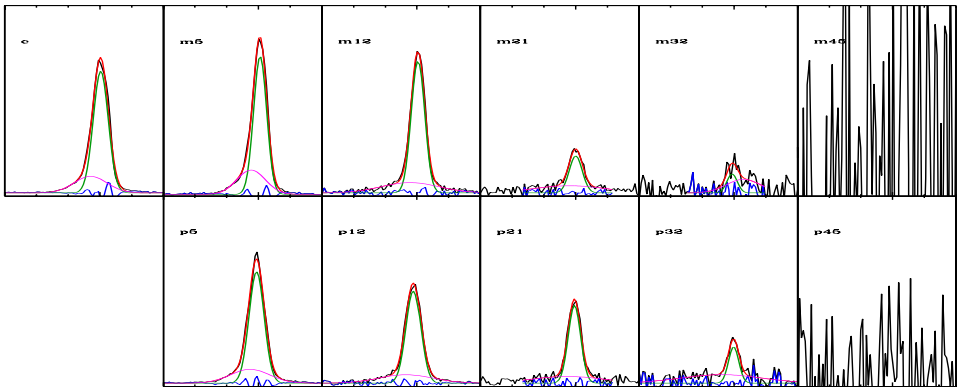

Figure B.148: DG-Object 58

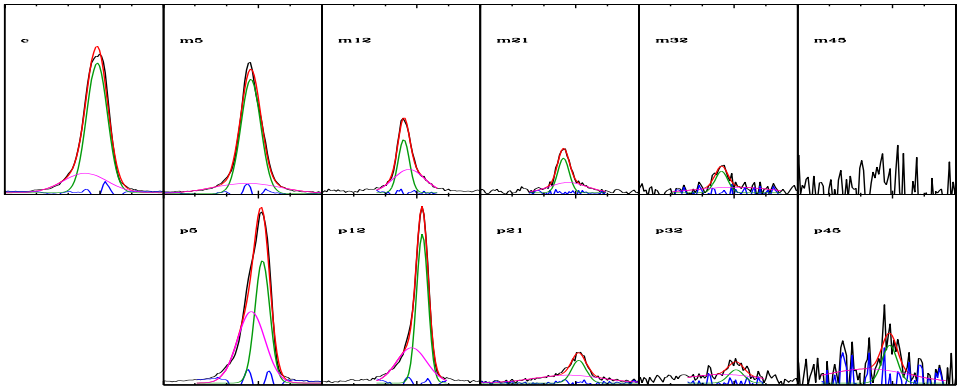

Figure B.149: DG-Object 59 [*]

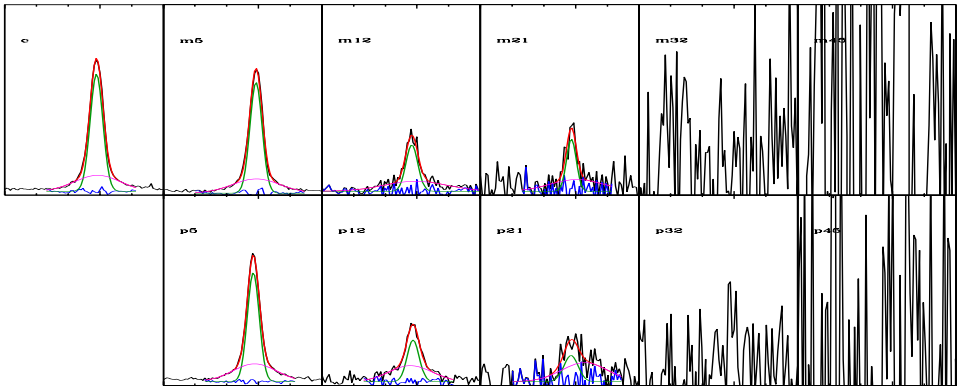

Figure B.150: DG-Object 60 [X]

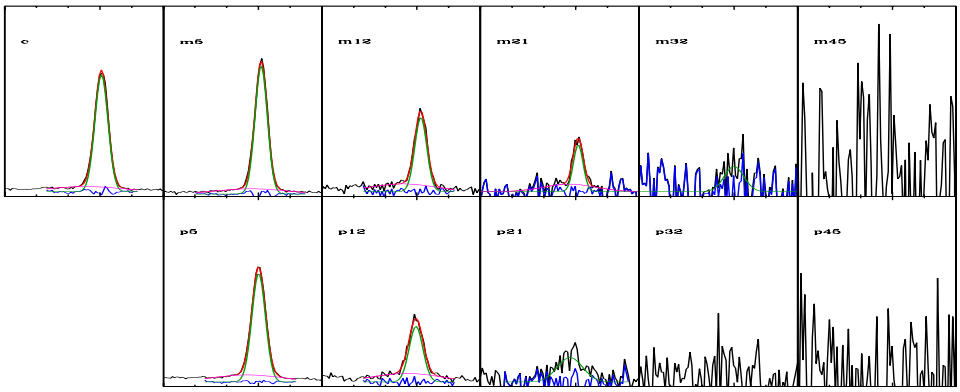

Figure B.151: DG-Object 61

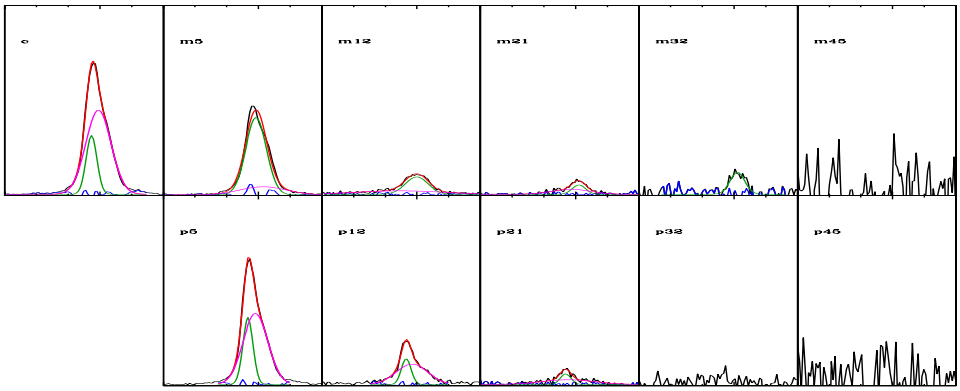

Figure B.152: DG-Object 62 [U]

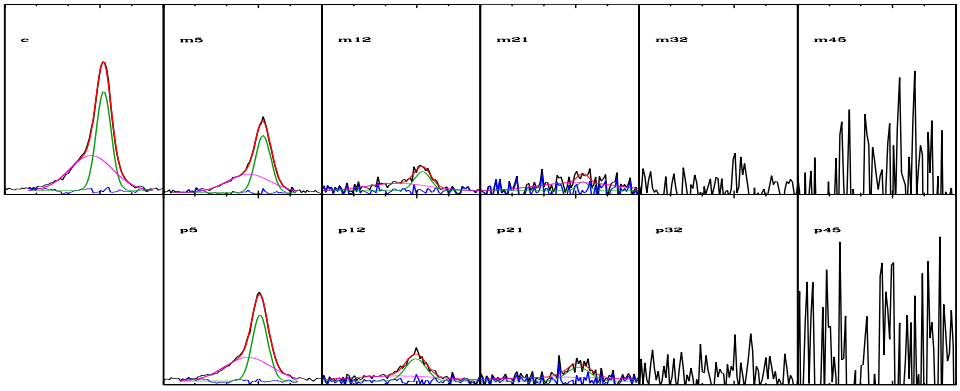

Figure B.153: DG-Object 63

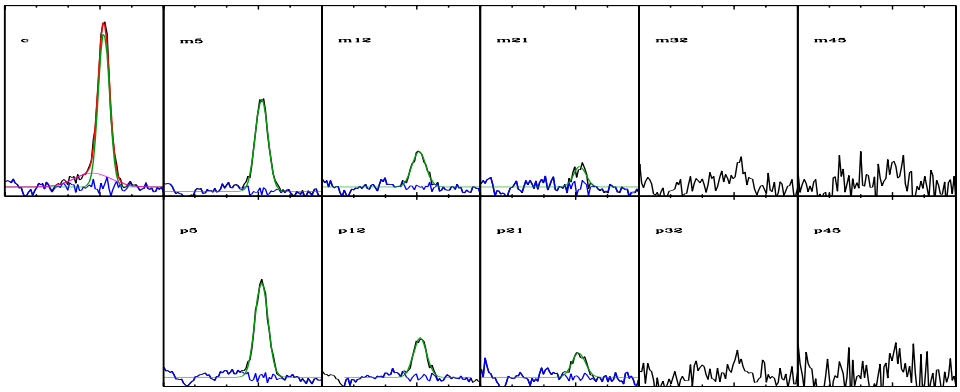

Figure B.154: DG-Object 64 [X]

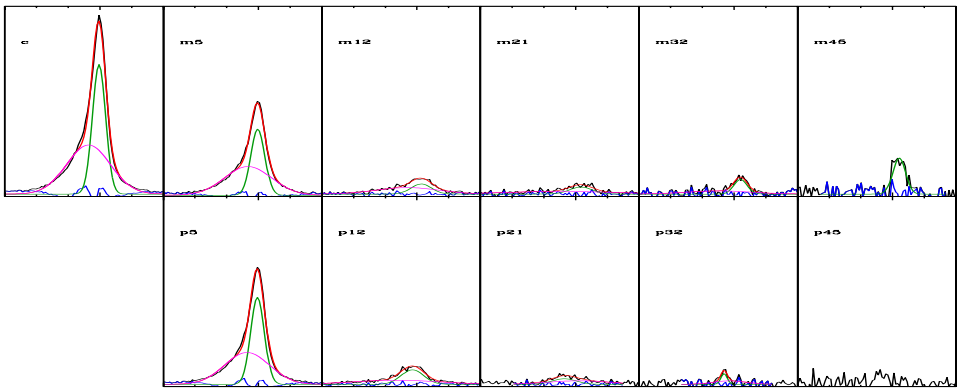

Figure B.155: DG-Object 70

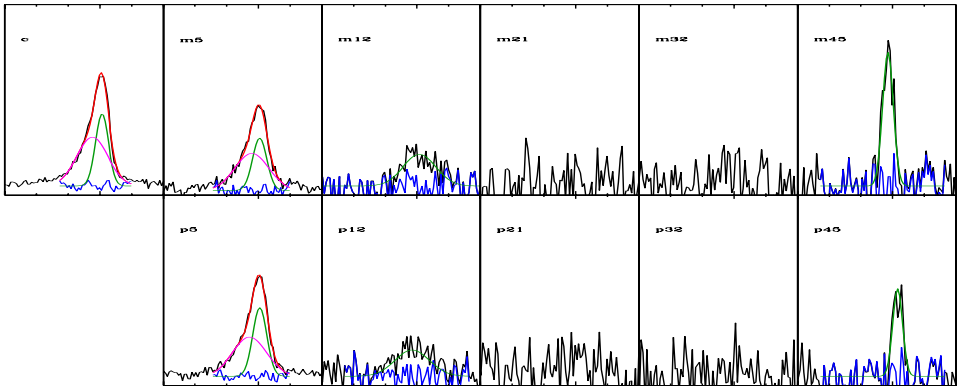

Figure B.156: DG-Object 71 [H]

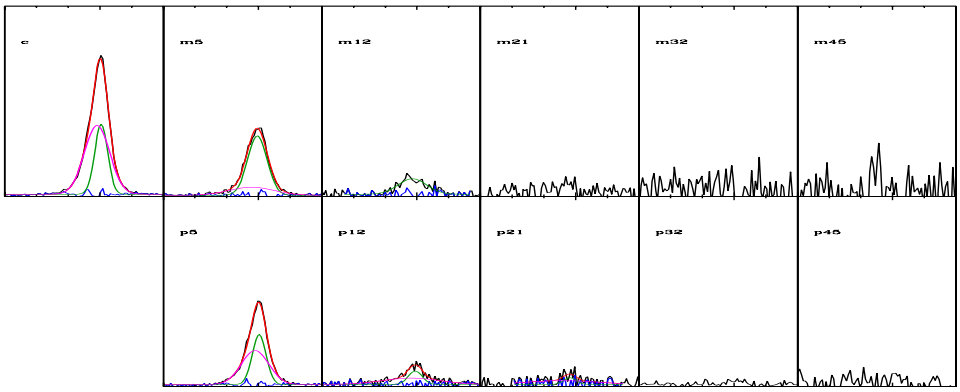

Figure B.157: DG-Object 73 [U]

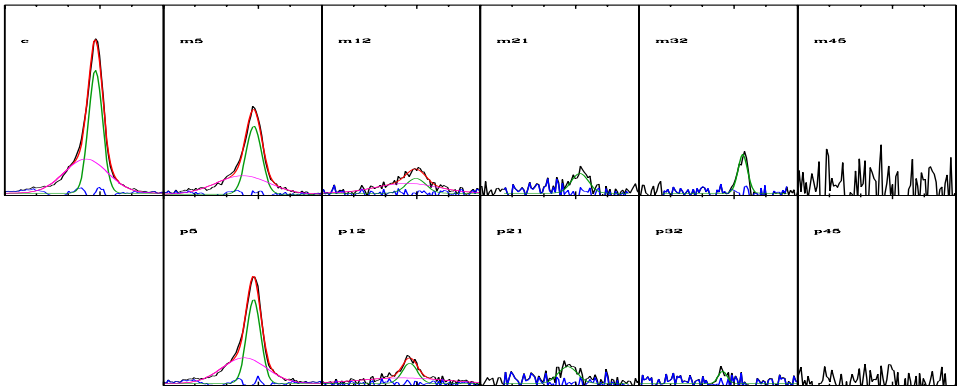

Figure B.158: DG-Object 74

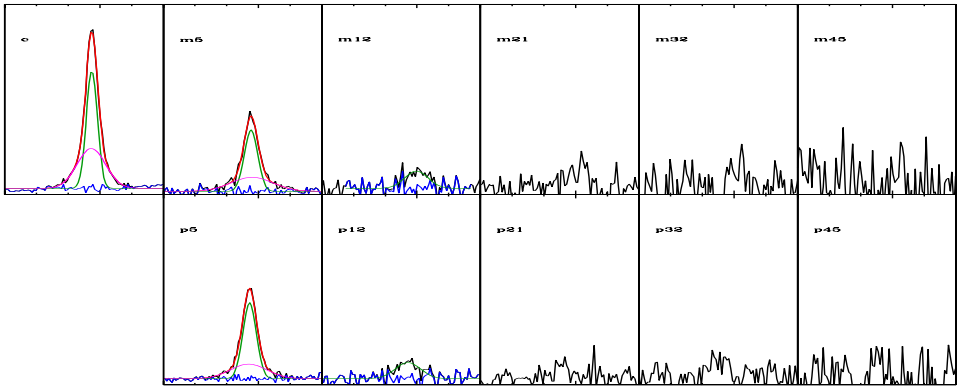

Figure B.159: DG-Object 76

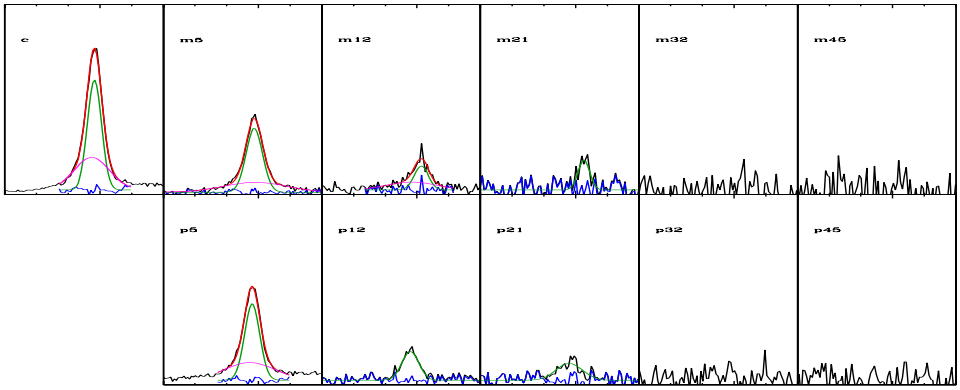

Figure B.160: DG-Object 77

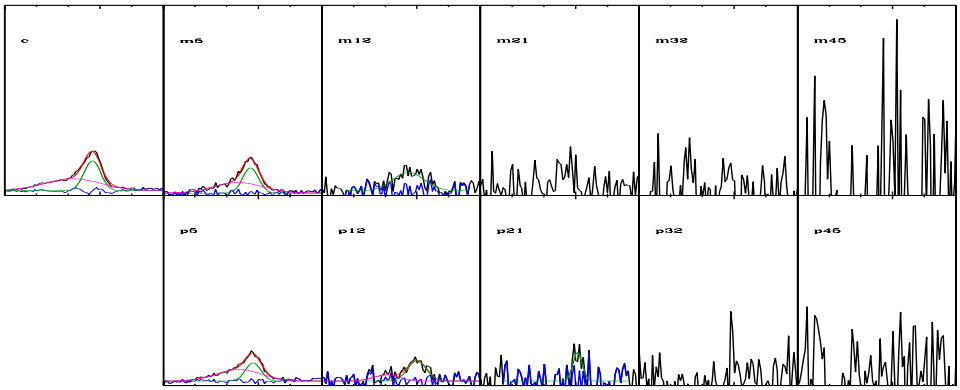

Figure B.161: DG-Object 78

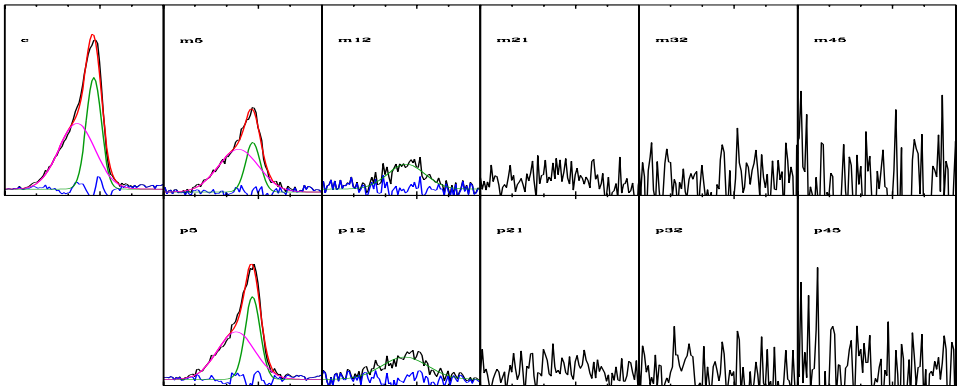

Figure B.162: DG-Object 79

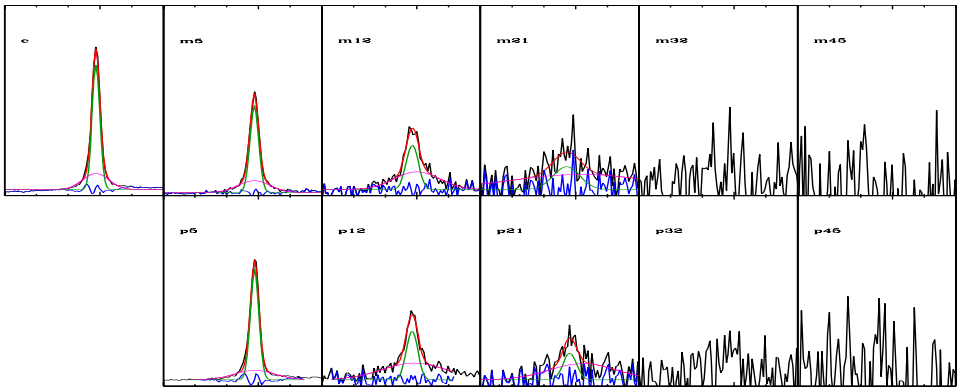

Figure B.163: DG-Object 80 [X]

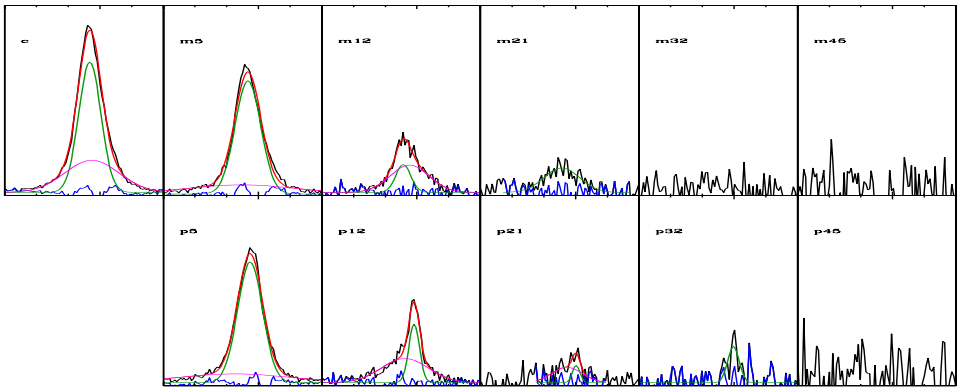

Figure B.164: DG-Object 81 [X]

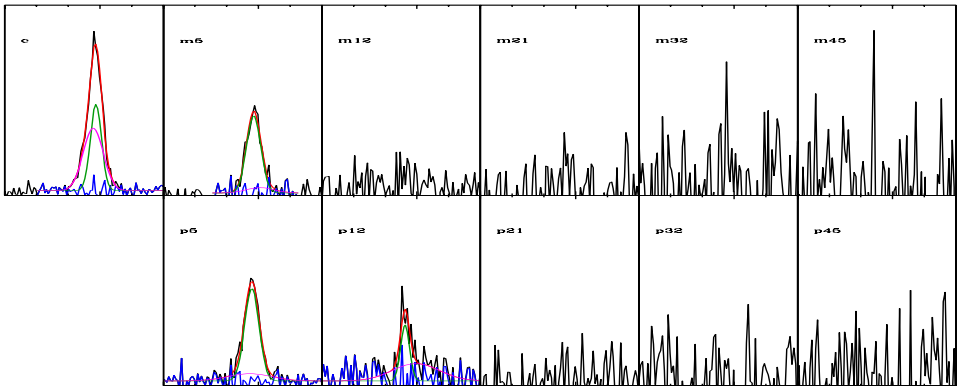

Figure B.165: DG-Object 82 [U]

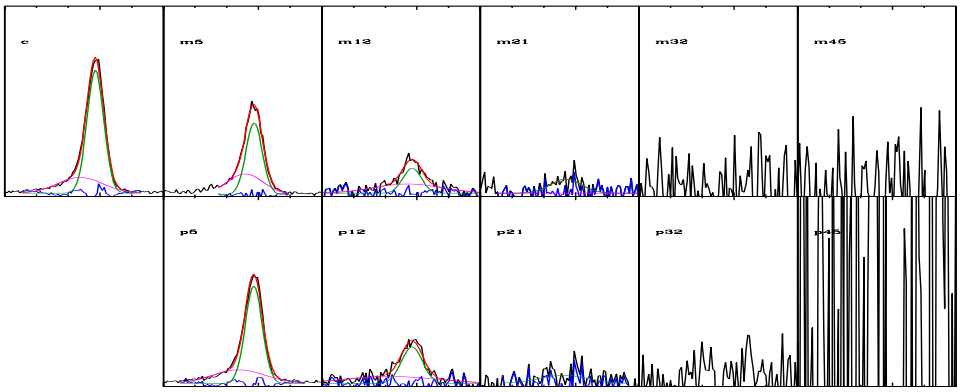

Figure B.166: DG-Object 83

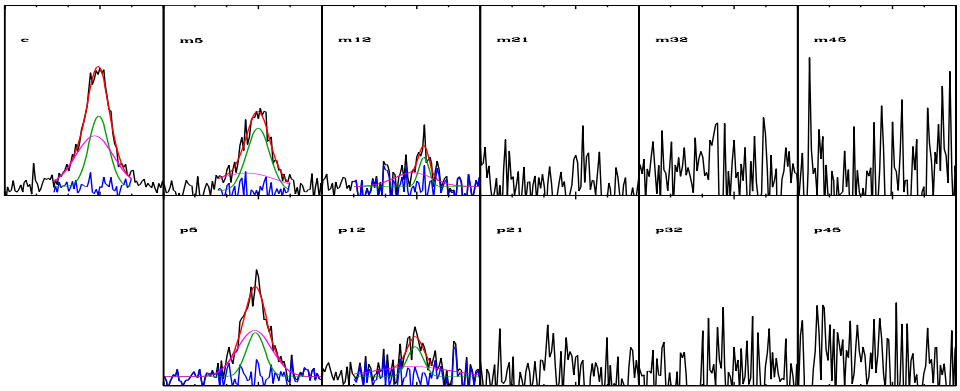

Figure B.167: DG-Object 88 [U]

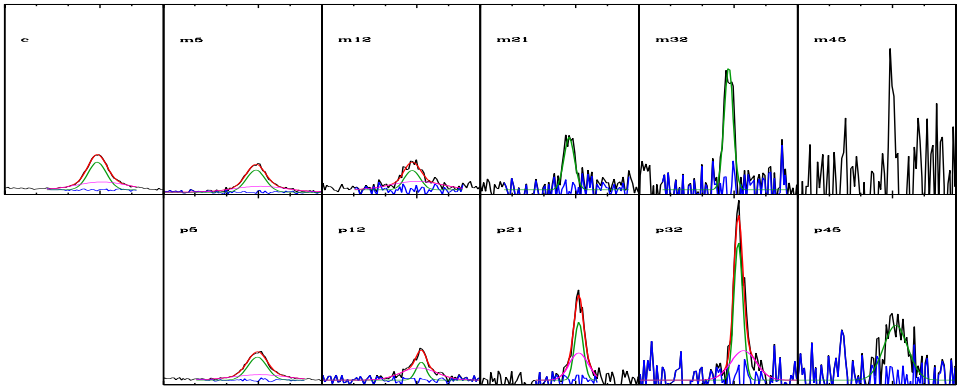

Figure B.168: DG-Object 91

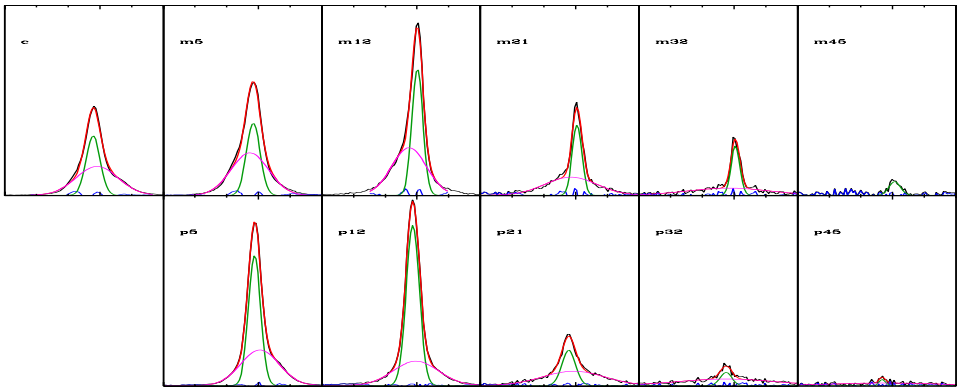

Figure B.169: DG-Object 96 [X,*]

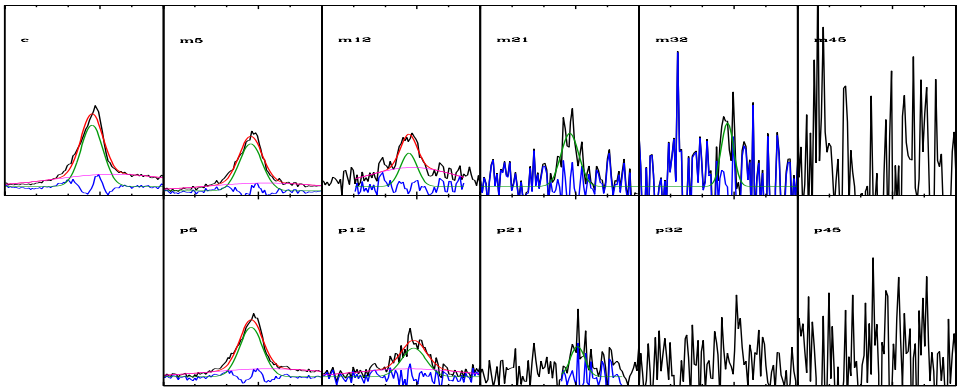

Figure B.170: DG-Object 99 [*]

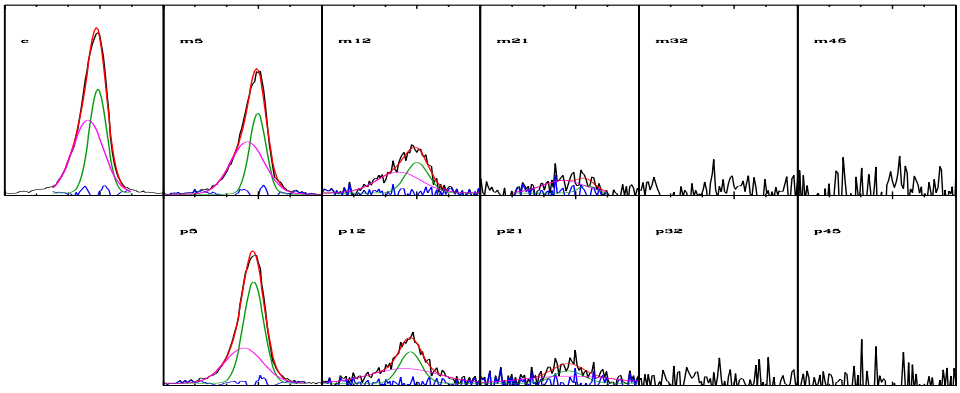

Figure B.171: DG-Object 100 [X]

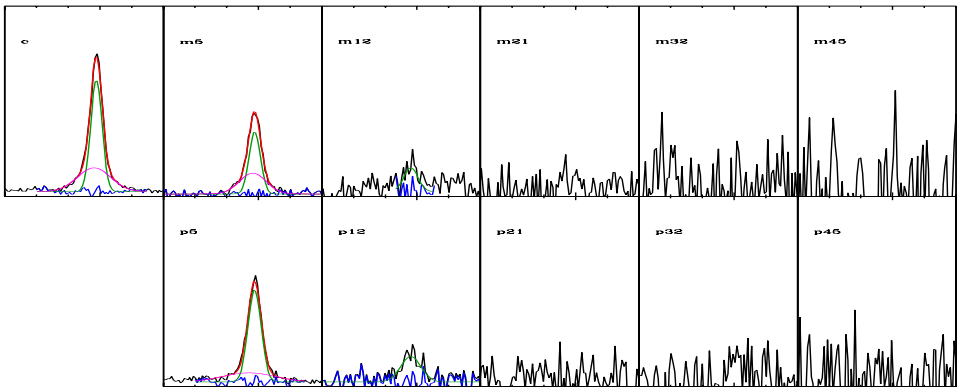

Figure B.172: DG-Object 102

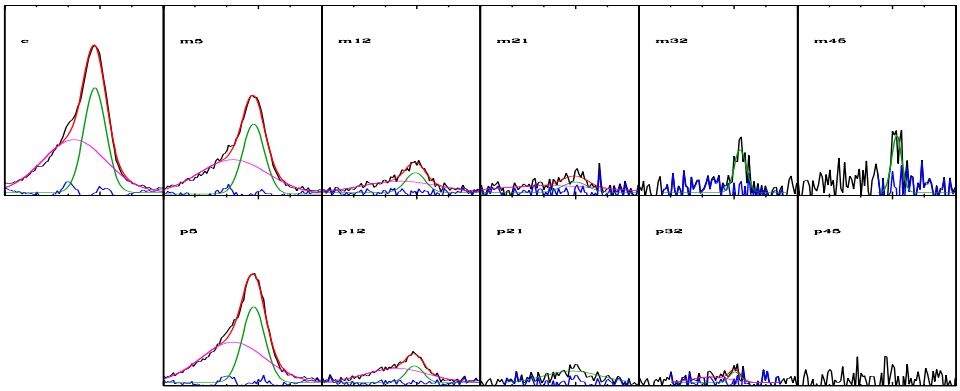

Figure B.173: DG-Object 103 [H]

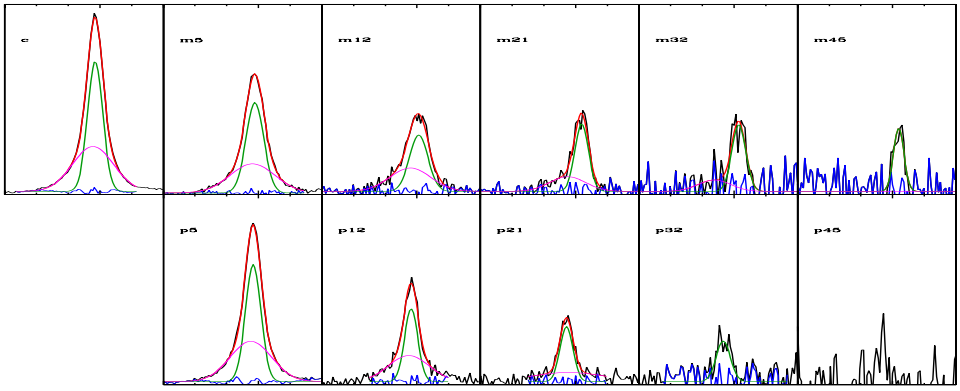

Figure B.174: DG-Object 106

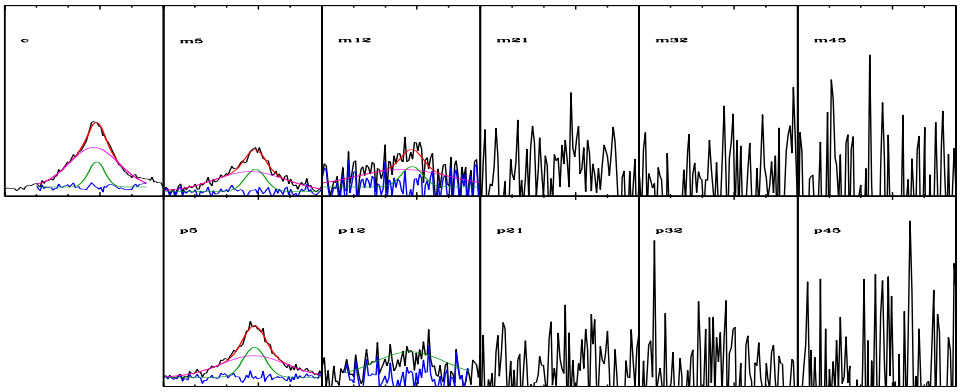

Figure B.175: DG-Object 108 [X,U,B]

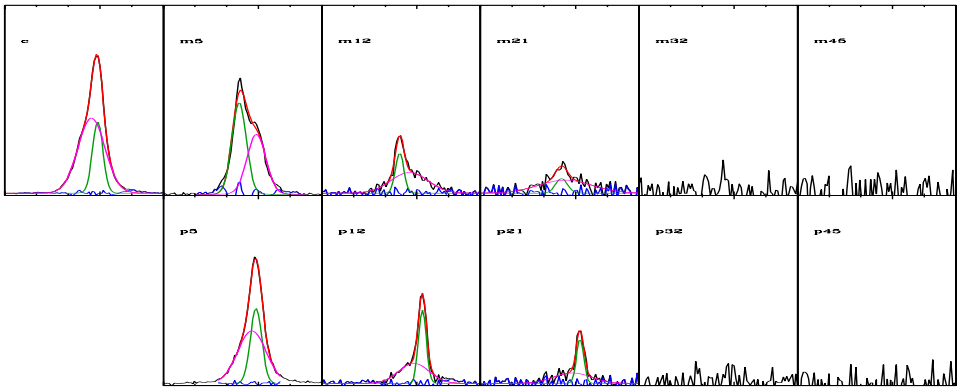

Figure B.176: DG-Object 109 [U,*]

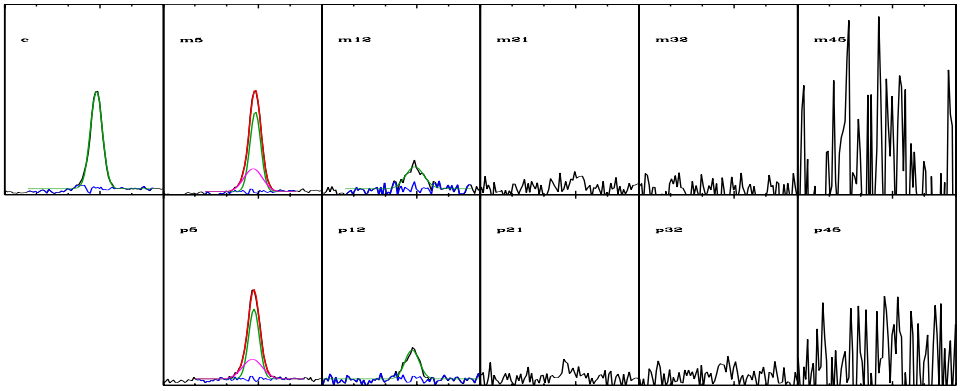

Figure B.177: DG-Object 114

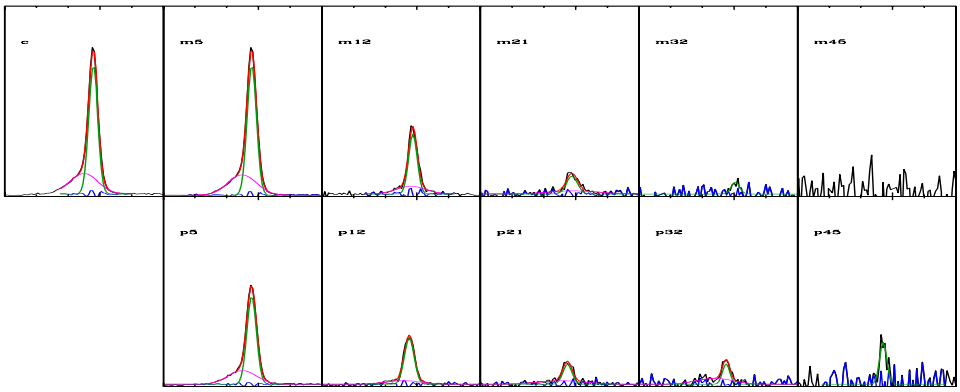

Figure B.178: DG-Object 126

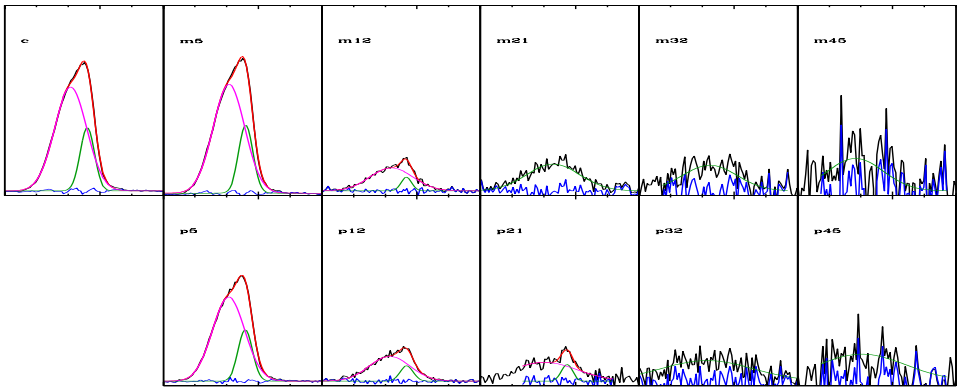

Figure B.179: DG-Object 130 [X,U,*]

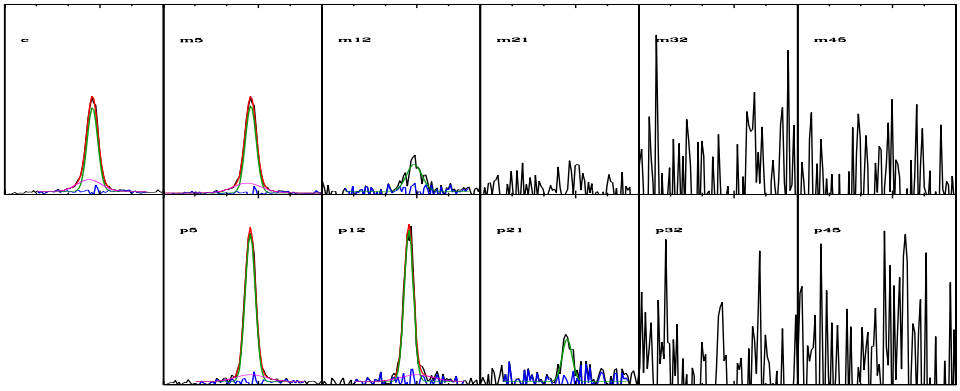

Figure B.180: DG-Object 138

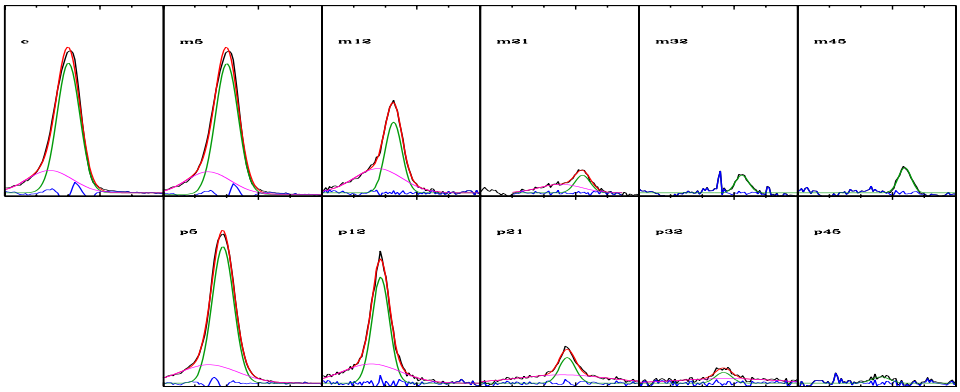

Figure B.181: DG-Object 143 [X,*]

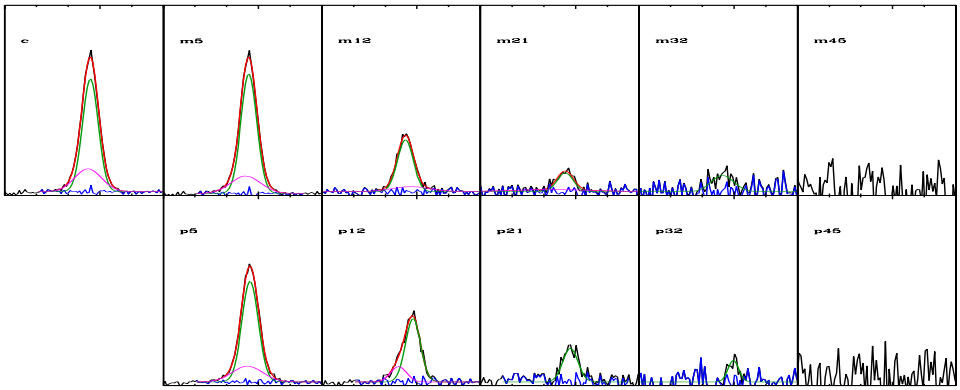

Figure B.182: DG-Object 155

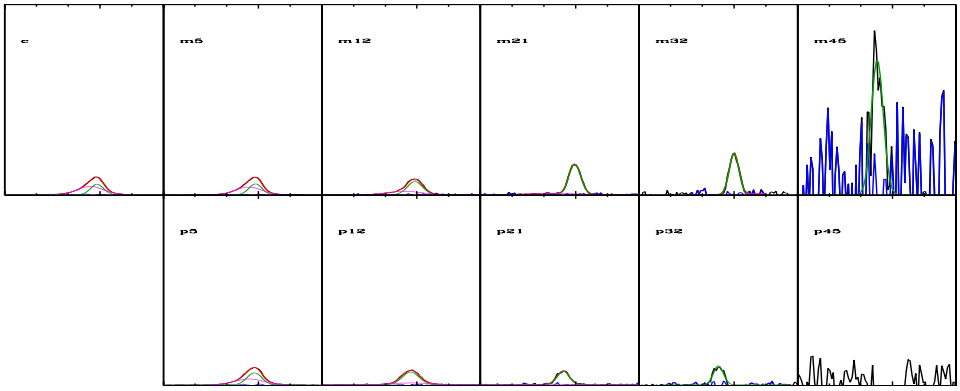

Figure B.183: DG-Object 156 [H]

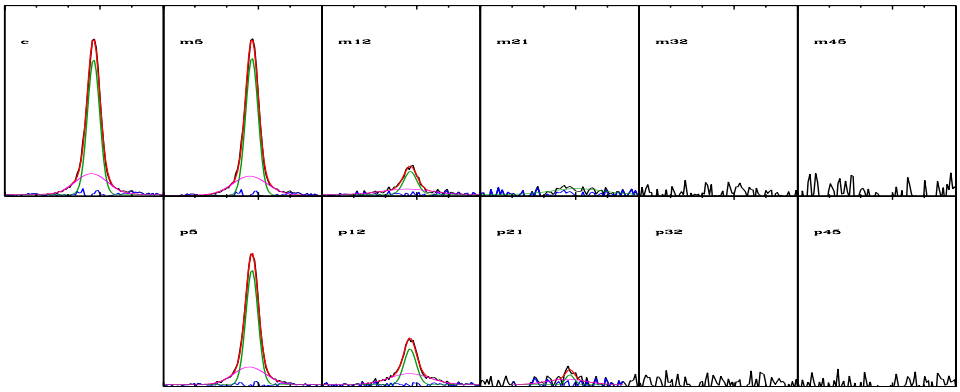

Figure B.184: DG-Object 157 [X]

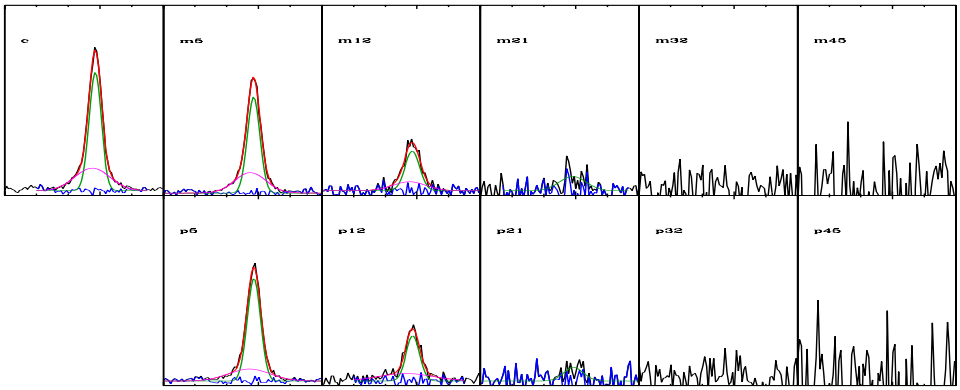

Figure B.185: DG-Object 162

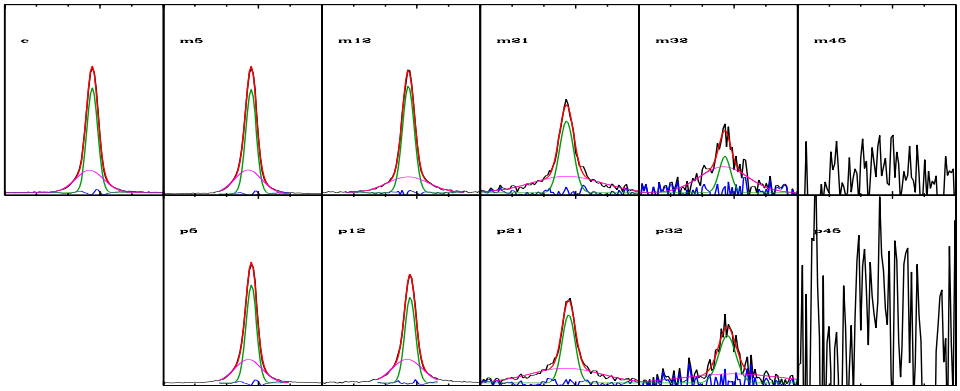

Figure B.186: DG-Object 174 [X]

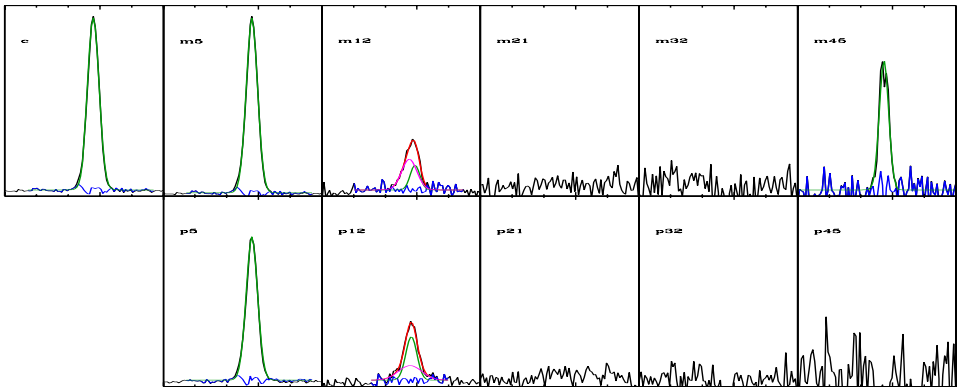

Figure B.187: DG-Object 177 [U,H]

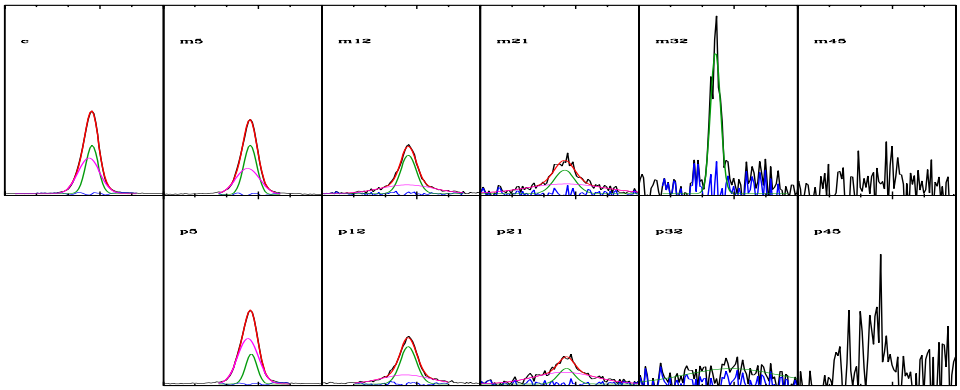

Figure B.188: DG-Object 180 [U,H]

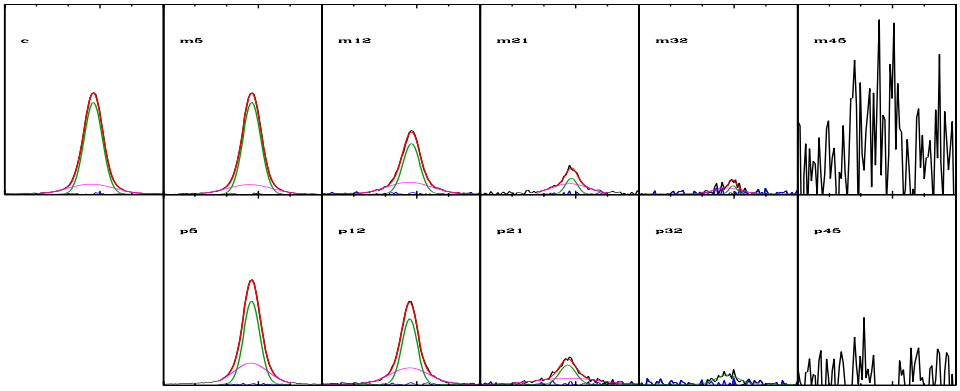

Figure B.189: DG-Object 187

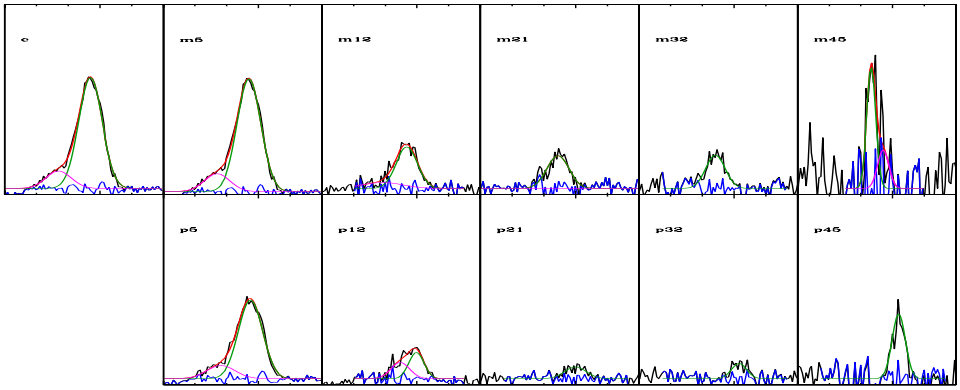

Figure B.190: DG-Object 196

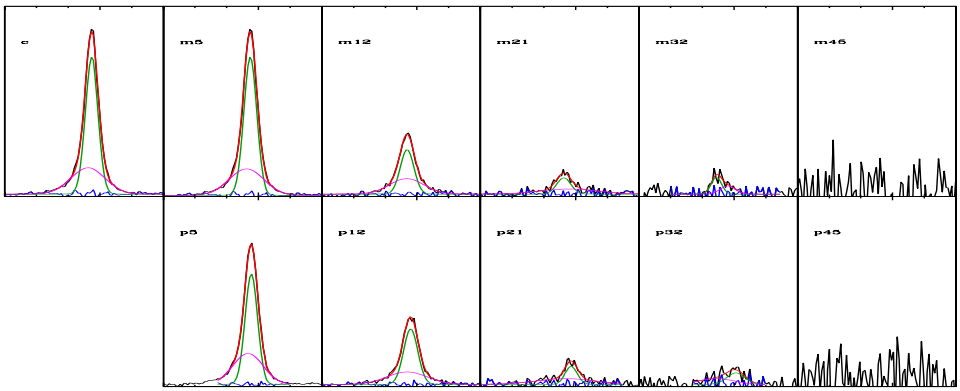

Figure B.191: DG-Object 197

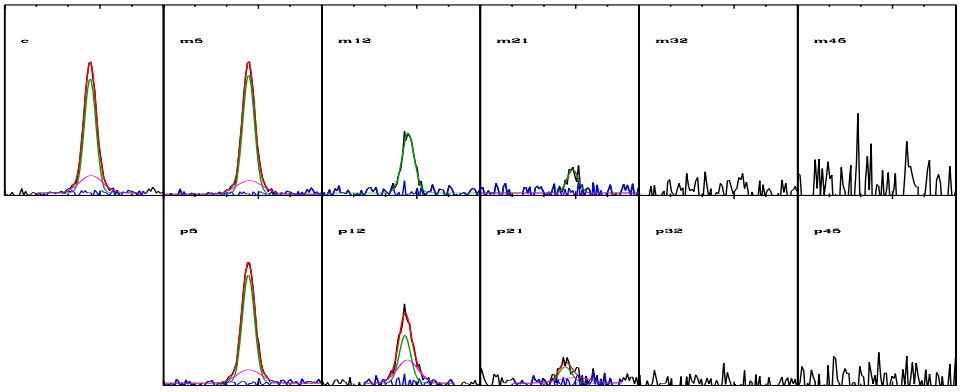

Figure B.192: DG-Object 202

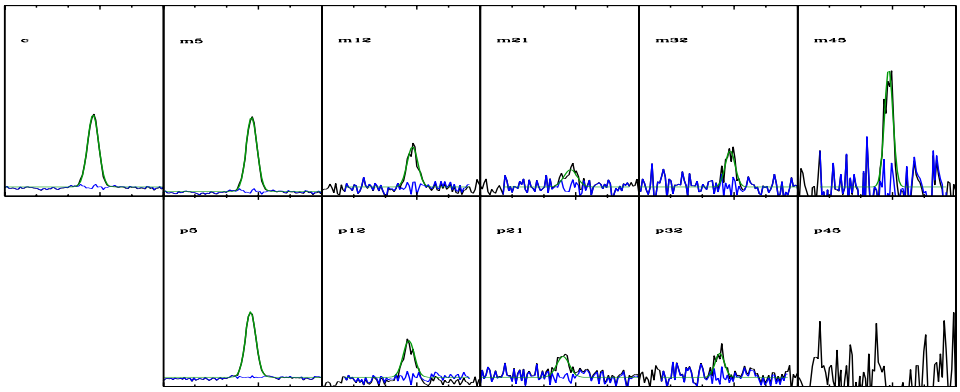

Figure B.193: DG-Object 204 [H]

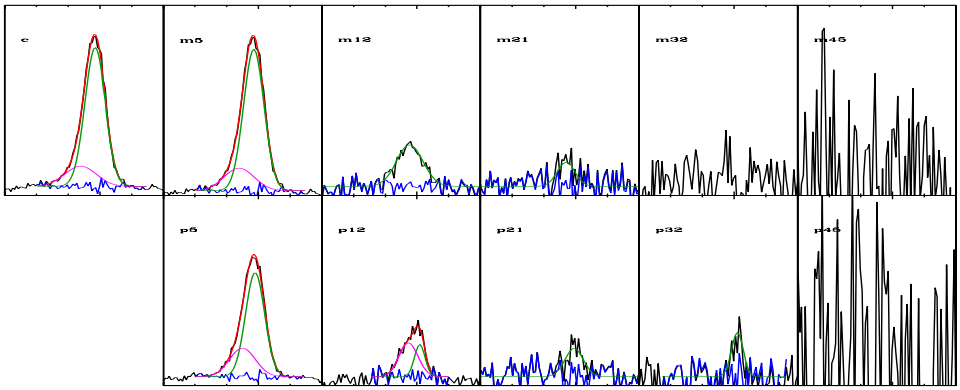

Figure B.194: DG-Object 205 [U]

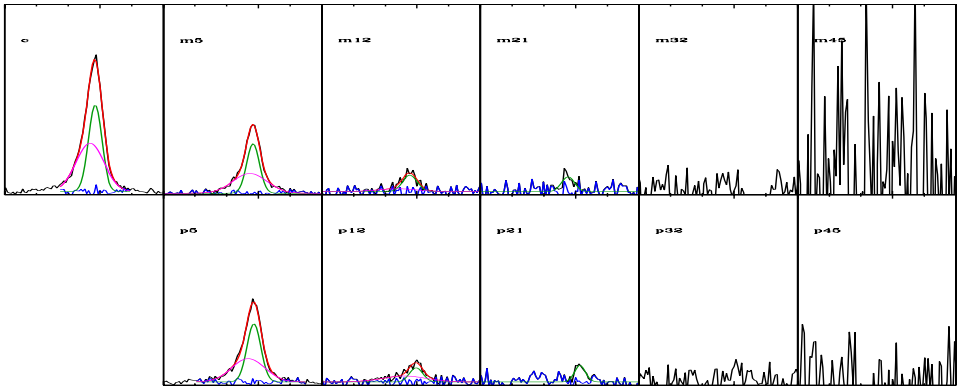

Figure B.195: DG-Object 207

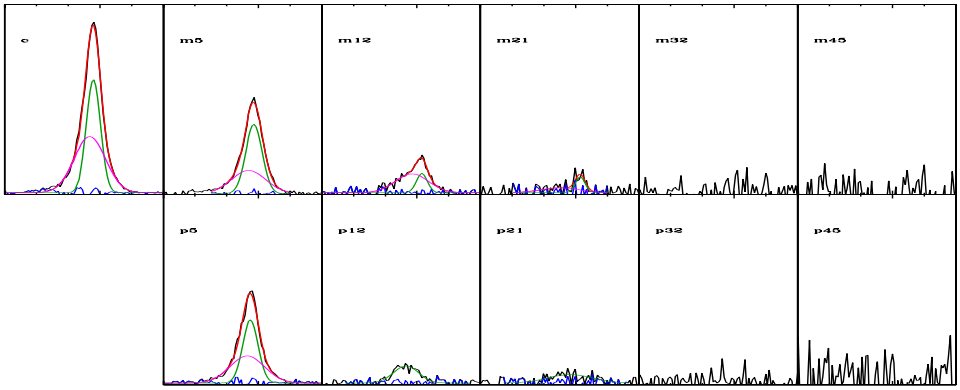

Figure B.196: DG-Object 208

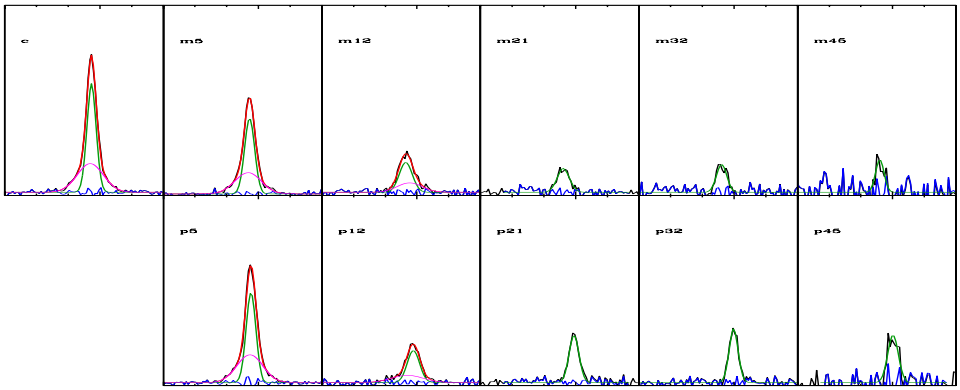

Figure B.197: DG-Object 209

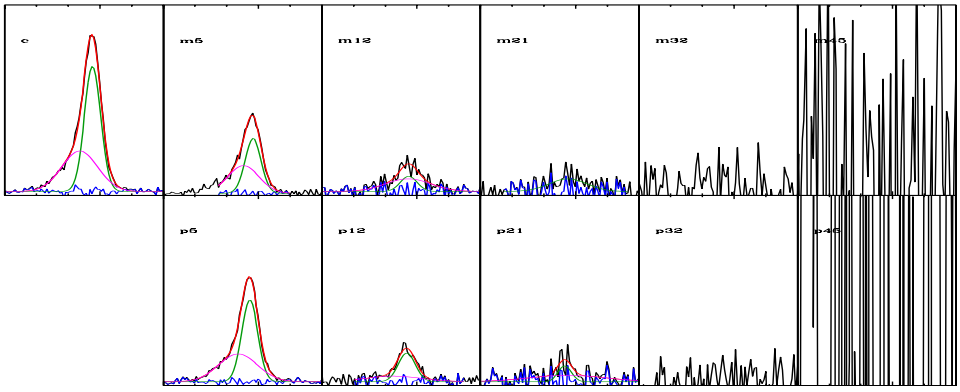

Figure B.198: DG-Object 210

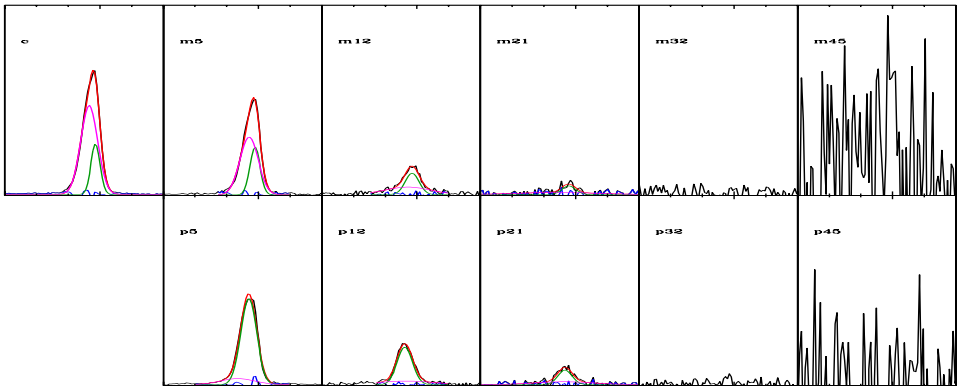

Figure B.199: DG-Object 213 [U]

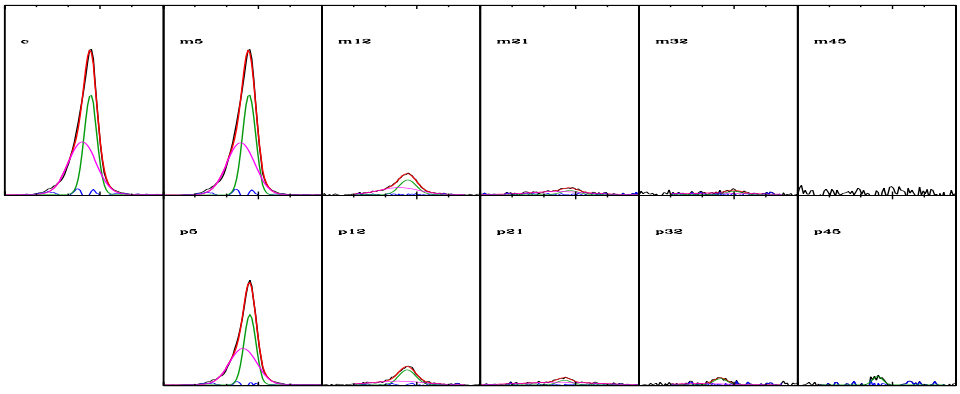

Figure B.200: DG-Object 214

B.3 Gauss-Hermite Fits

The following fits were performed using Gauss-Hermite polynomial profiles with orders 2-12.

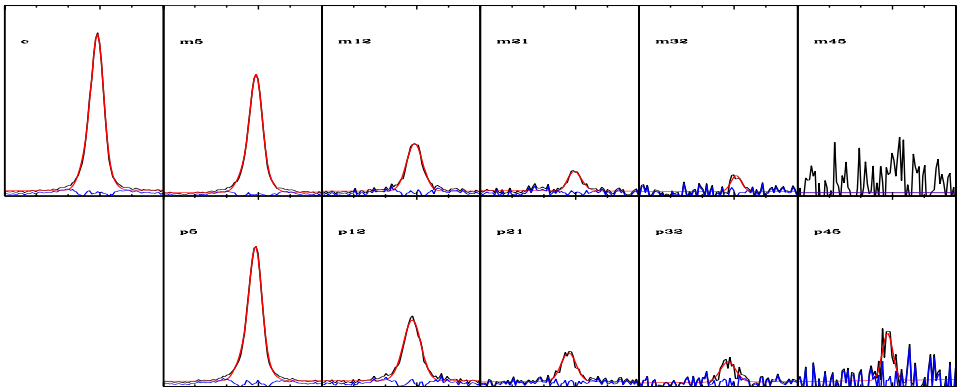

Figure B.201: GH-Object 1 [X]

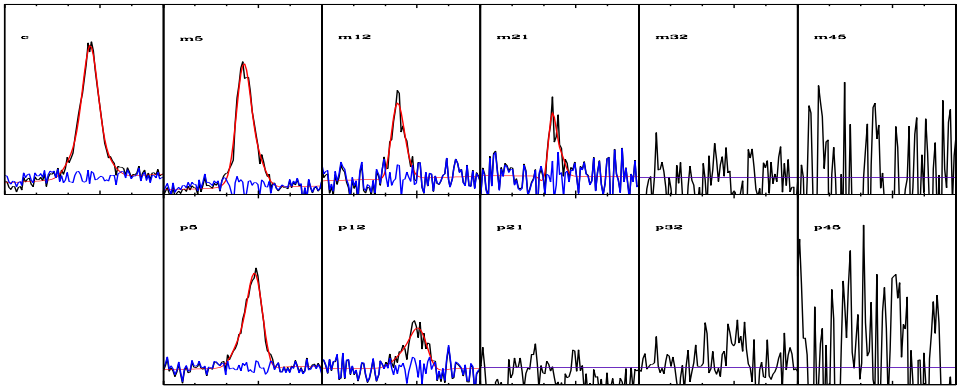

Figure B.202: GH-Object 5

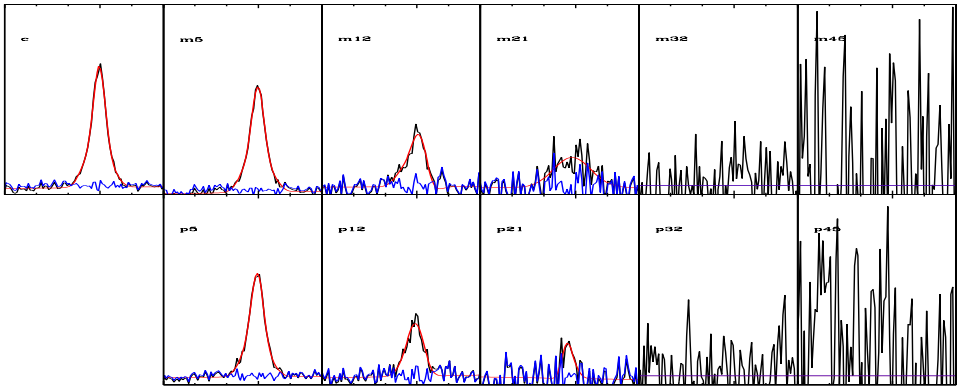

Figure B.203: GH-Object 6

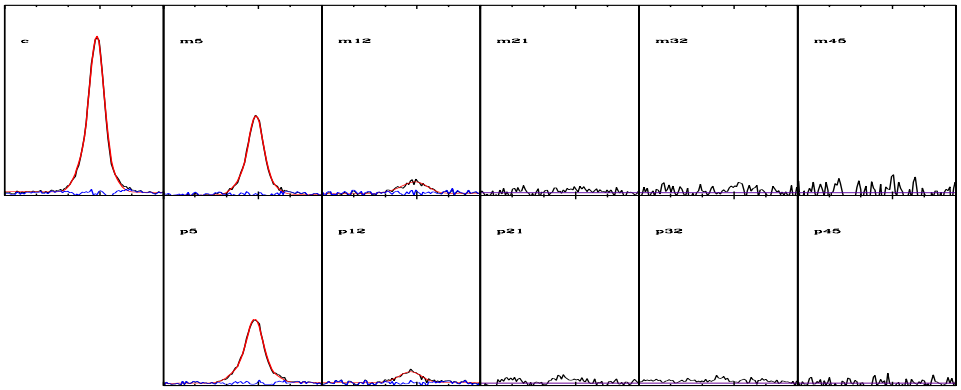

Figure B.204: GH-Object 9

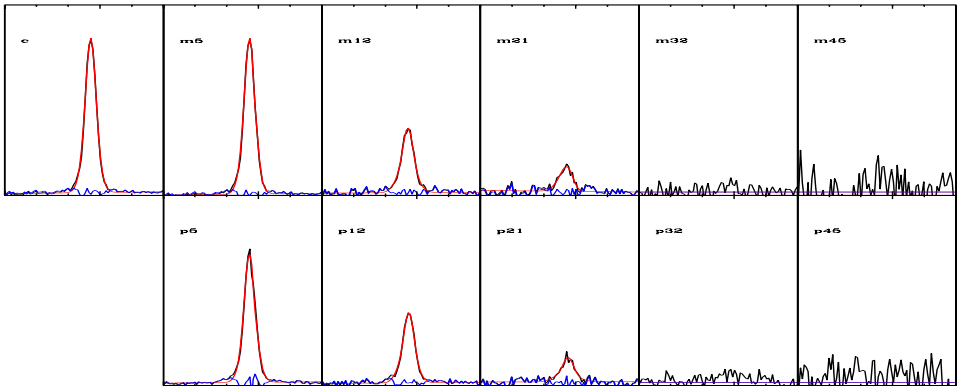

Figure B.205: GH-Object 10

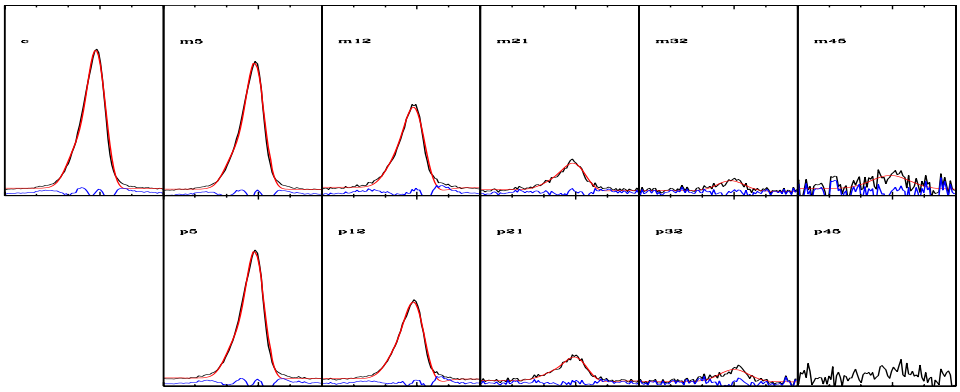

Figure B.206: GH-Object 11 [*]

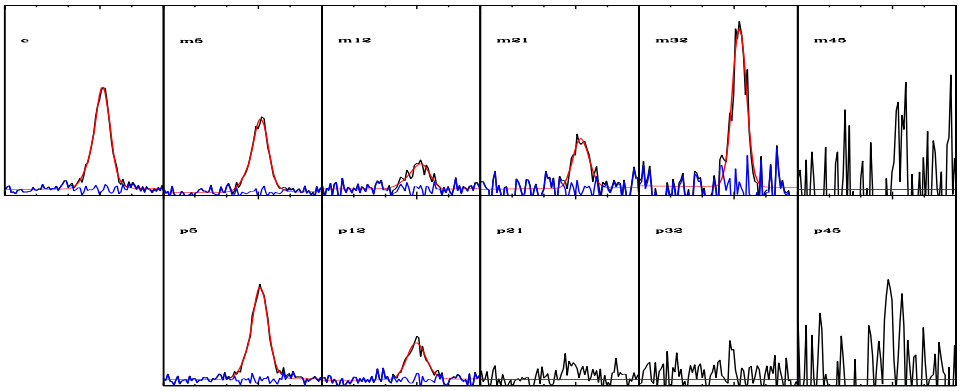

Figure B.207: GH-Object 13 [H]

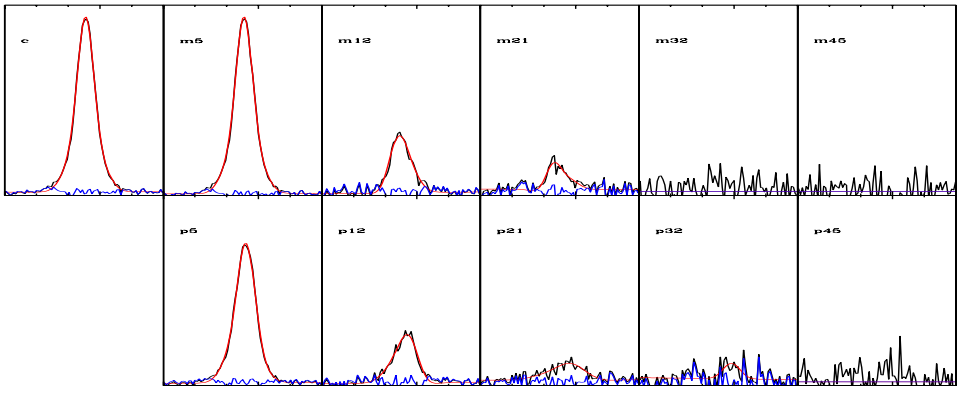

Figure B.208: GH-Object 14 [X]

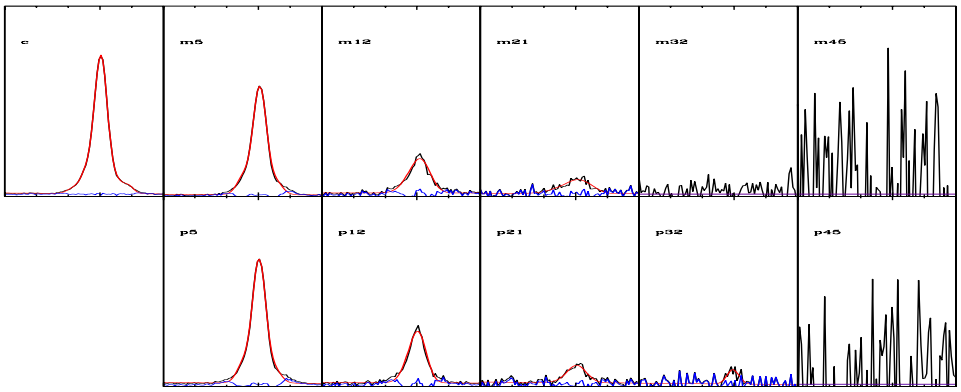

Figure B.209: GH-Object 15

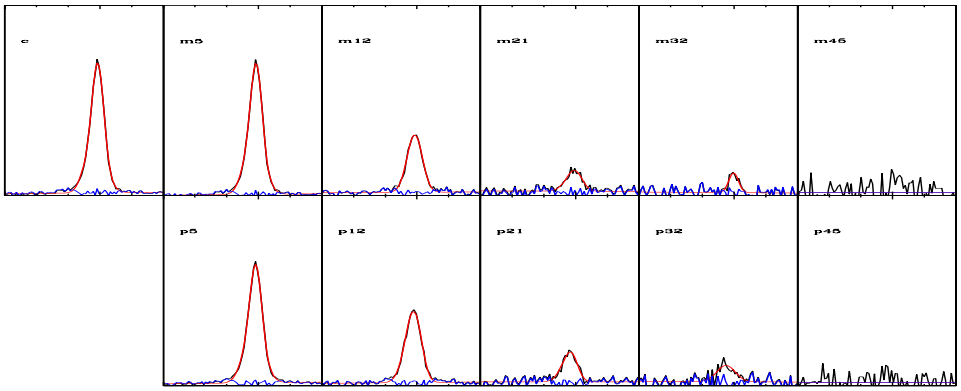

Figure B.210: GH-Object 16 [X]

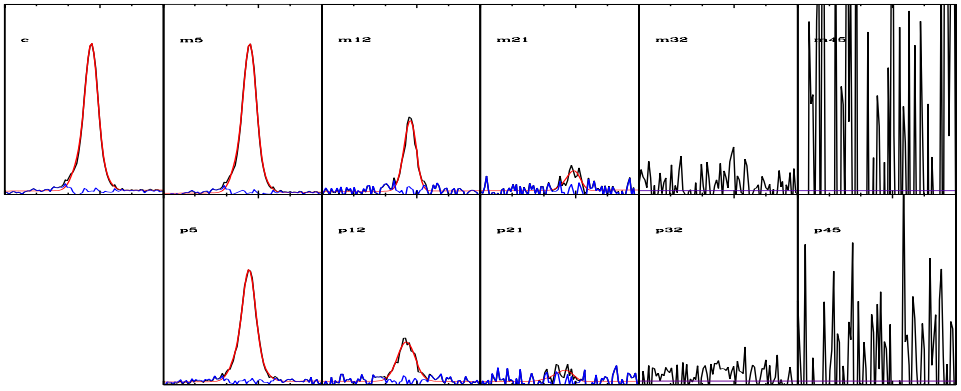

Figure B.211: GH-Object 19

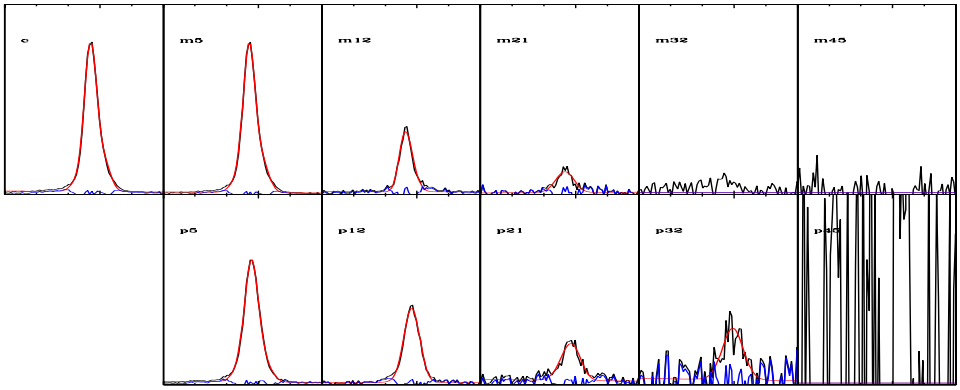

Figure B.212: GH-Object 20

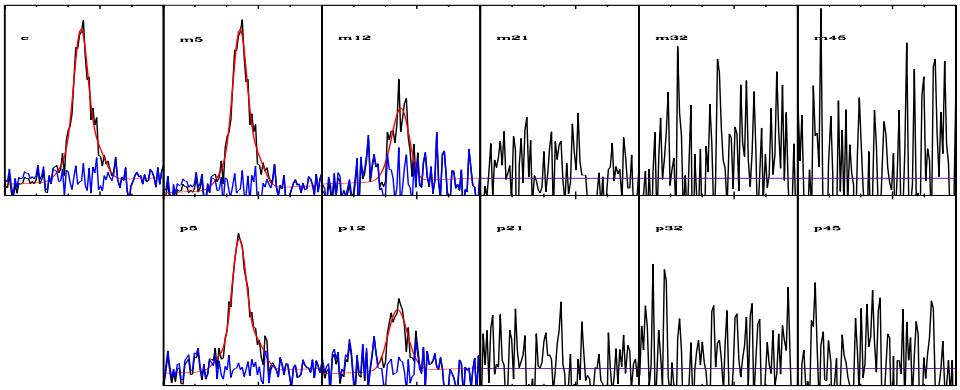

Figure B.213: GH-Object 21

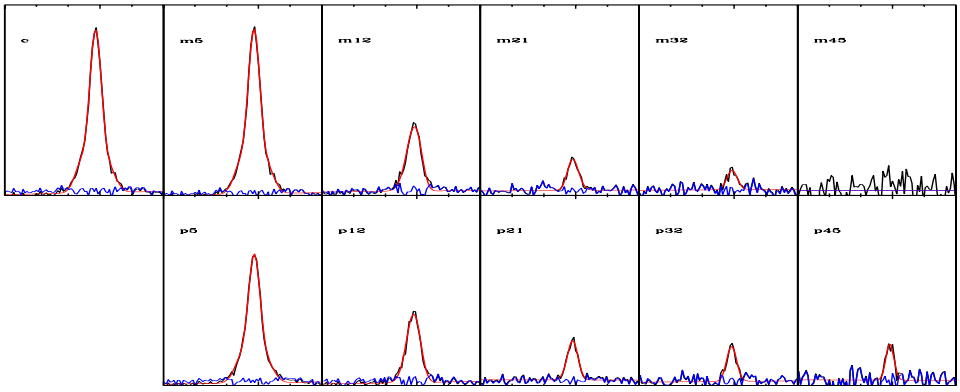

Figure B.214: GH-Object 22

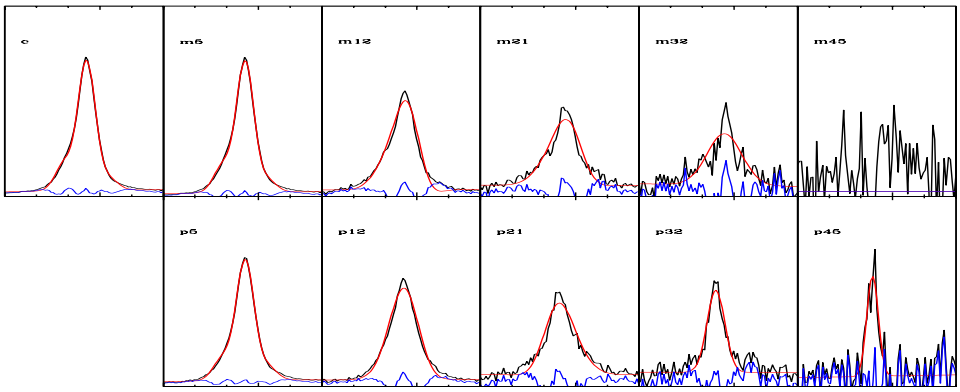

Figure B.215: GH-Object 23 [B]

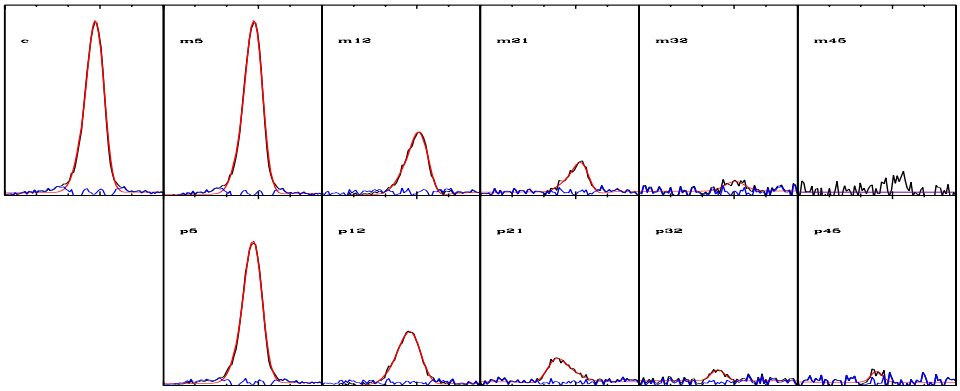

Figure B.216: GH-Object 24

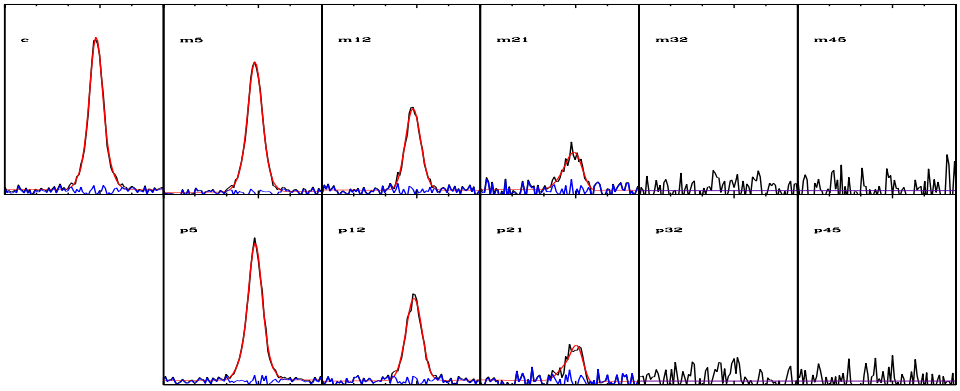

Figure B.217: GH-Object 26

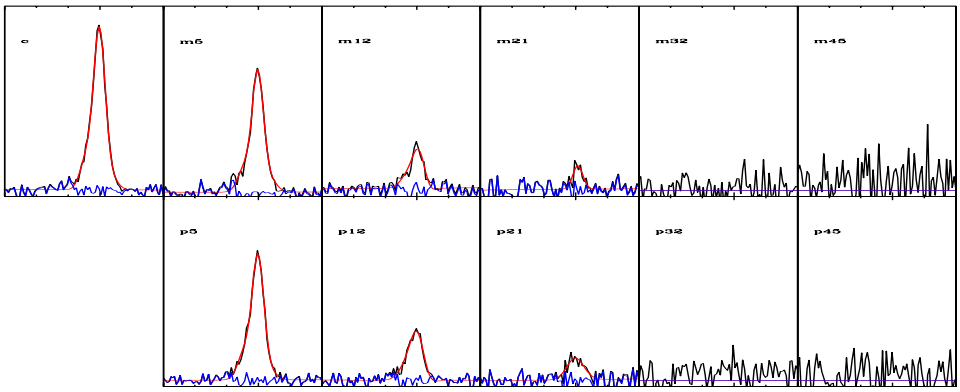

Figure B.218: GH-Object 27

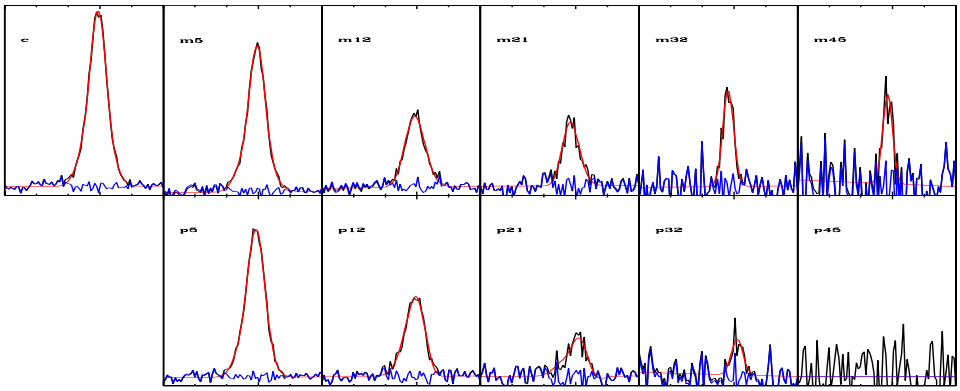

Figure B.219: GH-Object 28 [H]

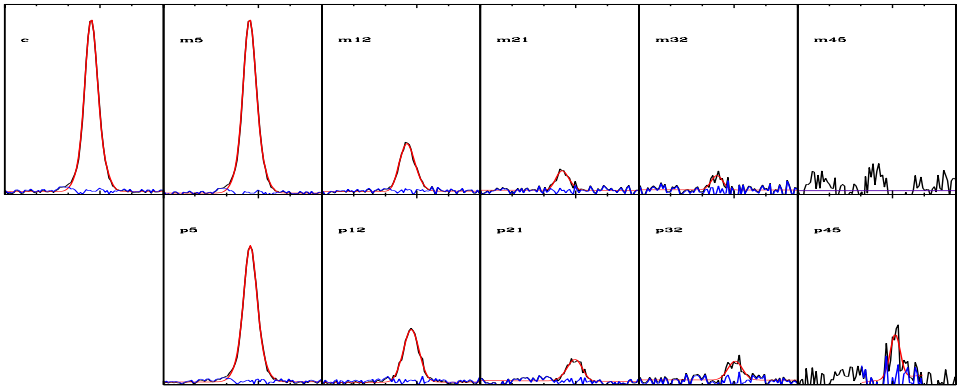

Figure B.220: GH-Object 29

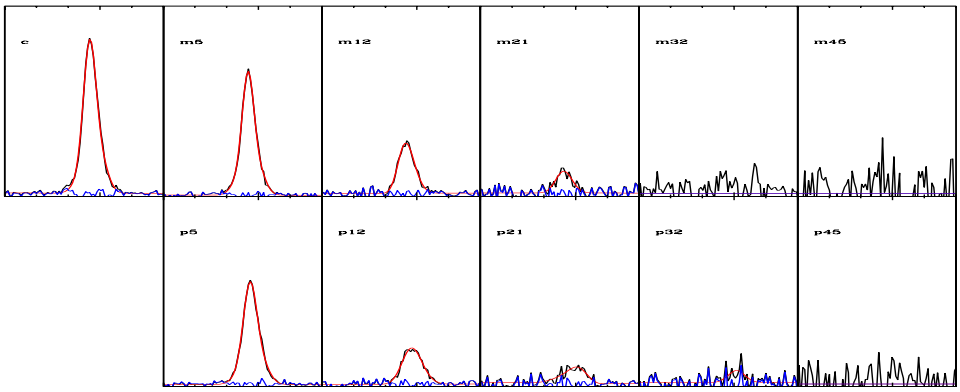

Figure B.221: GH-Object 30

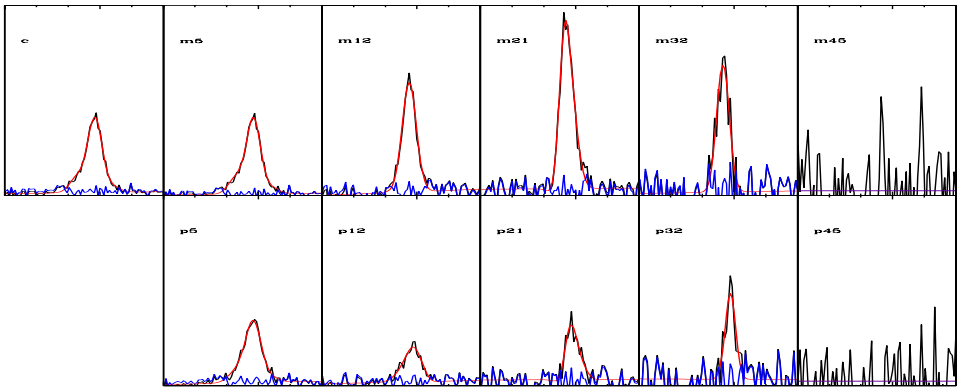

Figure B.222: GH-Object 31 [H]

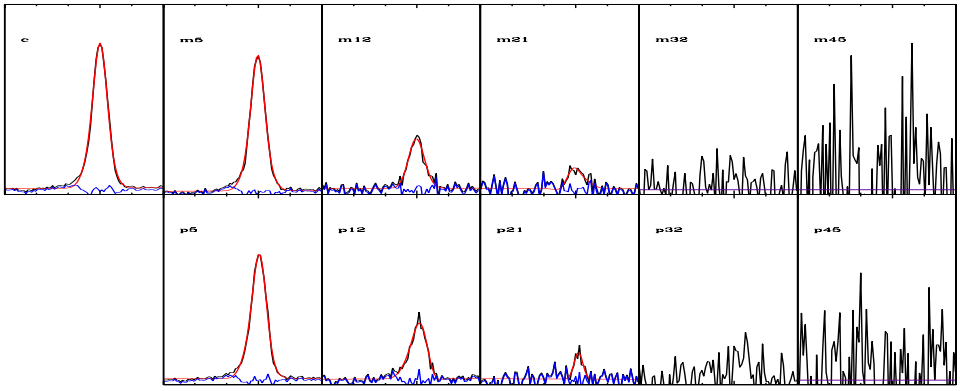

Figure B.223: GH-Object 32

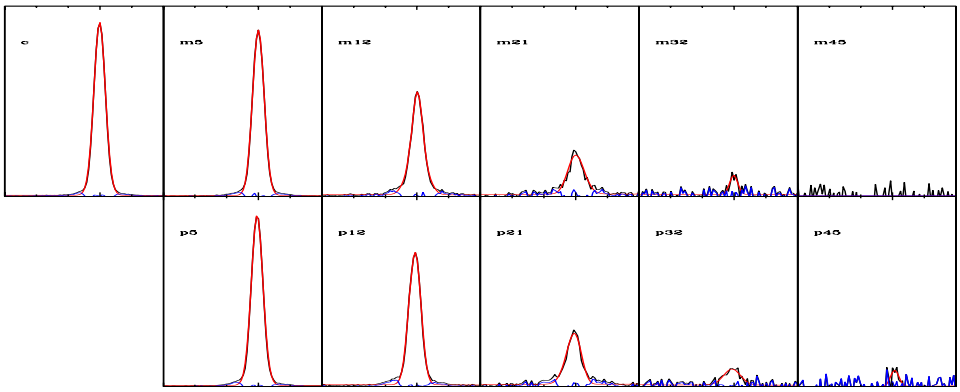

Figure B.224: GH-Object 33 [X]

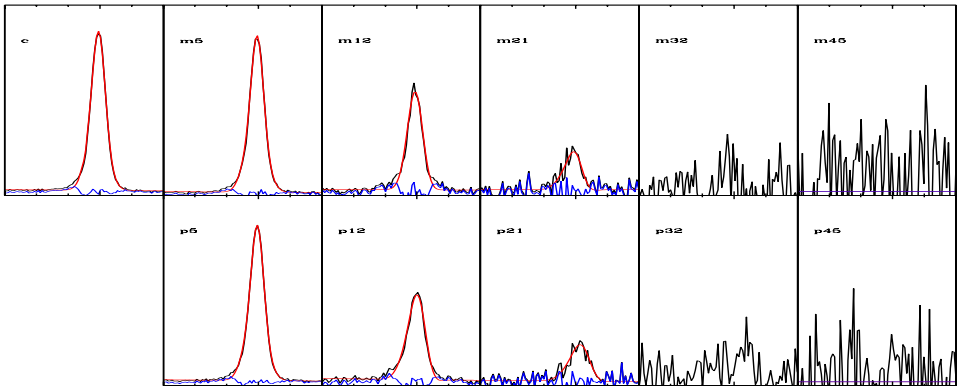

Figure B.225: GH-Object 34

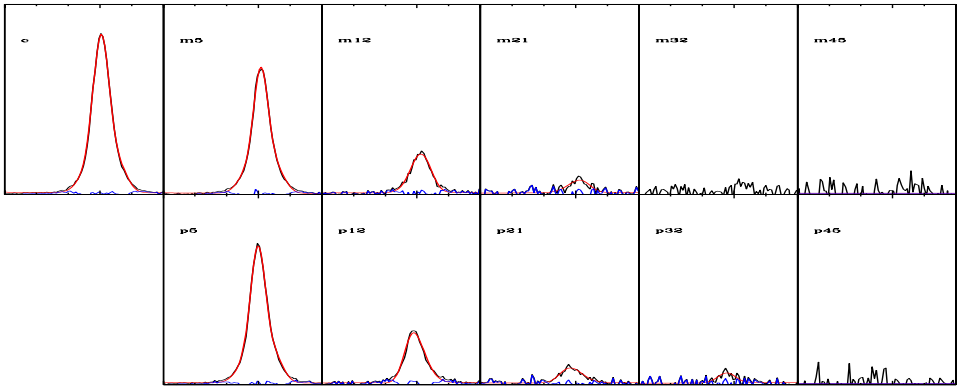

Figure B.226: GH-Object 35

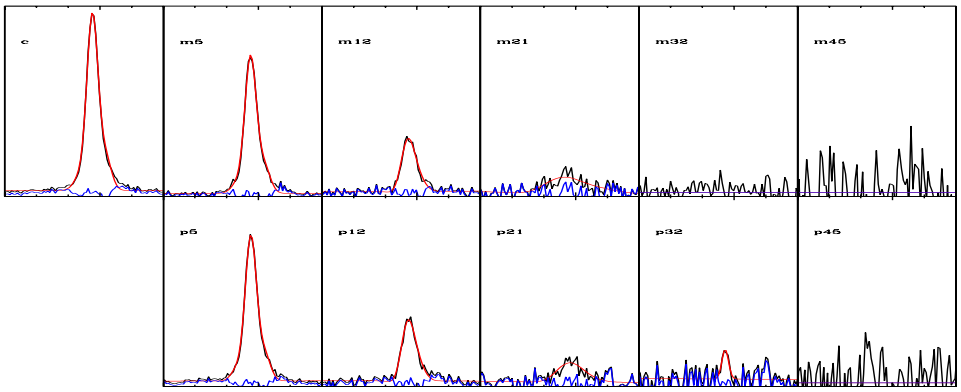

Figure B.227: GH-Object 36

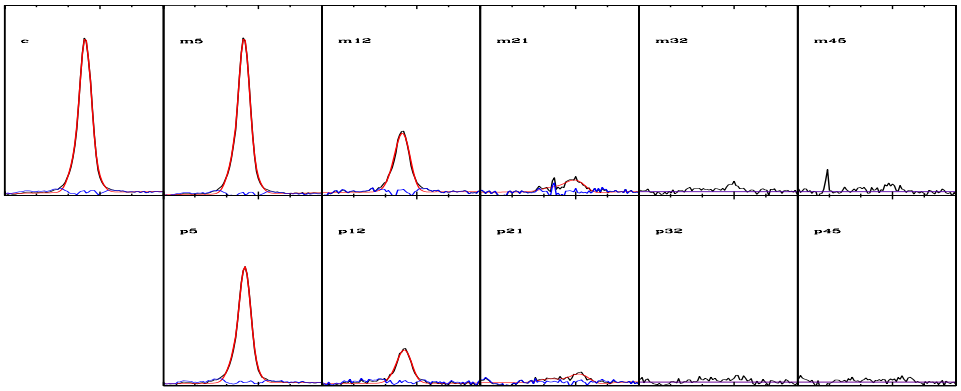

Figure B.228: GH-Object 37 [X]

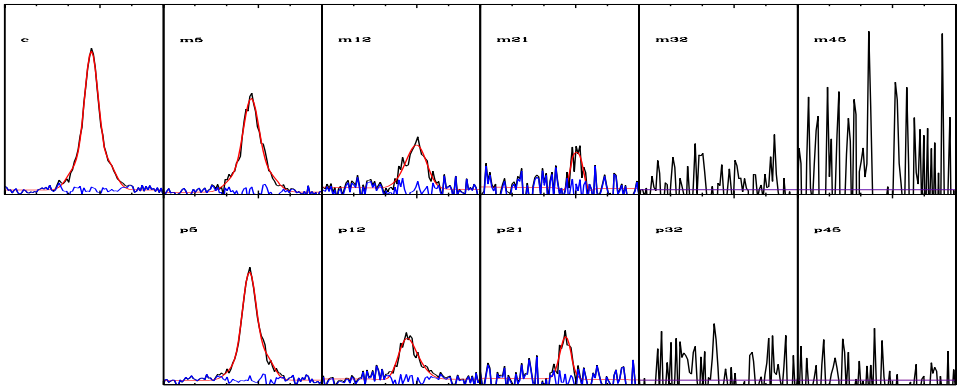

Figure B.229: GH-Object 38

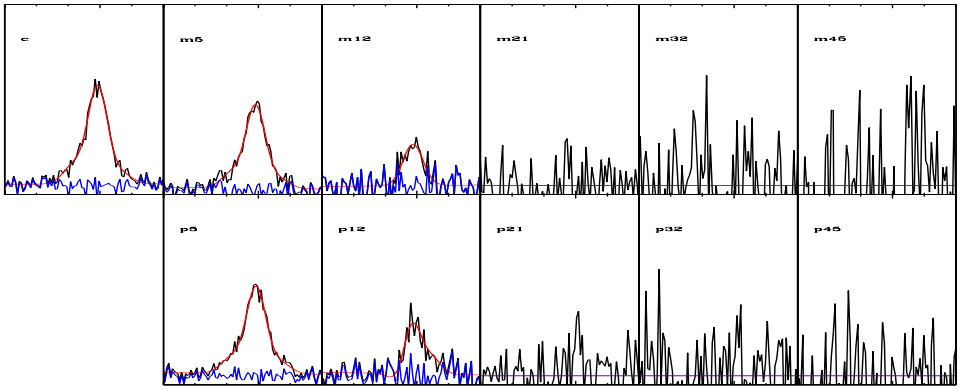

Figure B.230: GH-Object 39

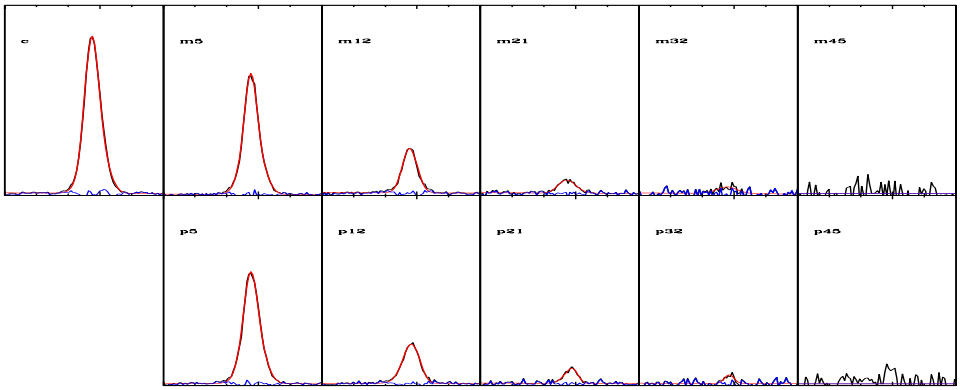

Figure B.231: GH-Object 40

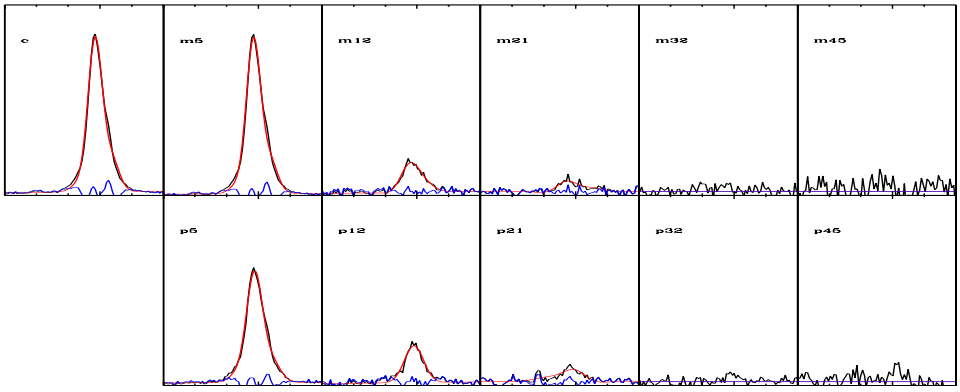

Figure B.232: GH-Object 41

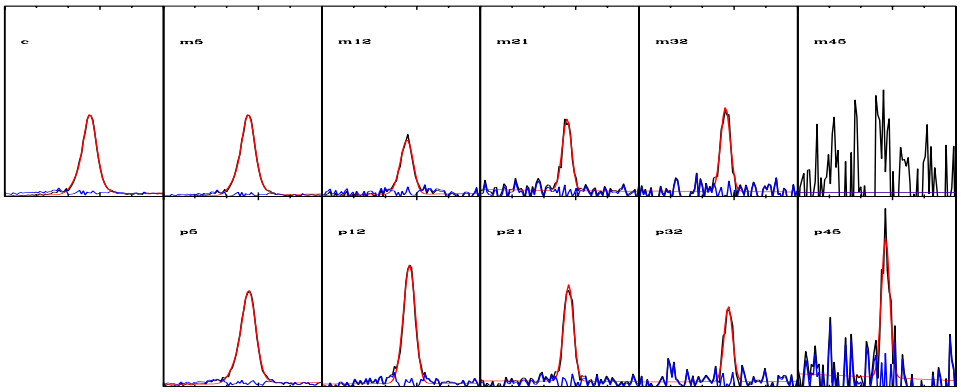

Figure B.233: GH-Object 42 [H]

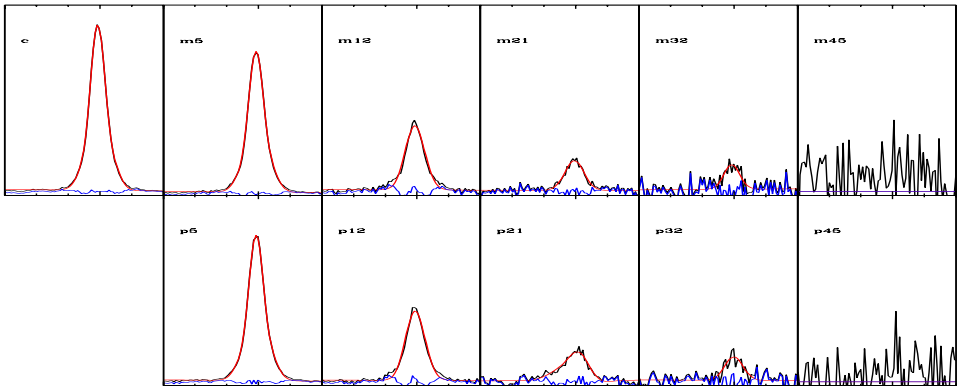

Figure B.234: GH-Object 43

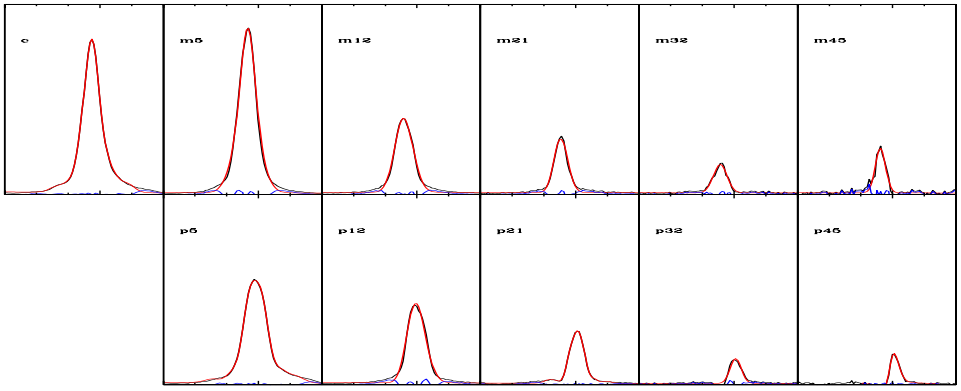

Figure B.235: GH-Object 44

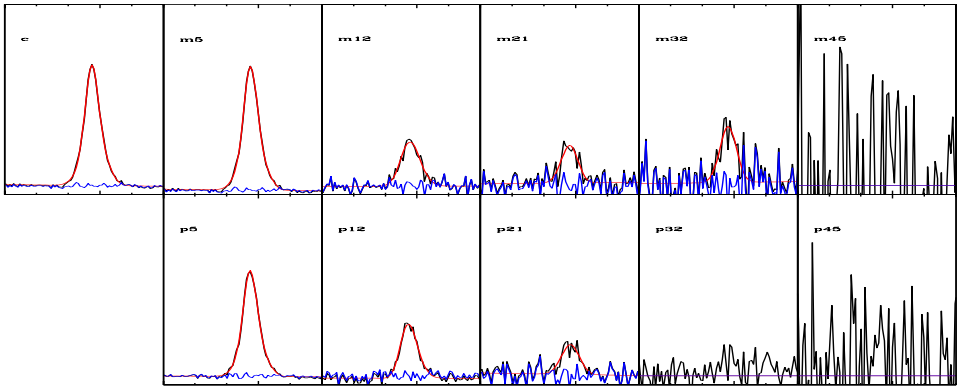

Figure B.236: GH-Object 45

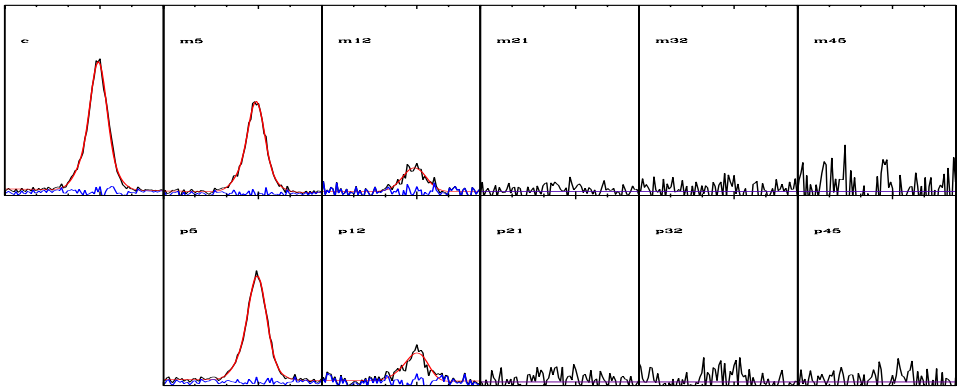

Figure B.237: GH-Object 46

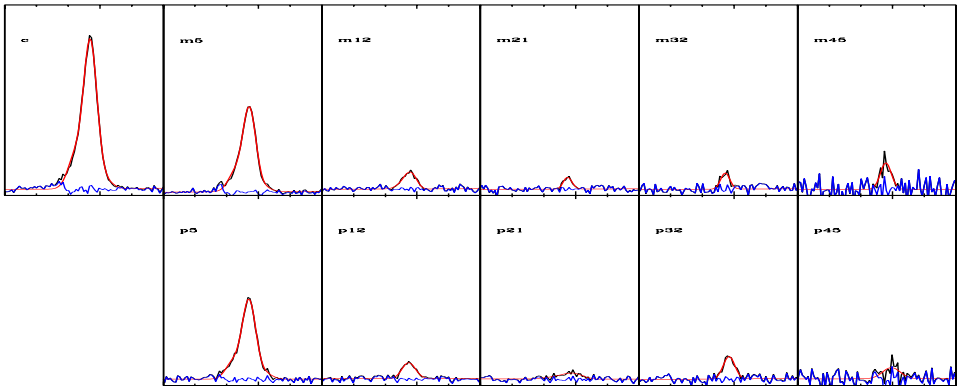

Figure B.238: GH-Object 47

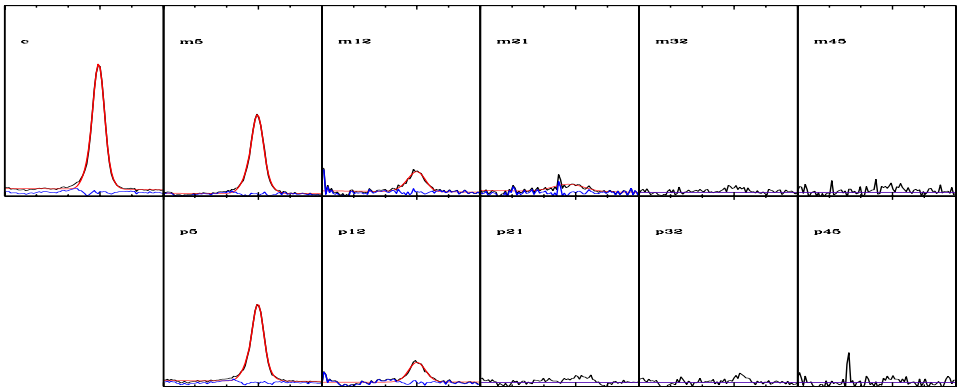

Figure B.239: GH-Object 48 [X]

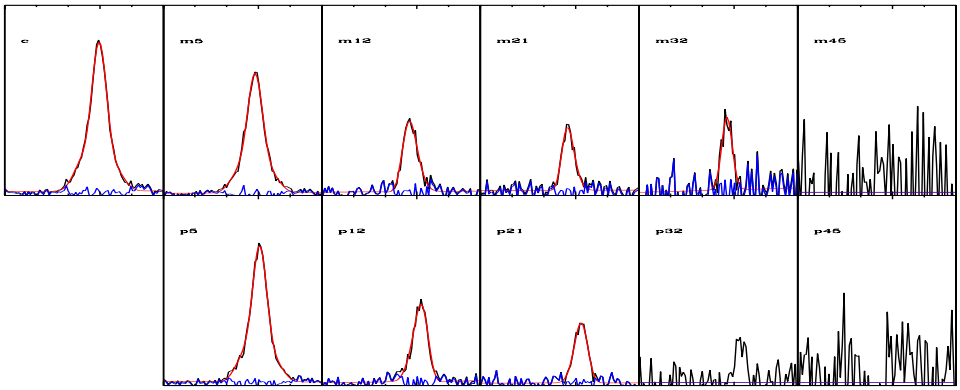

Figure B.240: GH-Object 49

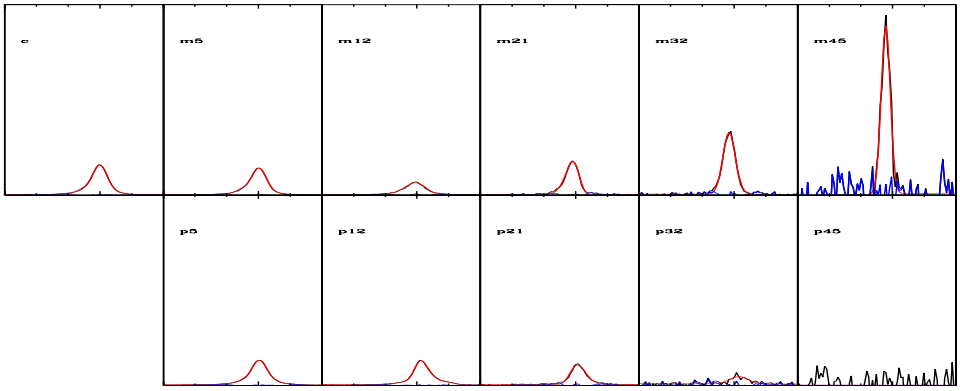

Figure B.241: GH-Object 50 [X,H]

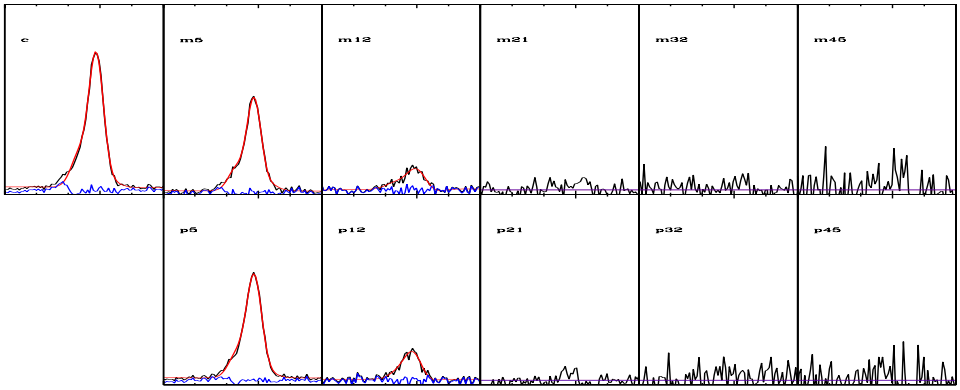

Figure B.242: GH-Object 51

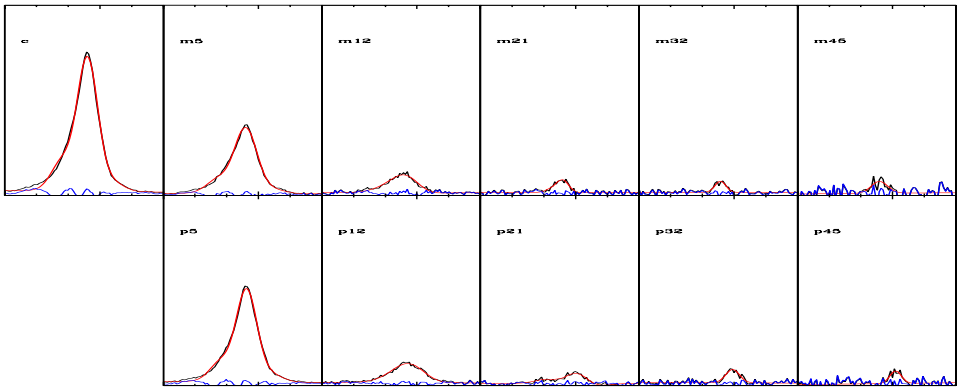

Figure B.243: GH-Object 52

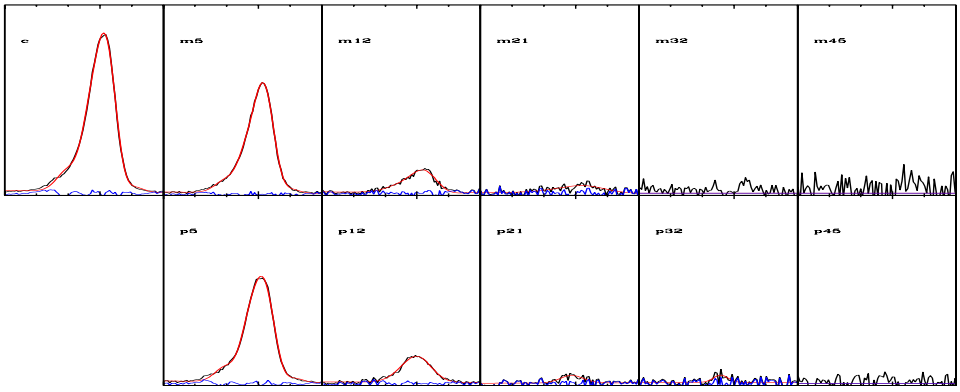

Figure B.244: GH-Object 53

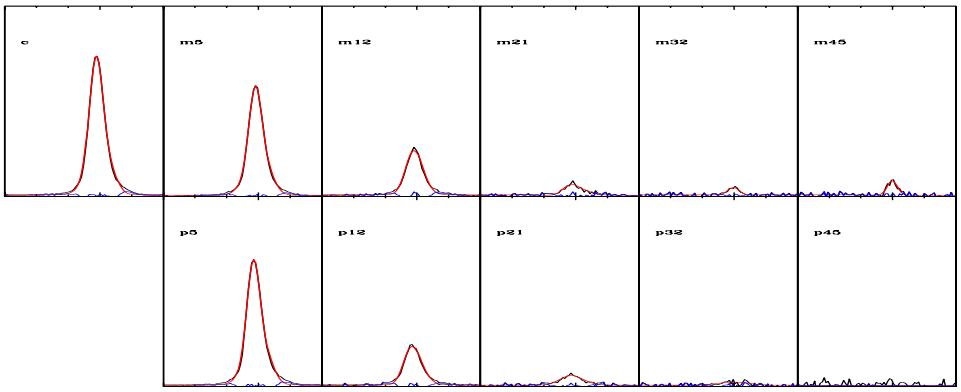

Figure B.245: GH-Object 54

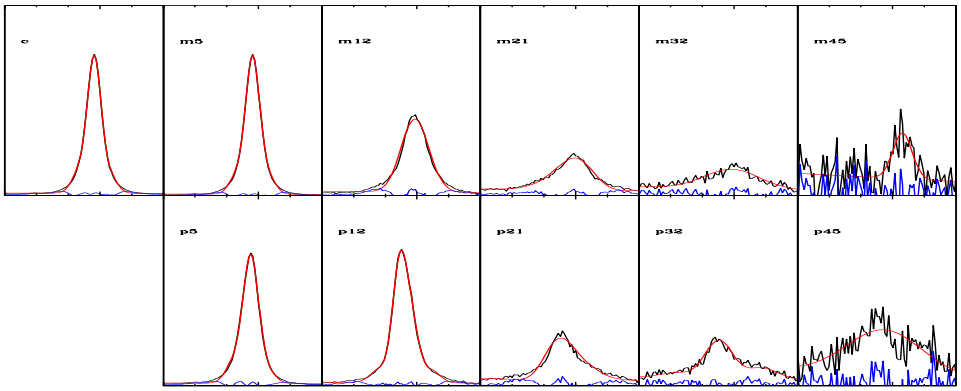

Figure B.246: GH-Object 56 X,[B]

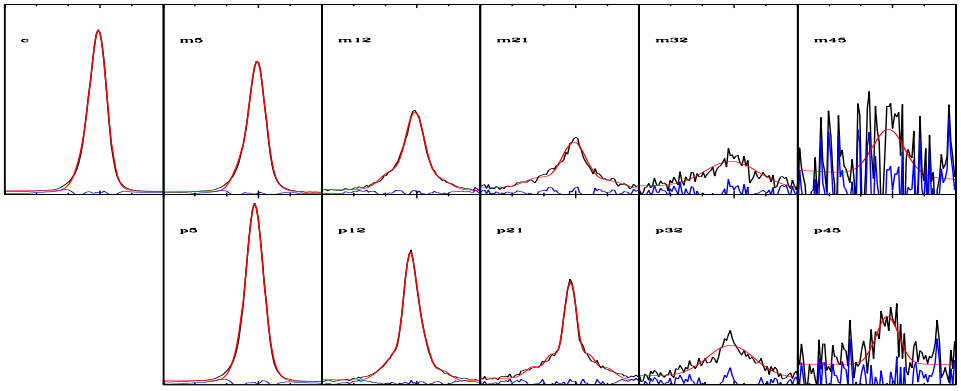

Figure B.247: GH-Object 57

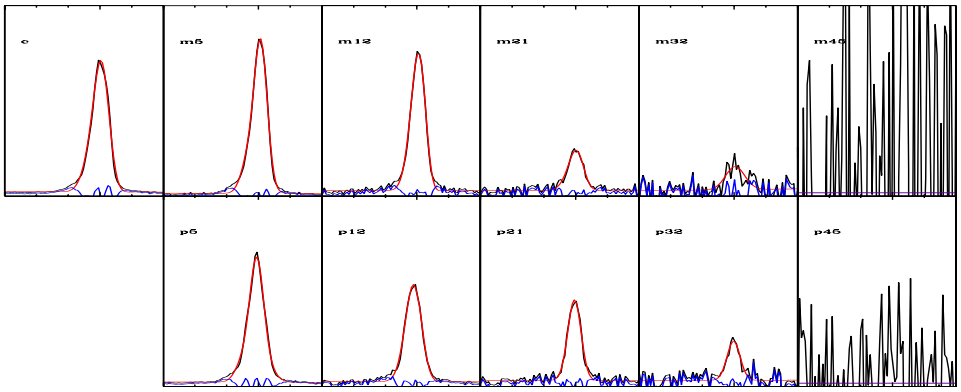

Figure B.248: GH-Object 58

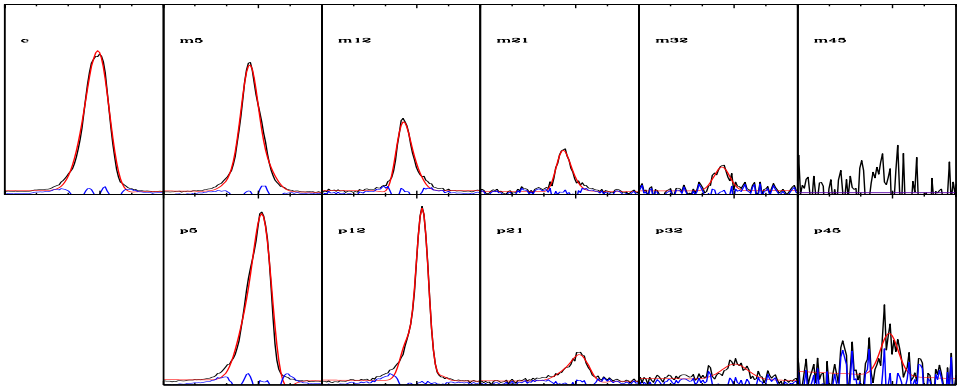

Figure B.249: GH-Object 59 [*]

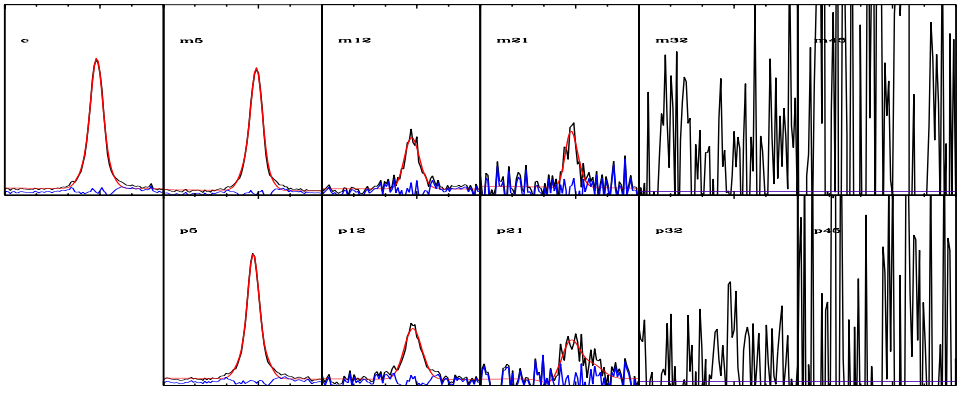

Figure B.250: GH-Object 60 [X]

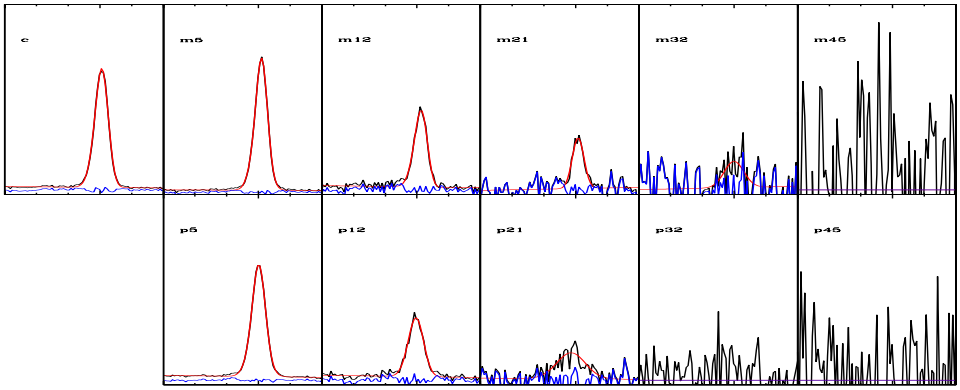

Figure B.251: GH-Object 61

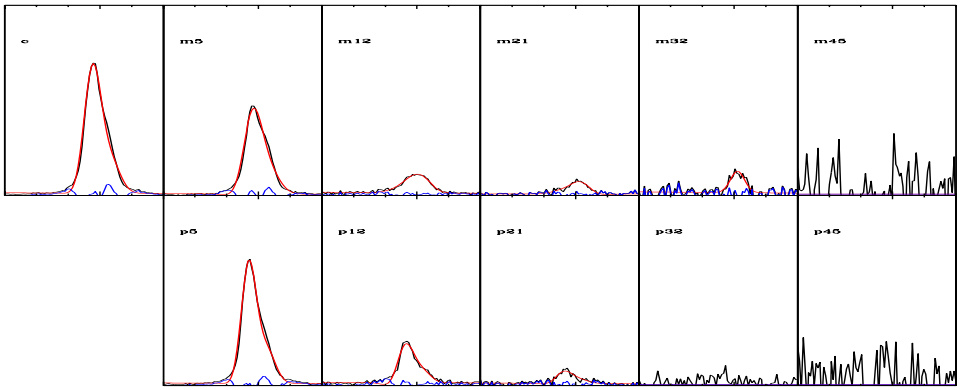

Figure B.252: GH-Object 62

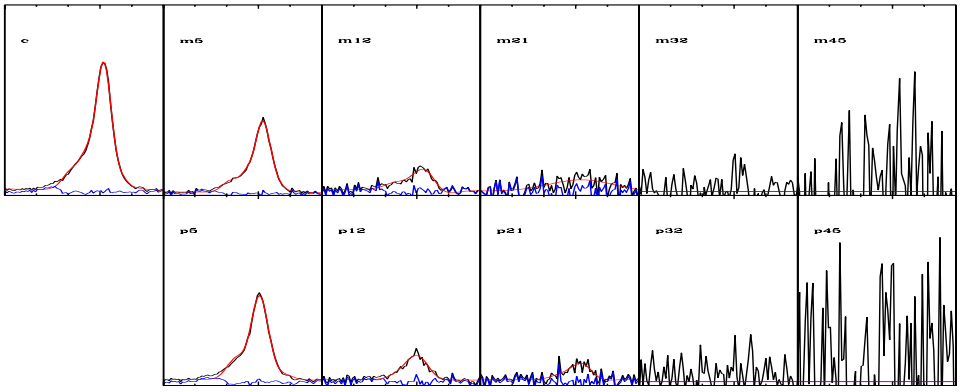

Figure B.253: GH-Object 63

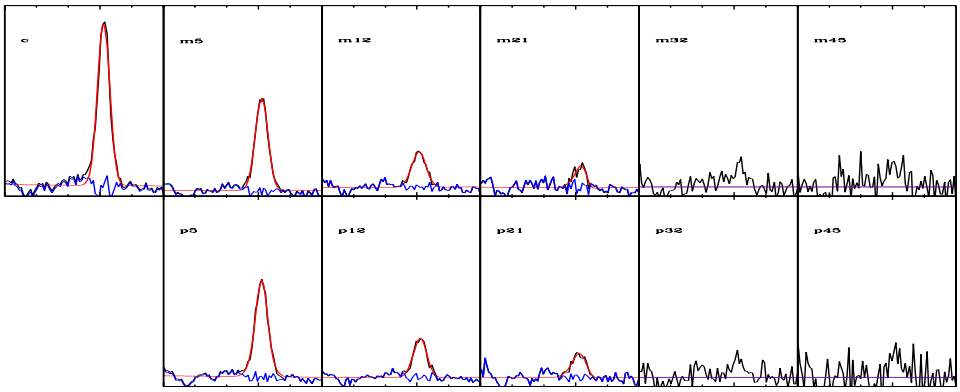

Figure B.254: GH-Object 64 [X]

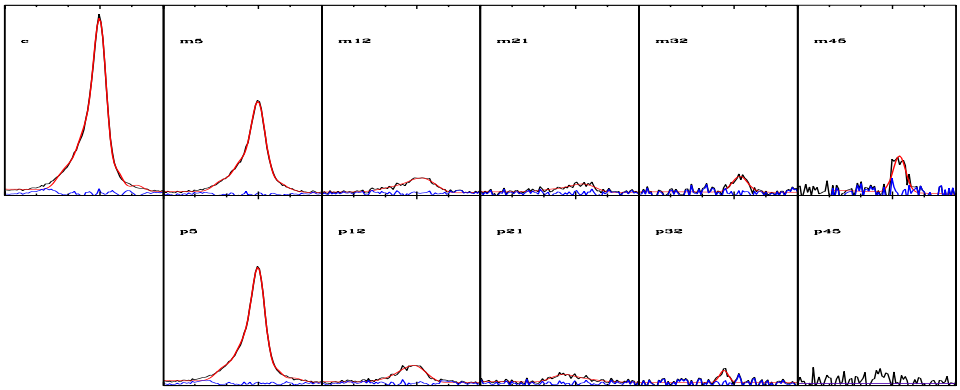

Figure B.255: GH-Object 70

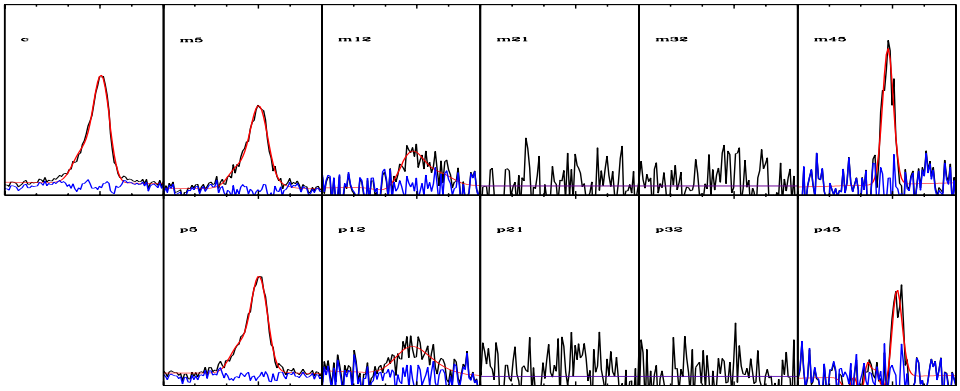

Figure B.256: GH-Object 71 [H]

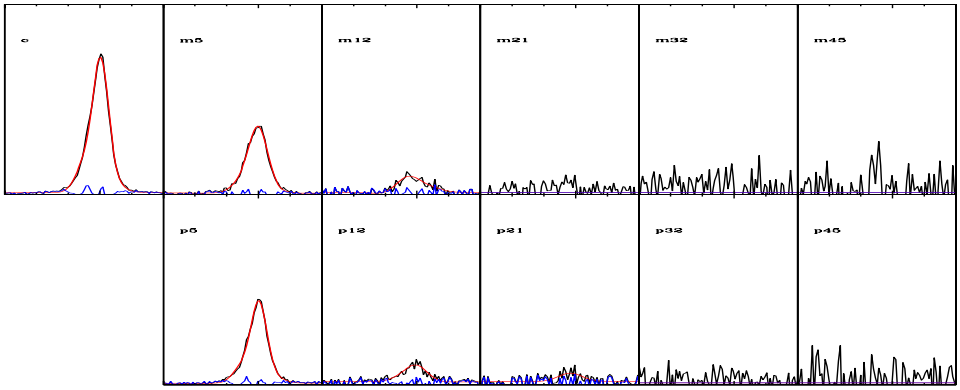

Figure B.257: GH-Object 73

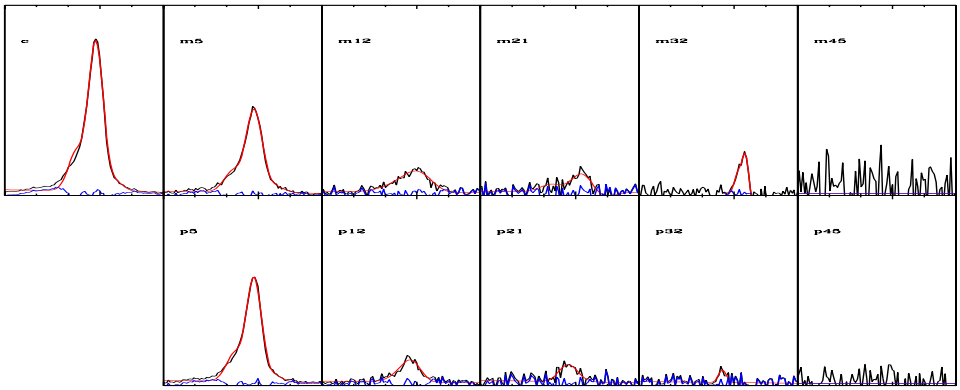

Figure B.258: GH-Object 74

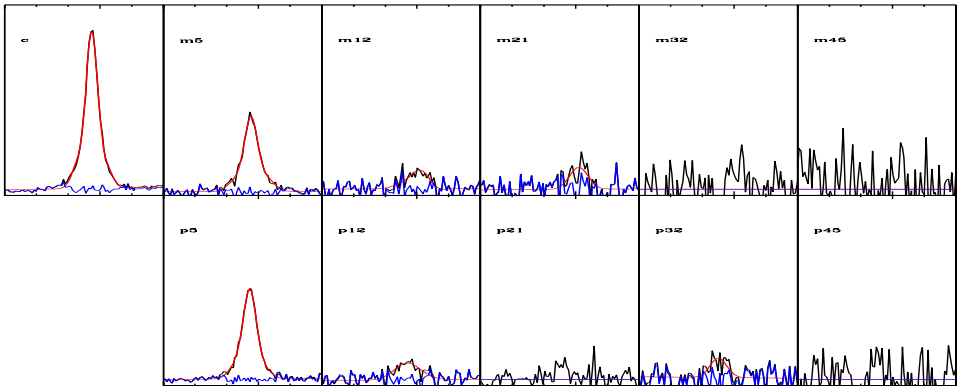

Figure B.259: GH-Object 76

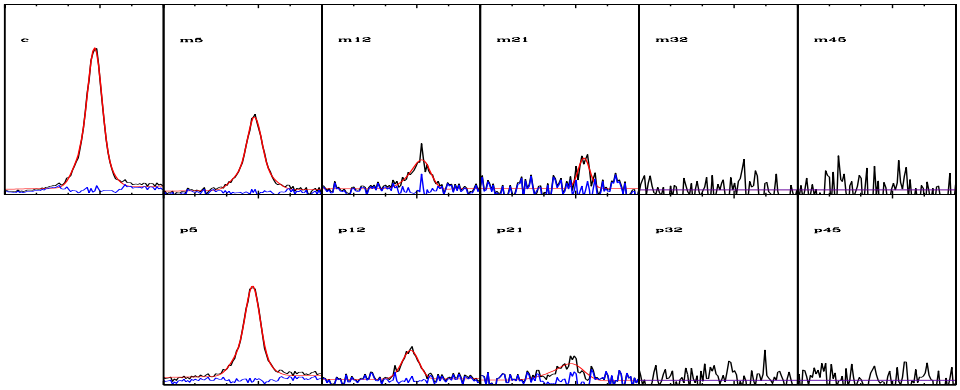

Figure B.260: GH-Object 77

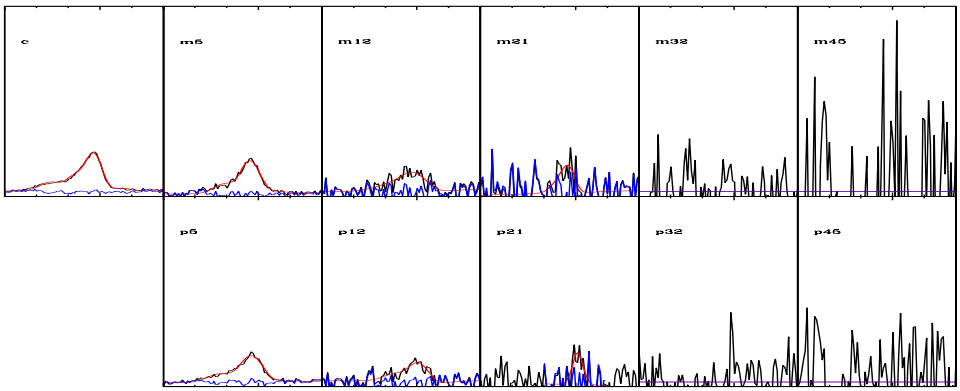

Figure B.261: GH-Object 78

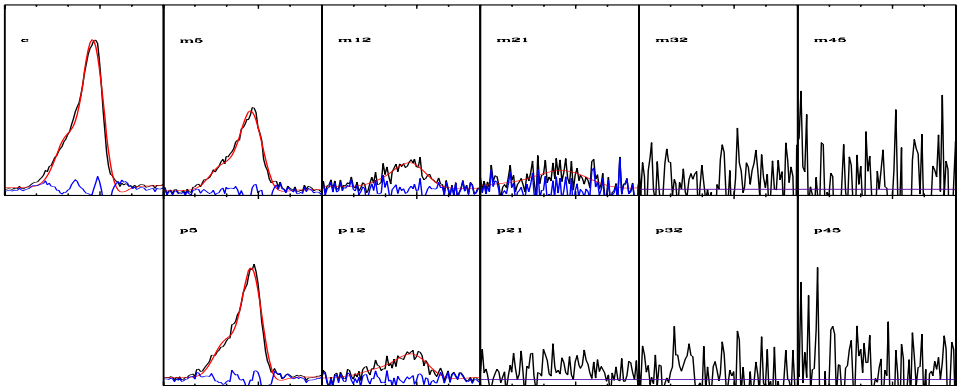

Figure B.262: GH-Object 79

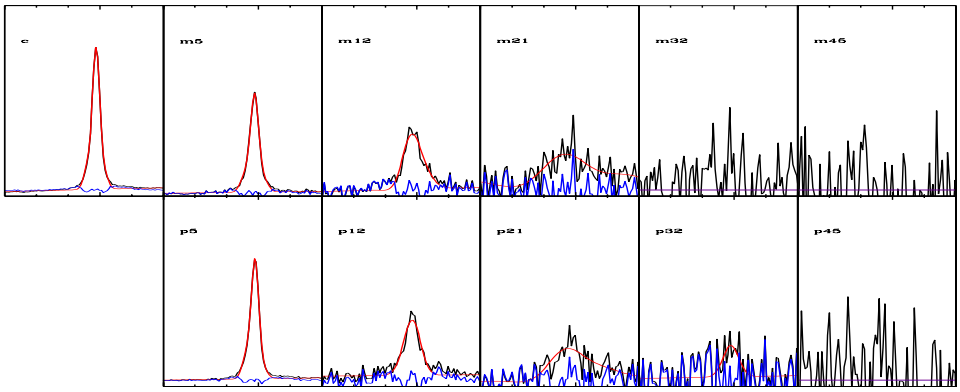

Figure B.263: GH-Object 80 [X]

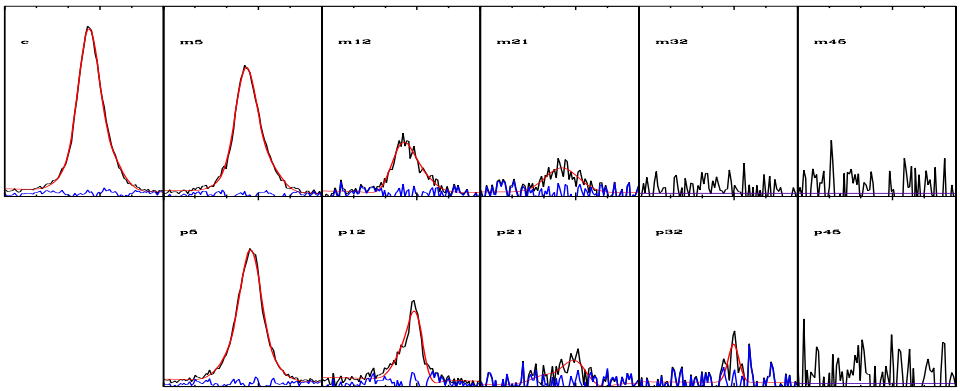

Figure B.264: GH-Object 81 [X]

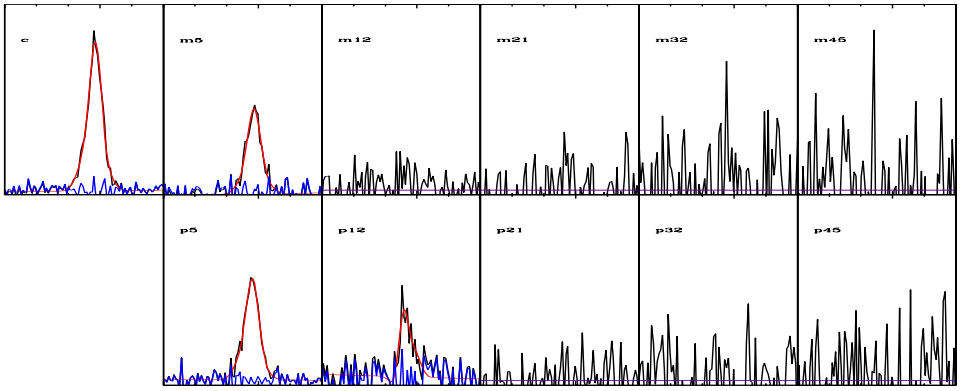

Figure B.265: GH-Object 82

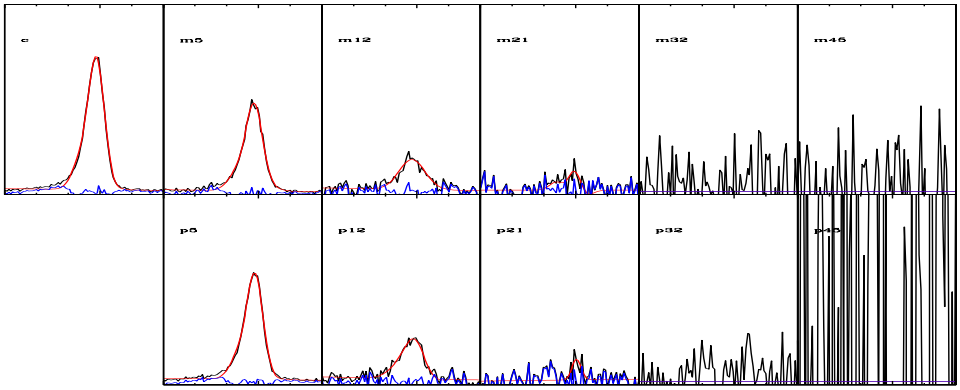

Figure B.266: GH-Object 83

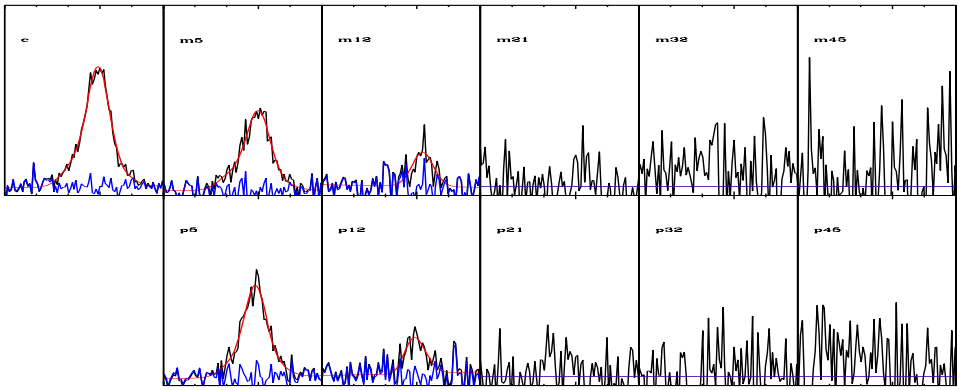

Figure B.267: GH-Object 88

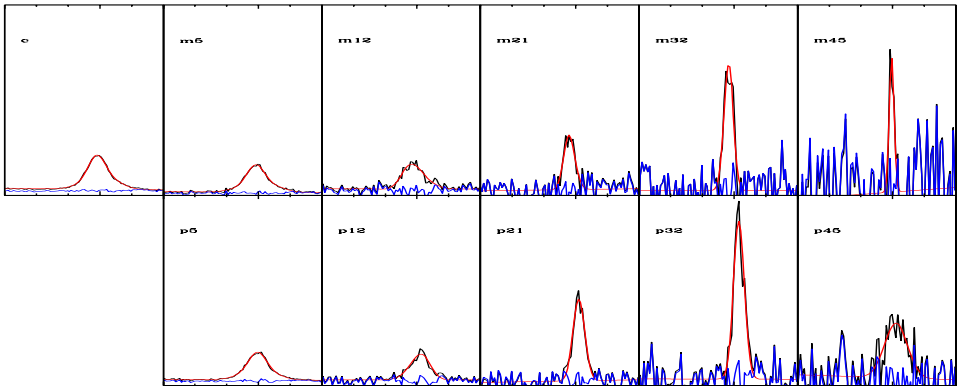

Figure B.268: GH-Object 91

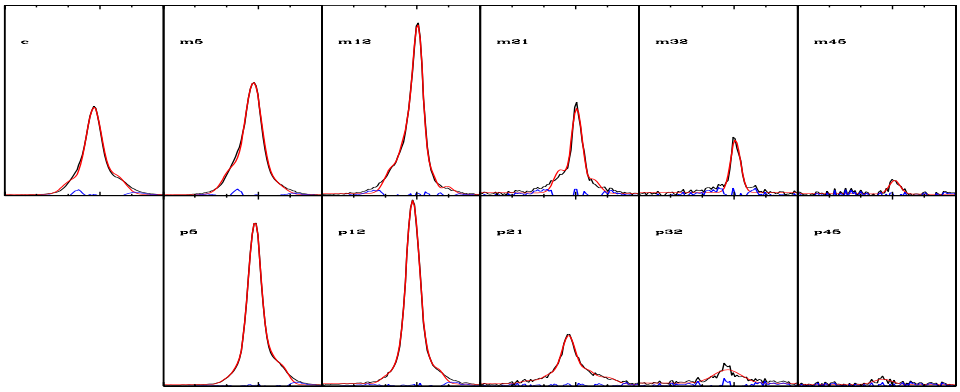

Figure B.269: GH-Object 96 [X,*]

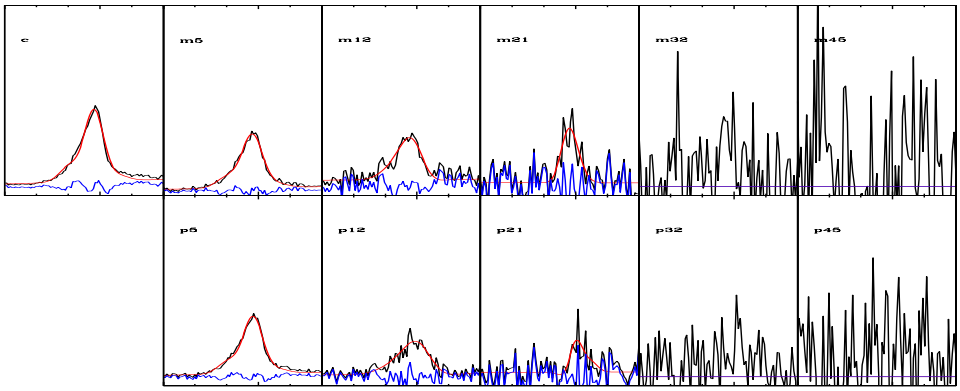

Figure B.270: GH-Object 99 [*]

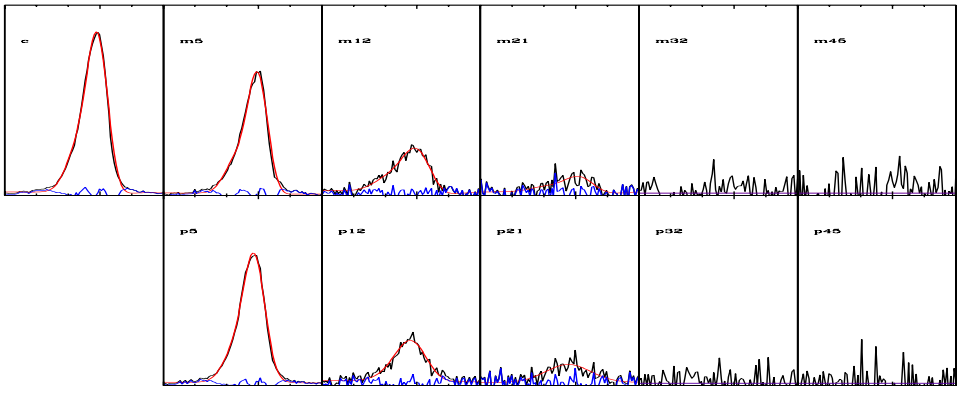

Figure B.271: GH-Object 100 [X]

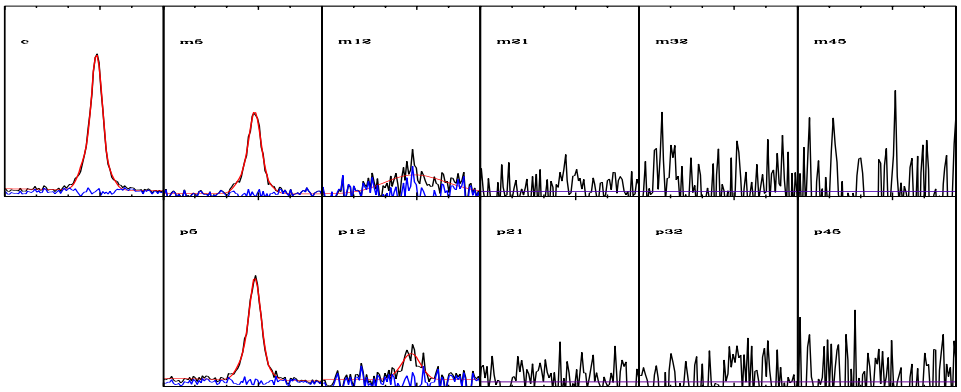

Figure B.272: GH-Object 102

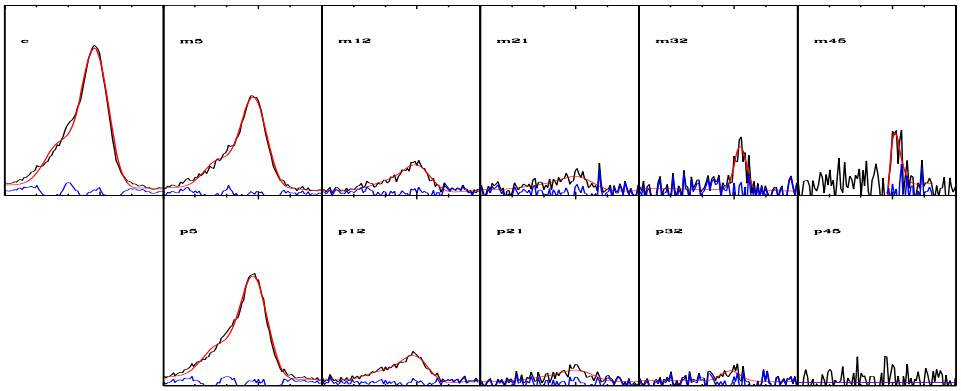

Figure B.273: GH-Object 103 [H]

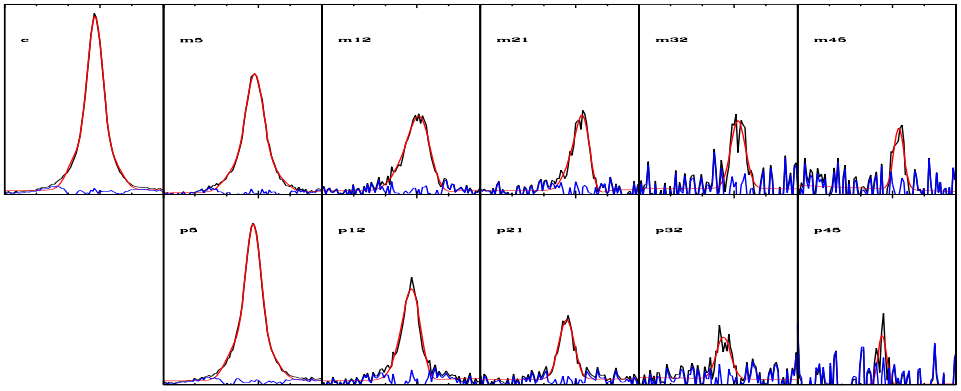

Figure B.274: GH-Object 106

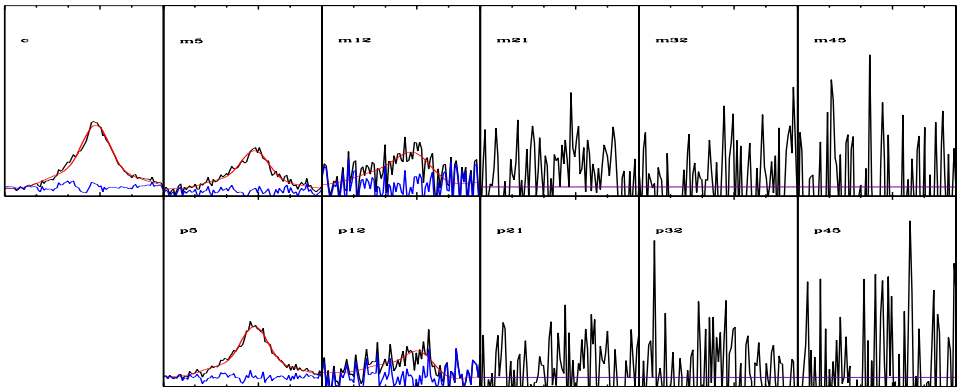

Figure B.275: GH-Object 108 [X,B]

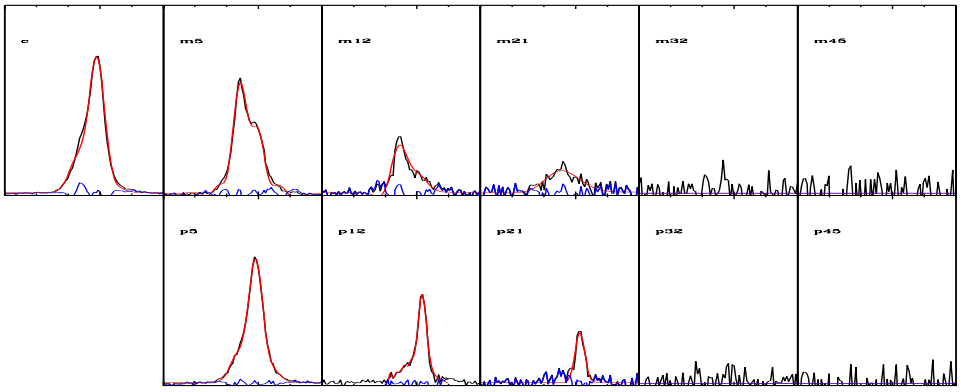

Figure B.276: GH-Object 109 [*]

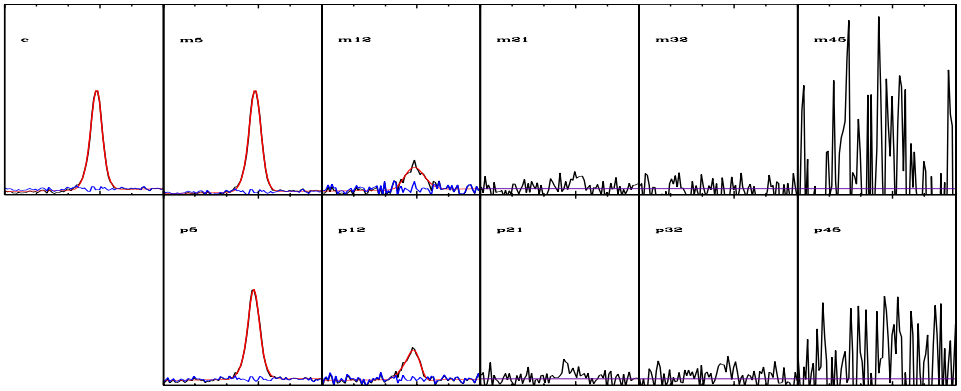

Figure B.277: GH-Object 114

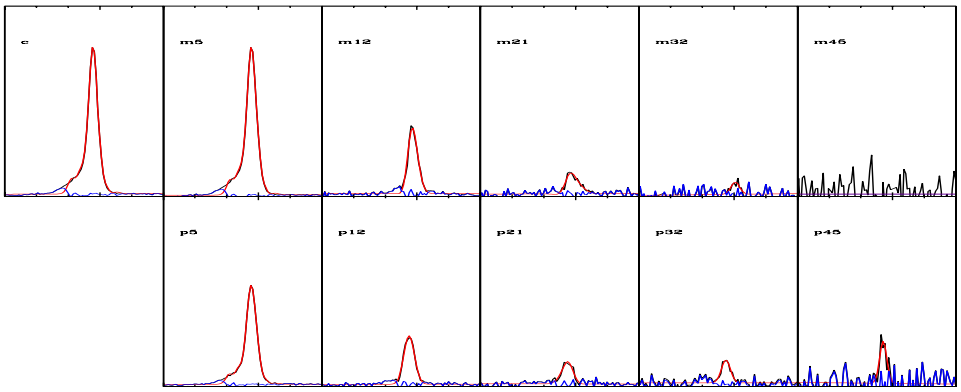

Figure B.278: GH-Object 126

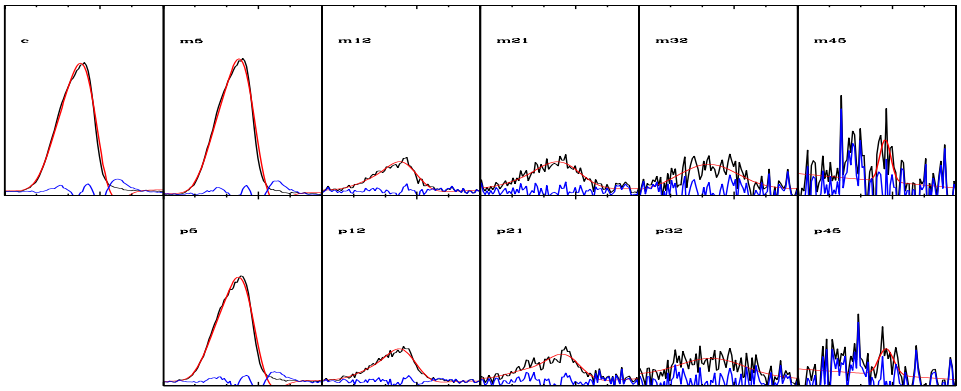

Figure B.279: GH-Object 130 [X,*]

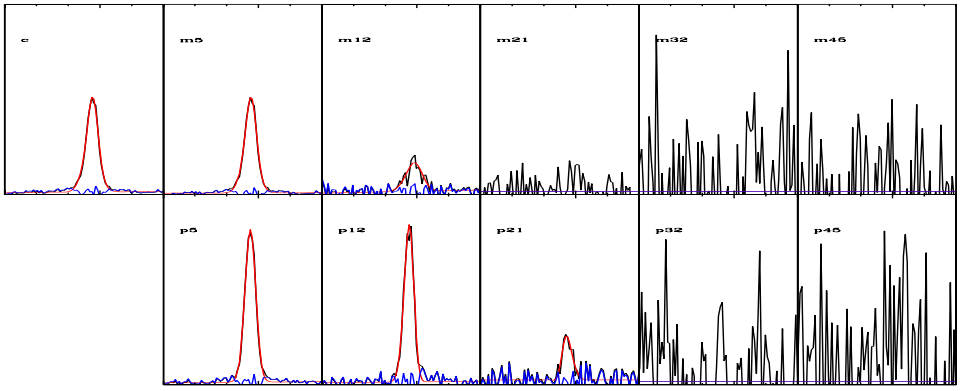

Figure B.280: GH-Object 138

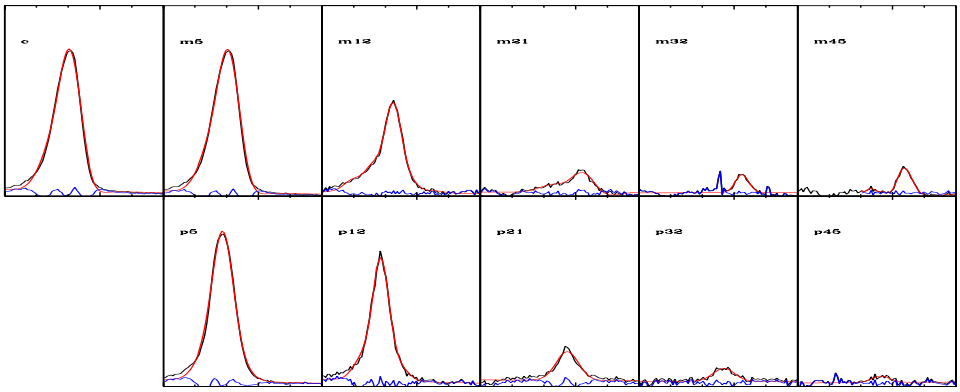

Figure B.281: GH-Object 143 [X,*]

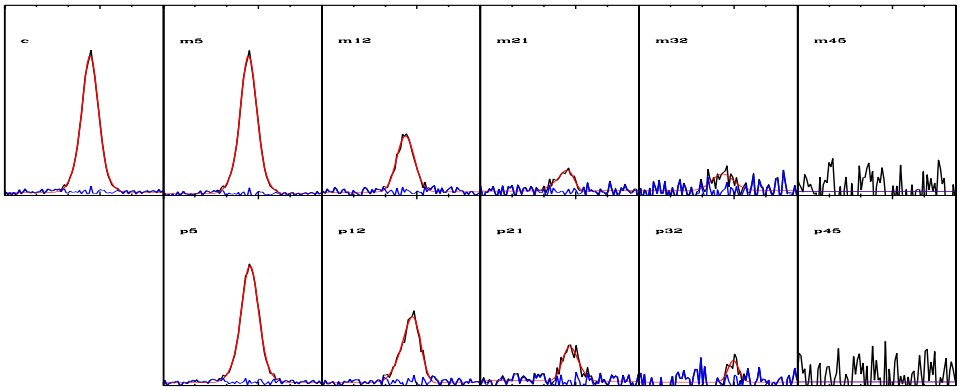

Figure B.282: GH-Object 155

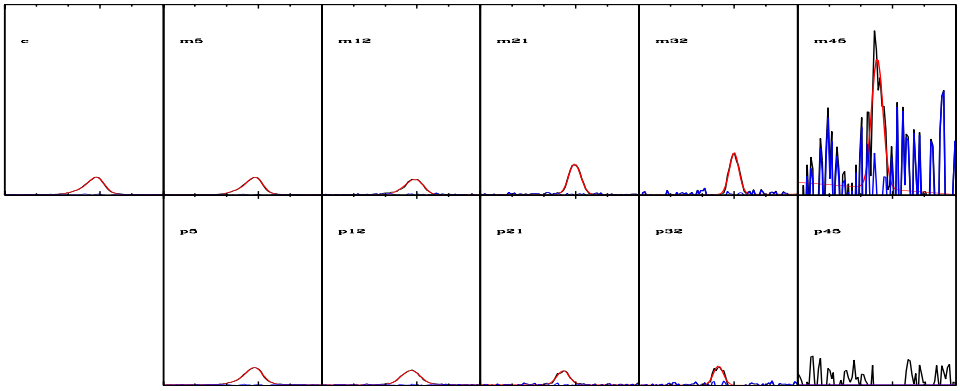

Figure B.283: GH-Object 156 [H]

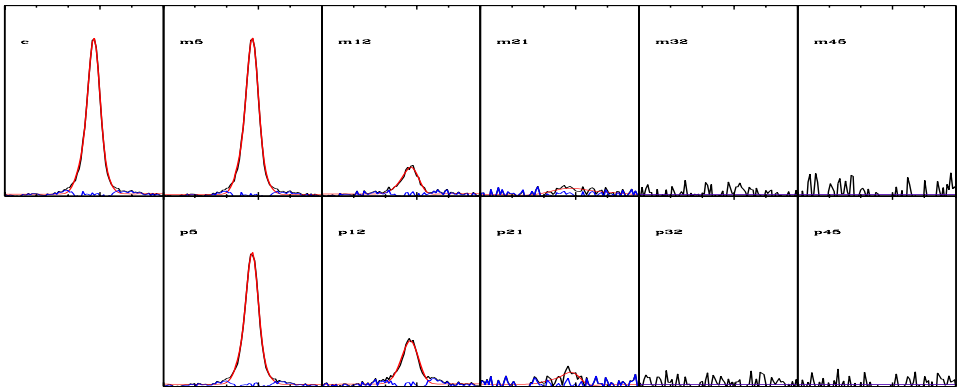

Figure B.284: GH-Object 157 [X]

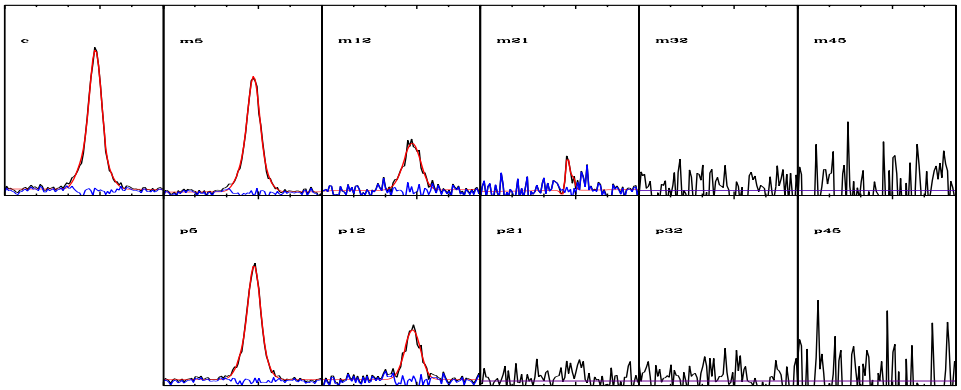

Figure B.285: GH-Object 162

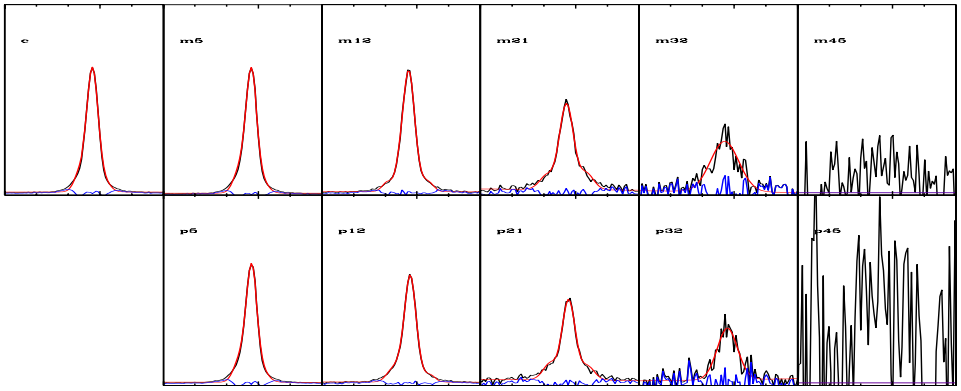

Figure B.286: GH-Object 174 [X]

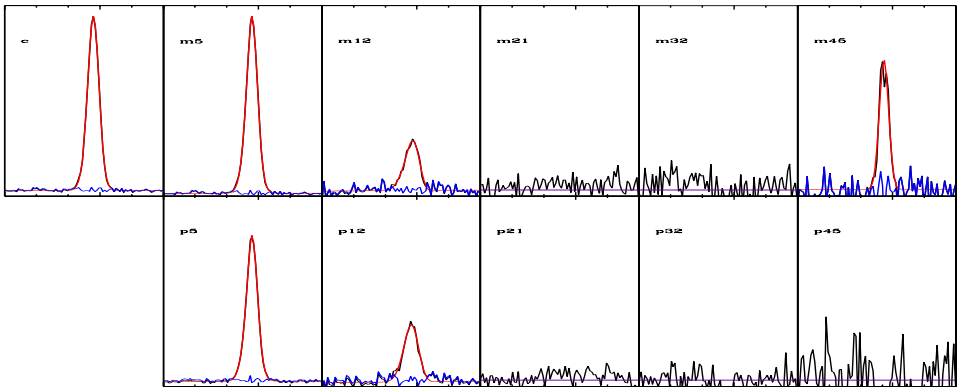

Figure B.287: GH-Object 177 [H]

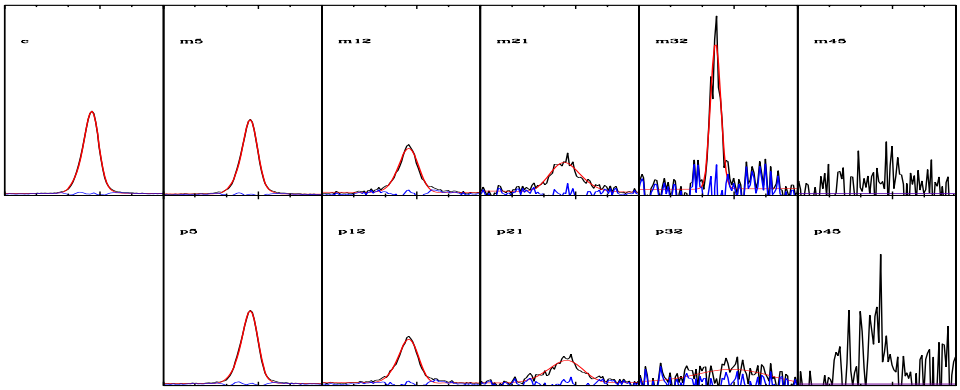

Figure B.288: GH-Object 180 [H]

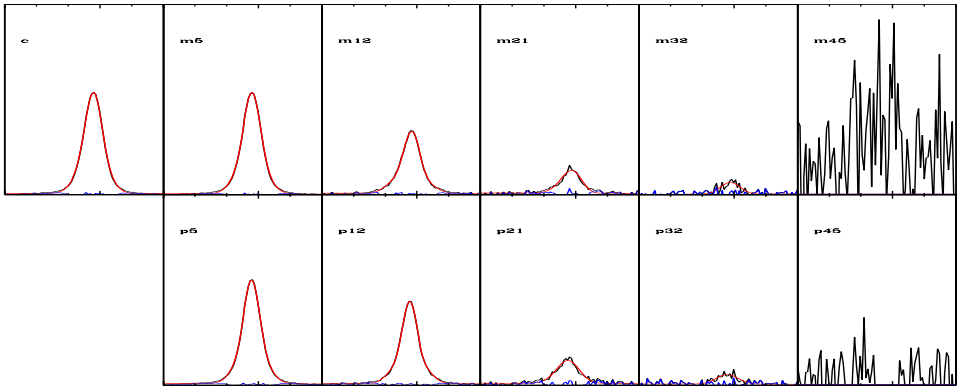

Figure B.289: GH-Object 187

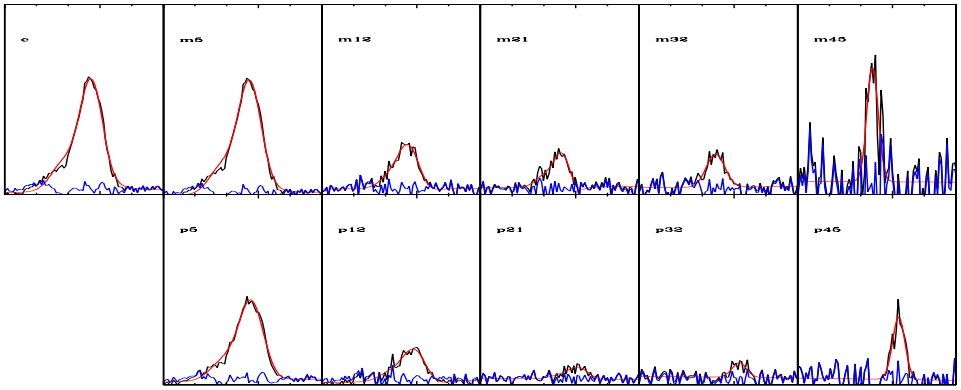

Figure B.290: GH-Object 196

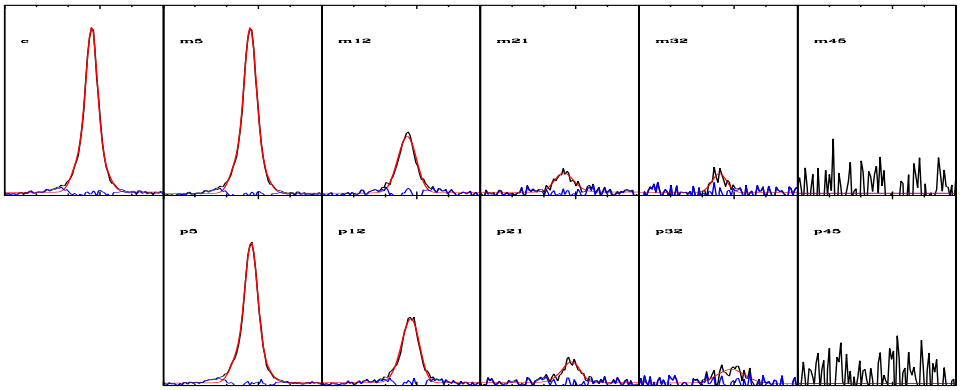

Figure B.291: GH-Object 197

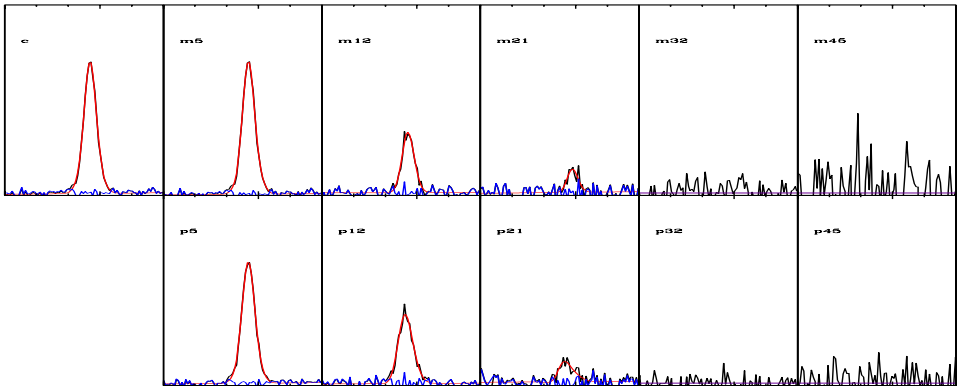

Figure B.292: GH-Object 202

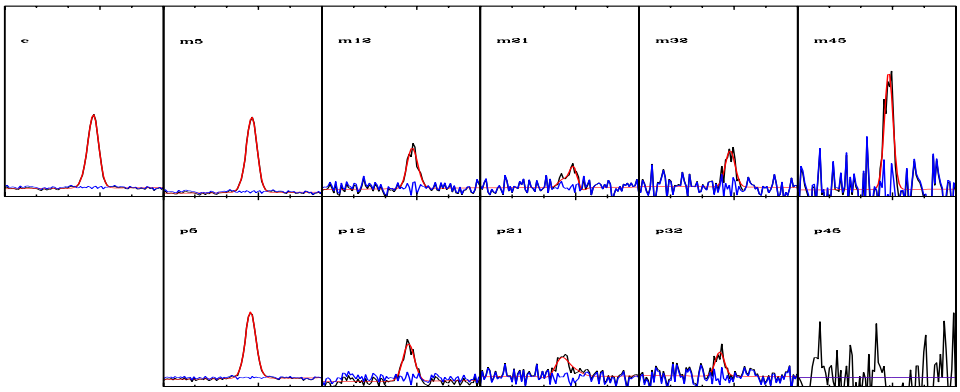

Figure B.293: GH-Object 204 [H]

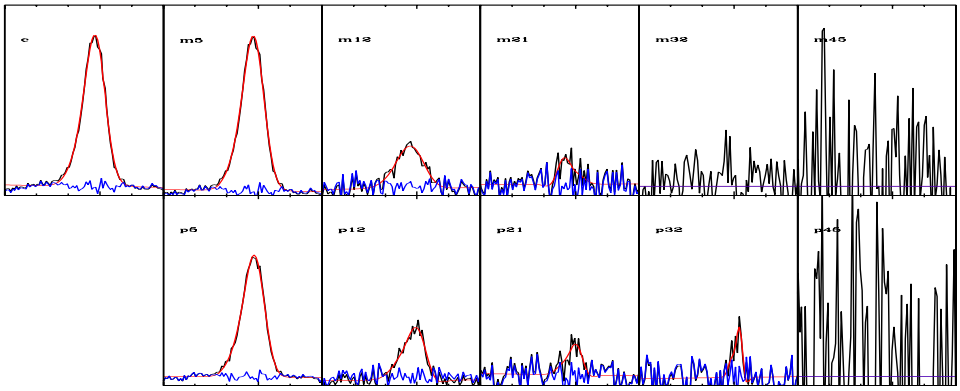

Figure B.294: GH-Object 205

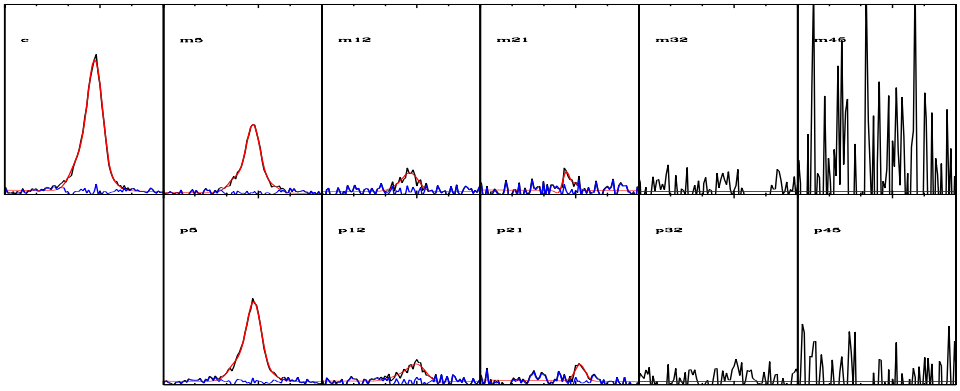

Figure B.295: GH-Object 207

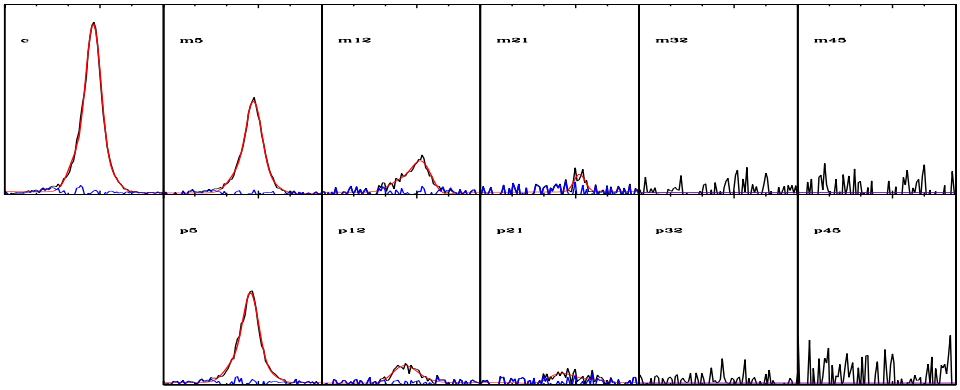

Figure B.296: GH-Object 208

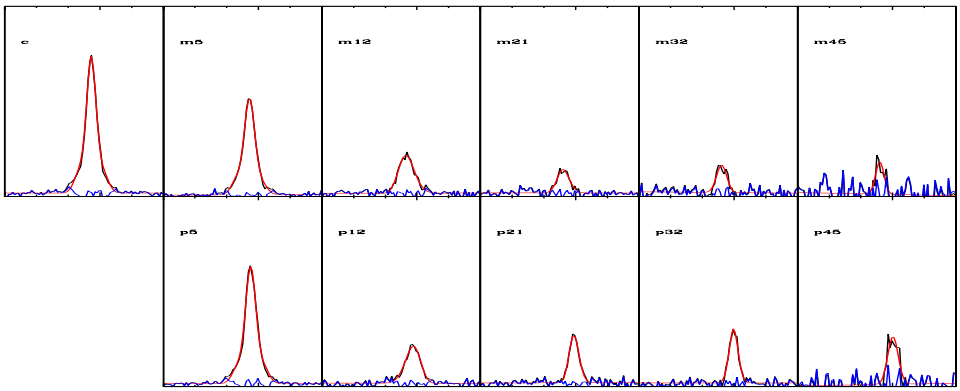

Figure B.297: GH-Object 209

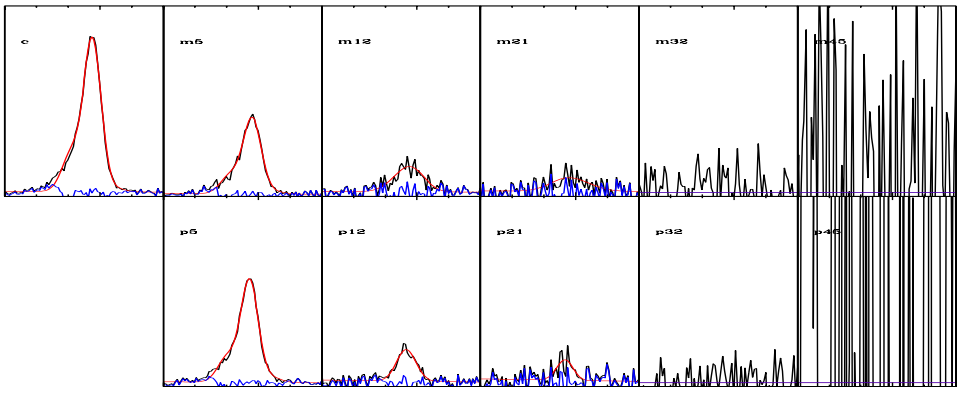

Figure B.298: GH-Object 210

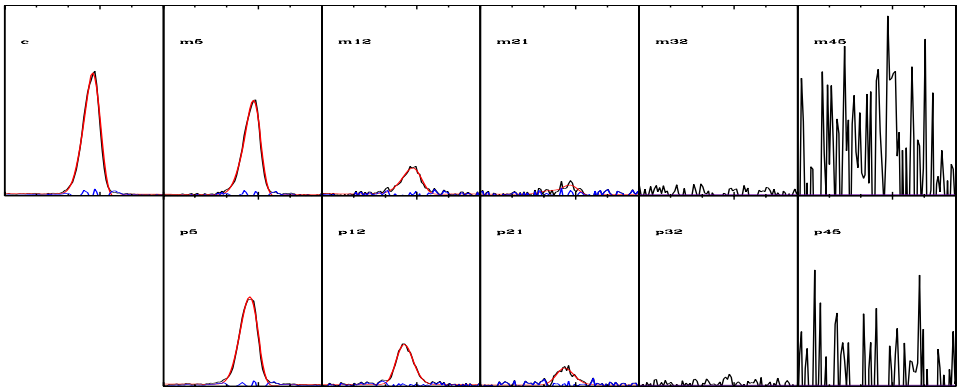

Figure B.299: GH-Object 213

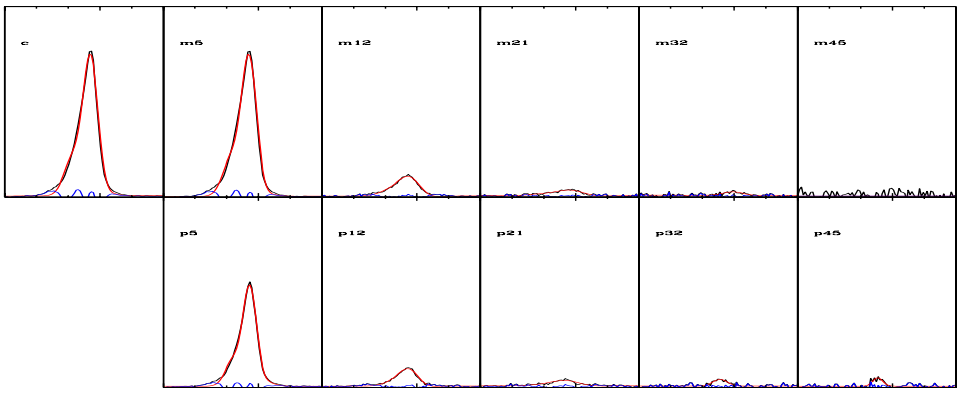

Figure B.300: GH-Object 214

Appendix C

Individual Object Discussion

Object 11/99/143 - Many of the profiles for these objects were such that the double Gaussian fitting code could not produce a realistic fit, yet they are clearly not single Gaussian in nature either. The data from these fits were left in their respective data sets regardless.

Object 59/96 - The profiles from these objects include both blue wings and red wings at different distances from the center, suggesting some form of bipolar outflow or a rotational component.

Object 109 - The profile for m5 is exceptionally odd, with a pronounced asymmetry very far from the main fit.

Object 130 - The innermost profiles for this object are also exceptionally odd, with pronounced asymmetries that appear even stronger than the main fit itself.

Appendix D

Tables

The following tables contain all of the final data produced for this project and is plotted in Fig. 4.1. The values for $\sigma_{[OIII]}$ were generated from the fits performed and the values for SVD were taken from Table 2 - σ_{best} in Harris et al. (2012).

D.1 Single Gaussian Results

Table D.1: Single Gaussian Results

Object	**Coordinate**	Distance From Center (Kpc)	$\sigma_{[\mathbf{OIII}]}$ **(km/s)**	**SVD (km/s)**	$\sigma_{[\mathbf{OIII}]}$/ SVD
5	c	0	179.82	170 ± 2	1.06
5	m5	5.8	159.92	170 ± 2	0.94
5	m12	13.92	119.55	170 ± 2	0.7
5	m21	24.36	99.09	170 ± 2	0.58
5	p5	5.8	168.16	170 ± 2	0.99
5	p12	13.92	180.71	170 ± 2	1.06
6	c	0	150.77	196 ± 11	0.77
6	m5	7.2	153.93	196 ± 11	0.79
6	m12	17.28	172.51	196 ± 11	0.88
6	m21	30.24	342.63	196 ± 11	1.75
6	p5	7.2	153.78	196 ± 11	0.79
6	p12	17.28	163.88	196 ± 11	0.84
6	p21	30.24	106.53	196 ± 11	0.54
9	c	0	169.36	246 ± 3	0.69
9	m5	9	170.29	246 ± 3	0.69
9	m12	21.6	239.54	246 ± 3	0.97
9	p5	9	197.09	246 ± 3	0.8
9	p12	21.6	215.27	246 ± 3	0.88
10	c	0	107.04	120 ± 4	0.89
10	m5	5.25	107.23	120 ± 4	0.89
10	m12	12.6	119.23	120 ± 4	0.99
10	m21	22.05	134.67	120 ± 4	1.12
10	p5	5.25	110.56	120 ± 4	0.92
10	p12	12.6	113.45	120 ± 4	0.95

Continued on next page

Table D.1 – *Continued from previous page*

Object	Coordinate	Distance From Center (Kpc)	$\sigma_{[OIII]}$ (km/s)	SVD (km/s)	$\sigma_{[OIII]}$/ SVD
10	p21	22.05	128.44	120 ± 4	1.07
11	c	0	229.28	107 ± 11	2.14
11	m5	5.25	234.99	107 ± 11	2.2
11	m12	12.6	254.63	107 ± 11	2.38
11	m21	22.05	295.95	107 ± 11	2.77
11	m32	33.6	351.82	107 ± 11	3.29
11	m45	47.25	803.99	107 ± 11	7.51
11	p5	5.25	231.72	107 ± 11	2.17
11	p12	12.6	245.49	107 ± 11	2.29
11	p21	22.05	296.63	107 ± 11	2.77
11	p32	33.6	311.88	107 ± 11	2.92
11	p45	47.25	1068.49	107 ± 11	9.99
13	c	0	157.59	131 ± 4	1.2
13	m5	2.15	161.31	131 ± 4	1.23
13	m12	5.16	196.97	131 ± 4	1.5
13	m21	9.03	152.09	131 ± 4	1.16
13	m32	13.76	134.9	131 ± 4	1.03
13	p5	2.15	162.49	131 ± 4	1.24
13	p12	5.16	177.1	131 ± 4	1.35
15	c	0	157.93	155 ± 8	1.02
15	m5	3.75	160.67	155 ± 8	1.04
15	m12	9	207.92	155 ± 8	1.34
15	m21	15.75	305.62	155 ± 8	1.97
15	p5	3.75	157.74	155 ± 8	1.02
15	p12	9	173.88	155 ± 8	1.12
15	p21	15.75	196.64	155 ± 8	1.27
15	p32	24	114.63	155 ± 8	0.74
19	c	0	144.15	127 ± 5	1.14
19	m5	5.65	143.58	127 ± 5	1.13
19	m12	13.56	116.72	127 ± 5	0.92
19	m21	23.73	138.82	127 ± 5	1.09
19	p5	5.65	151.14	127 ± 5	1.19
19	p12	13.56	167.64	127 ± 5	1.32
19	p21	23.73	177.69	127 ± 5	1.4
20	c	0	148.29	128 ± 9	1.16
20	m5	3.7	148.26	128 ± 9	1.16
20	m12	8.88	128.25	128 ± 9	1
20	m21	15.54	174.01	128 ± 9	1.36
20	p5	3.7	158.6	128 ± 9	1.24
20	p12	8.88	151.2	128 ± 9	1.18
20	p21	15.54	201.63	128 ± 9	1.58
20	p32	23.68	206.3	128 ± 9	1.61
21	c	0	171.52	91 ± 5	1.89
21	m5	4.95	168.75	91 ± 5	1.85
21	m12	11.88	157.49	91 ± 5	1.73
21	p5	4.95	173.35	91 ± 5	1.91
21	p12	11.88	166.82	91 ± 5	1.83
22	c	0	149.49	98 ± 3	1.53
22	m5	3.9	150.04	98 ± 3	1.53
22	m12	9.36	136.53	98 ± 3	1.39
22	m21	16.38	106.15	98 ± 3	1.08
22	m32	24.96	99.27	98 ± 3	1.01
22	p5	3.9	148.3	98 ± 3	1.51
22	p12	9.36	128.89	98 ± 3	1.32
22	p21	16.38	101.65	98 ± 3	1.04
22	p32	24.96	92.82	98 ± 3	0.95
22	p45	35.1	74.31	98 ± 3	0.76

Continued on next page

Table D.1 – *Continued from previous page*

Object	Coordinate	Distance From Center (Kpc)	$\sigma_{[OIII]}$ (km/s)	SVD (km/s)	$\sigma_{[OIII]}$/ SVD
23	c	0	226.56	129 ± 6	1.76
23	m5	3.3	227.26	129 ± 6	1.76
23	m12	7.92	281.6	129 ± 6	2.18
23	m21	13.86	344.95	129 ± 6	2.67
23	m32	21.12	418.26	129 ± 6	3.24
23	p5	3.3	229.15	129 ± 6	1.78
23	p12	7.92	283.59	129 ± 6	2.2
23	p21	13.86	328.57	129 ± 6	2.55
23	p32	21.12	193.24	129 ± 6	1.5
23	p45	29.7	110.04	129 ± 6	0.85
24	c	0	175.71	195 ± 2	0.9
24	m5	2.65	175.31	195 ± 2	0.9
24	m12	6.36	195.07	195 ± 2	1
24	m21	11.13	189.02	195 ± 2	0.97
24	m32	16.96	195.14	195 ± 2	1
24	m45	23.85	112.44	195 ± 2	0.58
24	p5	2.65	180.41	195 ± 2	0.93
24	p12	6.36	216.57	195 ± 2	1.11
24	p21	11.13	230.5	195 ± 2	1.18
24	p32	16.96	137.64	195 ± 2	0.71
24	p45	23.85	108.63	195 ± 2	0.56
26	c	0	144.33	124 ± 4	1.16
26	m5	5.5	148.01	124 ± 4	1.19
26	m12	13.2	144.97	124 ± 4	1.17
26	m21	23.1	171.18	124 ± 4	1.38
26	p5	5.5	148.06	124 ± 4	1.19
26	p12	13.2	150.18	124 ± 4	1.21
26	p21	23.1	142.55	124 ± 4	1.15
27	c	0	139.54	96 ± 6	1.45
27	m5	5.7	138.11	96 ± 6	1.44
27	m12	13.68	136.66	96 ± 6	1.42
27	m21	23.94	93.07	96 ± 6	0.97
27	p5	5.7	145.78	96 ± 6	1.52
27	p12	13.68	144.99	96 ± 6	1.51
27	p21	23.94	155.96	96 ± 6	1.63
28	c	0	182.09	124 ± 4	1.47
28	m5	2.2	178.51	124 ± 4	1.44
28	m12	5.28	188.27	124 ± 4	1.52
28	m21	9.24	162.26	124 ± 4	1.31
28	m32	14.08	102.6	124 ± 4	0.83
28	m45	19.8	95.3	124 ± 4	0.77
28	p5	2.2	185.62	124 ± 4	1.5
28	p12	5.28	186.43	124 ± 4	1.5
28	p21	9.24	164.46	124 ± 4	1.33
28	p32	14.08	112.46	124 ± 4	0.91
29	c	0	139.59	140 ± 3	1
29	m5	4.6	140.46	140 ± 3	1
29	m12	11.04	143.92	140 ± 3	1.03
29	m21	19.32	125.75	140 ± 3	0.9
29	m32	29.44	112.59	140 ± 3	0.8
29	p5	4.6	142.99	140 ± 3	1.02
29	p12	11.04	146.39	140 ± 3	1.05
29	p21	19.32	143.97	140 ± 3	1.03
29	p32	29.44	138.43	140 ± 3	0.99
29	p45	41.4	104.72	140 ± 3	0.75
30	c	0	148.19	154 ± 8	0.96
30	m5	5.05	140.96	154 ± 8	0.92

Continued on next page

Table D.1 – *Continued from previous page*

Object	Coordinate	Distance From Center (Kpc)	$\sigma_{[OIII]}$ (km/s)	SVD (km/s)	$\sigma_{[OIII]}$/ SVD
30	m12	12.12	153.13	154 ± 8	0.99
30	m21	21.21	158.19	154 ± 8	1.03
30	p5	5.05	157.3	154 ± 8	1.02
30	p12	12.12	188.34	154 ± 8	1.22
30	p21	21.21	217.57	154 ± 8	1.41
30	p32	32.32	165.81	154 ± 8	1.08
31	c	0	164.17	127 ± 6	1.29
31	m5	3.75	165.87	127 ± 6	1.31
31	m12	9	132.2	127 ± 6	1.04
31	m21	15.75	126.17	127 ± 6	0.99
31	m32	24	116.73	127 ± 6	0.92
31	p5	3.75	174.48	127 ± 6	1.37
31	p12	9	166.77	127 ± 6	1.31
31	p21	15.75	130.81	127 ± 6	1.03
31	p32	24	101.02	127 ± 6	0.8
32	c	0	149.41	108 ± 10	1.38
32	m5	5.1	144.51	108 ± 10	1.34
32	m12	12.24	151.58	108 ± 10	1.4
32	m21	21.42	161.9	108 ± 10	1.5
32	p5	5.1	149.07	108 ± 10	1.38
32	p12	12.24	154.14	108 ± 10	1.43
32	p21	21.42	82.59	108 ± 10	0.77
32	p32	32.64	140.16	108 ± 10	1.3
34	c	0	144.72	77 ± 17	1.88
34	m5	5.35	144.03	77 ± 17	1.87
34	m12	12.84	147.07	77 ± 17	1.91
34	m21	22.47	172.66	77 ± 17	2.24
34	p5	5.35	146.26	77 ± 17	1.9
34	p12	12.84	169.3	77 ± 17	2.2
34	p21	22.47	188.25	77 ± 17	2.45
35	c	0	197.26	144 ± 14	1.37
35	m5	3.55	189.54	144 ± 14	1.32
35	m12	8.52	193.24	144 ± 14	1.34
35	m21	14.91	199.14	144 ± 14	1.38
35	m32	22.72	137.2	144 ± 14	0.95
35	p5	3.55	191.84	144 ± 14	1.33
35	p12	8.52	191.4	144 ± 14	1.33
35	p21	14.91	217	144 ± 14	1.51
35	p32	22.72	165.69	144 ± 14	1.15
36	c	0	134.17	91 ± 7	1.47
36	m5	4.8	136.81	91 ± 7	1.5
36	m12	11.52	142.46	91 ± 7	1.57
36	m21	20.16	402.27	91 ± 7	4.42
36	p5	4.8	135.9	91 ± 7	1.49
36	p12	11.52	140.84	91 ± 7	1.55
36	p21	20.16	261.72	91 ± 7	2.88
36	p32	30.72	66.99	91 ± 7	0.74
38	c	0	178.38	119 ± 3	1.5
38	m5	5.8	196.28	119 ± 3	1.65
38	m12	13.92	203.12	119 ± 3	1.71
38	m21	24.36	98.86	119 ± 3	0.83
38	p5	5.8	172.11	119 ± 3	1.45
38	p12	13.92	188.87	119 ± 3	1.59
38	p21	24.36	108.92	119 ± 3	0.92
39	c	0	237.97	166 ± 7	1.43
39	m5	5.25	231.23	166 ± 7	1.39
39	m12	12.6	186.91	166 ± 7	1.13

Continued on next page

Table D.1 – *Continued from previous page*

Object	Coordinate	Distance From Center (Kpc)	$\sigma_{[OIII]}$ (km/s)	SVD (km/s)	$\sigma_{[OIII]}$/ SVD
39	p5	5.25	251.49	166 ± 7	1.52
39	p12	12.6	192.39	166 ± 7	1.16
40	c	0	161	82 ± 2	1.96
40	m5	3.45	152.78	82 ± 2	1.86
40	m12	8.28	141.77	82 ± 2	1.73
40	m21	14.49	171.57	82 ± 2	2.09
40	m32	22.08	198.14	82 ± 2	2.42
40	p5	3.45	161.9	82 ± 2	1.97
40	p12	8.28	160.36	82 ± 2	1.96
40	p21	14.49	122.74	82 ± 2	1.5
40	p32	22.08	91.08	82 ± 2	1.11
41	c	0	176.25	118 ± 6	1.49
41	m5	5.2	176.55	118 ± 6	1.5
41	m12	12.48	194.8	118 ± 6	1.65
41	m21	21.84	223.79	118 ± 6	1.9
41	p5	5.2	189.31	118 ± 6	1.6
41	p12	12.48	175.08	118 ± 6	1.48
41	p21	21.84	202.64	118 ± 6	1.72
42	c	0	142.66	157 ± 6	0.91
42	m5	5.05	143.73	157 ± 6	0.92
42	m12	12.12	116.92	157 ± 6	0.75
42	m21	21.21	89.06	157 ± 6	0.57
42	m32	32.32	91.08	157 ± 6	0.58
42	p5	5.05	147.67	157 ± 6	0.94
42	p12	12.12	111.31	157 ± 6	0.71
42	p21	21.21	92.47	157 ± 6	0.59
42	p32	32.32	81.02	157 ± 6	0.52
42	p45	45.45	81.44	157 ± 6	0.52
43	c	0	171.39	144 ± 5	1.19
43	m5	2.3	172.56	144 ± 5	1.2
43	m12	5.52	188.88	144 ± 5	1.31
43	m21	9.66	185.03	144 ± 5	1.29
43	m32	14.72	156.41	144 ± 5	1.09
43	p5	2.3	173.21	144 ± 5	1.2
43	p12	5.52	188.21	144 ± 5	1.31
43	p21	9.66	241.99	144 ± 5	1.68
43	p32	14.72	182.47	144 ± 5	1.27
44	c	0	197.17	172 ± 7	1.15
44	m5	3.1	179.55	172 ± 7	1.04
44	m12	7.44	176.53	172 ± 7	1.03
44	m21	13.02	133.35	172 ± 7	0.78
44	m32	19.84	132.41	172 ± 7	0.77
44	m45	27.9	98.39	172 ± 7	0.57
44	p5	3.1	222.07	172 ± 7	1.29
44	p12	7.44	175.28	172 ± 7	1.02
44	p21	13.02	134.2	172 ± 7	0.78
44	p32	19.84	103.54	172 ± 7	0.6
44	p45	27.9	80.17	172 ± 7	0.47
45	c	0	161.11	97 ± 8	1.66
45	m5	2.35	160.74	97 ± 8	1.66
45	m12	5.64	180.7	97 ± 8	1.86
45	m21	9.87	157.16	97 ± 8	1.62
45	m32	15.04	158.85	97 ± 8	1.64
45	p5	2.35	159.79	97 ± 8	1.65
45	p12	5.64	158.77	97 ± 8	1.64
45	p21	9.87	178.25	97 ± 8	1.84
46	c	0	197.71	107 ± 8	1.85

Continued on next page

Table D.1 – *Continued from previous page*

Object	Coordinate	Distance From Center (Kpc)	$\sigma_{[OIII]}$ (km/s)	SVD (km/s)	$\sigma_{[OIII]}$/ SVD
46	m5	4.6	194.05	107 ± 8	1.81
46	m12	11.04	222	107 ± 8	2.08
46	p5	4.6	203.5	107 ± 8	1.9
46	p12	11.04	235.02	107 ± 8	2.2
47	c	0	159.84	100 ± 4	1.6
47	m5	4.95	151.29	100 ± 4	1.51
47	m12	11.88	126.23	100 ± 4	1.26
47	m21	20.79	79.53	100 ± 4	0.8
47	m32	31.68	84.28	100 ± 4	0.84
47	m45	44.55	102.38	100 ± 4	1.02
47	p5	4.95	161.11	100 ± 4	1.61
47	p12	11.88	130.26	100 ± 4	1.3
47	p21	20.79	249.86	100 ± 4	2.5
47	p32	31.68	107.59	100 ± 4	1.08
47	p45	44.55	172.01	100 ± 4	1.72
49	c	0	191.43	122 ± 9	1.57
49	m5	5.45	186.34	122 ± 9	1.53
49	m12	13.08	140.64	122 ± 9	1.15
49	m21	22.89	117.26	122 ± 9	0.96
49	m32	34.88	99.55	122 ± 9	0.82
49	p5	5.45	178.18	122 ± 9	1.46
49	p12	13.08	139.95	122 ± 9	1.15
49	p21	22.89	126.81	122 ± 9	1.04
49	p32	34.88	88.3	122 ± 9	0.72
51	c	0	176.81	123 ± 4	1.44
51	m5	5.25	175.5	123 ± 4	1.43
51	m12	12.6	202.7	123 ± 4	1.65
51	p5	5.25	178.77	123 ± 4	1.45
51	p12	12.6	184.49	123 ± 4	1.5
52	c	0	268.98	149 ± 4	1.81
52	m5	5.25	282.08	149 ± 4	1.89
52	m12	12.6	286.37	149 ± 4	1.92
52	m21	22.05	140.83	149 ± 4	0.95
52	m32	33.6	106.65	149 ± 4	0.72
52	m45	47.25	149.49	149 ± 4	1
52	p5	5.25	271.79	149 ± 4	1.82
52	p12	12.6	317.86	149 ± 4	2.13
52	p21	22.05	204.87	149 ± 4	1.38
52	p32	33.6	132.42	149 ± 4	0.89
52	p45	47.25	105.51	149 ± 4	0.71
53	c	0	260.48	185 ± 10	1.41
53	m5	5.4	256.18	185 ± 10	1.39
53	m12	12.96	313.98	185 ± 10	1.7
53	m21	22.68	514.34	185 ± 10	2.78
53	p5	5.4	263.17	185 ± 10	1.42
53	p12	12.96	292.94	185 ± 10	1.58
53	p21	22.68	217.27	185 ± 10	1.17
53	p32	34.56	142.23	185 ± 10	0.77
54	c	0	157.74	114 ± 7	1.38
54	m5	3.65	156.88	114 ± 7	1.38
54	m12	8.76	164.9	114 ± 7	1.45
54	m21	15.33	187.3	114 ± 7	1.64
54	m32	23.36	109.78	114 ± 7	0.96
54	m45	32.85	93.76	114 ± 7	0.82
54	p5	3.65	158.27	114 ± 7	1.39
54	p12	8.76	170.16	114 ± 7	1.49
54	p21	15.33	232.04	114 ± 7	2.04

Continued on next page

Table D.1 – *Continued from previous page*

Object	Coordinate	Distance From Center (Kpc)	$\sigma_{[OIII]}$ (km/s)	SVD (km/s)	$\sigma_{[OIII]}$/ SVD
54	p32	23.36	306.47	114 ± 7	2.69
57	c	0	183.07	116 ± 4	1.58
57	m5	3.05	188.05	116 ± 4	1.62
57	m12	7.32	266.12	116 ± 4	2.29
57	m21	12.81	423.84	116 ± 4	3.65
57	m32	19.52	776.16	116 ± 4	6.69
57	p5	3.05	181.79	116 ± 4	1.57
57	p12	7.32	208.57	116 ± 4	1.8
57	p21	12.81	233.31	116 ± 4	2.01
57	p32	19.52	607.3	116 ± 4	5.24
57	p45	27.45	1023.84	116 ± 4	8.83
58	c	0	161.3	171 ± 5	0.94
58	m5	4.7	146.74	171 ± 5	0.86
58	m12	11.28	136.35	171 ± 5	0.8
58	m21	19.74	148.75	171 ± 5	0.87
58	m32	30.08	188.28	171 ± 5	1.1
58	p5	4.7	163.14	171 ± 5	0.95
58	p12	11.28	153.86	171 ± 5	0.9
58	p21	19.74	127.58	171 ± 5	0.75
58	p32	30.08	129.92	171 ± 5	0.76
59	c	0	220.49	159 ± 4	1.39
59	m5	4.75	209.4	159 ± 4	1.32
59	m12	11.4	161.34	159 ± 4	1.02
59	m21	19.95	143.82	159 ± 4	0.91
59	m32	30.4	153.75	159 ± 4	0.97
59	p5	4.75	208.91	159 ± 4	1.31
59	p12	11.4	142.61	159 ± 4	0.9
59	p21	19.95	213.78	159 ± 4	1.34
59	p32	30.4	638.54	159 ± 4	4.02
59	p45	42.75	198.27	159 ± 4	1.25
61	c	0	128.38	186 ± 8	0.69
61	m5	5.2	121.66	186 ± 8	0.65
61	m12	12.48	124.14	186 ± 8	0.67
61	m21	21.84	109.13	186 ± 8	0.59
61	m32	33.28	184.96	186 ± 8	0.99
61	p5	5.2	135.17	186 ± 8	0.73
61	p12	12.48	150.97	186 ± 8	0.81
61	p21	21.84	287.19	186 ± 8	1.54
62	c	0	207.71	170 ± 8	1.22
62	m5	5.65	213.47	170 ± 8	1.26
62	m12	13.56	254.19	170 ± 8	1.5
62	m21	23.73	208.66	170 ± 8	1.23
62	m32	36.16	135.81	170 ± 8	0.8
62	p5	5.65	199.54	170 ± 8	1.17
62	p12	13.56	198.84	170 ± 8	1.17
62	p21	23.73	185.56	170 ± 8	1.09
63	c	0	214.03	120 ± 5	1.78
63	m5	4.05	202.43	120 ± 5	1.69
63	m12	9.72	255.78	120 ± 5	2.13
63	m21	17.01	650.35	120 ± 5	5.42
63	p5	4.05	218.43	120 ± 5	1.82
63	p12	9.72	244.75	120 ± 5	2.04
63	p21	17.01	267.95	120 ± 5	2.23
70	c	0	220.39	266 ± 3	0.83
70	m5	4.5	234.3	266 ± 3	0.88
70	m12	10.8	350.09	266 ± 3	1.32
70	m21	18.9	329.34	266 ± 3	1.24

Continued on next page

Table D.1 – *Continued from previous page*

Object	Coordinate	Distance From Center (Kpc)	$\sigma_{[OIII]}$ (km/s)	SVD (km/s)	$\sigma_{[OIII]}$/ SVD
70	m32	28.8	148.87	266 ± 3	0.56
70	m45	40.5	115.95	266 ± 3	0.44
70	p5	4.5	212.16	266 ± 3	0.8
70	p12	10.8	288.43	266 ± 3	1.08
70	p21	18.9	313.84	266 ± 3	1.18
70	p32	28.8	85.13	266 ± 3	0.32
71	c	0	209.28	134 ± 5	1.56
71	m5	5.95	217.77	134 ± 5	1.63
71	m12	14.28	308.57	134 ± 5	2.3
71	m45	53.55	100.89	134 ± 5	0.75
71	p5	5.95	208.85	134 ± 5	1.56
71	p12	14.28	356.61	134 ± 5	2.66
71	p45	53.55	90.82	134 ± 5	0.68
73	c	0	192.34	131 ± 6	1.47
73	m5	7.6	205.67	131 ± 6	1.57
73	m12	18.24	272.57	131 ± 6	2.08
73	p5	7.6	189.67	131 ± 6	1.45
73	p12	18.24	247.57	131 ± 6	1.89
73	p21	31.92	298.2	131 ± 6	2.28
74	c	0	197.24	165 ± 17	1.2
74	m5	8.65	217.37	165 ± 17	1.32
74	m12	20.76	350.47	165 ± 17	2.12
74	m21	36.33	172.59	165 ± 17	1.05
74	m32	55.36	89.32	165 ± 17	0.54
74	p5	8.65	199.95	165 ± 17	1.21
74	p12	20.76	238.81	165 ± 17	1.45
74	p21	36.33	210.62	165 ± 17	1.28
74	p32	55.36	81.68	165 ± 17	0.5
76	c	0	144.3	193 ± 4	0.75
76	m5	7.95	162.26	193 ± 4	0.84
76	m12	19.08	217.63	193 ± 4	1.13
76	m21	33.39	169.89	193 ± 4	0.88
76	p5	7.95	152.48	193 ± 4	0.79
76	p12	19.08	239.33	193 ± 4	1.24
76	p32	50.88	167.02	193 ± 4	0.87
77	c	0	170.91	188 ± 4	0.91
77	m5	5.95	185.11	188 ± 4	0.99
77	m12	14.28	190.16	188 ± 4	1.01
77	m21	24.99	109.08	188 ± 4	0.58
77	p5	5.95	178.68	188 ± 4	0.95
77	p12	14.28	157.97	188 ± 4	0.84
77	p21	24.99	247.96	188 ± 4	1.32
78	c	0	248.31	97 ± 4	2.56
78	m5	6.8	224.18	97 ± 4	2.31
78	m12	16.32	277.38	97 ± 4	2.86
78	m21	28.56	147.34	97 ± 4	1.52
78	p5	6.8	270.21	97 ± 4	2.79
78	p12	16.32	217.9	97 ± 4	2.25
78	p21	28.56	93.01	97 ± 4	0.96
79	c	0	269.04	90 ± 6	2.99
79	m5	7.1	304.49	90 ± 6	3.38
79	m12	17.04	353.83	90 ± 6	3.93
79	m21	29.82	590.89	90 ± 6	6.57
79	p5	7.1	262.37	90 ± 6	2.92
79	p12	17.04	435.73	90 ± 6	4.84
82	c	0	144.84	156 ± 23	0.93
82	m5	8.9	143.09	156 ± 23	0.92

Continued on next page

Table D.1 – *Continued from previous page*

Object	Coordinate	Distance From Center (Kpc)	$\sigma_{[OIII]}$ (km/s)	SVD (km/s)	$\sigma_{[OIII]}$/ SVD
82	p5	8.9	147.76	156 ± 23	0.95
82	p12	21.36	117.07	156 ± 23	0.75
83	c	0	181.17	90 ± 18	2.01
83	m5	8.25	193.71	90 ± 18	2.15
83	m12	19.8	271.01	90 ± 18	3.01
83	m21	34.65	282.28	90 ± 18	3.14
83	p5	8.25	186.51	90 ± 18	2.07
83	p12	19.8	240.36	90 ± 18	2.67
83	p21	34.65	511.43	90 ± 18	5.68
88	c	0	258.23	199 ± 6	1.3
88	m5	7.9	280.35	199 ± 6	1.41
88	m12	18.96	213.39	199 ± 6	1.07
88	p5	7.9	249.46	199 ± 6	1.25
88	p12	18.96	202.84	199 ± 6	1.02
91	c	0	224.08	172 ± 13	1.3
91	m5	6.9	226.13	172 ± 13	1.32
91	m12	16.56	216.62	172 ± 13	1.26
91	m21	28.98	105	172 ± 13	0.61
91	m32	44.16	88.5	172 ± 13	0.52
91	p5	6.9	222.71	172 ± 13	1.3
91	p12	16.56	193.53	172 ± 13	1.13
91	p21	28.98	109.75	172 ± 13	0.64
91	p32	44.16	103.58	172 ± 13	0.6
91	p45	62.1	225.75	172 ± 13	1.31
99	c	0	247.95	71 ± 28	3.49
99	m5	7.85	251.82	71 ± 28	3.55
99	m12	18.84	336.66	71 ± 28	4.74
99	m21	32.97	166.61	71 ± 28	2.35
99	p5	7.85	249.55	71 ± 28	3.52
99	p12	18.84	298.6	71 ± 28	4.21
99	p21	32.97	136.05	71 ± 28	1.92
102	c	0	138.34	115 ± 17	1.2
102	m5	8.5	140.88	115 ± 17	1.23
102	m12	20.4	560.63	115 ± 17	4.88
102	p5	8.5	142.34	115 ± 17	1.24
102	p12	20.4	191.59	115 ± 17	1.67
103	c	0	394	99 ± 8	3.98
103	m5	7.75	390.14	99 ± 8	3.94
103	m12	18.6	377.39	99 ± 8	3.81
103	m21	32.55	576.12	99 ± 8	5.82
103	m32	49.6	115.81	99 ± 8	1.17
103	m45	69.75	906.35	99 ± 8	9.16
103	m45	69.75	83.62	99 ± 8	0.85
103	p5	7.75	399.23	99 ± 8	4.03
103	p12	18.6	430.17	99 ± 8	4.35
103	p21	32.55	384.29	99 ± 8	3.88
103	p32	49.6	231.8	99 ± 8	2.34
106	c	0	209.13	198 ± 6	1.06
106	m5	8.7	225.06	198 ± 6	1.14
106	m12	20.88	236.11	198 ± 6	1.19
106	m21	36.54	156.07	198 ± 6	0.79
106	m32	55.68	141.18	198 ± 6	0.71
106	m45	78.3	97.01	198 ± 6	0.49
106	p5	8.7	210.07	198 ± 6	1.06
106	p12	20.88	180.21	198 ± 6	0.91
106	p21	36.54	146.7	198 ± 6	0.74
106	p32	55.68	140.19	198 ± 6	0.71

Continued on next page

Table D.1 – *Continued from previous page*

Object	Coordinate	Distance From Center (Kpc)	$\sigma_{[OIII]}$ (km/s)	SVD (km/s)	$\sigma_{[OIII]}$/ SVD
106	p45	78.3	73.29	198 ± 6	0.37
109	c	0	210.82	237 ± 9	0.89
109	m5	8.9	243.72	237 ± 9	1.03
109	m12	21.36	209.82	237 ± 9	0.89
109	m21	37.38	312.45	237 ± 9	1.32
109	p5	8.9	190.97	237 ± 9	0.81
109	p12	21.36	104.15	237 ± 9	0.44
109	p21	37.38	92.16	237 ± 9	0.39
114	c	0	115.83	136 ± 6	0.85
114	m5	6.25	116.21	136 ± 6	0.86
114	m12	15	168.49	136 ± 6	1.24
114	p5	6.25	117.77	136 ± 6	0.87
114	p12	15	132.92	136 ± 6	0.98
126	c	0	105.68	1211 ± 5	0.09
126	m5	6.3	105.68	1211 ± 5	0.09
126	m12	15.12	93.2	1211 ± 5	0.08
126	m21	26.46	132.16	1211 ± 5	0.11
126	m32	40.32	79.91	1211 ± 5	0.07
126	p5	6.3	106.34	1211 ± 5	0.09
126	p12	15.12	99.45	1211 ± 5	0.08
126	p21	26.46	106.16	1211 ± 5	0.09
126	p32	40.32	85.88	1211 ± 5	0.07
126	p45	56.7	68.35	1211 ± 5	0.06
138	c	0	113.85	143 ± 3	0.8
138	m5	6	113.98	143 ± 3	0.8
138	m12	14.4	149.32	143 ± 3	1.04
138	p5	6	100.7	143 ± 3	0.7
138	p12	14.4	93.59	143 ± 3	0.65
138	p21	25.2	94.81	143 ± 3	0.66
155	c	0	166.23	197 ± 5	0.84
155	m5	5.85	167.28	197 ± 5	0.85
155	m12	14.04	163.66	197 ± 5	0.83
155	m21	24.57	165.51	197 ± 5	0.84
155	m32	37.44	211.54	197 ± 5	1.07
155	p5	5.85	173.31	197 ± 5	0.88
155	p12	14.04	176.3	197 ± 5	0.9
155	p21	24.57	148.91	197 ± 5	0.76
155	p32	37.44	100.07	197 ± 5	0.51
156	c	0	189.28	165 ± 6	1.15
156	m5	6.45	189.22	165 ± 6	1.15
156	m12	15.48	170.37	165 ± 6	1.03
156	m21	27.09	114.3	165 ± 6	0.69
156	m32	41.28	91.66	165 ± 6	0.56
156	m45	58.05	111.66	165 ± 6	0.68
156	p5	6.45	186.88	165 ± 6	1.13
156	p12	15.48	179.7	165 ± 6	1.09
156	p21	27.09	120.82	165 ± 6	0.73
156	p32	41.28	93.05	165 ± 6	0.56
162	c	0	142.48	121 ± 3	1.18
162	m5	6.45	142.14	121 ± 3	1.18
162	m12	15.48	161.7	121 ± 3	1.34
162	m21	27.09	251.5	121 ± 3	2.08
162	p5	6.45	141.5	121 ± 3	1.17
162	p12	15.48	150.54	121 ± 3	1.24
177	c	0	109.31	121 ± 6	0.9
177	m5	6.05	109.57	121 ± 6	0.91
177	m12	14.52	134.7	121 ± 6	1.11

Continued on next page

Table D.1 – *Continued from previous page*

Object	Coordinate	Distance From Center (Kpc)	$\sigma_{[OIII]}$ (km/s)	SVD (km/s)	$\sigma_{[OIII]}$/ SVD
177	m45	54.45	87.95	121 ± 6	0.73
177	p5	6.05	110.36	121 ± 6	0.91
177	p12	14.52	134.96	121 ± 6	1.12
180	c	0	158.93	120 ± 18	1.32
180	m5	6.6	160.52	120 ± 18	1.34
180	m12	15.84	195.99	120 ± 18	1.63
180	m21	27.72	313.68	120 ± 18	2.61
180	m32	42.24	97.14	120 ± 18	0.81
180	p5	6.6	165.4	120 ± 18	1.38
180	p12	15.84	198.29	120 ± 18	1.65
180	p21	27.72	347.25	120 ± 18	2.89
180	p32	42.24	869.02	120 ± 18	7.24
187	c	0	194.64	166 ± 6	1.17
187	m5	6.05	194.63	166 ± 6	1.17
187	m12	14.52	203.43	166 ± 6	1.23
187	m21	25.41	204.34	166 ± 6	1.23
187	m32	38.72	177.12	166 ± 6	1.07
187	p5	6.05	191.2	166 ± 6	1.15
187	p12	14.52	188.28	166 ± 6	1.13
187	p21	25.41	223.55	166 ± 6	1.35
187	p32	38.72	211.3	166 ± 6	1.27
196	c	0	253.27	228 ± 7	1.11
196	m5	6	254.05	228 ± 7	1.11
196	m12	14.4	228.4	228 ± 7	1
196	m21	25.2	195.98	228 ± 7	0.86
196	m32	38.4	175.03	228 ± 7	0.77
196	m45	54	114.13	228 ± 7	0.5
196	p5	6	263.5	228 ± 7	1.16
196	p12	14.4	237.21	228 ± 7	1.04
196	p21	25.2	212.21	228 ± 7	0.93
196	p32	38.4	140.96	228 ± 7	0.62
196	p45	54	115.57	228 ± 7	0.51
197	c	0	151.2	144 ± 4	1.05
197	m5	6.1	151.36	144 ± 4	1.05
197	m12	14.64	173.18	144 ± 4	1.2
197	m21	25.62	187.62	144 ± 4	1.3
197	m32	39.04	139.89	144 ± 4	0.97
197	p5	6.1	152.37	144 ± 4	1.06
197	p12	14.64	167.96	144 ± 4	1.17
197	p21	25.62	170.72	144 ± 4	1.19
197	p32	39.04	270.23	144 ± 4	1.88
202	c	0	120.63	113 ± 5	1.07
202	m5	6.4	120.53	113 ± 5	1.07
202	m12	15.36	116.27	113 ± 5	1.03
202	m21	26.88	99.58	113 ± 5	0.88
202	p5	6.4	125.03	113 ± 5	1.11
202	p12	15.36	139.11	113 ± 5	1.23
202	p21	26.88	146.63	113 ± 5	1.3
204	c	0	103.9	133 ± 9	0.78
204	m5	5.85	103.76	133 ± 9	0.78
204	m12	14.04	97.24	133 ± 9	0.73
204	m21	24.57	128.44	133 ± 9	0.97
204	m32	37.44	91.64	133 ± 9	0.69
204	m45	52.65	78.76	133 ± 9	0.59
204	p5	5.85	102.25	133 ± 9	0.77
204	p12	14.04	102.55	133 ± 9	0.77
204	p21	24.57	118.9	133 ± 9	0.89

Continued on next page

Table D.1 – *Continued from previous page*

Object	Coordinate	Distance From Center (Kpc)	$\sigma_{[OIII]}$ (km/s)	SVD (km/s)	$\sigma_{[OIII]}$/ SVD
204	p32	37.44	88.97	133 ± 9	0.67
205	c	0	213.27	144 ± 10	1.48
205	m5	5.9	214.65	144 ± 10	1.49
205	m12	14.16	250.62	144 ± 10	1.74
205	m21	24.78	169.09	144 ± 10	1.17
205	p5	5.9	209.66	144 ± 10	1.46
205	p12	14.16	204.36	144 ± 10	1.42
205	p21	24.78	174.88	144 ± 10	1.21
205	p32	37.76	95.38	144 ± 10	0.66
207	c	0	183.49	168 ± 11	1.09
207	m5	6.05	175.4	168 ± 11	1.04
207	m12	14.52	168.52	168 ± 11	1
207	m21	25.41	123.7	168 ± 11	0.74
207	p5	6.05	183.38	168 ± 11	1.09
207	p12	14.52	202.17	168 ± 11	1.2
207	p21	25.41	103.93	168 ± 11	0.62
208	c	0	196.21	201 ± 13	0.98
208	m5	6.1	200.06	201 ± 13	1
208	m12	14.64	249.72	201 ± 13	1.24
208	m21	25.62	104.5	201 ± 13	0.52
208	p5	6.1	202.77	201 ± 13	1.01
208	p12	14.64	232.73	201 ± 13	1.16
208	p21	25.62	382.61	201 ± 13	1.9
209	c	0	120.66	128 ± 7	0.94
209	m5	6.15	124.85	128 ± 7	0.98
209	m12	14.76	147.42	128 ± 7	1.15
209	m21	25.83	116.76	128 ± 7	0.91
209	m32	39.36	95.85	128 ± 7	0.75
209	m45	55.35	79.05	128 ± 7	0.62
209	p5	6.15	126.11	128 ± 7	0.99
209	p12	14.76	141.37	128 ± 7	1.1
209	p21	25.83	93.97	128 ± 7	0.73
209	p32	39.36	87.06	128 ± 7	0.68
209	p45	55.35	96.49	128 ± 7	0.75
210	c	0	209.71	184 ± 10	1.14
210	m5	6.15	212.02	184 ± 10	1.15
210	m12	14.76	286.25	184 ± 10	1.56
210	m21	25.83	389.39	184 ± 10	2.12
210	p5	6.15	211.79	184 ± 10	1.15
210	p12	14.76	190.02	184 ± 10	1.03
210	p21	25.83	174.48	184 ± 10	0.95
213	c	0	151.55	183 ± 24	0.83
213	m5	6.4	152.68	183 ± 24	0.83
213	m12	15.36	185.78	183 ± 24	1.02
213	m21	26.88	169.2	183 ± 24	0.93
213	p5	6.4	158.9	183 ± 24	0.87
213	p12	15.36	160.26	183 ± 24	0.88
213	p21	26.88	171.75	183 ± 24	0.94
214	c	0	191.97	119 ± 9	1.61
214	m5	6.45	191.8	119 ± 9	1.61
214	m12	15.48	233.76	119 ± 9	1.96
214	m21	27.09	327.73	119 ± 9	2.75
214	m32	41.28	248.32	119 ± 9	2.09
214	p5	6.45	178.21	119 ± 9	1.5
214	p12	15.48	204.85	119 ± 9	1.72
214	p21	27.09	353.59	119 ± 9	2.97
214	p32	41.28	139.86	119 ± 9	1.18

Continued on next page

Table D.1 – *Continued from previous page*

Object	**Coordinate**	Distance From Center (Kpc)	$\sigma_{[\mathbf{OIII}]}$ **(km/s)**	**SVD (km/s)**	$\sigma_{[\mathbf{OIII}]}$/ SVD
214	p45	58.05	93.66	119 ± 9	0.79

Column 1 - Object I.D. Given for Project, Column 2 - Spectrum Coordinate, Column 3 - Distance from Galactic Center Spectrum was Taken at, Column 4 - [OIII] Line Width Value, Column 5 - Stellar Velocity Dispersion, Column 6 - [OIII] line width Divided by the Stellar Velocity Dispersion

D.2 Double Gaussian Results

The following table contains the line widths collected from the main Gaussian fits (the green profile from the images above).

Table D.2: Double Gaussian Results

Object	Coordinate	Distance From Center (Kpc)	$\sigma_{[OIII]}$ (km/s)	SVD (km/s)	$\sigma_{[OIII]}$/ SVD
5	c	0	161.1	170 ± 2	0.95
5	m5	5.8	165.84	170 ± 2	0.98
5	m12	13.92	119.55	170 ± 2	0.7
5	m21	24.36	99.09	170 ± 2	0.58
5	p5	5.8	188.69	170 ± 2	1.11
5	p12	13.92	180.71	170 ± 2	1.06
6	c	0	102.25	196 ± 11	0.52
6	m5	7.2	118.35	196 ± 11	0.6
6	m12	17.28	96.63	196 ± 11	0.49
6	m21	30.24	342.63	196 ± 11	1.75
6	p5	7.2	117.98	196 ± 11	0.6
6	p12	17.28	121.05	196 ± 11	0.62
6	p21	30.24	98.34	196 ± 11	0.5
9	c	0	129.08	246 ± 3	0.53
9	m5	9	131.08	246 ± 3	0.53
9	m12	21.6	229.37	246 ± 3	0.93
9	p5	9	135.56	246 ± 3	0.55
9	p12	21.6	158.21	246 ± 3	0.64
10	c	0	96.13	120 ± 4	0.8
10	m5	5.25	96.27	120 ± 4	0.8
10	m12	12.6	104.69	120 ± 4	0.87
10	m21	22.05	99.08	120 ± 4	0.83
10	p5	5.25	99.5	120 ± 4	0.83
10	p12	12.6	98.28	120 ± 4	0.82
10	p21	22.05	110.24	120 ± 4	0.92
11	c	0	209.81	107 ± 11	1.96
11	m5	5.25	203.95	107 ± 11	1.91
11	m12	12.6	217.2	107 ± 11	2.03
11	m21	22.05	211.87	107 ± 11	1.98
11	m32	33.6	134.41	107 ± 11	1.26
11	m45	47.25	233.21	107 ± 11	2.18
11	p5	5.25	202.99	107 ± 11	1.9
11	p12	12.6	218.5	107 ± 11	2.04
11	p21	22.05	230.68	107 ± 11	2.16
11	p32	33.6	116.66	107 ± 11	1.09
11	p45	47.25	249.4	107 ± 11	2.33
13	c	0	140.31	131 ± 4	1.07
13	m5	2.15	143.02	131 ± 4	1.09
13	m12	5.16	196.6	131 ± 4	1.5
13	m21	9.03	152.09	131 ± 4	1.16
13	m32	13.76	134.9	131 ± 4	1.03
13	p5	2.15	146.39	131 ± 4	1.12
13	p12	5.16	177.1	131 ± 4	1.35
15	c	0	115.64	155 ± 8	0.75
15	m5	3.75	114.29	155 ± 8	0.74
15	m12	9	114.95	155 ± 8	0.74
15	m21	15.75	138.79	155 ± 8	0.9
15	p5	3.75	118.53	155 ± 8	0.77

Continued on next page

Table D.2 – *Continued from previous page*

Object	Coordinate	Distance From Center (Kpc)	$\sigma_{[OIII]}$ (km/s)	SVD (km/s)	$\sigma_{[OIII]}$/ SVD
15	p12	9	124.69	155 ± 8	0.8
15	p21	15.75	152.56	155 ± 8	0.98
15	p32	24	114.63	155 ± 8	0.74
19	c	0	119.35	127 ± 5	0.94
19	m5	5.65	118.81	127 ± 5	0.94
19	m12	13.56	98.04	127 ± 5	0.77
19	m21	23.73	138.82	127 ± 5	1.09
19	p5	5.65	124.76	127 ± 5	0.98
19	p12	13.56	131.24	127 ± 5	1.03
20	c	0	105.64	128 ± 9	0.83
20	m5	3.7	105.67	128 ± 9	0.83
20	m12	8.88	101.97	128 ± 9	0.8
20	m21	15.54	146.89	128 ± 9	1.15
20	p5	3.7	134.96	128 ± 9	1.05
20	p12	8.88	130.95	128 ± 9	1.02
20	p21	15.54	127.04	128 ± 9	0.99
20	p32	23.68	174.46	128 ± 9	1.36
21	c	0	109.02	91 ± 5	1.2
21	m5	4.95	115.66	91 ± 5	1.27
21	m12	11.88	159.02	91 ± 5	1.75
21	p5	4.95	112.7	91 ± 5	1.24
21	p12	11.88	166.82	91 ± 5	1.83
22	c	0	96.74	98 ± 3	0.99
22	m5	3.9	99.34	98 ± 3	1.01
22	m12	9.36	92.55	98 ± 3	0.94
22	m21	16.38	106.15	98 ± 3	1.08
22	m32	24.96	96.53	98 ± 3	0.99
22	p5	3.9	102.49	98 ± 3	1.05
22	p12	9.36	91.91	98 ± 3	0.94
22	p21	16.38	101.65	98 ± 3	1.04
22	p32	24.96	89.52	98 ± 3	0.91
22	p45	35.1	74.31	98 ± 3	0.76
23	c	0	132.81	129 ± 6	1.03
23	m5	3.3	134.67	129 ± 6	1.04
23	m12	7.92	146.78	129 ± 6	1.14
23	m21	13.86	161.01	129 ± 6	1.25
23	m32	21.12	88.23	129 ± 6	0.68
23	p5	3.3	146.91	129 ± 6	1.14
23	p12	7.92	181.21	129 ± 6	1.41
23	p21	13.86	213.45	129 ± 6	1.66
23	p32	21.12	113.5	129 ± 6	0.88
23	p45	29.7	106.71	129 ± 6	0.83
24	c	0	156.06	195 ± 2	0.8
24	m5	2.65	156.28	195 ± 2	0.8
24	m12	6.36	194.63	195 ± 2	1
24	m21	11.13	81.48	195 ± 2	0.42
24	m32	16.96	179.52	195 ± 2	0.92
24	m45	23.85	112.44	195 ± 2	0.58
24	p5	2.65	162.19	195 ± 2	0.83
24	p12	6.36	216.95	195 ± 2	1.11
24	p21	11.13	203	195 ± 2	1.04
24	p32	16.96	129.82	195 ± 2	0.67
24	p45	23.85	108.63	195 ± 2	0.56
26	c	0	120.38	124 ± 4	0.97
26	m5	5.5	139.48	124 ± 4	1.13
26	m12	13.2	138.9	124 ± 4	1.12
26	m21	23.1	163.76	124 ± 4	1.32

Continued on next page

Table D.2 – *Continued from previous page*

Object	Coordinate	Distance From Center (Kpc)	$\sigma_{[OIII]}$ (km/s)	SVD (km/s)	$\sigma_{[OIII]}$/ SVD
26	p5	5.5	134.97	124 ± 4	1.09
26	p12	13.2	133.81	124 ± 4	1.08
26	p21	23.1	141.84	124 ± 4	1.14
27	c	0	116.72	96 ± 6	1.22
27	m5	5.7	114.42	96 ± 6	1.19
27	m12	13.68	75.58	96 ± 6	0.79
27	m21	23.94	83.92	96 ± 6	0.87
27	p5	5.7	108.24	96 ± 6	1.13
27	p12	13.68	118.85	96 ± 6	1.24
27	p21	23.94	155.96	96 ± 6	1.63
28	c	0	167.18	124 ± 4	1.35
28	m5	2.2	147.97	124 ± 4	1.19
28	m12	5.28	184.54	124 ± 4	1.49
28	m21	9.24	98.78	124 ± 4	0.8
28	m32	14.08	102.6	124 ± 4	0.83
28	m45	19.8	95.3	124 ± 4	0.77
28	p5	2.2	158.64	124 ± 4	1.28
28	p12	5.28	151.98	124 ± 4	1.23
28	p21	9.24	165.85	124 ± 4	1.34
28	p32	14.08	116.86	124 ± 4	0.94
29	c	0	111.8	140 ± 3	0.8
29	m5	4.6	116.05	140 ± 3	0.83
29	m12	11.04	86.11	140 ± 3	0.62
29	m21	19.32	125.75	140 ± 3	0.9
29	m32	29.44	113.61	140 ± 3	0.81
29	p5	4.6	123.97	140 ± 3	0.89
29	p12	11.04	146.39	140 ± 3	1.05
29	p21	19.32	150.89	140 ± 3	1.08
29	p32	29.44	133.46	140 ± 3	0.95
29	p45	41.4	105.78	140 ± 3	0.76
30	c	0	118.71	154 ± 8	0.77
30	m5	5.05	101.7	154 ± 8	0.66
30	m12	12.12	144.7	154 ± 8	0.94
30	m21	21.21	153.71	154 ± 8	1
30	p5	5.05	79.9	154 ± 8	0.52
30	p12	12.12	188.1	154 ± 8	1.22
30	p21	21.21	234.82	154 ± 8	1.53
30	p32	32.32	150.19	154 ± 8	0.98
31	c	0	122.16	127 ± 6	0.96
31	m5	3.75	145.78	127 ± 6	1.15
31	m12	9	132.2	127 ± 6	1.04
31	m21	15.75	119.82	127 ± 6	0.94
31	m32	24	116.73	127 ± 6	0.92
31	p5	3.75	149.85	127 ± 6	1.18
31	p12	9	163.84	127 ± 6	1.29
31	p21	15.75	114.21	127 ± 6	0.9
31	p32	24	70.78	127 ± 6	0.56
32	c	0	136.76	108 ± 10	1.27
32	m5	5.1	130.22	108 ± 10	1.21
32	m12	12.24	135.48	108 ± 10	1.25
32	m21	21.42	170.97	108 ± 10	1.58
32	p5	5.1	134.84	108 ± 10	1.25
32	p12	12.24	126.22	108 ± 10	1.17
32	p21	21.42	82.59	108 ± 10	0.77
32	p32	32.64	103.62	108 ± 10	0.96
34	c	0	129.49	77 ± 17	1.68
34	m5	5.35	126.15	77 ± 17	1.64

Continued on next page

Table D.2 – *Continued from previous page*

Object	Coordinate	Distance From Center (Kpc)	$\sigma_{[OIII]}$ (km/s)	SVD (km/s)	$\sigma_{[OIII]}$/ SVD
34	m12	12.84	114.84	77 ± 17	1.49
34	m21	22.47	112.41	77 ± 17	1.46
34	p5	5.35	129.68	77 ± 17	1.68
34	p12	12.84	133.05	77 ± 17	1.73
34	p21	22.47	152.18	77 ± 17	1.98
35	c	0	147.33	144 ± 14	1.02
35	m5	3.55	142.18	144 ± 14	0.99
35	m12	8.52	146.47	144 ± 14	1.02
35	m21	14.91	101.14	144 ± 14	0.7
35	m32	22.72	121.52	144 ± 14	0.84
35	p5	3.55	141.73	144 ± 14	0.98
35	p12	8.52	139.88	144 ± 14	0.97
35	p21	14.91	159.34	144 ± 14	1.11
35	p32	22.72	165.69	144 ± 14	1.15
36	c	0	106.16	91 ± 7	1.17
36	m5	4.8	105.43	91 ± 7	1.16
36	m12	11.52	120.34	91 ± 7	1.32
36	m21	20.16	76.78	91 ± 7	0.84
36	p5	4.8	103.13	91 ± 7	1.13
36	p12	11.52	112.79	91 ± 7	1.24
36	p21	20.16	114.96	91 ± 7	1.26
36	p32	30.72	66.99	91 ± 7	0.74
38	c	0	110.98	119 ± 3	0.93
38	m5	5.8	129.98	119 ± 3	1.09
38	m12	13.92	199.01	119 ± 3	1.67
38	m21	24.36	97.16	119 ± 3	0.82
38	p5	5.8	111.3	119 ± 3	0.94
38	p12	13.92	117.03	119 ± 3	0.98
38	p21	24.36	112.77	119 ± 3	0.95
39	c	0	162.52	166 ± 7	0.98
39	m5	5.25	182.82	166 ± 7	1.1
39	m12	12.6	185.58	166 ± 7	1.12
39	p5	5.25	161.81	166 ± 7	0.98
39	p12	12.6	121.45	166 ± 7	0.73
40	c	0	92.59	82 ± 2	1.13
40	m5	3.45	113.86	82 ± 2	1.39
40	m12	8.28	123.86	82 ± 2	1.51
40	m21	14.49	145.94	82 ± 2	1.78
40	m32	22.08	198.14	82 ± 2	2.42
40	p5	3.45	145.82	82 ± 2	1.78
40	p12	8.28	143.77	82 ± 2	1.75
40	p21	14.49	105.74	82 ± 2	1.29
40	p32	22.08	86.48	82 ± 2	1.06
40	p45	31.05	81.76	82 ± 2	1
41	c	0	86.55	118 ± 6	0.73
41	m5	5.2	86.33	118 ± 6	0.73
41	m12	12.48	190.17	118 ± 6	1.61
41	m21	21.84	117.45	118 ± 6	1
41	p5	5.2	87.98	118 ± 6	0.75
41	p12	12.48	114.45	118 ± 6	0.97
41	p21	21.84	111.13	118 ± 6	0.94
42	c	0	130.44	157 ± 6	0.83
42	m5	5.05	103.91	157 ± 6	0.66
42	m12	12.12	83.55	157 ± 6	0.53
42	m21	21.21	80.56	157 ± 6	0.51
42	m32	32.32	90.7	157 ± 6	0.58
42	p5	5.05	123.52	157 ± 6	0.79

Continued on next page

Table D.2 – *Continued from previous page*

Object	Coordinate	Distance From Center (Kpc)	$\sigma_{[OIII]}$ (km/s)	SVD (km/s)	$\sigma_{[OIII]}$/ SVD
42	p12	12.12	92.12	157 ± 6	0.59
42	p21	21.21	87.17	157 ± 6	0.56
42	p32	32.32	76.73	157 ± 6	0.49
42	p45	45.45	76.5	157 ± 6	0.49
43	c	0	139.96	144 ± 5	0.97
43	m5	2.3	141.56	144 ± 5	0.98
43	m12	5.52	135.34	144 ± 5	0.94
43	m21	9.66	150.06	144 ± 5	1.04
43	m32	14.72	127.74	144 ± 5	0.89
43	p5	2.3	139.3	144 ± 5	0.97
43	p12	5.52	141.55	144 ± 5	0.98
43	p21	9.66	157.35	144 ± 5	1.09
43	p32	14.72	131.1	144 ± 5	0.91
44	c	0	152.85	172 ± 7	0.89
44	m5	3.1	154.12	172 ± 7	0.9
44	m12	7.44	155.48	172 ± 7	0.9
44	m21	13.02	115.72	172 ± 7	0.67
44	m32	19.84	117.91	172 ± 7	0.69
44	m45	27.9	87.83	172 ± 7	0.51
44	p5	3.1	185.7	172 ± 7	1.08
44	p12	7.44	158.36	172 ± 7	0.92
44	p21	13.02	123.67	172 ± 7	0.72
44	p32	19.84	100.62	172 ± 7	0.59
44	p45	27.9	80.17	172 ± 7	0.47
45	c	0	151.54	97 ± 8	1.56
45	m5	2.35	105.78	97 ± 8	1.09
45	m12	5.64	180.7	97 ± 8	1.86
45	m21	9.87	157.16	97 ± 8	1.62
45	m32	15.04	158.85	97 ± 8	1.64
45	p5	2.35	113.76	97 ± 8	1.17
45	p12	5.64	158.77	97 ± 8	1.64
45	p21	9.87	178.25	97 ± 8	1.84
46	c	0	163.65	107 ± 8	1.53
46	m5	4.6	164.16	107 ± 8	1.53
46	m12	11.04	121.84	107 ± 8	1.14
46	p5	4.6	180.79	107 ± 8	1.69
46	p12	11.04	89.81	107 ± 8	0.84
47	c	0	120.67	100 ± 4	1.21
47	m5	4.95	118.76	100 ± 4	1.19
47	m12	11.88	124.3	100 ± 4	1.24
47	m21	20.79	77.42	100 ± 4	0.77
47	m32	31.68	79.38	100 ± 4	0.79
47	m45	44.55	102.38	100 ± 4	1.02
47	p5	4.95	119.87	100 ± 4	1.2
47	p12	11.88	130.26	100 ± 4	1.3
47	p21	20.79	249.86	100 ± 4	2.5
47	p32	31.68	106.95	100 ± 4	1.07
49	c	0	131.36	122 ± 9	1.08
49	m5	5.45	146.4	122 ± 9	1.2
49	m12	13.08	113.81	122 ± 9	0.93
49	m21	22.89	104.1	122 ± 9	0.85
49	m21	22.89	106.95	122 ± 9	0.88
49	m32	34.88	95.82	122 ± 9	0.79
49	p5	5.45	129.86	122 ± 9	1.06
49	p12	13.08	112.66	122 ± 9	0.92
49	p21	22.89	115.45	122 ± 9	0.95
49	p32	34.88	91.89	122 ± 9	0.75

Continued on next page

Table D.2 – *Continued from previous page*

Object	Coordinate	Distance From Center (Kpc)	$\sigma_{[OIII]}$ (km/s)	SVD (km/s)	$\sigma_{[OIII]}$/ SVD
51	c	0	132.65	123 ± 4	1.08
51	m5	5.25	124.17	123 ± 4	1.01
51	m12	12.6	214.85	123 ± 4	1.75
51	p5	5.25	135.81	123 ± 4	1.1
51	p12	12.6	162.46	123 ± 4	1.32
51	p21	22.05	126.8	123 ± 4	1.03
52	c	0	183.77	149 ± 4	1.23
52	m5	5.25	175.92	149 ± 4	1.18
52	m12	12.6	180.15	149 ± 4	1.21
52	m21	22.05	140.83	149 ± 4	0.95
52	m32	33.6	104.03	149 ± 4	0.7
52	m45	47.25	149.03	149 ± 4	1
52	p5	5.25	177.73	149 ± 4	1.19
52	p12	12.6	317.86	149 ± 4	2.13
52	p21	22.05	236.1	149 ± 4	1.59
52	p32	33.6	125	149 ± 4	0.84
52	p45	47.25	105.89	149 ± 4	0.71
53	c	0	213.61	185 ± 10	1.16
53	m5	5.4	195.69	185 ± 10	1.06
53	m12	12.96	145.77	185 ± 10	0.79
53	m21	22.68	514.34	185 ± 10	2.78
53	m32	34.56	94.03	185 ± 10	0.51
53	p5	5.4	213.62	185 ± 10	1.16
53	p12	12.96	241.71	185 ± 10	1.31
53	p21	22.68	217.27	185 ± 10	1.17
53	p32	34.56	142.23	185 ± 10	0.77
54	c	0	128.5	114 ± 7	1.13
54	m5	3.65	131.84	114 ± 7	1.16
54	m12	8.76	130.21	114 ± 7	1.14
54	m21	15.33	105.78	114 ± 7	0.93
54	m32	23.36	83.44	114 ± 7	0.73
54	m45	32.85	93.76	114 ± 7	0.82
54	p5	3.65	126.44	114 ± 7	1.11
54	p12	8.76	136.48	114 ± 7	1.2
54	p21	15.33	129.57	114 ± 7	1.14
54	p32	23.36	306.47	114 ± 7	2.69
57	c	0	150.52	116 ± 4	1.3
57	m5	3.05	150.91	116 ± 4	1.3
57	m12	7.32	178.53	116 ± 4	1.54
57	m21	12.81	194.59	116 ± 4	1.68
57	m32	19.52	185.42	116 ± 4	1.6
57	p5	3.05	162.24	116 ± 4	1.4
57	p12	7.32	140.29	116 ± 4	1.21
57	p21	12.81	103.83	116 ± 4	0.9
57	p32	19.52	163.82	116 ± 4	1.41
57	p45	27.45	158.83	116 ± 4	1.37
58	c	0	142.49	171 ± 5	0.83
58	m5	4.7	124.08	171 ± 5	0.73
58	m12	11.28	124.64	171 ± 5	0.73
58	m21	19.74	123.06	171 ± 5	0.72
58	m32	30.08	96.99	171 ± 5	0.57
58	p5	4.7	143.18	171 ± 5	0.84
58	p12	11.28	139.33	171 ± 5	0.82
58	p21	19.74	117.97	171 ± 5	0.69
58	p32	30.08	121.07	171 ± 5	0.71
58	p32	30.08	97.06	171 ± 5	0.57
59	c	0	193.15	159 ± 4	1.22

Continued on next page

Table D.2 – *Continued from previous page*

Object	Coordinate	Distance From Center (Kpc)	$\sigma_{[OIII]}$ (km/s)	SVD (km/s)	$\sigma_{[OIII]}$/ SVD
59	m5	4.75	186.93	159 ± 4	1.18
59	m12	11.4	106.12	159 ± 4	0.67
59	m21	19.95	107.41	159 ± 4	0.68
59	m32	30.4	118.13	159 ± 4	0.74
59	p5	4.75	140.7	159 ± 4	0.89
59	p12	11.4	109.46	159 ± 4	0.69
59	p21	19.95	134.27	159 ± 4	0.84
59	p32	30.4	142.1	159 ± 4	0.89
59	p45	42.75	143.68	159 ± 4	0.9
61	c	0	123.44	186 ± 8	0.66
61	m5	5.2	116.63	186 ± 8	0.63
61	m12	12.48	113.66	186 ± 8	0.61
61	m21	21.84	93.5	186 ± 8	0.5
61	m32	33.28	184.96	186 ± 8	0.99
61	p5	5.2	127.56	186 ± 8	0.69
61	p12	12.48	130.38	186 ± 8	0.7
61	p21	21.84	238.93	186 ± 8	1.29
62	c	0	101.81	170 ± 8	0.6
62	m5	5.65	194.65	170 ± 8	1.15
62	m12	13.56	211.91	170 ± 8	1.25
62	m21	23.73	124.67	170 ± 8	0.73
62	m32	36.16	137.98	170 ± 8	0.81
62	p5	5.65	97.99	170 ± 8	0.58
62	p12	13.56	90.52	170 ± 8	0.53
62	p21	23.73	100.45	170 ± 8	0.59
63	c	0	141.61	120 ± 5	1.18
63	m5	4.05	143.25	120 ± 5	1.19
63	m12	9.72	151.38	120 ± 5	1.26
63	m21	17.01	110.54	120 ± 5	0.92
63	p5	4.05	147.75	120 ± 5	1.23
63	p12	9.72	191.2	120 ± 5	1.59
63	p21	17.01	219.13	120 ± 5	1.83
70	c	0	125.01	266 ± 3	0.47
70	m5	4.5	130.52	266 ± 3	0.49
70	m12	10.8	191.21	266 ± 3	0.72
70	m21	18.9	215.51	266 ± 3	0.81
70	m32	28.8	125.15	266 ± 3	0.47
70	m45	40.5	118.52	266 ± 3	0.45
70	p5	4.5	128.62	266 ± 3	0.48
70	p12	10.8	211.03	266 ± 3	0.79
70	p21	18.9	229.7	266 ± 3	0.86
70	p32	28.8	59.6	266 ± 3	0.22
71	c	0	122.74	134 ± 5	0.92
71	m5	5.95	132.75	134 ± 5	0.99
71	m12	14.28	308.57	134 ± 5	2.3
71	m45	53.55	100.3	134 ± 5	0.75
71	p5	5.95	131.14	134 ± 5	0.98
71	p12	14.28	326.59	134 ± 5	2.44
71	p45	53.55	91.73	134 ± 5	0.69
73	c	0	122.41	131 ± 6	0.93
73	m5	7.6	183.32	131 ± 6	1.4
73	m12	18.24	270.31	131 ± 6	2.06
73	p5	7.6	129.19	131 ± 6	0.99
73	p12	18.24	133.36	131 ± 6	1.02
73	p21	31.92	117.96	131 ± 6	0.9
74	c	0	131.71	165 ± 17	0.8
74	m5	8.65	148.15	165 ± 17	0.9

Continued on next page

Table D.2 – *Continued from previous page*

Object	Coordinate	Distance From Center (Kpc)	$\sigma_{[OIII]}$ (km/s)	SVD (km/s)	$\sigma_{[OIII]}$/ SVD
74	m12	20.76	180.84	165 ± 17	1.1
74	m21	36.33	162.04	165 ± 17	0.98
74	m32	55.36	89.7	165 ± 17	0.54
74	p5	8.65	131.2	165 ± 17	0.8
74	p12	20.76	142.8	165 ± 17	0.87
74	p21	36.33	181.38	165 ± 17	1.1
74	p32	55.36	81.68	165 ± 17	0.5
76	c	0	104.98	193 ± 4	0.54
76	m5	7.95	126.43	193 ± 4	0.66
76	m12	19.08	220.83	193 ± 4	1.14
76	p5	7.95	126.99	193 ± 4	0.66
76	p12	19.08	239.33	193 ± 4	1.24
77	c	0	132.23	188 ± 4	0.7
77	m5	5.95	157.64	188 ± 4	0.84
77	m12	14.28	135.18	188 ± 4	0.72
77	m21	24.99	109.08	188 ± 4	0.58
77	p5	5.95	145.09	188 ± 4	0.77
77	p12	14.28	157.97	188 ± 4	0.84
77	p21	24.99	247.96	188 ± 4	1.32
78	c	0	156.04	97 ± 4	1.61
78	m5	6.8	147.31	97 ± 4	1.52
78	m12	16.32	296.51	97 ± 4	3.06
78	p5	6.8	141.48	97 ± 4	1.46
78	p12	16.32	178.77	97 ± 4	1.84
78	p21	28.56	89.77	97 ± 4	0.93
79	c	0	142.73	90 ± 6	1.59
79	m5	7.1	138.44	90 ± 6	1.54
79	m12	17.04	353.83	90 ± 6	3.93
79	p5	7.1	141.93	90 ± 6	1.58
79	p12	17.04	435.73	90 ± 6	4.84
82	c	0	105.22	156 ± 23	0.68
82	m5	8.9	134.58	156 ± 23	0.86
82	p5	8.9	135.72	156 ± 23	0.87
82	p12	21.36	83.7	156 ± 23	0.54
83	c	0	157.2	90 ± 18	1.75
83	m5	8.25	153.62	90 ± 18	1.71
83	m12	19.8	174.13	90 ± 18	1.94
83	m21	34.65	293.43	90 ± 18	3.26
83	p5	8.25	159.81	90 ± 18	1.78
83	p12	19.8	197.69	90 ± 18	2.2
83	p21	34.65	462.55	90 ± 18	5.14
88	c	0	183.01	199 ± 6	0.92
88	m5	7.9	216.55	199 ± 6	1.09
88	m12	18.96	94.09	199 ± 6	0.47
88	p5	7.9	173.41	199 ± 6	0.87
88	p12	18.96	150.48	199 ± 6	0.76
91	c	0	175.27	172 ± 13	1.02
91	m5	6.9	177.99	172 ± 13	1.04
91	m12	16.56	145.8	172 ± 13	0.85
91	m21	28.98	99.34	172 ± 13	0.58
91	m32	44.16	85.89	172 ± 13	0.5
91	p5	6.9	181.44	172 ± 13	1.06
91	p12	16.56	95.82	172 ± 13	0.56
91	p21	28.98	81.39	172 ± 13	0.47
91	p32	44.16	83.07	172 ± 13	0.48
91	p45	62.1	225.75	172 ± 13	1.31
99	c	0	209.15	71 ± 28	2.95

Continued on next page

Table D.2 – *Continued from previous page*

Object	Coordinate	Distance From Center (Kpc)	$\sigma_{[OIII]}$ (km/s)	SVD (km/s)	$\sigma_{[OIII]}$/ SVD
99	m5	7.85	217.28	71 ± 28	3.06
99	m12	18.84	154.62	71 ± 28	2.18
99	m21	32.97	166.61	71 ± 28	2.35
99	m32	50.24	115.22	71 ± 28	1.62
99	p5	7.85	216.19	71 ± 28	3.05
99	p12	18.84	231.52	71 ± 28	3.26
99	p21	32.97	136.05	71 ± 28	1.92
102	c	0	107.39	115 ± 17	0.93
102	m5	8.5	106.93	115 ± 17	0.93
102	m12	20.4	134.8	115 ± 17	1.17
102	p5	8.5	125.12	115 ± 17	1.09
102	p12	20.4	191.59	115 ± 17	1.67
103	c	0	208.37	99 ± 8	2.11
103	m5	7.75	206.85	99 ± 8	2.09
103	m12	18.6	184.19	99 ± 8	1.86
103	m21	32.55	234.64	99 ± 8	2.37
103	m32	49.6	111.59	99 ± 8	1.13
103	m45	69.75	93.73	99 ± 8	0.95
103	p5	7.75	212.26	99 ± 8	2.14
103	p12	18.6	164.7	99 ± 8	1.66
103	p21	32.55	514.78	99 ± 8	5.2
103	p32	49.6	106.81	99 ± 8	1.08
106	c	0	143.56	198 ± 6	0.73
106	m5	8.7	168	198 ± 6	0.85
106	m12	20.88	174.63	198 ± 6	0.88
106	m21	36.54	129.08	198 ± 6	0.65
106	m32	55.68	132.06	198 ± 6	0.67
106	m45	78.3	98.38	198 ± 6	0.5
106	p5	8.7	146.67	198 ± 6	0.74
106	p12	20.88	124.61	198 ± 6	0.63
106	p21	36.54	121.53	198 ± 6	0.61
106	p32	55.68	134.62	198 ± 6	0.68
109	c	0	98.66	237 ± 9	0.42
109	c	0	98.66	237 ± 9	0.42
109	m5	8.9	136.56	237 ± 9	0.58
109	m5	8.9	136.56	237 ± 9	0.58
109	m12	21.36	78.46	237 ± 9	0.33
109	m12	21.36	78.46	237 ± 9	0.33
109	m21	37.38	111.79	237 ± 9	0.47
109	m21	37.38	111.79	237 ± 9	0.47
109	p5	8.9	107.46	237 ± 9	0.45
109	p5	8.9	107.46	237 ± 9	0.45
109	p12	21.36	73.13	237 ± 9	0.31
109	p12	21.36	73.13	237 ± 9	0.31
109	p21	37.38	68.14	237 ± 9	0.29
109	p21	37.38	68.14	237 ± 9	0.29
114	c	0	115.95	136 ± 6	0.85
114	m5	6.25	100.71	136 ± 6	0.74
114	m12	15	169.36	136 ± 6	1.25
114	p5	6.25	100.07	136 ± 6	0.74
114	p12	15	132.92	136 ± 6	0.98
126	c	0	86.49	1211 ± 5	0.07
126	m5	6.3	86.81	1211 ± 5	0.07
126	m12	15.12	79.71	1211 ± 5	0.07
126	m21	26.46	104.72	1211 ± 5	0.09
126	m32	40.32	80.04	1211 ± 5	0.07
126	p5	6.3	88.76	1211 ± 5	0.07

Continued on next page

Table D.2 – *Continued from previous page*

Object	Coordinate	Distance From Center (Kpc)	$\sigma_{[OIII]}$ (km/s)	SVD (km/s)	$\sigma_{[OIII]}$/ SVD
126	p12	15.12	91.25	1211 ± 5	0.08
126	p21	26.46	87.69	1211 ± 5	0.07
126	p32	40.32	68.25	1211 ± 5	0.06
126	p45	56.7	66.75	1211 ± 5	0.06
138	c	0	99.47	143 ± 3	0.7
138	m5	6	100.99	143 ± 3	0.71
138	m12	14.4	146.73	143 ± 3	1.03
138	p5	6	94.83	143 ± 3	0.66
138	p12	14.4	88.67	143 ± 3	0.62
138	p21	25.2	91.42	143 ± 3	0.64
155	c	0	147.54	197 ± 5	0.75
155	m5	5.85	150.4	197 ± 5	0.76
155	m12	14.04	148.68	197 ± 5	0.76
155	m21	24.57	150.66	197 ± 5	0.77
155	m32	37.44	211.54	197 ± 5	1.07
155	p5	5.85	155.31	197 ± 5	0.79
155	p12	14.04	143.19	197 ± 5	0.73
155	p21	24.57	141.61	197 ± 5	0.72
155	p32	37.44	100.07	197 ± 5	0.51
156	c	0	120.66	165 ± 6	0.73
156	m5	6.45	124.03	165 ± 6	0.75
156	m12	15.48	138.38	165 ± 6	0.84
156	m21	27.09	111.26	165 ± 6	0.67
156	m32	41.28	91.7	165 ± 6	0.56
156	m45	58.05	111.66	165 ± 6	0.68
156	p5	6.45	139.1	165 ± 6	0.84
156	p12	15.48	157.67	165 ± 6	0.96
156	p21	27.09	115.11	165 ± 6	0.7
156	p32	41.28	92.47	165 ± 6	0.56
162	c	0	115.16	121 ± 3	0.95
162	m5	6.45	116.36	121 ± 3	0.96
162	m12	15.48	137.8	121 ± 3	1.14
162	m21	27.09	255.03	121 ± 3	2.11
162	p5	6.45	123.89	121 ± 3	1.02
162	p12	15.48	126.58	121 ± 3	1.05
162	p21	27.09	185.42	121 ± 3	1.53
177	c	0	109.52	121 ± 6	0.91
177	m5	6.05	109.73	121 ± 6	0.91
177	m12	14.52	89.58	121 ± 6	0.74
177	m45	54.45	87.95	121 ± 6	0.73
177	p5	6.05	110.59	121 ± 6	0.91
177	p12	14.52	104.1	121 ± 6	0.86
180	c	0	117.05	120 ± 18	0.98
180	m5	6.6	120.55	120 ± 18	1.01
180	m12	15.84	148.56	120 ± 18	1.24
180	m21	27.72	193.66	120 ± 18	1.61
180	m32	42.24	93.98	120 ± 18	0.78
180	p5	6.6	103.53	120 ± 18	0.86
180	p12	15.84	152.68	120 ± 18	1.27
180	p21	27.72	151.06	120 ± 18	1.26
180	p32	42.24	869.02	120 ± 18	7.24
187	c	0	171.09	166 ± 6	1.03
187	m5	6.05	171.25	166 ± 6	1.03
187	m12	14.52	159.93	166 ± 6	0.96
187	m21	25.41	107.72	166 ± 6	0.65
187	m32	38.72	71.14	166 ± 6	0.43
187	p5	6.05	153.99	166 ± 6	0.93

Continued on next page

Table D.2 – *Continued from previous page*

Object	Coordinate	Distance From Center (Kpc)	$\sigma_{[OIII]}$ (km/s)	SVD (km/s)	$\sigma_{[OIII]}$/ SVD
187	p12	14.52	145.29	166 ± 6	0.88
187	p21	25.41	151.64	166 ± 6	0.91
187	p32	38.72	211.3	166 ± 6	1.27
196	c	0	222.03	228 ± 7	0.97
196	c	0	222.03	228 ± 7	0.97
196	m5	6	222.58	228 ± 7	0.98
196	m5	6	222.58	228 ± 7	0.98
196	m12	14.4	200.97	228 ± 7	0.88
196	m12	14.4	200.97	228 ± 7	0.88
196	m21	25.2	207.89	228 ± 7	0.91
196	m21	25.2	207.89	228 ± 7	0.91
196	m32	38.4	180.74	228 ± 7	0.79
196	m32	38.4	180.74	228 ± 7	0.79
196	m45	54	85.86	228 ± 7	0.38
196	m45	54	85.86	228 ± 7	0.38
196	p5	6	271.05	228 ± 7	1.19
196	p5	6	227.6	228 ± 7	1
196	p12	14.4	141.55	228 ± 7	0.62
196	p12	14.4	141.55	228 ± 7	0.62
196	p21	25.2	208.43	228 ± 7	0.91
196	p21	25.2	208.43	228 ± 7	0.91
196	p32	38.4	145.1	228 ± 7	0.64
196	p32	38.4	145.1	228 ± 7	0.64
196	p45	54	122.97	228 ± 7	0.54
196	p45	54	122.97	228 ± 7	0.54
197	c	0	120.74	144 ± 4	0.84
197	m5	6.1	120.88	144 ± 4	0.84
197	m12	14.64	126.39	144 ± 4	0.88
197	m21	25.62	136.24	144 ± 4	0.95
197	m32	39.04	97	144 ± 4	0.67
197	p5	6.1	116.24	144 ± 4	0.81
197	p12	14.64	132.81	144 ± 4	0.92
197	p21	25.62	115.83	144 ± 4	0.8
197	p32	39.04	171.67	144 ± 4	1.19
202	c	0	107.23	113 ± 5	0.95
202	m5	6.4	108.89	113 ± 5	0.96
202	m12	15.36	116.27	113 ± 5	1.03
202	m21	26.88	103.71	113 ± 5	0.92
202	p5	6.4	113.6	113 ± 5	1.01
202	p12	15.36	109.84	113 ± 5	0.97
202	p21	26.88	119.31	113 ± 5	1.06
204	c	0	103.9	133 ± 9	0.78
204	m5	5.85	103.76	133 ± 9	0.78
204	m12	14.04	99.58	133 ± 9	0.75
204	m21	24.57	126.04	133 ± 9	0.95
204	m32	37.44	91.64	133 ± 9	0.69
204	m45	52.65	79.69	133 ± 9	0.6
204	p5	5.85	102.25	133 ± 9	0.77
204	p12	14.04	105.07	133 ± 9	0.79
204	p21	24.57	118.9	133 ± 9	0.89
204	p32	37.44	87.02	133 ± 9	0.65
205	c	0	191.44	144 ± 10	1.33
205	m5	5.9	191.26	144 ± 10	1.33
205	m12	14.16	250.62	144 ± 10	1.74
205	m21	24.78	169.09	144 ± 10	1.17
205	p5	5.9	178.44	144 ± 10	1.24
205	p12	14.16	98.89	144 ± 10	0.69

Continued on next page

Table D.2 – *Continued from previous page*

Object	Coordinate	Distance From Center (Kpc)	$\sigma_{[OIII]}$ (km/s)	SVD (km/s)	$\sigma_{[OIII]}$/ SVD
205	p21	24.78	174.88	144 ± 10	1.21
205	p32	37.76	110.5	144 ± 10	0.77
207	c	0	125.99	168 ± 11	0.75
207	m5	6.05	119.13	168 ± 11	0.71
207	m12	14.52	140.11	168 ± 11	0.83
207	m21	25.41	123.7	168 ± 11	0.74
207	p5	6.05	129.48	168 ± 11	0.77
207	p12	14.52	124.56	168 ± 11	0.74
207	p21	25.41	103.93	168 ± 11	0.62
208	c	0	132.71	201 ± 13	0.66
208	m5	6.1	155.61	201 ± 13	0.77
208	m12	14.64	104.73	201 ± 13	0.52
208	m21	25.62	89.84	201 ± 13	0.45
208	p12	14.64	236.05	201 ± 13	1.17
208	p21	25.62	422.02	201 ± 13	2.1
209	c	0	89.79	128 ± 7	0.7
209	m5	6.15	94.06	128 ± 7	0.74
209	m12	14.76	121.59	128 ± 7	0.95
209	m21	25.83	118.12	128 ± 7	0.92
209	m32	39.36	95.85	128 ± 7	0.75
209	m45	55.35	79.05	128 ± 7	0.62
209	p5	6.15	91.24	128 ± 7	0.71
209	p12	14.76	115.23	128 ± 7	0.9
209	p21	25.83	93.32	128 ± 7	0.73
209	p32	39.36	87.06	128 ± 7	0.68
209	p45	55.35	98.63	128 ± 7	0.77
210	c	0	154.34	184 ± 10	0.84
210	m5	6.15	150.96	184 ± 10	0.82
210	m12	14.76	156.68	184 ± 10	0.85
210	m21	25.83	358.05	184 ± 10	1.95
210	p5	6.15	152.44	184 ± 10	0.83
210	p12	14.76	160.24	184 ± 10	0.87
210	p21	25.83	124.91	184 ± 10	0.68
213	c	0	86.6	183 ± 24	0.47
213	m5	6.4	96.17	183 ± 24	0.53
213	m12	15.36	128.54	183 ± 24	0.7
213	m21	26.88	128.28	183 ± 24	0.7
213	p5	6.4	149.11	183 ± 24	0.82
213	p12	15.36	143.39	183 ± 24	0.78
213	p21	26.88	134.34	183 ± 24	0.73
214	c	0	121.21	119 ± 9	1.02
214	m5	6.45	121.76	119 ± 9	1.02
214	m12	15.48	157.78	119 ± 9	1.33
214	m21	27.09	154.7	119 ± 9	1.3
214	m32	41.28	149.07	119 ± 9	1.25
214	p5	6.45	111.09	119 ± 9	0.93
214	p12	15.48	156.49	119 ± 9	1.32
214	p21	27.09	129.5	119 ± 9	1.09
214	p32	41.28	123	119 ± 9	1.03
214	p45	58.05	94.51	119 ± 9	0.79

Column 1 - Object I.D. Given for Project, Column 2 - Spectrum Coordinate, Column 3 - Distance from Galactic Center Spectrum was Taken at, Column 4 - [OIII] Line Width Value, Column 5 - Stellar Velocity Dispersion, Column 6 - [OIII] line width Divided by the Stellar Velocity Dispersion

D.3 Combined Gaussian Selection

The following is a table compiling which spectra were fit with a double Gaussian fit for the combined Gaussian method. The remainder were fit using a single Gaussian method.

Table D.3: Combined Gaussian Selection

Object	Coordinate
36	c
36	m5
36	m12
36	m21
36	p5
36	p12
36	p21
51	c
51	m5
51	p5
51	p12
52	c
52	m5
52	m12
52	p5
53	c
53	m5
53	m12
53	p5
53	p12
57	c
57	m5
57	m12
57	m21
57	m32
57	p5
57	p12
57	p21
57	p32
57	p45
63	c
63	m5
63	m12
63	m21
63	p5
63	p12
63	p21
70	c
70	m5
70	m12
70	m21
70	m32
70	p5
70	p12
70	p21
70	p32
71	c

Continued on next page

Table D.3 – *Continued from previous page*

Object	Coordinate
71	m5
71	p5
74	c
74	m5
74	m12
74	p5
74	p12
78	c
78	m5
78	p5
78	p12
79	c
79	m5
79	p5
103	c
103	m5
103	m12
103	m21
103	p5
103	p12
103	p32
109	c
109	m5
109	m12
109	m21
109	p5
109	p12
109	p21
126	c
126	m5
126	m12
126	m21
126	m32
126	p5
126	p12
126	p21
126	p32
196	c
196	m5
196	m12
196	m21
196	m45
196	p5
196	p12
210	c
210	m5
210	m12
210	p5
210	p12
210	p21

Column 1 - Object I.D. Given for Project, Column 2 - Spectrum Coordinate

D.4 Gauss-Hermite Results

Table D.4: Gauss-Hermite Results

Object	**Coordinate**	Order	Distance From Center (Kpc)	$\sigma_{[OIII]}$ **(km/s)**	**SVD (km/s)**	$\sigma_{[OIII]}$/ SVD
5	c	4	0	187.11	170 ± 2	1.1
5	m5	4	5.8	162.06	170 ± 2	0.95
5	m12	3	13.92	123.17	170 ± 2	0.72
5	m21	3	24.36	94.1	170 ± 2	0.55
5	p5	4	5.8	170.06	170 ± 2	1
5	p12	3	13.92	193.03	170 ± 2	1.14
6	c	4	0	151.08	196 ± 11	0.77
6	m5	4	7.2	157.97	196 ± 11	0.81
6	m12	3	17.28	175.62	196 ± 11	0.9
6	m21	3	30.24	349.07	196 ± 11	1.78
6	p5	4	7.2	155.2	196 ± 11	0.79
6	p12	3	17.28	166.27	196 ± 11	0.85
6	p21	3	30.24	108.26	196 ± 11	0.55
9	c	4	0	165.2	246 ± 3	0.67
9	m5	4	9	170.85	246 ± 3	0.69
9	m12	3	21.6	246.93	246 ± 3	1
9	p5	4	9	195.43	246 ± 3	0.79
9	p12	3	21.6	210.4	246 ± 3	0.86
10	c	4	0	108.23	120 ± 4	0.9
10	m5	4	5.25	108.38	120 ± 4	0.9
10	m12	4	12.6	122.37	120 ± 4	1.02
10	m21	3	22.05	125.57	120 ± 4	1.05
10	p5	4	5.25	111.13	120 ± 4	0.93
10	p12	4	12.6	116.93	120 ± 4	0.97
10	p21	4	22.05	131.29	120 ± 4	1.09
11	c	4	0	217.81	107 ± 11	2.04
11	m5	4	5.25	220.32	107 ± 11	2.06
11	m12	3	12.6	233.68	107 ± 11	2.18
11	m21	3	22.05	260.38	107 ± 11	2.43
11	m32	2	33.6	260.31	107 ± 11	2.43
11	m45	2	47.25	361.06	107 ± 11	3.37
11	p5	4	5.25	219.74	107 ± 11	2.05
11	p12	3	12.6	229.07	107 ± 11	2.14
11	p21	3	22.05	266.23	107 ± 11	2.49
11	p32	2	33.6	275.59	107 ± 11	2.58
13	c	4	0	157.37	131 ± 4	1.2
13	m5	4	2.15	162.8	131 ± 4	1.24
13	m12	3	5.16	192.88	131 ± 4	1.47
13	m21	3	9.03	151.77	131 ± 4	1.16
13	m32	2	13.76	133.79	131 ± 4	1.02
13	p5	4	2.15	163.25	131 ± 4	1.25
13	p12	3	5.16	178.75	131 ± 4	1.36
15	c	10	0	149.22	155 ± 8	0.96
15	m5	4	3.75	157.53	155 ± 8	1.02
15	m12	3	9	202.2	155 ± 8	1.3
15	m21	3	15.75	278.23	155 ± 8	1.8
15	p5	4	3.75	154.02	155 ± 8	0.99
15	p12	3	9	169.38	155 ± 8	1.09
15	p21	3	15.75	184.26	155 ± 8	1.19
15	p32	2	24	111.46	155 ± 8	0.72
19	c	4	0	144.85	127 ± 5	1.14
19	m5	4	5.65	144.52	127 ± 5	1.14
19	m12	3	13.56	117.73	127 ± 5	0.93

Continued on next page

Table D.4 – *Continued from previous page*

Object	**Coordinate**	Order	Distance From Center (Kpc)	$\sigma_{[OIII]}$ **(km/s)**	**SVD (km/s)**	$\sigma_{[OIII]}$/ SVD
19	m21	3	23.73	133.29	127 ± 5	1.05
19	p5	4	5.65	151.42	127 ± 5	1.19
19	p12	3	13.56	167.72	127 ± 5	1.32
19	p21	3	23.73	180.04	127 ± 5	1.42
20	c	4	0	142.41	128 ± 9	1.11
20	m5	4	3.7	142.38	128 ± 9	1.11
20	m12	3	8.88	127.21	128 ± 9	0.99
20	m21	3	15.54	171.99	128 ± 9	1.34
20	p5	4	3.7	154.13	128 ± 9	1.2
20	p12	3	8.88	150.28	128 ± 9	1.17
20	p21	3	15.54	181.67	128 ± 9	1.42
20	p32	2	23.68	197.09	128 ± 9	1.54
21	c	4	0	176.27	91 ± 5	1.94
21	m5	4	4.95	174.53	91 ± 5	1.92
21	m12	3	11.88	165.73	91 ± 5	1.82
21	p5	4	4.95	179.21	91 ± 5	1.97
21	p12	3	11.88	182.56	91 ± 5	2.01
22	c	4	0	148	98 ± 3	1.51
22	m5	4	3.9	147.89	98 ± 3	1.51
22	m12	3	9.36	137.47	98 ± 3	1.4
22	m21	3	16.38	106.88	98 ± 3	1.09
22	m32	2	24.96	98.97	98 ± 3	1.01
22	p5	4	3.9	149.23	98 ± 3	1.52
22	p12	3	9.36	131.78	98 ± 3	1.34
22	p21	3	16.38	100.5	98 ± 3	1.03
22	p32	2	24.96	94.47	98 ± 3	0.96
22	p45	2	35.1	73.7	98 ± 3	0.75
23	c	4	0	213.47	129 ± 6	1.65
23	m5	4	3.3	213.48	129 ± 6	1.65
23	m12	3	7.92	268.61	129 ± 6	2.08
23	m21	3	13.86	301.06	129 ± 6	2.33
23	m32	2	21.12	326.42	129 ± 6	2.53
23	p5	4	3.3	218.11	129 ± 6	1.69
23	p12	3	7.92	276	129 ± 6	2.14
23	p21	3	13.86	292.67	129 ± 6	2.27
23	p32	2	21.12	168.18	129 ± 6	1.3
23	p45	2	29.7	107.7	129 ± 6	0.83
24	c	4	0	178.24	195 ± 2	0.91
24	m5	4	2.65	177.85	195 ± 2	0.91
24	m12	3	6.36	198.71	195 ± 2	1.02
24	m21	3	11.13	178.07	195 ± 2	0.91
24	m32	2	16.96	190.07	195 ± 2	0.97
24	p5	4	2.65	183.7	195 ± 2	0.94
24	p12	3	6.36	223.42	195 ± 2	1.15
24	p21	3	11.13	221.81	195 ± 2	1.14
24	p32	2	16.96	128.7	195 ± 2	0.66
24	p45	2	23.85	106.85	195 ± 2	0.55
26	c	4	0	142.36	124 ± 4	1.15
26	m5	4	5.5	146.43	124 ± 4	1.18
26	m12	3	13.2	144.12	124 ± 4	1.16
26	m21	3	23.1	166.95	124 ± 4	1.35
26	p5	4	5.5	145.37	124 ± 4	1.17
26	p12	3	13.2	150.22	124 ± 4	1.21
26	p21	3	23.1	149.21	124 ± 4	1.2
27	c	4	0	136.15	96 ± 6	1.42
27	m5	4	5.7	140.84	96 ± 6	1.47

Continued on next page

Table D.4 – *Continued from previous page*

Object	**Coordinate**	Order	Distance From Center (Kpc)	$\sigma_{[OIII]}$ **(km/s)**	**SVD (km/s)**	$\sigma_{[OIII]}$/ SVD
27	m12	3	13.68	138.45	96 ± 6	1.44
27	m21	2	23.94	93.04	96 ± 6	0.97
27	p5	4	5.7	144.74	96 ± 6	1.51
27	p12	3	13.68	146.97	96 ± 6	1.53
27	p21	3	23.94	159.34	96 ± 6	1.66
28	c	4	0	181.54	124 ± 4	1.46
28	m5	4	2.2	180.03	124 ± 4	1.45
28	m12	3	5.28	190.88	124 ± 4	1.54
28	m21	3	9.24	160.14	124 ± 4	1.29
28	m32	2	14.08	103.05	124 ± 4	0.83
28	m45	2	19.8	92.81	124 ± 4	0.75
28	p5	4	2.2	185.85	124 ± 4	1.5
28	p12	3	5.28	185.87	124 ± 4	1.5
28	p21	3	9.24	191.84	124 ± 4	1.55
28	p32	2	14.08	108.46	124 ± 4	0.87
29	c	4	0	137.59	140 ± 3	0.98
29	m5	4	4.6	138.15	140 ± 3	0.99
29	m12	3	11.04	144.04	140 ± 3	1.03
29	m21	3	19.32	123.77	140 ± 3	0.88
29	m32	2	29.44	109.22	140 ± 3	0.78
29	p5	4	4.6	141.94	140 ± 3	1.01
29	p12	3	11.04	148.35	140 ± 3	1.06
29	p21	3	19.32	143.96	140 ± 3	1.03
29	p32	2	29.44	135.98	140 ± 3	0.97
29	p45	2	41.4	95.68	140 ± 3	0.68
30	c	4	0	145.34	154 ± 8	0.94
30	m5	4	5.05	138.18	154 ± 8	0.9
30	m12	3	12.12	153.52	154 ± 8	1
30	m21	3	21.21	153.73	154 ± 8	1
30	p5	4	5.05	155.14	154 ± 8	1.01
30	p12	3	12.12	188.75	154 ± 8	1.23
30	p21	3	21.21	214.78	154 ± 8	1.39
30	p32	2	32.32	155.83	154 ± 8	1.01
31	c	4	0	172.02	127 ± 6	1.35
31	m5	4	3.75	172.1	127 ± 6	1.36
31	m12	3	9	135.41	127 ± 6	1.07
31	m21	3	15.75	126.93	127 ± 6	1
31	m32	2	24	117.77	127 ± 6	0.93
31	p5	4	3.75	183.47	127 ± 6	1.44
31	p12	3	9	170.89	127 ± 6	1.35
31	p21	3	15.75	124.27	127 ± 6	0.98
31	p32	2	24	99.1	127 ± 6	0.78
32	c	4	0	149.24	108 ± 10	1.38
32	m5	4	5.1	144.94	108 ± 10	1.34
32	m12	3	12.24	149.33	108 ± 10	1.38
32	m21	3	21.42	147.73	108 ± 10	1.37
32	p5	4	5.1	149.73	108 ± 10	1.39
32	p12	3	12.24	156.82	108 ± 10	1.45
32	p21	2	21.42	80.89	108 ± 10	0.75
34	c	4	0	143.8	77 ± 17	1.87
34	m5	4	5.35	142.59	77 ± 17	1.85
34	m12	3	12.84	144.42	77 ± 17	1.88
34	m21	3	22.47	161.67	77 ± 17	2.1
34	p5	4	5.35	143.99	77 ± 17	1.87
34	p12	3	12.84	165.82	77 ± 17	2.15
34	p21	3	22.47	185.36	77 ± 17	2.41

Continued on next page

Table D.4 – *Continued from previous page*

Object	**Coordinate**	Order	Distance From Center (Kpc)	$\sigma_{[OIII]}$ **(km/s)**	**SVD (km/s)**	$\sigma_{[OIII]}$/ SVD
35	c	4	0	189.67	144 ± 14	1.32
35	m5	4	3.55	182.9	144 ± 14	1.27
35	m12	3	8.52	191.79	144 ± 14	1.33
35	m21	3	14.91	201.85	144 ± 14	1.4
35	p5	4	3.55	184.09	144 ± 14	1.28
35	p12	3	8.52	189.54	144 ± 14	1.32
35	p21	3	14.91	208.96	144 ± 14	1.45
35	p32	2	22.72	164.12	144 ± 14	1.14
36	c	4	0	132.48	91 ± 7	1.46
36	m5	4	4.8	136.37	91 ± 7	1.5
36	m12	3	11.52	142.95	91 ± 7	1.57
36	m21	3	20.16	407.46	91 ± 7	4.48
36	p5	4	4.8	134.83	91 ± 7	1.48
36	p12	3	11.52	140.82	91 ± 7	1.55
36	p21	3	20.16	254.6	91 ± 7	2.8
36	p32	2	30.72	62.38	91 ± 7	0.69
38	c	4	0	173	119 ± 3	1.45
38	m5	4	5.8	193.27	119 ± 3	1.62
38	m12	3	13.92	195.11	119 ± 3	1.64
38	m21	4	24.36	96.5	119 ± 3	0.81
38	p5	4	5.8	170.37	119 ± 3	1.43
38	p12	3	13.92	180.14	119 ± 3	1.51
38	p21	3	24.36	106.31	119 ± 3	0.89
39	c	4	0	238.59	166 ± 7	1.44
39	m5	4	5.25	235.84	166 ± 7	1.42
39	m12	3	12.6	188.78	166 ± 7	1.14
39	p5	4	5.25	240.7	166 ± 7	1.45
39	p12	3	12.6	200.11	166 ± 7	1.21
40	c	4	0	156.39	82 ± 2	1.91
40	m5	4	3.45	149.96	82 ± 2	1.83
40	m12	3	8.28	139.8	82 ± 2	1.7
40	m21	3	14.49	164.23	82 ± 2	2
40	m32	2	22.08	187.49	82 ± 2	2.29
40	p5	4	3.45	160.12	82 ± 2	1.95
40	p12	3	8.28	158.74	82 ± 2	1.94
40	p21	3	14.49	120.75	82 ± 2	1.47
40	p32	2	22.08	88.36	82 ± 2	1.08
41	c	4	0	168.57	118 ± 6	1.43
41	m5	4	5.2	168.83	118 ± 6	1.43
41	m12	3	12.48	200.83	118 ± 6	1.7
41	m21	3	21.84	245.65	118 ± 6	2.08
41	p5	4	5.2	186.67	118 ± 6	1.58
41	p12	3	12.48	180.8	118 ± 6	1.53
41	p21	3	21.84	274.01	118 ± 6	2.32
42	c	4	0	144.59	157 ± 6	0.92
42	m5	4	5.05	144.58	157 ± 6	0.92
42	m12	3	12.12	120.17	157 ± 6	0.77
42	m21	3	21.21	87.16	157 ± 6	0.56
42	m32	2	32.32	90.13	157 ± 6	0.57
42	p5	4	5.05	149.58	157 ± 6	0.95
42	p12	3	12.12	111.8	157 ± 6	0.71
42	p21	3	21.21	91.69	157 ± 6	0.58
42	p32	2	32.32	80.71	157 ± 6	0.51
42	p45	2	45.45	78.83	157 ± 6	0.5
43	c	4	0	166.13	144 ± 5	1.15
43	m5	4	2.3	168.63	144 ± 5	1.17

Continued on next page

Table D.4 – *Continued from previous page*

Object	**Coordinate**	Order	Distance From Center (Kpc)	$\sigma_{[OIII]}$ **(km/s)**	**SVD (km/s)**	$\sigma_{[OIII]}$/ SVD
43	m12	3	5.52	184.19	144 ± 5	1.28
43	m21	3	9.66	180.73	144 ± 5	1.26
43	m32	2	14.72	150.6	144 ± 5	1.05
43	p5	4	2.3	167.94	144 ± 5	1.17
43	p12	3	5.52	184.61	144 ± 5	1.28
43	p21	3	9.66	241.64	144 ± 5	1.68
43	p32	2	14.72	173.03	144 ± 5	1.2
44	c	12	0	180.76	172 ± 7	1.05
44	m5	4	3.1	175.85	172 ± 7	1.02
44	m12	3	7.44	172.76	172 ± 7	1
44	m21	3	13.02	130.12	172 ± 7	0.76
44	m32	2	19.84	128.43	172 ± 7	0.75
44	m45	2	27.9	96.52	172 ± 7	0.56
44	p5	10	3.1	215.93	172 ± 7	1.26
44	p12	3	7.44	172.61	172 ± 7	1
44	p21	12	13.02	135.97	172 ± 7	0.79
44	p32	2	19.84	102.82	172 ± 7	0.6
44	p45	10	27.9	144.17	172 ± 7	0.84
45	c	4	0	157.05	97 ± 8	1.62
45	m5	4	2.35	156.86	97 ± 8	1.62
45	m12	3	5.64	183.18	97 ± 8	1.89
45	m21	3	9.87	155.59	97 ± 8	1.6
45	m32	2	15.04	156.84	97 ± 8	1.62
45	p5	4	2.35	158.08	97 ± 8	1.63
45	p12	3	5.64	162.53	97 ± 8	1.68
45	p21	3	9.87	167.85	97 ± 8	1.73
46	c	4	0	191.24	107 ± 8	1.79
46	m5	4	4.6	189.69	107 ± 8	1.77
46	m12	3	11.04	220.39	107 ± 8	2.06
46	p5	4	4.6	198.78	107 ± 8	1.86
46	p12	3	11.04	223.04	107 ± 8	2.08
47	c	4	0	159.91	100 ± 4	1.6
47	m5	4	4.95	153.21	100 ± 4	1.53
47	m12	3	11.88	127.82	100 ± 4	1.28
47	m21	3	20.79	81.04	100 ± 4	0.81
47	m32	2	31.68	85.52	100 ± 4	0.86
47	m45	2	44.55	102.66	100 ± 4	1.03
47	p5	4	4.95	162.14	100 ± 4	1.62
47	p12	3	11.88	126.76	100 ± 4	1.27
47	p21	3	20.79	231.05	100 ± 4	2.31
47	p32	2	31.68	108.37	100 ± 4	1.08
47	p45	2	44.55	165.27	100 ± 4	1.65
49	c	4	0	184.29	122 ± 9	1.51
49	m5	4	5.45	184.26	122 ± 9	1.51
49	m12	3	13.08	140.38	122 ± 9	1.15
49	m21	3	22.89	116.79	122 ± 9	0.96
49	m32	2	34.88	99.91	122 ± 9	0.82
49	p5	4	5.45	176.18	122 ± 9	1.44
49	p12	3	13.08	140.96	122 ± 9	1.16
49	p21	3	22.89	126.81	122 ± 9	1.04
51	c	4	0	176.37	123 ± 4	1.43
51	m5	4	5.25	175.78	123 ± 4	1.43
51	m12	3	12.6	220.4	123 ± 4	1.79
51	p5	4	5.25	179.77	123 ± 4	1.46
51	p12	3	12.6	185.11	123 ± 4	1.5
52	c	4	0	249.92	149 ± 4	1.68

Continued on next page

Table D.4 – *Continued from previous page*

Object	**Coordinate**	Order	Distance From Center (Kpc)	$\sigma_{[OIII]}$ **(km/s)**	**SVD (km/s)**	$\sigma_{[OIII]}$/ SVD
52	m5	4	5.25	269.72	149 ± 4	1.81
52	m12	3	12.6	279.44	149 ± 4	1.88
52	m21	3	22.05	138.87	149 ± 4	0.93
52	m32	2	33.6	104.3	149 ± 4	0.7
52	m45	2	47.25	155.35	149 ± 4	1.04
52	p5	4	5.25	253.3	149 ± 4	1.7
52	p12	3	12.6	305.42	149 ± 4	2.05
52	p21	3	22.05	273.79	149 ± 4	1.84
52	p32	2	33.6	129.03	149 ± 4	0.87
52	p45	2	47.25	108.68	149 ± 4	0.73
53	c	8	0	255.2	185 ± 10	1.38
53	m5	8	5.4	250.7	185 ± 10	1.36
53	m12	3	12.96	293.29	185 ± 10	1.59
53	m21	3	22.68	447.7	185 ± 10	2.42
53	p5	8	5.4	259.36	185 ± 10	1.4
53	p12	3	12.96	285	185 ± 10	1.54
53	p21	3	22.68	216.7	185 ± 10	1.17
53	p32	2	34.56	134.21	185 ± 10	0.73
54	c	4	0	155.29	114 ± 7	1.36
54	m5	4	3.65	155.18	114 ± 7	1.36
54	m12	3	8.76	163	114 ± 7	1.43
54	m21	3	15.33	183.43	114 ± 7	1.61
54	m32	2	23.36	106.24	114 ± 7	0.93
54	m45	2	32.85	92.14	114 ± 7	0.81
54	p5	4	3.65	156.84	114 ± 7	1.38
54	p12	3	8.76	167.03	114 ± 7	1.47
54	p21	3	15.33	219.07	114 ± 7	1.92
54	p32	2	23.36	278.08	114 ± 7	2.44
57	c	4	0	179.98	116 ± 4	1.55
57	m5	4	3.05	182.1	116 ± 4	1.57
57	m12	4	7.32	245.41	116 ± 4	2.12
57	m21	4	12.81	331.05	116 ± 4	2.85
57	m32	2	19.52	503.82	116 ± 4	4.34
57	m45	2	27.45	299.33	116 ± 4	2.58
57	p5	4	3.05	178.64	116 ± 4	1.54
57	p12	8	7.32	191.95	116 ± 4	1.65
57	p21	10	12.81	212.35	116 ± 4	1.83
57	p32	2	19.52	446.18	116 ± 4	3.85
57	p45	2	27.45	211.66	116 ± 4	1.82
58	c	4	0	164.17	171 ± 5	0.96
58	m5	4	4.7	147.72	171 ± 5	0.86
58	m12	3	11.28	135.11	171 ± 5	0.79
58	m21	3	19.74	145.3	171 ± 5	0.85
58	m32	2	30.08	179.97	171 ± 5	1.05
58	p5	4	4.7	159.42	171 ± 5	0.93
58	p12	3	11.28	152.61	171 ± 5	0.89
58	p21	3	19.74	125.79	171 ± 5	0.74
58	p32	2	30.08	124.12	171 ± 5	0.73
59	c	4	0	225.42	159 ± 4	1.42
59	m5	4	4.75	198.94	159 ± 4	1.25
59	m12	3	11.4	156.54	159 ± 4	0.98
59	m21	3	19.95	141.96	159 ± 4	0.89
59	m32	2	30.4	145.91	159 ± 4	0.92
59	p5	4	4.75	209.26	159 ± 4	1.32
59	p12	6	11.4	138.95	159 ± 4	0.87
59	p21	3	19.95	197.26	159 ± 4	1.24

Continued on next page

Table D.4 – *Continued from previous page*

Object	**Coordinate**	Order	Distance From Center (Kpc)	$\sigma_{[OIII]}$ **(km/s)**	**SVD (km/s)**	$\sigma_{[OIII]}$/ SVD
59	p32	2	30.4	247.03	159 ± 4	1.55
59	p45	2	42.75	167.32	159 ± 4	1.05
61	c	4	0	127.41	186 ± 8	0.68
61	m5	4	5.2	120.06	186 ± 8	0.65
61	m12	3	12.48	121.88	186 ± 8	0.66
61	m21	2	21.84	109.91	186 ± 8	0.59
61	m32	2	33.28	185.03	186 ± 8	0.99
61	p5	4	5.2	132.02	186 ± 8	0.71
61	p12	3	12.48	144.58	186 ± 8	0.78
61	p21	3	21.84	269.8	186 ± 8	1.45
62	c	4	0	197.08	170 ± 8	1.16
62	m5	4	5.65	208.75	170 ± 8	1.23
62	m12	3	13.56	242.09	170 ± 8	1.42
62	m21	3	23.73	212.09	170 ± 8	1.25
62	m32	2	36.16	132.45	170 ± 8	0.78
62	p5	4	5.65	185.08	170 ± 8	1.09
62	p12	3	13.56	182.7	170 ± 8	1.07
62	p21	3	23.73	183.4	170 ± 8	1.08
63	c	8	0	207.46	120 ± 5	1.73
63	m5	8	4.05	201.07	120 ± 5	1.68
63	m12	3	9.72	264.89	120 ± 5	2.21
63	m21	2	17.01	611.54	120 ± 5	5.1
63	p5	4	4.05	217.78	120 ± 5	1.81
63	p12	3	9.72	231.09	120 ± 5	1.93
63	p21	3	17.01	234.61	120 ± 5	1.96
70	c	10	0	196.37	266 ± 3	0.74
70	m5	8	4.5	215.16	266 ± 3	0.81
70	m12	3	10.8	315.56	266 ± 3	1.19
70	m21	3	18.9	304	266 ± 3	1.14
70	m32	2	28.8	144.46	266 ± 3	0.54
70	m45	2	40.5	118.26	266 ± 3	0.44
70	p5	10	4.5	196.68	266 ± 3	0.74
70	p12	3	10.8	262.41	266 ± 3	0.99
70	p21	3	18.9	283.26	266 ± 3	1.06
70	p32	2	28.8	82.64	266 ± 3	0.31
71	c	4	0	200.18	134 ± 5	1.49
71	m5	4	5.95	212.9	134 ± 5	1.59
71	m12	3	14.28	288.69	134 ± 5	2.15
71	m45	2	53.55	101.22	134 ± 5	0.76
71	p5	4	5.95	202.38	134 ± 5	1.51
71	p12	3	14.28	332.99	134 ± 5	2.49
71	p45	9	53.55	137.13	134 ± 5	1.02
73	c	4	0	185.41	131 ± 6	1.42
73	m5	4	7.6	204.25	131 ± 6	1.56
73	m12	3	18.24	262.21	131 ± 6	2
73	p5	4	7.6	186.58	131 ± 6	1.42
73	p12	3	18.24	231.32	131 ± 6	1.77
73	p21	2	31.92	222.02	131 ± 6	1.69
74	c	4	0	186.63	165 ± 17	1.13
74	m5	4	8.65	203.51	165 ± 17	1.23
74	m12	3	20.76	315.56	165 ± 17	1.91
74	m21	3	36.33	269.26	165 ± 17	1.63
74	m32	4	55.36	84.07	165 ± 17	0.51
74	p5	4	8.65	188.83	165 ± 17	1.14
74	p12	3	20.76	204.49	165 ± 17	1.24
74	p21	3	36.33	174.78	165 ± 17	1.06

Continued on next page

Table D.4 – *Continued from previous page*

Object	**Coordinate**	Order	Distance From Center (Kpc)	$\sigma_{[OIII]}$ **(km/s)**	**SVD (km/s)**	$\sigma_{[OIII]}$/ SVD
74	p32	2	55.36	71.61	165 ± 17	0.43
76	c	4	0	140.88	193 ± 4	0.73
76	m5	4	7.95	163.43	193 ± 4	0.85
76	m12	3	19.08	196.24	193 ± 4	1.02
76	m21	2	33.39	172.82	193 ± 4	0.9
76	p5	4	7.95	153.12	193 ± 4	0.79
76	p12	3	19.08	251.65	193 ± 4	1.3
76	p32	2	50.88	159.7	193 ± 4	0.83
77	c	4	0	168.44	188 ± 4	0.9
77	m5	4	5.95	184.14	188 ± 4	0.98
77	m12	3	14.28	187.32	188 ± 4	1
77	m21	2	24.99	107.33	188 ± 4	0.57
77	p5	4	5.95	176	188 ± 4	0.94
77	p12	3	14.28	156.15	188 ± 4	0.83
77	p21	3	24.99	277.1	188 ± 4	1.47
78	c	8	0	258.17	97 ± 4	2.66
78	m5	4	6.8	244.51	97 ± 4	2.52
78	m12	3	16.32	295.24	97 ± 4	3.04
78	m21	3	28.56	153.64	97 ± 4	1.58
78	p5	4	6.8	288.58	97 ± 4	2.98
78	p12	3	16.32	247.75	97 ± 4	2.55
78	p21	2	28.56	101.52	97 ± 4	1.05
79	c	4	0	254.37	90 ± 6	2.83
79	m5	4	7.1	276.69	90 ± 6	3.07
79	m12	3	17.04	329.01	90 ± 6	3.66
79	m21	3	29.82	677.11	90 ± 6	7.52
79	p5	4	7.1	252.08	90 ± 6	2.8
79	p12	3	17.04	381.76	90 ± 6	4.24
82	c	4	0	142.82	156 ± 23	0.92
82	m5	4	8.9	144.64	156 ± 23	0.93
82	p5	4	8.9	145.26	156 ± 23	0.93
82	p12	3	21.36	118.99	156 ± 23	0.76
83	c	4	0	179.42	90 ± 18	1.99
83	m5	4	8.25	190.36	90 ± 18	2.12
83	m12	3	19.8	244.32	90 ± 18	2.71
83	m21	3	34.65	158.74	90 ± 18	1.76
83	p5	4	8.25	183.7	90 ± 18	2.04
83	p12	3	19.8	216.45	90 ± 18	2.4
83	p21	2	34.65	85.13	90 ± 18	0.95
88	c	4	0	263.4	199 ± 6	1.32
88	m5	4	7.9	281.36	199 ± 6	1.41
88	m12	2	18.96	201.59	199 ± 6	1.01
88	p5	4	7.9	252.6	199 ± 6	1.27
88	p12	3	18.96	195.65	199 ± 6	0.98
91	c	4	0	216.99	172 ± 13	1.26
91	m5	4	6.9	222.43	172 ± 13	1.29
91	m12	3	16.56	208.32	172 ± 13	1.21
91	m21	3	28.98	106.04	172 ± 13	0.62
91	m32	2	44.16	88.44	172 ± 13	0.51
91	m45	2	62.1	45.06	172 ± 13	0.26
91	p5	4	6.9	216.58	172 ± 13	1.26
91	p12	3	16.56	187.75	172 ± 13	1.09
91	p21	3	28.98	110.67	172 ± 13	0.64
91	p32	2	44.16	102.85	172 ± 13	0.6
91	p45	2	62.1	215.44	172 ± 13	1.25
99	c	4	0	233.17	71 ± 28	3.28

Continued on next page

Table D.4 – *Continued from previous page*

Object	**Coordinate**	Order	Distance From Center (Kpc)	$\sigma_{[OIII]}$ **(km/s)**	**SVD (km/s)**	$\sigma_{[OIII]}$/ SVD
99	m5	4	7.85	244.8	71 ± 28	3.45
99	m12	3	18.84	245.79	71 ± 28	3.46
99	m21	3	32.97	160.2	71 ± 28	2.26
99	p5	4	7.85	237.18	71 ± 28	3.34
99	p12	3	18.84	294.41	71 ± 28	4.15
99	p21	3	32.97	147.28	71 ± 28	2.07
102	c	4	0	132.75	115 ± 17	1.15
102	m5	4	8.5	141.73	115 ± 17	1.23
102	m12	3	20.4	597.84	115 ± 17	5.2
102	p5	4	8.5	136.72	115 ± 17	1.19
102	p12	3	20.4	179.62	115 ± 17	1.56
103	c	4	0	338.62	99 ± 8	3.42
103	m5	4	7.75	332.98	99 ± 8	3.36
103	m12	3	18.6	329.42	99 ± 8	3.33
103	m21	3	32.55	389.1	99 ± 8	3.93
103	m32	2	49.6	111.42	99 ± 8	1.13
103	m45	2	69.75	7.02	99 ± 8	0.07
103	m45	4	69.75	223.7	99 ± 8	2.26
103	p5	4	7.75	346.16	99 ± 8	3.5
103	p12	3	18.6	339.85	99 ± 8	3.43
103	p21	3	32.55	390.95	99 ± 8	3.95
103	p32	2	49.6	177.1	99 ± 8	1.79
106	c	4	0	197.6	198 ± 6	1
106	m5	4	8.7	222.84	198 ± 6	1.13
106	m12	3	20.88	233.34	198 ± 6	1.18
106	m21	3	36.54	159.02	198 ± 6	0.8
106	m32	2	55.68	139.25	198 ± 6	0.7
106	m45	2	78.3	95.16	198 ± 6	0.48
106	p5	4	8.7	200.35	198 ± 6	1.01
106	p12	3	20.88	177.91	198 ± 6	0.9
106	p21	3	36.54	144.18	198 ± 6	0.73
106	p32	2	55.68	133.96	198 ± 6	0.68
106	p45	2	78.3	78.04	198 ± 6	0.39
109	c	4	0	190.51	237 ± 9	0.8
109	m5	9	8.9	232	237 ± 9	0.98
109	m12	3	21.36	194.71	237 ± 9	0.82
109	m21	3	37.38	317.59	237 ± 9	1.34
109	p5	4	8.9	175.51	237 ± 9	0.74
109	p12	12	21.36	127.54	237 ± 9	0.54
109	p21	2	37.38	91.46	237 ± 9	0.39
114	c	4	0	117.48	136 ± 6	0.86
114	m5	4	6.25	117.25	136 ± 6	0.86
114	m12	3	15	180.97	136 ± 6	1.33
114	p5	4	6.25	118.44	136 ± 6	0.87
114	p12	3	15	136.24	136 ± 6	1
126	c	12	0	103.65	1211 ± 5	0.09
126	m5	12	6.3	103.59	1211 ± 5	0.09
126	m12	3	15.12	91.73	1211 ± 5	0.08
126	m21	3	26.46	122.38	1211 ± 5	0.1
126	m32	2	40.32	84.11	1211 ± 5	0.07
126	p5	12	6.3	105.79	1211 ± 5	0.09
126	p12	3	15.12	99.63	1211 ± 5	0.08
126	p21	3	26.46	106.52	1211 ± 5	0.09
126	p32	2	40.32	83.27	1211 ± 5	0.07
126	p45	2	56.7	66.65	1211 ± 5	0.06
138	c	4	0	115.71	143 ± 3	0.81

Continued on next page

Table D.4 – *Continued from previous page*

Object	Coordinate	Order	Distance From Center (Kpc)	$\sigma_{[OIII]}$ (km/s)	SVD (km/s)	$\sigma_{[OIII]}$/ SVD
138	m5	4	6	115.26	143 ± 3	0.81
138	m12	3	14.4	155.84	143 ± 3	1.09
138	p5	4	6	102.49	143 ± 3	0.72
138	p12	3	14.4	93.43	143 ± 3	0.65
138	p21	3	25.2	92.06	143 ± 3	0.64
155	c	4	0	164.94	197 ± 5	0.84
155	m5	4	5.85	165.45	197 ± 5	0.84
155	m12	3	14.04	164.75	197 ± 5	0.84
155	m21	3	24.57	154.11	197 ± 5	0.78
155	m32	2	37.44	205.97	197 ± 5	1.05
155	p5	4	5.85	173.69	197 ± 5	0.88
155	p12	3	14.04	175.72	197 ± 5	0.89
155	p21	3	24.57	147.33	197 ± 5	0.75
155	p32	2	37.44	100.26	197 ± 5	0.51
156	c	4	0	185.95	165 ± 6	1.13
156	m5	4	6.45	185.88	165 ± 6	1.13
156	m12	3	15.48	173.78	165 ± 6	1.05
156	m21	3	27.09	114.27	165 ± 6	0.69
156	m32	2	41.28	91.84	165 ± 6	0.56
156	m45	2	58.05	106.47	165 ± 6	0.65
156	p5	4	6.45	184.75	165 ± 6	1.12
156	p12	3	15.48	179.04	165 ± 6	1.09
156	p21	3	27.09	119.79	165 ± 6	0.73
156	p32	2	41.28	93.15	165 ± 6	0.56
162	c	4	0	140.75	121 ± 3	1.16
162	m5	4	6.45	140.55	121 ± 3	1.16
162	m12	3	15.48	162.01	121 ± 3	1.34
162	m21	3	27.09	51.91	121 ± 3	0.43
162	p5	4	6.45	139.75	121 ± 3	1.15
162	p12	3	15.48	148.46	121 ± 3	1.23
177	c	4	0	109.28	121 ± 6	0.9
177	m5	4	6.05	109.43	121 ± 6	0.9
177	m12	3	14.52	135.48	121 ± 6	1.12
177	m45	2	54.45	87.82	121 ± 6	0.73
177	p5	4	6.05	110.5	121 ± 6	0.91
177	p12	3	14.52	138.07	121 ± 6	1.14
180	c	4	0	155.05	120 ± 18	1.29
180	m5	4	6.6	155.39	120 ± 18	1.29
180	m12	3	15.84	188.93	120 ± 18	1.57
180	m21	3	27.72	285.74	120 ± 18	2.38
180	m32	2	42.24	95.04	120 ± 18	0.79
180	p5	4	6.6	161.01	120 ± 18	1.34
180	p12	3	15.84	191.23	120 ± 18	1.59
180	p21	3	27.72	323.9	120 ± 18	2.7
180	p32	2	42.24	701.49	120 ± 18	5.85
187	c	4	0	189.73	166 ± 6	1.14
187	m5	4	6.05	189.71	166 ± 6	1.14
187	m12	4	14.52	196.65	166 ± 6	1.18
187	m21	3	25.41	192.88	166 ± 6	1.16
187	m32	2	38.72	180.03	166 ± 6	1.08
187	p5	4	6.05	184.35	166 ± 6	1.11
187	p12	4	14.52	179.59	166 ± 6	1.08
187	p21	3	25.41	212.13	166 ± 6	1.28
187	p32	2	38.72	205.41	166 ± 6	1.24
196	c	4	0	278.99	228 ± 7	1.22
196	m5	4	6	278.93	228 ± 7	1.22

Continued on next page

Table D.4 – *Continued from previous page*

Object	**Coordinate**	Order	Distance From Center (Kpc)	$\sigma_{[OIII]}$ **(km/s)**	**SVD (km/s)**	$\sigma_{[OIII]}$/ SVD
196	m12	3	14.4	229.76	228 ± 7	1.01
196	m21	3	25.2	185.47	228 ± 7	0.81
196	m32	2	38.4	172.58	228 ± 7	0.76
196	m45	2	54	107.96	228 ± 7	0.47
196	p5	4	6	287.31	228 ± 7	1.26
196	p12	3	14.4	255.87	228 ± 7	1.12
196	p21	3	25.2	222.65	228 ± 7	0.98
196	p32	2	38.4	136.3	228 ± 7	0.6
196	p45	2	54	115.04	228 ± 7	0.5
197	c	4	0	145.15	144 ± 4	1.01
197	m5	4	6.1	145.25	144 ± 4	1.01
197	m12	3	14.64	172.91	144 ± 4	1.2
197	m21	3	25.62	182.98	144 ± 4	1.27
197	m32	2	39.04	136.62	144 ± 4	0.95
197	p5	4	6.1	149.28	144 ± 4	1.04
197	p12	3	14.64	166.51	144 ± 4	1.16
197	p21	3	25.62	173.89	144 ± 4	1.21
197	p32	2	39.04	261.21	144 ± 4	1.81
202	c	4	0	121.29	113 ± 5	1.07
202	m5	4	6.4	120.91	113 ± 5	1.07
202	m12	3	15.36	116.06	113 ± 5	1.03
202	m21	3	26.88	100.26	113 ± 5	0.89
202	p5	4	6.4	125.72	113 ± 5	1.11
202	p12	3	15.36	139.72	113 ± 5	1.24
202	p21	3	26.88	138.96	113 ± 5	1.23
204	c	4	0	104.84	133 ± 9	0.79
204	m5	4	5.85	104.71	133 ± 9	0.79
204	m12	3	14.04	99.74	133 ± 9	0.75
204	m21	3	24.57	102.61	133 ± 9	0.77
204	m32	2	37.44	90.69	133 ± 9	0.68
204	m45	2	52.65	79.25	133 ± 9	0.6
204	p5	4	5.85	103.75	133 ± 9	0.78
204	p12	3	14.04	107.19	133 ± 9	0.81
204	p21	3	24.57	148.04	133 ± 9	1.11
204	p32	2	37.44	85.69	133 ± 9	0.64
205	c	4	0	213.06	144 ± 10	1.48
205	m5	4	5.9	214.68	144 ± 10	1.49
205	m12	3	14.16	261.7	144 ± 10	1.82
205	m21	3	24.78	153	144 ± 10	1.06
205	p5	4	5.9	210.78	144 ± 10	1.46
205	p12	3	14.16	208.41	144 ± 10	1.45
205	p21	3	24.78	147.92	144 ± 10	1.03
205	p32	3	37.76	76.21	144 ± 10	0.53
207	c	4	0	178.35	168 ± 11	1.06
207	m5	4	6.05	174.74	168 ± 11	1.04
207	m12	3	14.52	168.33	168 ± 11	1
207	m21	3	25.41	83.56	168 ± 11	0.5
207	p5	4	6.05	180.94	168 ± 11	1.08
207	p12	3	14.52	206.68	168 ± 11	1.23
207	p21	2	25.41	97.68	168 ± 11	0.58
208	c	4	0	183.63	201 ± 13	0.91
208	m5	4	6.1	194.13	201 ± 13	0.97
208	m12	3	14.64	240.07	201 ± 13	1.19
208	m21	2	25.62	103.8	201 ± 13	0.52
208	p5	4	6.1	195.65	201 ± 13	0.97
208	p12	3	14.64	236.05	201 ± 13	1.17

Continued on next page

Table D.4 – *Continued from previous page*

Object	**Coordinate**	Order	Distance From Center (Kpc)	$\sigma_{[\mathbf{OIII}]}$ **(km/s)**	**SVD (km/s)**	$\sigma_{[\mathbf{OIII}]}$/ SVD
208	p21	3	25.62	296.65	201 ± 13	1.48
209	c	4	0	119.95	128 ± 7	0.94
209	m5	4	6.15	124.24	128 ± 7	0.97
209	m12	3	14.76	147.73	128 ± 7	1.15
209	m21	3	25.83	115.75	128 ± 7	0.9
209	m32	2	39.36	94.05	128 ± 7	0.73
209	m45	2	55.35	78.13	128 ± 7	0.61
209	p5	4	6.15	125.73	128 ± 7	0.98
209	p12	3	14.76	141.5	128 ± 7	1.11
209	p21	3	25.83	93.4	128 ± 7	0.73
209	p32	2	39.36	86.68	128 ± 7	0.68
209	p45	2	55.35	97.65	128 ± 7	0.76
210	c	4	0	210.45	184 ± 10	1.14
210	m5	4	6.15	218.16	184 ± 10	1.19
210	m12	3	14.76	277.86	184 ± 10	1.51
210	m21	3	25.83	355.91	184 ± 10	1.93
210	p5	4	6.15	214.85	184 ± 10	1.17
210	p12	3	14.76	180.68	184 ± 10	0.98
210	p21	3	25.83	152.37	184 ± 10	0.83
213	c	4	0	155.12	183 ± 24	0.85
213	m5	4	6.4	153.16	183 ± 24	0.84
213	m12	3	15.36	178.79	183 ± 24	0.98
213	m21	3	26.88	201.43	183 ± 24	1.1
213	p5	4	6.4	162.62	183 ± 24	0.89
213	p12	3	15.36	157.17	183 ± 24	0.86
213	p21	3	26.88	166.82	183 ± 24	0.91
214	c	4	0	183.83	119 ± 9	1.54
214	m5	4	6.45	183.8	119 ± 9	1.54
214	m12	3	15.48	232.71	119 ± 9	1.96
214	m21	3	27.09	303.47	119 ± 9	2.55
214	m32	2	41.28	188.55	119 ± 9	1.58
214	p5	4	6.45	168.54	119 ± 9	1.42
214	p12	3	15.48	201.23	119 ± 9	1.69
214	p21	3	27.09	277.74	119 ± 9	2.33
214	p32	2	41.28	136.98	119 ± 9	1.15
214	p45	2	58.05	93.4	119 ± 9	0.78

Column 1 - Object I.D. Given for Project, Column 2 - Spectrum Coordinate, Column 3 - Fitting Order Used, Column 4 - Distance from Galactic Center Spectrum was Taken at, Column 5 - [OIII] Line Width Value, Column 6 - Stellar Velocity Dispersion, Column 7 - [OIII] line width Divided by the Stellar Velocity Dispersion

Appendix E

Double Gaussian Automation Code

To automize the double Gaussian fitting procedure, the following code appeared near the end of the first python code used. This code determined if the fit was adequate by judging if the width of the wing fit was too big or too small in relation to the width of the main fit (smaller than the main fit or larger than 6 times the main fit), or if the two fits were too far apart (more than 8 $\mathring{A}$ apart). If the fit was unrealistic, one of two things would occur depending of the nature of the fit. If the wing fit were thinner than the main fit, thicker than 20 times the main fit, or more that 100$\mathring{A}$ away from the main fit, it appended the object to a command list (2.com) wherein another double Gaussian fitting code (2.py) is used with a different initial guess location for the wing fit, to which the fitting code was sensitive to (each code also iterated through many different wavelength ranges). The initial guess locations used for each fitting code was (in the written order): 5000$\mathring{A}$, 5014$\mathring{A}$, 5007$\mathring{A}$, 4900$\mathring{A}$, and 5010$\mathring{A}$. If the wing fit were thinner than 20 times the main fit but thicker than 6 times the main fit or if it were less that 100$\mathring{A}$ away from the main fit but more than 8$\mathring{A}$ away from the main fit, that object was added to a different command list (supercomlist2.com) wherein a single Gaussian fit would be performed (NM_SuperSingle.py). The reasoning behind this is as follows: if the fit is extremely unrealistic as described under the first set of conditions, the fit has failed and a new set of initial conditions should be used. If the fit were unrealistic but somewhat

less extreme as defined by the second set of conditions, the fit was a success, but the double Gaussian fitting method was unsuitable and a single Gaussian should be used instead. This chain of fitting would continue through 5 double Gaussian command lists, and if by the end no realistic double Gaussian fit was found using any set of initial conditions, a single Gaussian fit would be performed.

```
#Here, the code judges if the fit was successful. If not, it appends the
    object to 2.com and ends the process.
if abs(sigmaOiii) > abs(sigmaOiiib) or abs(20*sigmaOiii) <
    abs(sigmaOiiib) or abs(coeff[0]-coeff[2])>100:
   file = open('2.com','a')

   line = '{0:5}'.format\
         ('ipython 2.py')

   line+= '{0:5}{1:5}{2:5}{3:5}'.format\
         (" "+obj,"y",coordinate,'5000')

   file.write(line+"\n")

   sys.exit()

#Here, the code judges if the fit was suitable. If not, it appends the
    object to 2.com and ends the process.
if abs(6*sigmaOiii)<abs(sigmaOiiib) or abs(coeff[0]-coeff[2])>8:
   if dowrite == 'y':
       file = open('supercomlist2.com','a')

       line = '{0:5}'.format\
              ('ipython NM_SuperSingle.py')

       line+= '{0:5}{1:5}{2:5}{3:5}'.format\
             (" "+obj,"y",coordinate,'5000')
```

```
        file.write(line+"\n")


        sys.exit()

#Here, the code writes the line width data to a file if the fit is both
    successful and suitable.
if dowrite == 'y':
   file = open('Data.txt','a')

   line = '{0:5}'.format\
              (obj)

   line+= '{0:5}{1:5}{2:5}'.format\
             (coordinate,sigmaOiii," Double")

   file.write(line+"\n")
```